Infection by the gastrointestinal parasite *Trichuris muris*: Defining the microbiota of the parasite and the host

A thesis submitted to the University of Manchester for the degree of Doctor of Philosophy in Microbiology in the Faculty of Biology, Medicine and Health.

2016

Emily Claire White

School of Biological Sciences

Division of Infection, Immunity and Respiratory Medicine

Table of Contents

Word count – 59,586

List of Figures

Chapter 1:

Chapter 3:

Chapter 4:

Chapter 5:

Chapter 6:

List of Tables

Chapter 2:

Chapter 5:

Appendices (on DVD):

Abstract

Infection by the gastrointestinal parasite *Trichuris muris*: Defining the microbiota of the parasite and the host

The University of Manchester: Doctor of Philosophy in Microbiology
Emily Claire White, September 2016

Intestinal dwelling parasites live in close association with the complex microbiota that inhabit our intestinal tracts. The intestinal helminth, *Trichuris muris*, depends on these bacteria for egg hatching and successful establishment of infection within the epithelium of the caecum and colon. Infection causes significant alterations to the host intestinal microbiota, including a decrease in bacterial diversity and shifts in proportions of certain bacterial groups. This is accompanied by a decrease in Foxp3+ regulatory T cells and changes to the metabolic potential of the host microbiota, consequently impacting host health. However, the factor(s) driving these changes and the existence and role of its own intestinal microbiota is unknown.

Infection of C57BL/6 and immunodeficient SCID mice with a high dose (~ 200 embryonated eggs) and a low dose (~ 20 embryonated eggs) of *T. muris* was used to determine the impact of worm burden and the adaptive immune system on the host intestinal microbiota, in comparison to naïve controls. Microbiota analysis was performed by 16S rRNA gene denaturing gradient gel electrophoresis (DGGE) and Illumina sequencing. This revealed that infection-induced microbiota changes were dose dependent and high level infection caused an increase in the *Bacteroidaceae* and *Enterobacteriaceae* families, independently of the host adaptive immune system.

Development of a surface sterilisation protocol enabled the internal *T. muris* microbiota to be analysed by 16S rRNA gene DGGE and fluorescence *in situ* hybridisation (FISH). The resulting data indicated that *T. muris* requires its own diverse intestinal microbiota that is derived from, but distinct to, that of its host. A core microbiota is selected and maintained by the parasite regardless of the surrounding host microbiota. The parasite microbiota is important for its fitness, shown *in vitro* using an antibiotic motility assay and *in vivo* using germ free (GF) mice.

Furthermore, infection with *T. muris* causes a significant reduction in caecal butyrate concentrations and consequently a decrease in the expression of butyrate transporters in caecal tissue. Interestingly, the *T. muris* microbiota is able to produce the short-chain fatty acid (SCFA) butyrate, which the parasite is unable to make itself yet secretes into its local environment.

Together these strategies promote the long term survival of *T. muris* within the intestinal niche, adding a new level of complexity to the interaction between the pathogen, the host and their respective microbiotas that underpins successful chronic nematode infection.

Declaration

No portion of the work referred to in the thesis has been submitted in support of an application for another degree or qualification of this or any other university or other institute of learning.

Copyright statement

Acknowledgement

Firstly, I'd like to thank my supervisors Ian Roberts and Richard Grencis for all their support and encouragement over the past four years. I couldn't have asked for a better project or PhD experience. Thanks to my advisor, Jen Cavet, for encouraging me to do a PhD and for all her advice over the years. Thanks also to the BBSRC for funding my PhD project.

Big thanks goes to Allison Bancroft, Kelly Hayes and Ashley Houlden for all their help in and out of the lab; without you guys I wouldn't have been able to achieve half as much! Thanks also goes to Helen Toogood for helping me with GC-MS, Andy Hayes and the rest of the Genomic Technologies team for sequencing help and advice, the Bioimaging core facility for training and everyone from the Grencis group for their invaluable help in the lab. I'd also like to thank everyone in the Microbiology group for keeping me sane, listening to me moan, being great company and helping me in the lab, especially Jane King, Marie Goldrick, Liz Lord, Eric Miller, Ange Thistlewaite, Nader Masri, Danielle Weaver and anyone else who has helped me over the years. My PhD wouldn't have been the same without you all!

I also have to thank my friends Ruth Brignall, Katie Muddiman, Jessica Llewellyn, Sophie Haslett and Tom Leach, for sharing the PhD pains of failed experiments and second year blues, being a great laugh and always being up for a well needed cake break or gin(s). Thanks to all my friends outside of the lab for making my time in Manchester amazing and for listening to me whine about worms and pretending to care, especially Ellie Chinnock, Helen Marsden and Toya Stokes.

Last but by no means least, thanks to my family, especially my mum Tina, for all your support, encouragement and for believing in me.

List of Abbreviations

Ang4	Angiogenin 4
ANOVA	Analysis of variance
APCs	Antigen presenting cells
b.p.	Base pairs
BSA	Bovine serum albumin
cDNA	Complementary DNA
Cfu	Colony forming units
CoA	Coenzyme A
Cq	Quantitation cycle
Ct	Threshold cycle
CTAB	Hexadecyltrimethylammonium bromide
DAPI	4', 6'-diamidino-2-phenylindole
DGGE	Denaturing gradient gel electrophoresis
D p.i.	Days post infection
dsDNA	Double stranded DNA
EDTA	Ethylenediaminetetraacetic acid
ELISA	Enzyme-linked immunosorbent assay
E/S	Excretory/secretory
FAE	Follicle associated epithelium
Fiaf	Fasting-induced adipocyte protein
FISH	Fluorescence *in situ* hybridisation
GC-MS	Gas chromatography – mass spectrometry
gDNA	Genomic DNA
GF	Germ free
gfp	Green fluorescent protein
GI	Gastrointestinal
GPCRs	G protein coupled receptors
HD	High dose
HDACs	Histone deacetylases

IBD	Inflammatory bowel disease
ICD	Idiopathic chronic diarrhoea
Ig	Immunoglobulin
IκB	Inhibitor of Nf-κB
IL	Interleukin
ILCs	Innate lymphoid cells
i.p.	Intraperitoneal
KAAS	KEGG Automatic Annotation Server
KEGG	Kyoto Encyclopaedia of Genes and Genomes
LAB	Lactic acid bacteria
LB	Luria-Bertani
LD	Low dose
LPL	Lipoprotein lipase
MAMPs	Microbial-associated molecular patterns
MCT-1	Monocarboxylate transporter isoform 1
MGF	Manchester Gnotobiotic Facility
MHC II	Major Histocompatibility complex II
MVAN	Metronidazole, vancomycin, ampicillin, neomycin
NADH	Nicotinamide adenine dinucleotide hydride
NBF	Neutral buffered formalin
Nf-κB	Nuclear factor kappa-light-chain-enhancer of activated B cells
NGS	Next generation sequencing
NLRs	Nod-like receptors
NMDS	Non-parametric multidimensional scaling analysis
NOD	Nucleotide-binding oligomerisation domain
OTUs	Operational taxonomic units
PBS	Phosphate buffered saline
PBS-T	PBS-tween 20
PCR	Polymerase chain reaction
PEG	Polyethylene glycol

PFA	Paraformaldehyde
p.i.	Post infection
PRR	Pattern recognition receptor
PSA	Polysaccharide A
QIIME	Quantitative Insights into Microbial Ecology
qPCR	Quantitative PCR
qRT-PCR	Quantitative reverse transcription PCR
Rag	Recombination-activating gene
rIL-12	Recombinant IL-12
rRNA	Ribosomal RNA
RT	Room temperature
SBB	Sudan black B
SBS	Sequencing by synthesis
SCFAs	Short chain fatty acids
SCID	Severe combined immune deficiency
SDS	Sodium dodecyl sulphate
SEM	Standard error of the mean
SIGIRR	Single Ig domain containing IL-1 receptor (IL-1R)-related protein
SPF	Specific pathogen free
ssDNA	single stranded DNA
STAT6	Signal transducer and activator of transcription 6
TAE	Tris-acetate
TEMED	Tetramethylethylenediamine
TGF-β	Tumour necrosis factor β
TLRs	Toll-like receptors
Tollip	TLR inhibitor Toll-interacting protein
Tregs	Regulatory T cells
TSB	Tryptone soy broth
UV	Ultraviolet
WT	Wild type

Chapter 1

Introduction

1.1. The mammalian intestinal microbiota

Our bodies are home to vast microbial communities which outnumber our own cells by a factor of ten, with around 10^{14} prokaryotic cells and approximately 3 x 10^{12} viruses, as well as fungi (mostly yeasts) and archaea (Whitman *et al.,* 1998; Haynes and Rohwer 2011). Altogether the collective genomes of the microbiota, known as the microbiome, contain 100 times as many genes as we encode in our own genome. As a result, our microbiota can fulfil many functions that we cannot perform ourselves, such as the digestion of certain dietary carbohydrates, and are therefore extremely important for host health (Gill *et al.,* 2006). Most of these bacteria are commensals living in symbiosis with the host, although certain environmental conditions such as immunodeficiency, compromised barrier function or antibiotic use can cause them to become opportunistic pathogens. Many members of the microbiota can switch between these two states and are becoming increasingly linked to disease (Round and Mazmanian, 2009).

The intestinal tract is home to the majority of these microorganisms, all interacting in an extremely complex and diverse ecosystem. Throughout the intestinal tract, physiological conditions vary and with this so do microbial numbers and composition, with the caecum and colon harbouring the greatest numbers (Gill *et al.,* 2006). Thus, the intestinal microbiota is often referred to as the "forgotten organ" (O'Hara and Shanahan, 2006).

1.2. Studying the intestinal microbiota

1.2.1. Culture-dependent methods

Traditionally, bacteria have been isolated from a variety of clinical and environmental samples using culture-dependent methods. However, many bacteria are believed to be unculturable and this poses a range of obstacles for research into bacterial communities, their interactions and functions as a whole (Wilson & Blitchington 1996; Amann *et al.,* 1995). Using selective media we cannot mimic the intestinal environment exactly and many bacteria are dependent on other community members to thrive; therefore this method can give us a limited view of what constitutes our intestinal microbiota. Further to this, culturing bacteria individually hinders our ability to define microbiota size and diversity, the major players and their roles within the environment, gene expression and the metabolic networks present. It is therefore necessary to study bacterial communities as a 'macro-organism', not as individual cultured species (Vieites *et al.,* 2009). Thanks to recent developments in molecular

and sequencing tools we can now use culture-independent methods, which allow us to study whole communities based on the detection of bacterial genes.

1.2.2. Molecular methods

Molecular methods are commonly used to study the intestinal microbiota. These methods are culture-independent and are based on the detection of common molecular markers found in microorganisms, for example 16S (Svedberg) ribosomal RNA (rRNA) and its relevant gene (Fig. 1.1). This RNA molecule is contained within the 30S subunit (small subunit) of 70S ribosomes found in the cytoplasm of bacterial cells. It is highly conserved between bacteria, but also contains 9 hypervariable regions for species and genus identification and other phylogenetic analyses (Petrosino *et al.,* 2009; Saiki *et al.,* 1988). Primers are usually designed to target one or more of these variable regions such as the V3 and V4 regions. Consequently, this gene is ideal for the identification and phylogenetic analysis of bacterial communities, together with its relatively small size (~1,500 base pairs) and abundance within prokaryotes.

Figure 1.1 Conserved and variable regions in the 16S rRNA gene. Conserved regions are found in all bacterial species (grey). Regions V1 – V9 are hypervariable regions (pink) that can be used to discriminate between bacterial groups or species. Numbers across the top indicate base pairs (b.p). Adapted from Petrosino *et al.,* (2009).

1.2.2.1. Denaturing gradient gel electrophoresis (DGGE)

Denaturing gradient gel electrophoresis (DGGE) is one technique that utilises 16S rDNA polymerase chain reaction (PCR) products. This method separates PCR fragments of the same length, but that differ by sequence (Muyzer *et al.,* 1993; Saiki *et al.,* 1988) (Fig. 1.2). Separation occurs using a linearly increasing gradient of DNA denaturants, containing urea and formamide through a polyacrylamide gel. As the double-stranded DNA (dsDNA) fragments travel through the gel, they become partially melted at areas on the sequence with identical melting points known as ‘melting domains’. Melting depends on sequence composition as areas high in GC content need higher temperatures or denaturant concentrations to melt. Once all the domains in a given sequence have melted, the fragment changes from helical to

partially melted and no longer continues to move through the gel (Muyzer and Smalla, 1998) Including a GC-clamp, a GC rich sequence, to one primer prevents the complete denaturation of the DNA fragments, allowing almost 100% of all sequences to be detected (Myers *et al.,* 1985; Sheffield *et al.,* 1992; Muyzer & Smalla 1998). Therefore the separation of partially melted fragments is based on their electrophoretic mobility through a gradient gel (Muyzer and Smalla, 1998).

One advantage of this method is that it removes the need to culture bacteria present in a sample, which is not only time-saving but allows whole communities to be studied, not just individual species. It also gives a visual representation or genetic profile with each band corresponding to a certain species, allowing analysis of bacterial diversity. It has a high reproducibility rate (>98%) so different samples can be compared through the presence and absence of bands (Green *et al.,* 2006; Muyzer & Smalla 1998).

However, there are several drawbacks. Although this technique gives an important insight into bacterial diversity, it does not give us any information about the dynamics or interactions between the community and its environment. It can also only separate fragments up to 500 base pairs and bacteria present in low abundance may not be shown, limiting the number of sequences for phylogenetic analysis (Myers *et al.,* 1985). There is also the chance of co-migration of sequences, which can infer the presence of only one species instead of several (Muyzer and Smalla, 1998). Nevertheless, DGGE profiling is an extremely helpful tool enabling visualisation of bacterial diversity within a sample, before more expensive or time consuming analysis is performed.

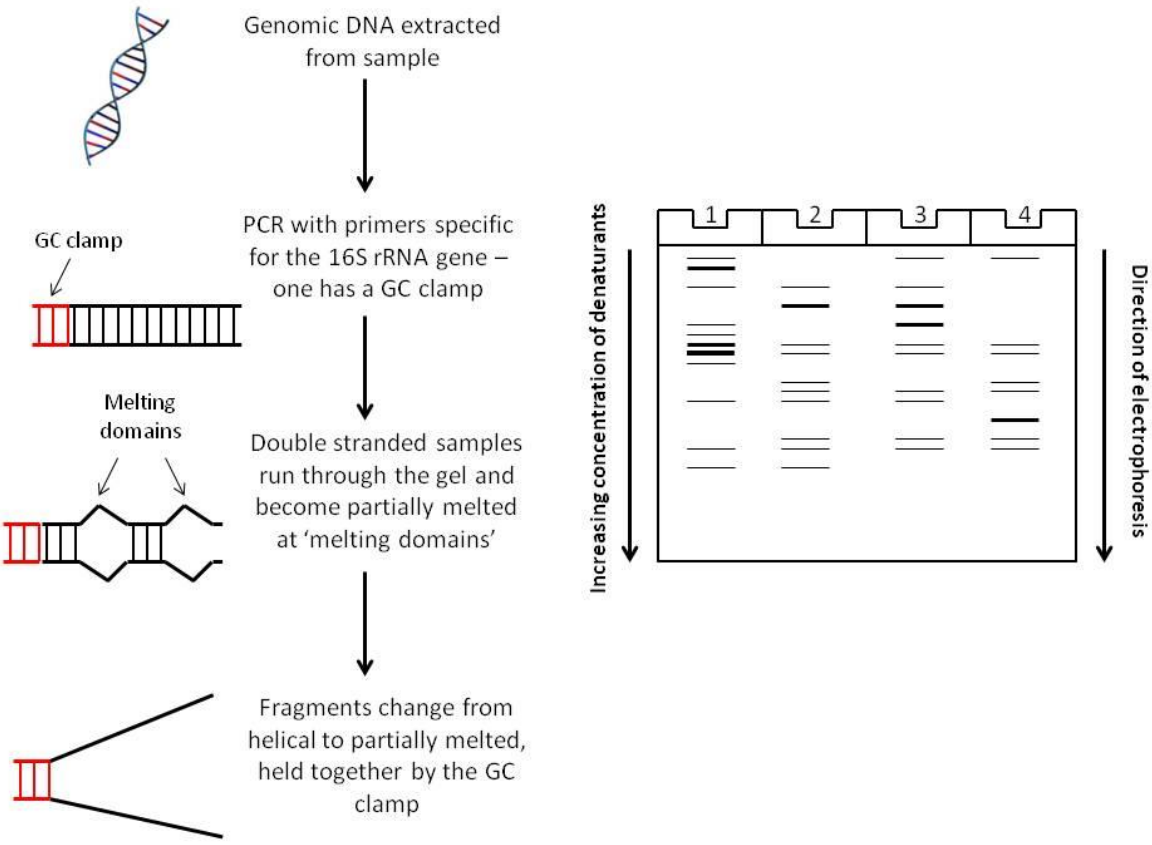

Figure 1.2 Using denaturing gradient gel electrophoresis (DGGE) to determine the diversity of complex microbial populations within a sample. DNA extracted from each sample is subjected to PCR with primers specific for the 16S rRNA gene present in all bacteria. One of these primers has the addition of a GC clamp at the 5' end. PCR products of the same size run down a linearly increasing concentration of denaturants in a polyacrylamide gel, and are consequently separated due to differences in base pair sequences. As the fragments move down the gel, melting occurs at stretches of base pairs with identical melting temperatures, known as 'melting domains'. Once the last domain with the lowest melting temperature has melted, the fragments change from helical to partially melted and migration through the gel stops. The fragment is still held together with the GC clamp preventing complete denaturation, allowing the majority of fragments to be identified on the gel. Sequence variation in 'melting domains' causes melting temperatures to differ and therefore fragments to stop migrating at different distances allowing separation.

1.2.2.2. Quantitative PCR (qPCR)

The 16S rRNA gene can also be employed for use with qPCR, also known as real-time PCR, which allows the exact concentration (relative or absolute) of the target sequence to be quantified in a sample. During PCR, the target sequence is doubled every cycle allowing exponential amplification. However, in qPCR, the dsDNA amplicon is fluorescently labelled and the reaction is monitored in real time, with the amount of fluorescence detected being directly proportional to the amount of target sequence. The cycle that detects fluorescence above background levels is called the Cq (quantitation cycle) or Ct (threshold cycle) value. Therefore, the more target sequence that is present in a sample, the lower the Ct value. Absolute quantification can be performed by creating a standard curve of Ct values from reference samples with known amounts of DNA. RNA can also be used as a template once it has been reverse transcribed into complementary DNA (cDNA) for qPCR. This method is known as quantitative reverse transcription PCR (qRT-PCR) and allows quantification of gene expression from host or bacterial cells (Nolan *et al.,* 2006).

For microbiota analyses, qPCR using 16S rRNA gene primers is a useful, accurate and fast method for quantification of the total bacterial load within a sample. Specific primers for bacterial phyla or species can be used to determine the composition of bacterial communities and to detect the presence or absence of a bacterium within a sample (Yang *et al.,* 2015). However, this method is not ideal for overall analysis of community composition as many primer sets would be necessary, and unknown species would not be detected.

1.2.2.3. Fluorescence *in situ* hybridisation (FISH)

FISH uses fluorescently tagged oligonucleotide probes that can be specific for the 16S rRNA gene (Moter and Göbel, 2000). This can be performed on a range of samples, including paraffin fixed tissues, stool samples or whole mounts. Probes specific for certain bacterial species or different phyla can be used to visually compare the microbiota of different samples. However, although this method has proved successful for visualising the localisation of bacteria within its natural habitat, it is not ideal for quantifying the ecology of the human intestinal tract at species level as it is so diverse (Franks *et al.,* 1998).

1.2.3. Sequencing methods

Next-generation sequencing (NGS), also known as high-throughput sequencing, is a DNA sequencing technique that produces millions of short reads in parallel. This process uses DNA polymerase that catalyses the incorporation of fluorescently labelled nucleotides into a DNA template strand during cycles of DNA synthesis. With

each cycle, fluorescence is detected when a nucleotide is incorporated into the DNA strand and this can be performed with millions of different fragments at the same time. Several commercial technologies can be used for this, which all use slightly different chemistries, including 454 Pyrosequencing (Roche) and Illumina (San Diego, CA, USA) (Reuter *et al.,* 2015).

NGS can be used for the sequencing of target regions, such as the 16S rRNA gene (Fig. 1.3). For Illumina sequencing, the library is first prepared by amplifying the V3 and V4 region of the 16S rRNA gene from sample DNA using specific primers containing adapter sequences. Many samples can be pooled together using an additional PCR step with dual-index barcodes. This attaches unique index sequences to each library allowing identification later on when performing data analysis (Kozich *et al.,* 2013; Fadrosh *et al.,* 2014). The DNA is then denatured into single-stranded fragments and loaded onto a solid substrate, such as a flow cell for Illumina (Bentley *et al.,* 2008). Here the fragments attach to surface bound oligonucleotides complementary to the library adapters and are then amplified into distinct, clonal clusters in a process called bridge amplification. Bridge PCR involves the addition of dNTPs and DNA polymerase to extend DNA strands before further denaturation and repeated PCR to form high density regions of the same fragment (Adessi *et al.,* 2000). The fragments can then be sequenced using sequencing by synthesis (SBS) technology, which uses four fluorescently labelled nucleotides. Single nucleotides are added during each sequencing cycle to the DNA strand and emit a fluorescent signal to identify the incorporated base (Guo *et al.,* 2008; Reuter *et al.,* 2015). The resulting short reads are aligned to reference genomes and can be clustered to produce operational taxonomic units (OTUs) or 'species' depending on phylogenetic similarity or sequence similarity (Petrosino *et al.,* 2009; Vieites *et al.,* 2009).

This method is extremely useful for microbiota analysis as it can be used to sequence millions of 16S amplicons accurately and quickly, meaning bacteria in low abundance or those that are unknown can be detected (Petrosino *et al.,* 2009). This is aided by the use of paired end sequencing, where DNA fragments are sequenced from both ends and analysed as pairs, giving more accurate read alignment (Kozich *et al.,* 2013; Fadrosh *et al.,* 2014). Although this method is more expensive than other techniques, it generates huge amounts of data for the comparison of microbiotas from different treatments e.g. infected vs. uninfected. In addition, the sensitivity of the NGS run can be adjusted by increasing or decreasing the number of sequencing reads depending on the resolution and range needed. For example, a low resolution but wide range over an entire genome, or a high resolution on certain areas of the genome (Fadrosh *et al.,* 2014).

Metagenomics is the sequencing of the total DNA within a sample rather than specific fragments, such as 16S rRNA genes. This can also be performed using NGS, although for library preparation the genomic DNA is randomly fragmented before adapters are attached to each end. This has facilitated the analysis of bacterial communities as a whole enabling greater understanding of genetic diversity, microbial dynamics and the functional capacity of microbes present in a specific environment (Wooley and Ye, 2009). Several other complementary techniques including proteomics, metabolomics and transcriptomics can be employed to further analyse the proteins produced within the community, the metabolic reactions occurring and gene expression, giving a better insight into how the microbial community functions and its impact on the host or environment (Franzosa *et al.,* 2015).

1.2.4. Gas Chromatography-Mass Spectrometry (GC-MS)

There are various methods that can be used for analysis of metabolic compounds produced by the intestinal microbiota. GC-MS is one of these techniques and is particularly useful for the identification and quantification of volatile or semi-volatile organic compounds from complex mixtures, such as stool or caecal samples (García-Villalba *et al.,* 2012). Gas chromatography (GC) works by separating compounds with great resolution, which are then identified by the mass spectrometer (MS). Prior to loading onto the GC-MS system, solid samples must be chemically derivatised depending on what is being detected. This can involve the use of solvents, such as ethyl acetate, to extract the target compounds. The samples are then injected into the GC, volatilised and carried by an inert gas, for example hydrogen or helium, down a column. Different columns can be used for different target compounds. Compounds can then be identified by their retention time when compared to a standard, i.e. the time it takes for a specific compound to travel through the column to the detector in the MS. After exiting the column, compounds become charged fragments after electron impact. These fragments are detected by the MS and produce fragmentation patterns or spectrums that can be used for quantitative measurements (Hites, 1997).

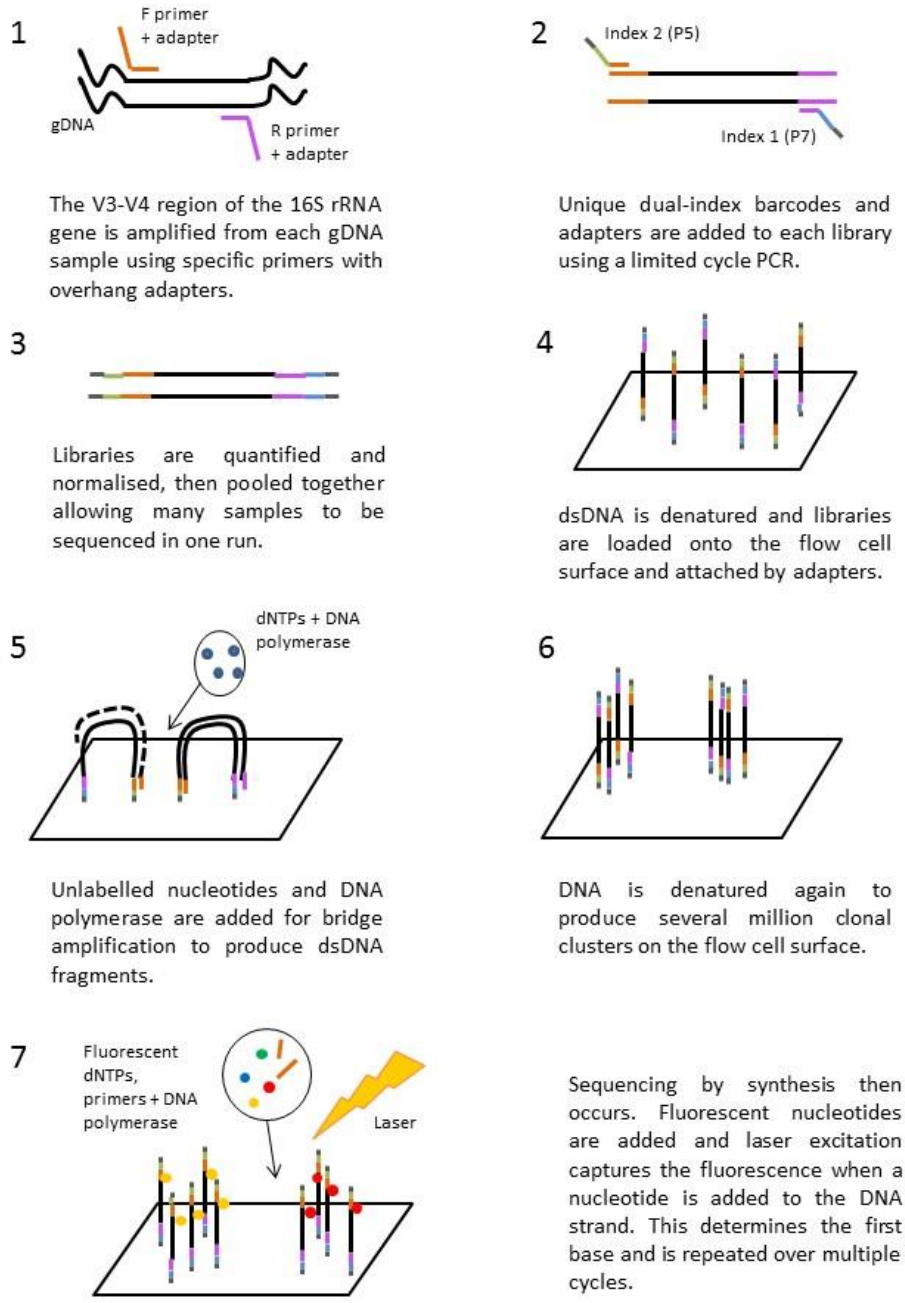

Figure 1.3 Preparation and sequencing of 16S rRNA gene libraries using Illumina. (**1**) The 16S gene is amplified from genomic DNA (gDNA) using primers specific for the V3 and V4 region, with the addition of overhang adapters. (**2** + **3**) If many libraries are to be sequenced, individual libraries can be barcoded with unique dual-indexes allowing several libraries to be pooled after normalisation. (**4** + **5**) The dsDNA fragments are denatured and then attached to the flow cell surface via adapters where bridge amplification occurs. (**6**) This is repeated until several million clonal clusters are formed. (**7**) Sequencing by synthesis (SBS) occurs by the addition of fluorescent nucleotides to the DNA strand and excitation by a laser signifying the nucleotide that has been added. Adapted from Illumina 2016.

1.3. Composition of the mammalian intestinal microbiota

Establishment of our intestinal microbiota was thought to occur immediately after birth, but studies indicate that this may not be the case with low numbers of bacteria being identified in various samples including amniotic fluid *in utero* (Jiménez *et al.,* 2008). In addition, meconium harbours a complex bacterial community dominated by Firmicutes and Proteobacteria (Ardissone *et al.,* 2014). It has been suggested that bacteria reach the foetus by transportation via dendritic cells from the maternal intestinal lumen, through the bloodstream, to lymphoid organs and the placenta (Rodríguez *et al.,* 2015). Work by Jimenez *et al.,* using pregnant mice given a genetically labelled *Enterococcus* species supports this hypothesis. These specific bacteria were recovered from the amniotic fluid and meconium after sterile C-section (Jiménez *et al.,* 2005; Jiménez *et al.,* 2008). Nevertheless, newborns are rapidly colonised with their mother's microbiota immediately after birth, with delivery method having an impact on the initial bacterial communities that colonise the intestinal tract. Vaginal delivery introduces the mother's vaginal microbiota with taxa such as *Lactobacillus* and *Prevotella* dominating, whereas caesarean section confers a skin-like microbiota with taxa including *Staphylococcus* and *Corynebacterium* (Dominguez-Bello *et al.,* 2010; Jakobsson *et al.,* 2014). Initial colonisers of the newborn intestinal tract are typically facultative anaerobes. Their metabolic capabilities prepare the intestinal environment for future commensals, for example reducing oxygen concentrations favourable for obligate anaerobic colonisers (Shin *et al.,* 2015; Morelli 2008). The initial low diversity increases over time and changes with the addition of breast milk and then solid food, so that the microbiota matures and resembles an adult microbiota (Clemente *et al.,* 2012; Dominguez-Bello *et al.,* 2010).

Bacterial community composition in the digestive tracts of healthy individuals is primarily determined by body habitat and time (Costello *et al.,* 2009). The adult intestinal microbiota is typically dominated by two main phylum, Firmicutes and Bacteroidetes (Eckburg *et al.,* 2005). Along the intestinal tract, bacterial composition and abundance changes with its environment, due to variations in pH, antimicrobial and oxygen concentrations, and nutrient availability (Donaldson *et al.,* 2015) (Fig. 1.4). Fast growing, facultative anaerobes that can withstand bile acids and antimicrobials are typically found in the small intestine (Gu *et al.,* 2013). As a result, there is reduced bacterial diversity and abundance in this intestinal niche, which increases in the caecum and colon. Here the pH is higher with fewer antimicrobials and lower oxygen concentrations. There are also differences between the microbiota associated with the mucus layer and the luminal microbiota in the large intestine (Li *et al.,* 2015). Firmicutes, such as *Lachnospiraceae* and *Ruminococcaceae*, are typically found associated with the outer mucus layer, which could act as a nutrient source (Nava *et*

al., 2011; Pédron *et al.,* 2012). However, Bacteroidetes families usually dominate the intestinal lumen (Nava *et al.,* 2011).

Bacterial community structure can be analysed in various ways. Species richness refers to the number of species present, whereas species diversity takes into account both species richness and species eveness (relative abundance) i.e. a community with low diversity may have a low number of different species with one species dominating, whereas high diversity can refer to a community with many different species all at similar abundance. There are different measures of diversity; alpha, beta and gamma. Alpha (intra-individual) diversity is the diversity within a group or treatment and a popular method to address this is to calculate the Shannon diversity index. This calculation accounts for the richness, abundance and eveness of the species present. Beta (inter-individual) diversity is the variation between the intestinal microbiotas of different individuals of the same group or treatment. This can be evaluated using a Bray-Curtis dissimilarity matrix to compare bacterial community similarity using species abundance, or using UniFrac, which determines community similarity using clustering and ordination techniques. These techniques also take into account various factors such as environment, treatment or time. Beta diversity is influenced by various factors such as genetics, diet and early microbial exposure. Using several genetically distinct mouse strains, it has been shown that host genetics has a greater effect on bacterial communities within the caecum than environmental factors (Campbell *et al.,* 2012). It was initially thought that a 'core microbiota' existed, conserved in all individuals (Turnbaugh *et al.,* 2007). Instead, a partially stable, temporal core microbiota is thought to exist at phylum level with around 40 shared species or OTUs that can persist for ~ 1 year in an individual (Caporaso *et al.,* 2011; Faith *et al.,* 2013; Tap *et al.,* 2009). Further to this, microbial genes and therefore microbial metabolic processes are conserved between hosts, especially within the intestinal tract. This minimal human gut metagenome comprises of essential housekeeping pathways necessary for cell survival, for example ATP synthesis, genes that are needed in all habitats and are therefore high in abundance, as well as habitat specific genes (Huttenhower *et al.,* 2012; Qin *et al.,* 2010; Kurokawa *et al.,* 2007). This stability in the face of biodiversity can be explained by some microorganisms sharing the same niche so that their functional potential overlaps, ensuring crucial functions are maintained (Ley, Peterson, *et al.,* 2006).

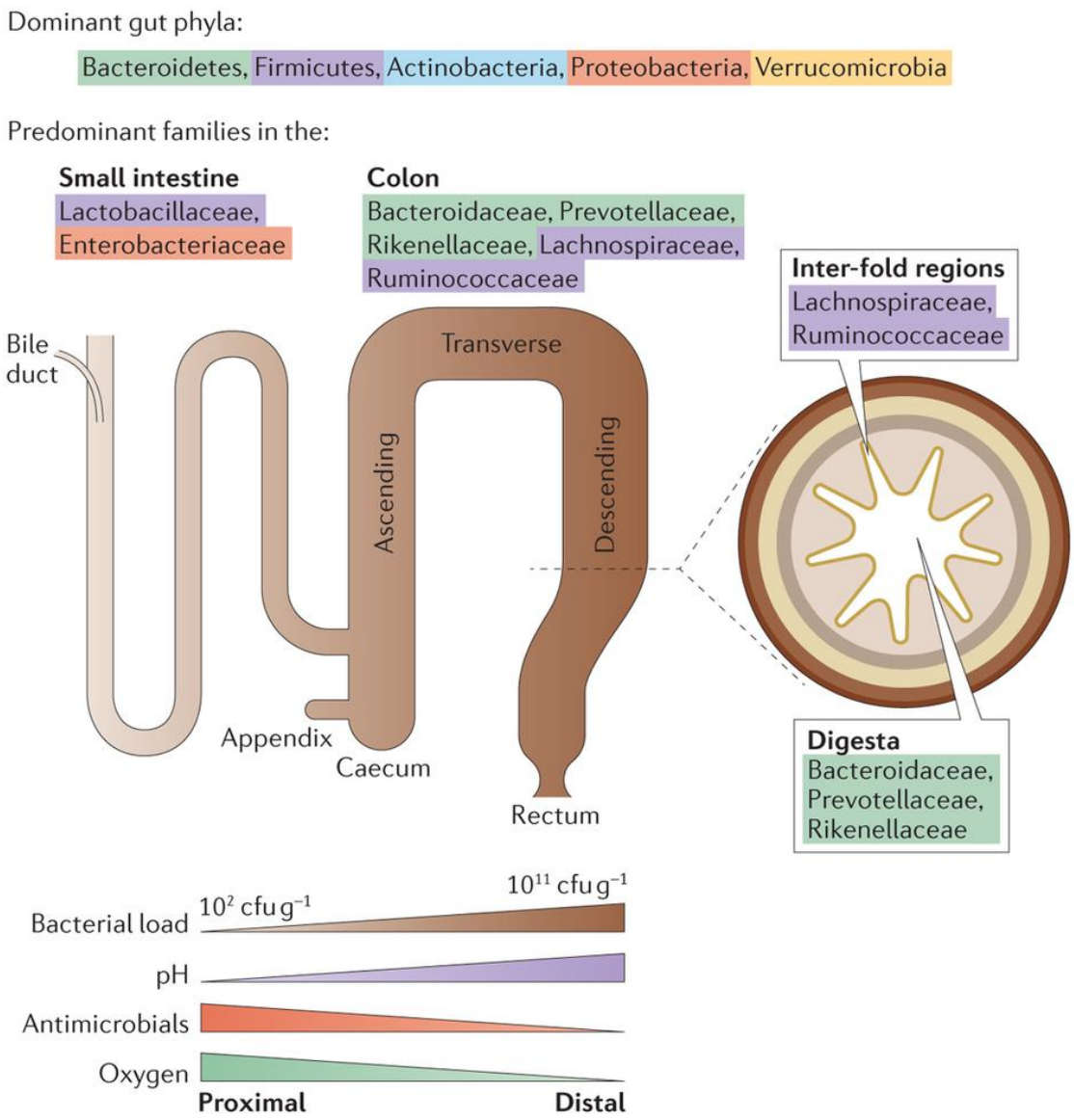

Figure 1.4 Spatial distribution of the microbiota throughout the lower intestinal tract. The bacterial communities that dominate the intestinal tract vary in accordance with their environment. The small intestine, which has a low pH, increased oxygen and antimicrobial concentrations, has a reduced bacterial load compared to the caecum and colon. Here, families *Lactobacillaceae* and *Enterobacteriaceae* dominate (colours represent corresponding phylum). However, in the caecum and colon, *Bacteroidaceae*, *Prevotellaceae*, *Rikenellaceae*, *Lachnospiraceae* and *Ruminococcaceae* dominate. The bacterial abundance is also significantly increased due to a higher pH and lower concentrations of oxygen and antimicrobials, making it a more habitable environment for bacteria. Within the crypts (inter-fold regions) of the caecum and colon, Firmicutes dominate. However, Bacteroidetes are more commonly found within the lumen of the intestinal tract. Cfu = colony-forming units. Taken from Donaldson, Melanie Lee, & Mazmanian, 2015.

1.4. Functions of the intestinal microbiota

1.4.1. Development and modulation of the host immune system

The intestinal microbiota has a great impact on the development and modulation of immune responses in the intestinal tract, vital for animal/mammalian health. There must be a fine balance between maintaining regulatory pathways enabling tolerance to commensals, whilst still protecting against and eliminating pathogens for optimum homeostasis. Development of the mammalian immune system is thought to be influenced early on as the infant intestinal tract becomes colonised with microbes. The introduction of maternal milk containing live microorganisms, immunoglobulin A (IgA), cytokines and immune cells has been shown to influence microbiota composition and therefore immune status (Belkaid and Hand, 2014). GF mice have extensive developmental defects associated with the immune system, including poorly formed Peyer's patches with altered populations of T and B cells in the lamina propria underlying the intestinal epithelial cell layer (Round & Mazmanian 2009; Bauer *et al.,* 1963). However, these immune defects can be corrected through the introduction of *Bacteroides fragilis*, a member of the phylum Bacteroidetes and therefore a known dominant commensal (Mazmanian *et al.,* 2005).

The first line of defence in the intestinal tract is the mucus layer, which limits contact between the microbiota and underlying epithelial cell layer. In the large intestine, there are two mucus layers where the internal layer closest to the epithelial cell layer is mostly sterile (Johansson *et al.,* 2008; Atuma *et al.,* 2001). However, the outer layer is less compact and is associated with a microbiota distinct from that found in the intestinal lumen (Li *et al.,* 2015). Goblet cells produce mucus and this production is influenced by the immune system and the microbiota (Jakobsson *et al.,* 2015). These cells, together with epithelial cells, also produce antibacterial peptides, which facilitate the regulation of numbers and spatial organisation of bacteria at the host barrier. Certain peptides also depend on the presence of a microbiota for their expression, for example RegIIIγ, which is at low levels in the intestinal tracts of GF mice (Natividad *et al.,* 2013).

The intestinal epithelial cell layer underlies the mucosal barrier and acts as a further barrier to microorganisms present in the lumen. However, some bacteria and their associated antigens can pass through using tight junctions when permeability of the intestinal epithelium is altered (Artis, 2008). Beneath this barrier is an array of lymphocytes, dendritic cells and macrophages present in Peyer's patches that can respond to any immunological stimulation and engulf translocating bacteria. There are several immune cells that constantly sample the contents of the intestinal lumen in search of microbial antigens. Dendritic cells can survey the intestinal lumen from

Peyer's patches beneath the epithelial cell barrier, by extending their dendrites through tight junctions after secretion of tight junction proteins for direct sampling (Rescigno *et al.,* 2001). Microfold (M) cells also sample the luminal contents and are situated in the follicle associated epithelium (FAE) over Peyer's patches delivering antigens to dendritic cells and other antigen presenting cells (APCs) via transcytosis (Artis, 2008). This enables constant sampling of the luminal contents and immunological surveillance of the intestinal tract. Intestinal epithelial cells can greatly influence underlying APCs such as dendritic cells, through the secretion of chemokines and cytokines to maintain intestinal homeostasis and direct appropriate immune responses (O'Hara and Shanahan, 2006). Intestinal epithelial cells, M cells and dendritic cells detect microbial antigens via two pattern recognition receptor (PRR) classes; toll-like receptors (TLRs) and nucleotide binding oligomerisation domain (Nod)-like receptors (NLRs), which both recognise microbial-associated molecular patterns (MAMPs), such as flagellin and lipopolysaccharide. Both pathogens and commensals express MAMPs and can consequently cause M cells and dendritic cells to present bacterial antigens to naïve T cells in Peyer's patches. Naïve T cells can differentiate into effector or regulatory T cells (Tregs) and therefore determines if an immune response is initiated against the microorganism. Dendritic cells can direct T cell development and cause the differentiation into Tregs promoting tolerance towards commensals (O'Hara and Shanahan, 2006).

A homeostatic balance between tolerance and protective immune responses is essential as the intestinal mucosal immune system faces constant immunological challenge, not only by commensal organisms, but by dietary and environmental antigens and pathogenic organisms (Artis, 2008). The need to be able to distinguish between commensals and pathogens is crucial. Serum from healthy individuals often contains antibodies and T cells against certain commensals, indicating that the host immune system detects these microbes but has developed tolerance to them to prevent pathogenesis (Macpherson *et al.,* 1996; Ergin *et al.,* 2011). Th17 and Th1 cells are often found in the lamina propria of the intestinal tract during homeostasis. IL-17 and IL-22 produced by Th17 cells, and also other cell lines, have been shown to be important for intestinal homeostasis with the microbiota by regulating epithelial cell function (Belkaid and Hand, 2014). IL-22 induces antimicrobial and mucus production and a lack of Th17 cells is related to increased bacterial translocation, indicating the importance of this lineage for barrier function and commensal containment (Wolk and Sabat, 2006).

There are several mechanisms thought to be employed by the intestinal microbiota and the host to dampen and avoid inflammatory responses within the intestinal tract. The selective distribution of PRRs in the intestinal epithelia is thought to be one

mechanism implemented by the host. Normally, there is little or no TLR2, TLR4 or CD14 expression on intestinal epithelial cells minimising recognition of commensals by the host immune system (Abreu *et al.,* 2001, Otte *et al.,* 2004). PRRs can also be intracellular and subcellular across the intestinal epithelial cell layer, meaning commensals that rarely breach this barrier would not normally encounter these PRRs. They are instead much more likely to interact with intracellular pathogens such as *Listeria monocytogenes* and illicit an appropriate protective immune response against the bacteria (Artis, 2008). Further interactions between commensal bacteria and the intestinal epithelia involving the TLR inhibitor Toll-interacting protein (Tollip) have indicated an inductive effect for commensals. High levels of Tollip have been detected on intestinal epithelial cells, with the highest being in healthy colonic mucosa where bacterial load tends to be the highest. Thus, expression directly correlates with luminal bacterial load *in vivo* (Otte *et al.,* 2004). Another TLR inhibitor, SIGIRR (single-immunoglobulin-domain-containing interleukin-1 receptor (IL-1R)-related protein), also known as TIR8, is present at high levels on intestinal epithelial cells and animals deficient in this protein are more susceptible to colitis (Garlanda *et al.,* 2004). This suggests a possible role for suppressing inflammatory cascades and modulating the immune system to tolerate commensals. There is a clear method employed by commensals to utilise host proteins in order to suppress inflammatory cascades, also seen with nucleotide-binding oligomerisation domain 2 (NOD2), as mutations in this gene can cause Crohn's Disease (Bairead *et al.,* 2003).

Certain lymphocytes can modulate the intestinal microbiota, such as Foxp3+ Treg cells, and maintain intestinal homeostasis. These cells differentiate in the thymus and can also be induced in the intestinal tract, allowing the generation of populations specific for particular commensals (Coombes *et al.,* 2007; Lathrop *et al.,* 2011). Certain members of the microbiota and their products can cause the induction and expansion of Treg cells within the intestinal tract, for example polysaccharide A (PSA) from *Bacteroides fragilis*. This microbial product induces IL-10-producing Tregs via TLR2 and consequently protects mice from colitis and the associated inflammation (Mazmanian *et al.,* 2008; Mazmanian *et al.,* 2005; Round *et al.,* 2011). The antibody, secretory IgA (sIgA), is produced by intestinal epithelial cells and has been shown to have a role in mediating tolerance towards the microbiota. It can prevent microbial stimulation of the adaptive and innate immune systems, reducing intestinal inflammation and can consequently promote host-microbial interactions (Peterson *et al.,* 2007). Further to this members of the intestinal microbiota can modulate the Nf-κB pathway present in intestinal epithelial cells. This pathway is usually activated by pathogenic bacteria leading to a pro-inflammatory immune response (Artis, 2008). However, commensals avoid this response by inhibiting three main pathway

components; proteosome function within epithelial cells, degradation of phosphorylated Nf-κB inhibitory IκB and the nuclear export of the Nf-κB subunit p65 (Neish *et al.,* 2000, Kelly *et al.,* 2004, Petrof *et al.,* 2004). In addition, intestinal epithelial cells have the ability to secrete tumour necrosis factor-β (TGF-β) in response to commensals, which can inhibit Nf-κB pathway gene expression, further limiting the pro-inflammatory response (Artis, 2008). Therefore intestinal epithelial cells are tolerant of TLR stimulation by the resident microbiota, so that under normal circumstances Nf-κB stimulation is low (Ben-Neriah and Schmidt-Supprian, 2007). Recent research has revealed a further mechanism used by the host immune system to maintain intestinal homeostasis. Group 3 innate lymphoid cells (ILCs) are a set of immune cells grouped according to their expression of the transcription factor RORγt and production of IL-17 and IL-22, as part of the innate immune system. These cells also express major histocompatibility complex II (MHC II) and as a result can regulate CD4+ T cell responses to commensal bacteria, preventing inflammatory responses by the adaptive immune system (Hepworth *et al.,* 2013). These methods are effective ways of enabling commensal bacteria to reside in the intestine without triggering pro-inflammatory immune responses that would remove them.

Members of the microbiota also promote protective responses against pathogens by colonisation resistance. The physical presence of commensals and the competition for nutrients limits the ability of pathogenic species to colonise the same intestinal niche (van der Waaij *et al.,* 1971; Belkaid & Hand 2014). As a result, alterations to the intestinal microbiota or nutrient availability can upset this balance and enable pathogens to colonise. It is therefore evident that our intestinal microbiota is essential for the healthy development and maintenance of our mucosal and peripheral immune system, having an overall regulatory and anti-inflammatory effect, maintaining homeostasis.

1.4.2. Nutrient metabolism

The intestinal microbiota has the capacity to generate a wide range of metabolites from the breakdown of host dietary components, as well as host and microbial products. In some cases, we lack the necessary genes, whose products breakdown these metabolites, ourselves. This has been shown in various animal models and using gnotobiotic zebrafish, which have a decreased ability to utilise nutrients compared to conventional zebrafish (Rawls *et al.,* 2004). Animals therefore rely on members of the microbiota to provide essential nutrients and vitamins. This is particularly true for the breakdown of non-digestible carbohydrates. Unlike digestible carbohydrates, which are mostly used and absorbed in the small intestine, non-digestible carbohydrates must be fermented by bacteria in the large intestine to

produce short chain fatty acids (SCFAs). Human studies have detected a high number of bacterial carbohydrate transport and metabolism genes in faecal samples, displaying their importance in human nutrition (Tap *et al.,* 2009; Qin *et al.,* 2010; Kurokawa *et al.,* 2007). The three main SCFAs produced primarily in the colon and lower intestinal tract are acetate, butyrate and propionate via multiple pathways. These SCFAs can be found at concentrations ranging from 20 – 140 mM depending on variables such as dietary fibre intake and microbiota composition (Cummings *et al.,* 1987). The majority of SCFAs produced by the microbiota are taken up by host intestinal epithelial cells as an energy source in a preferential order of butyrate (C4) > propionate (C3) > acetate (C2) (Clausen and Mortensen, 1994). Acetate is the most abundant SCFA in the intestinal tract and can travel to peripheral tissues such as the liver, together with propionate, via the portal circulation. These SCFAs can be used for gluconeogenesis and lipogenesis in various tissues (De Vadder *et al.,* 2014; Zambell *et al.,* 2003).

Butyrate is of particular interest due to its beneficial impact on host health and importance for maintaining intestinal homeostasis. The majority of butyrate producing bacteria belong to the Firmicutes phylum, for example the *Lachnospiraceae*, *Ruminococcaceae* and *Clostridiales* clusters IV and XIVa (Louis *et al.,* 2010). However, members of other intestinal phyla, including Actinobacteria, Bacteroidetes and Proteobacteria, all have the potential to produce butyrate. Production occurs by fermentative metabolism so that bacteria gain energy in the form of ATP by substrate-level phosphorylation, and this can be performed using different biosynthetic pathways, with the most prevalent being the acetyl-coenzyme A (CoA) pathway. All four known biosynthetic pathways merge where crotonyl-CoA is used to generate butyryl-CoA, which is then converted to butyrate (Vital *et al.,* 2014).

Intestinal epithelial cells take butyrate up in a number of ways, including non-ionic diffusion and via SCFA transporters on the cell surface, as depicted in figure 1.5. There are two main transporters; monocarboxylate transporter isoform 1 (MCT-1), which is coupled to a transmembrane H^+-gradient, and SLC5A8, which is a Na^+-coupled co-transporter. Expression of MCT-1 is influenced by butyrate concentrations in the intestine, with low concentrations of butyrate resulting in fewer transporters (Cuff *et al.,* 2002; Borthakur *et al.,* 2008). Butyrate can then be used by the cell as an energy source where it undergoes β-oxidation in the mitochondria to produce acetyl-CoA. This then enters the Krebs cycle producing NADH, which then enters the electron transport chain for ATP and CO_2 production (Donohoe *et al.,* 2011). A consequence of butyrate metabolism is reduced oxygen concentrations within the intestinal epithelium, which maintains a hypoxic barrier and an anaerobic lumen promoting the colonisation of obligate anaerobes that typically dominate the intestinal

microbiota. In the absence, or low concentrations of butyrate, glucose can be used as an alternative energy source by intestinal epithelial cells after conversion to acetyl-CoA by pyruvate dehydrogenase (Donohoe *et al.,* 2012; Rivera-Chávez *et al.,* 2016; Kelly *et al.,* 2015).

Apart from acting locally as an energy source, butyrate and other SCFAs can act as signalling molecules via several G protein couple receptors (GPCRs). These include GPR43 (FFAR2), GPR41 (FFAR3) and GPR109A (HCAR2) (Fig. 1.5). All three receptors are expressed by various cell types such as intestinal epithelial cells and immune cells, allowing butyrate to induce numerous regulatory properties (Rooks and Garrett, 2016). Butyrate can inhibit histone deacetylases (HDACs) impacting gene expression of numerous cell types. This is evident for Treg cells, as butyrate can promote their frequency within the colon, reducing inflammation and promoting intestinal homeostasis (Furusawa *et al.,* 2013). SCFAs are also important for maintaining barrier function within the intestinal tract, causing alterations to mucin production and tight junction integrity (Gaudier *et al.,* 2004; Fukuda *et al.,* 2011). Overall SCFAs are the primary energy source for intestinal epithelial cells and maintain intestinal homeostasis.

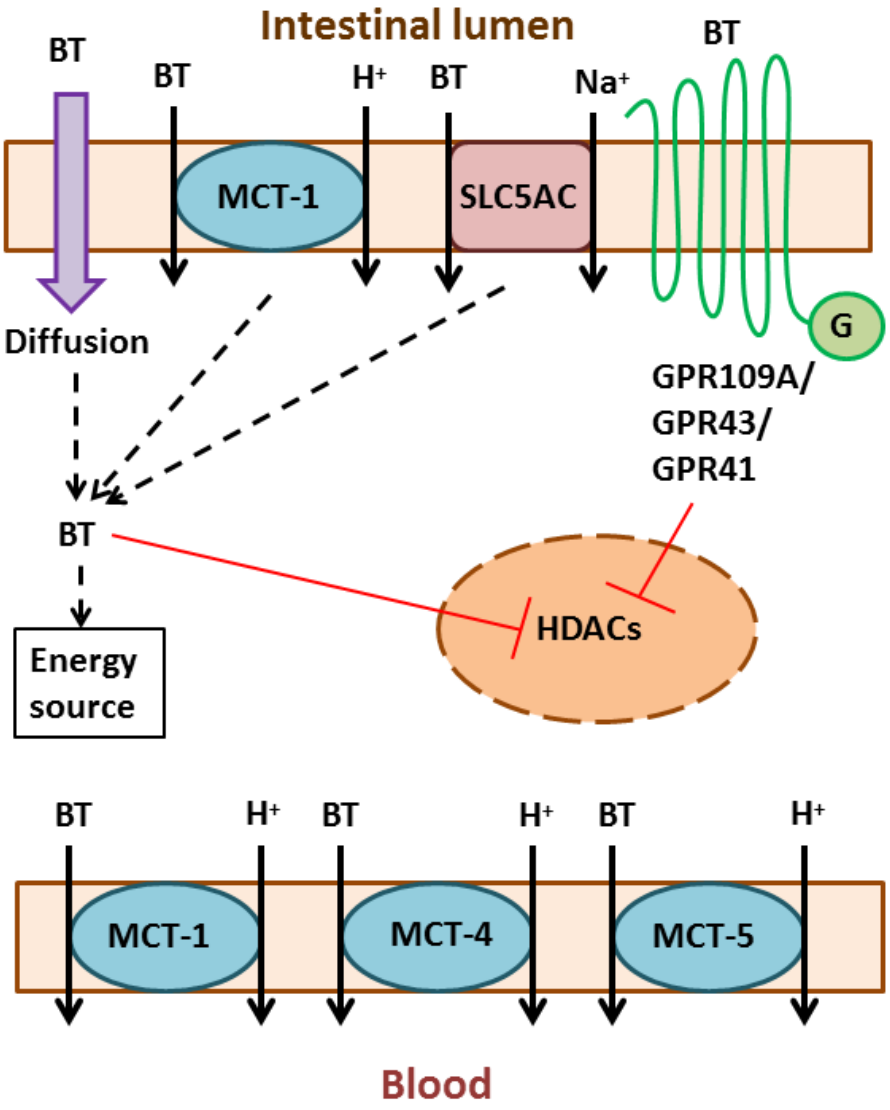

Figure 1.5 Butyrate transporters and receptors expressed by intestinal epithelial cells. Butyrate (BT) produced by bacterial fermentation within the intestinal lumen by members of the microbiota, can be taken up by intestinal epithelial cells by diffusion or transporters on the cell surface. Monocarboxylate transporter isoform 1 (MCT-1) is coupled to a transmembrane H^+-gradient, and SLC5A8 (sodium-coupled monocarboxylate transporter 1 (SMCT-1)), is a Na^+-coupled co-transporter. Once in the cell, butyrate can be used as an energy source using β-oxidation or can enter the nucleus and inhibit histone deacetylase (HDAC) activity. This can also occur via G protein-coupled receptors (GPCRs), including GPR109A, GPR43 and GPR41, which induce signal transduction. Inhibition of HDACs impacts gene expression in intestinal epithelial cells and other cell types. Cellular butyrate can also be transported into the circulation by MCT-1, 4 and 5 for interactions with other cell types. Adapted from Gill & Dudeja 2011.

1.5. Alterations to the intestinal microbiota

Although the intestinal microbiota is relatively stable within individuals over time, various changes in lifestyle, age, environment or disease state can cause major alterations to microbiota composition and diversity. Mouse models have been used extensively for these types of studies as their microbiotas, like humans, are dominated by the Firmicutes and Bacteroidetes, and consequently have very similar functionality. However, there are numerous differences in microbiota composition at lower taxanomic levels and intestinal physiology (Xiao *et al.,* 2015; Nguyen *et al.,* 2015). Nevertheless, there are numerous advantages to using mouse models for microbiota studies including their short life cycle, the availability of reagents and genetically modified mouse models, including GF animals, and the ability to control their environment allowing the comparison of individuals suffering microbiota changes to a 'healthy' naïve baseline.

1.5.1. Obesity

Several studies have revealed that obesity is associated with major changes to the intestinal microbiota, seen in both mouse models and human studies. GF mice have reduced adiposity compared to those colonised with an intestinal microbiota, and obese individuals have alterations to their intestinal microbiota (Ley, Turnbaugh, *et al.,* 2006; Bäckhed *et al.,* 2004). In genetically modified mice lacking the leptin gene needed for proper metabolism and energy intake, an obese phenotype is observed. Obesity is associated with a significant reduction in the abundance of Bacteroidetes and an increase in Firmicutes and Actinobacteria, when compared to lean mice with a functioning leptin gene (Ley *et al.,* 2005). This altered microbiota provides an increased ability to harvest energy from the diet, which is then stored in adipocytes (fat cells), due to an enrichment of genes encoding enzymes for the breakdown of carbohydrates, lipids and amino acids (Turnbaugh *et al.,* 2006). In 'lean' mice, intestinal epithelial cells express Fiaf (fasting-induced adipocyte protein), which inhibits lipoprotein lipase (LPL). However, the altered microbiota can suppress Fiaf, which in turn reduces LPL inhibitor levels causing an increase in LPL activity and storage of fatty acids in adipocytes (Bäckhed *et al.,* 2004). 'Obese' genes are associated with Firmicutes and Actinobacteria, resulting in reduced diversity for the obese phenotype, whereas 'lean' genes are encoded by the Bacteroidetes and other phyla (Turnbaugh, Hamady, *et al.,* 2009).

Furthermore, it is thought that both genetic background and diet have an impact on the development of obesity (Turnbaugh *et al.,* 2006). Giving mice a different diet has a great impact on the intestinal microbiota, with changes seen within a day (Turnbaugh, Ridaura, *et al.,* 2009). This has also been seen in human studies with

bacterial blooms occurring over time due to dietary changes (Walker, Ince, *et al.,* 2011). Individuals consuming a western diet high in fat and protein have a significantly different signature microbiota compared to those that consume a plant-based, high fibre diet. These changes are independent of geographical location with similar diets promoting conserved microbial features (Yatsunenko *et al.,* 2012; De Filippo *et al.,* 2010). In addition, high fibre diets provide the microbiota with increased levels of substrate for butyrate production, which consequently has beneficial effects on host health (Sonnenburg and Bäckhed, 2016).

1.5.2. Inflammatory bowel disease

Inflammatory bowel disease (IBD), which includes Crohn's Disease and Ulcerative Colitis, causes dysbiosis, defined as significant alterations to the intestinal microbiota resulting in ill-health. These disorders are characterised by inappropriate immune responses and chronic intestinal inflammation caused by a genetic predisposition and exposure to certain environmental factors. Although numerous studies have shown that dysbiosis is associated with IBD and the microbiota plays a key role, it is not known if these changes are a cause or consequence of these intestinal disorders (Sartor and Mazmanian, 2012).

Although IBD is associated with significant dysbiosis, there is not a defined altered intestinal microbiota shared between individuals with IBD. However, a common feature of these disorders is reduced diversity but an increase in the abundance of mucosa-associated bacteria (Swidsinski *et al.,* 2002; Wohlgemuth *et al.,* 2009). Firmicutes are also reduced and members of the Proteobacteria, particularly the *Enterobacteriaceae*, are enriched resulting in increased Proteobacterial diversity and an overall reduction in beneficial bacteria (Frank *et al.,* 2007; Lupp *et al.,* 2007; Garrett *et al.,* 2010). On the other hand, the Bacteroidetes have been found to both increase and decrease in patients with IBD (Walker, Sanderson, *et al.,* 2011; Andoh *et al.,* 2012). The variability seen between individuals could be a result of different factors such as diet, location of the disease in the intestinal tract and genetic background (Sartor and Mazmanian, 2012).

Genetic background can contribute to intestinal dysbiosis due to polymorphisms in particular genes, causing abnormalities in the recognition and processing of bacterial antigens, mucosal barrier function and immune regulation (Waterman *et al.,* 2011; Sartor & Mazmanian 2012). This can consequently impact spatial organisation and the composition and quantity of the intestinal microbiota. Genetic variants of the NOD2 receptor have been shown to increase the risk of susceptibility to disease (Frank *et al.,* 2011). Mutations in this gene result in defective production of the antimicrobial α-defensin, which may explain the increased bacterial attachment and

consequent mucosal inflammation associated with Crohn's disease (Wehkamp *et al.,* 2004).

A reduction in SCFA concentrations, including butyrate, is seen within the intestinal tract of IBD patients compared to healthy individuals, and is linked to a reduction in butyrate-producing bacteria (Huda-Faujan *et al.,* 2010). Further to this, oxidation of butyrate by intestinal epithelial cells is significantly decreased and is due to a down-regulation of the butyrate transporter, MCT-1, resulting in reduced butyrate uptake (Thibault *et al.,* 2007; Den Hond *et al.,* 1998). Rigottier-Gois has proposed that the dysbiosis seen with IBD is generally characterised by a decrease in obligate anaerobes in favour of facultative anaerobes, such as the *Enterobactericeae*, and this may be due to increasing oxygen concentrations within the intestinal tract as a result of inflammation (Rigottier-Gois, 2013). Antibiotic induced depletion of *Clostridia*, a group of butyrate producing Firmicutes, caused reduced intestinal butyrate concentrations and an increased abundance of the *Enterobacteriaceae* species, *Salmonella*. This was a result of increased epithelial oxygenation due to a shift in intestinal epithelial metabolism from butyrate oxidation to glucose fermentation, therefore selecting for facultative anaerobes (Rivera-Chávez *et al.,* 2016). This could also be occurring during IBD, facilitating the outgrowth of pathogenic *Enterobacteriaceae* and increasing intestinal inflammation.

1.5.3. Antibiotics

Antibiotics can also cause significant changes in the host microbiota and overuse has led to the development of many resistant strains. Broad-spectrum antibiotics can cause great alterations, as they are not specific to a certain groups of bacteria so can impact whole communities, not just the target pathogen. These changes can persist for long periods of time, with week-long treatment having an impact for 6 months to 2 years (Jernberg *et al.,* 2007). These changes include long term reduction in alpha diversity, proportional shifts in specific taxa and an enrichment of antibiotic resistant strains causing further health problems for the individual (Jernberg *et al.,* 2007). These microbiota changes can lead to increased susceptibility to opportunistic infections, such as *Clostridium difficile*, due to reduced colonisation resistance and altered metabolism, resulting in an environment more suited for pathogens (Ferreyra *et al.,* 2014; Bäckhed *et al.,* 2012).

1.6. Gastrointestinal helminth infections

1.6.1. *Trichuris muris*

Trichuris is one genus of gastrointestinal (GI) parasite infecting around 650 million people worldwide, although exact numbers are difficult to estimate, and there are over 50 species which infect the caecum and colon of a wide range of mammals (Mascie-Taylor and Karim, 2003; Panesar and Croll, 1980). This includes the human whipworm, *T. trichiura*, which is responsible for considerable morbidity and disability in the developing world where infection is endemic (Stephenson *et al.,* 2000).

The mouse whipworm, *T. muris*, is an extremely useful system for studying *Trichuris* infection, pathology and associated immune responses (Cliffe and Grencis, 2004). The *Trichuris* life cycle is similar between species and is shown in figure 1.6. Briefly, transmission occurs via the oral ingestion of embryonated eggs from the environment, which passively accumulate in the caecum and hatch in response to the intestinal microbiota and temperature (Panesar & Croll 1980; Cliffe & Grencis 2004; Hayes *et al.,* 2010). Direct contact of bacterial structural components, such as type 1 fimbriae, triggers hatching at 37 °C ensuring eggs only hatch within the host intestinal tract. The resulting L1 larvae penetrate the intestinal epithelial cell layer of the caecum and colon at the base of crypts and undergo three more moults. Male and female adult worms burrow their anterior end into the epithelial cell layer by day 32 post infection (p.i.) forming syncitial tunnels, with their posterior end free in the lumen for copulation. Following mating, female worms release unembryonated eggs, which are then transported through the intestinal tract by peristalsis and released in the faeces. Over two months these eggs become embryonated in the environment, infective for ingestion by a new host (Cliffe and Grencis, 2004).

In most cases, worm burden determines the severity of symptoms with low level infections usually asymptomatic and chronic infections leading to diarrhoea, weight loss, rectal prolapse, severe anaemia and clubbing of the fingers (Stephenson *et al.,* 2000; Klementowicz *et al.,* 2012). Current treatment involves the use of anthelmintics, such as mebendazole, but efficacy is waning and resistance is increasingly apparent in endemic areas, so novel treatments are needed (Cliffe and Grencis, 2004). Much research has been carried out using *T. muris* together with various genetically modified mouse strains generating a great deal of knowledge about *Trichuris* infection, host immune responses for resistance and susceptibility, and more recently the involvement of the intestinal microbiota (Klementowicz *et al.,* 2012).

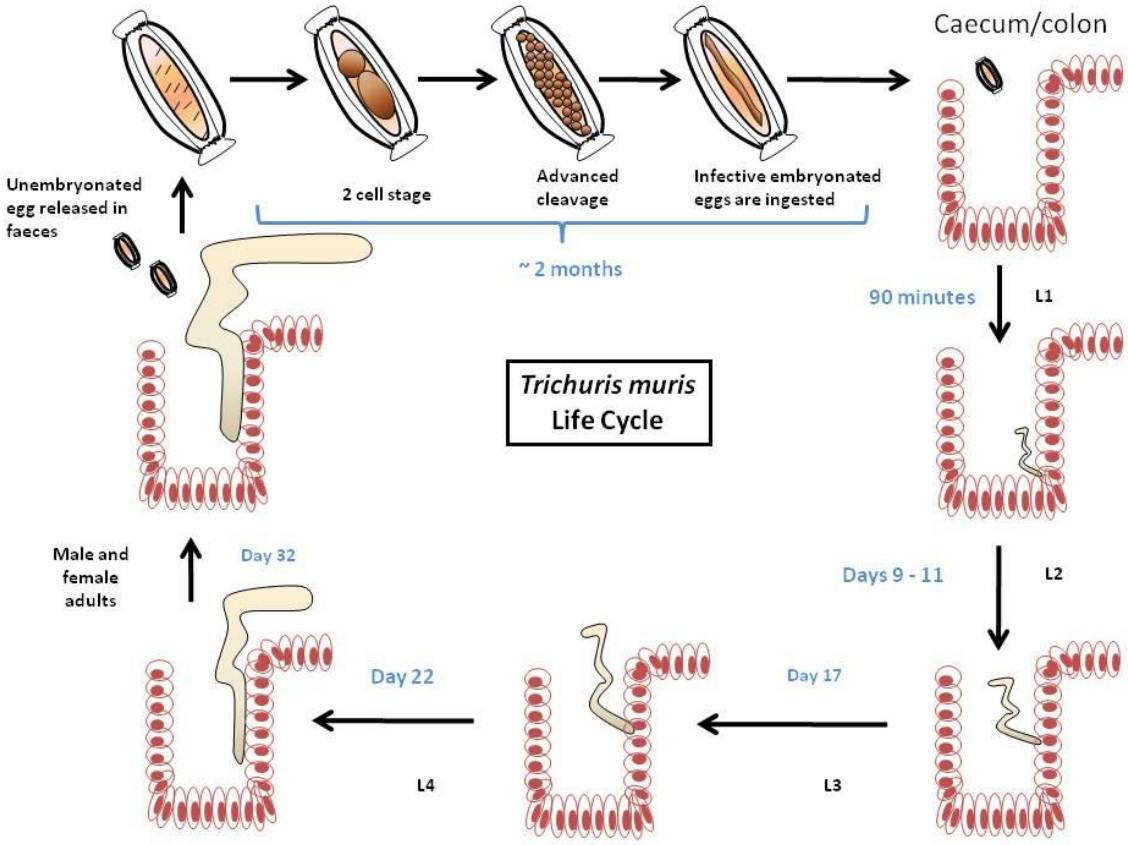

Figure 1.6 Life cycle of *Trichuris muris*. Ingestion of embryonated *Trichuris* eggs causes infection. Eggs accumulate in the caecum and hatching is initiated by interactions with the intestinal microbiota after 90 minutes, releasing L1 larvae. Larvae penetrate the crypts of the epithelial cell layers in the caecum and colon, and undergo three more moults. By day 32 p.i., male and female adult worms can be observed in the caecum and colon. The posterior end of the parasite is free in the lumen to allow copulation to occur. Eggs are released in faeces into the environment, where they embryonate over two months and become infective. Adapted from Klementowicz *et al.,* (2012).

1.6.2. *Trichuris* physiology and metabolism

There is a distinct difference in size between male and female *Trichuris* adult worms, with females being the larger of the two. Both are found with their anterior end embedded within the epithelial cell layer of the host intestine and the posterior end left free in the intestinal lumen. The majority of research on *Trichuris* anatomy and structure has focussed on the anterior end using electron microscopy, due to its intimate association with the host. This has revealed the presence of specialised organs including the bacillary band and stichosome (Fig. 1.7A). The bacillary band is present on the ventral surface of adult worms and is made up of around 50,000 subcuticular glands, or bacillary cells, that have pores through the cuticle (Tilney *et al.,* 2005; Wright & Chan 1973). Its exact role is yet to be fully defined although proposed functions include a role in the absorption of nutrients from the intestinal tract such as the cytoplasm of ruptured cells, enzyme or protein secretion, osmotic and ionic regulation or a chemosensory role (Artis *et al.,* 2004; Tilney *et al.,* 2005; Jenkins 1969; Wright & Chan 1973). The stichosome is an internal structure that runs through the parasite anterior end and is made up of stichocytes (Sheffield 1963). It surrounds the narrow oesophagus and is thought to have a secretory and digestive role due to the high level of enzymatic activity, also detected in the related nematode *Trichinella spiralis* (Despommier and Müller 1976; Sheffield 1963). Transcriptome analysis of the anterior end has identified a high number of chymotrypsin A-like serine proteases, which are also the largest group of proteases encoded by the *Trichuris* genome. These could explain the increased enzymatic activity and if secreted could facilitate the degradation of the host mucin layer for successful infiltration of the host barrier. Protease inhibitors were also enriched and could potentially have anti-inflammatory and anti-bacterial properties, which would be beneficial in the infected host intestinal tract (Foth *et al.,* 2014).

Conversely, there has been relatively little study on the posterior half of this parasite. The digestive tract of most nematodes is one continuous tube that spans the length of the worm but changes in shape and size throughout (Lee, 1965). The intestine is located in the posterior half together with the sexual organs, which dominate this portion of the worm (Fig. 1.7B). As a result, transcriptome analysis of the posterior region resulted in a high level of reproduction associated transcripts (Foth *et al.,* 2014).

Relatively little is known about the metabolism of *Trichuris* species, unlike other parasitic helminths. Many helminth parasites are able to metabolise and excrete the SCFA acetate, such as *Ascaris suum,* in the host intestinal tract (Tielens *et al.,* 2010). Nematodes have also been shown to excrete nitrogenous products, including

ammonia, through the body wall by diffusion and via the intestinal tract. Further to this, many worms secrete large amounts of amino acids. This may also be true for *Trichuris* species since the main food source is thought to be host cells and mucins, high in protein and therefore nitrogen (Lee, 1965).

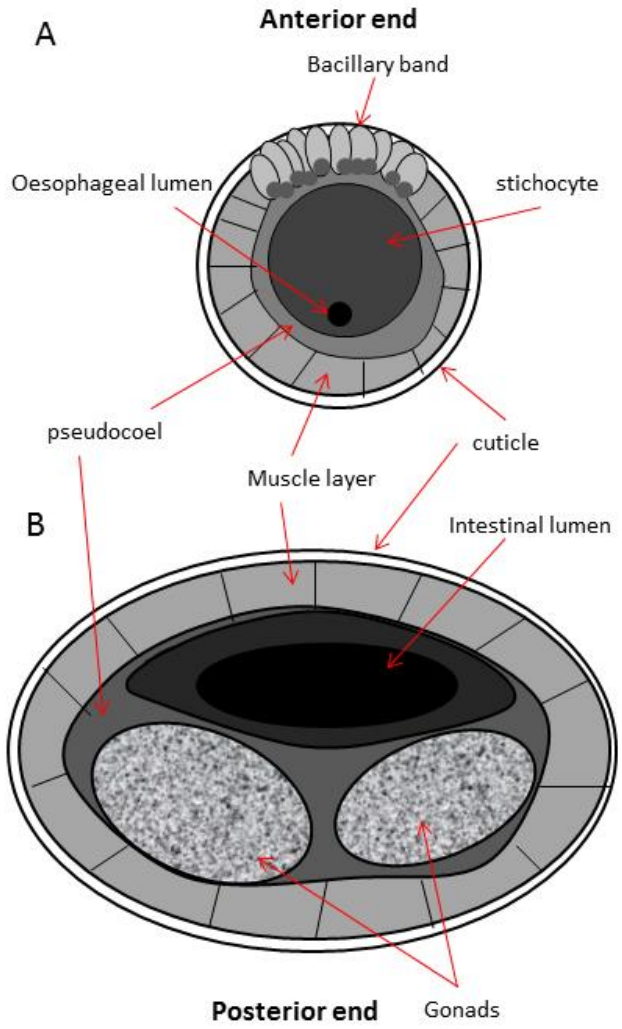

Figure 1.7 Structure of *Trichuris* adult worms. (**A**) Transverse section through a *Trichuris* adult worm showing the organs found in the anterior end found buried in the host intestinal epithelial cell layer and (**B**) a transverse section through a male adult *Trichuris* worm posterior end. This part of the parasite is found in the lumen of the intestinal tract. Not to scale.

1.6.3. Immune responses to *T. muris* infection

T. muris, or mouse whipworm, is used as a laboratory model for the human whipworm, *T. trichiura* (Cliffe and Grencis, 2004). Humans and wild-type (WT) animals are susceptible to infection by *Trichuris* species, but the majority do not display symptoms of chronic infection (Klementowicz *et al.,* 2012). This is due to modulation of the host immune system by the infecting parasite in order to keep the host alive and maintain long term infection. Susceptible mice mount a Th1 response and develop chronic infections with increased immunopathology, whereas resistant mice generate a Th2 response leading to parasite expulsion (Fig. 1.8).

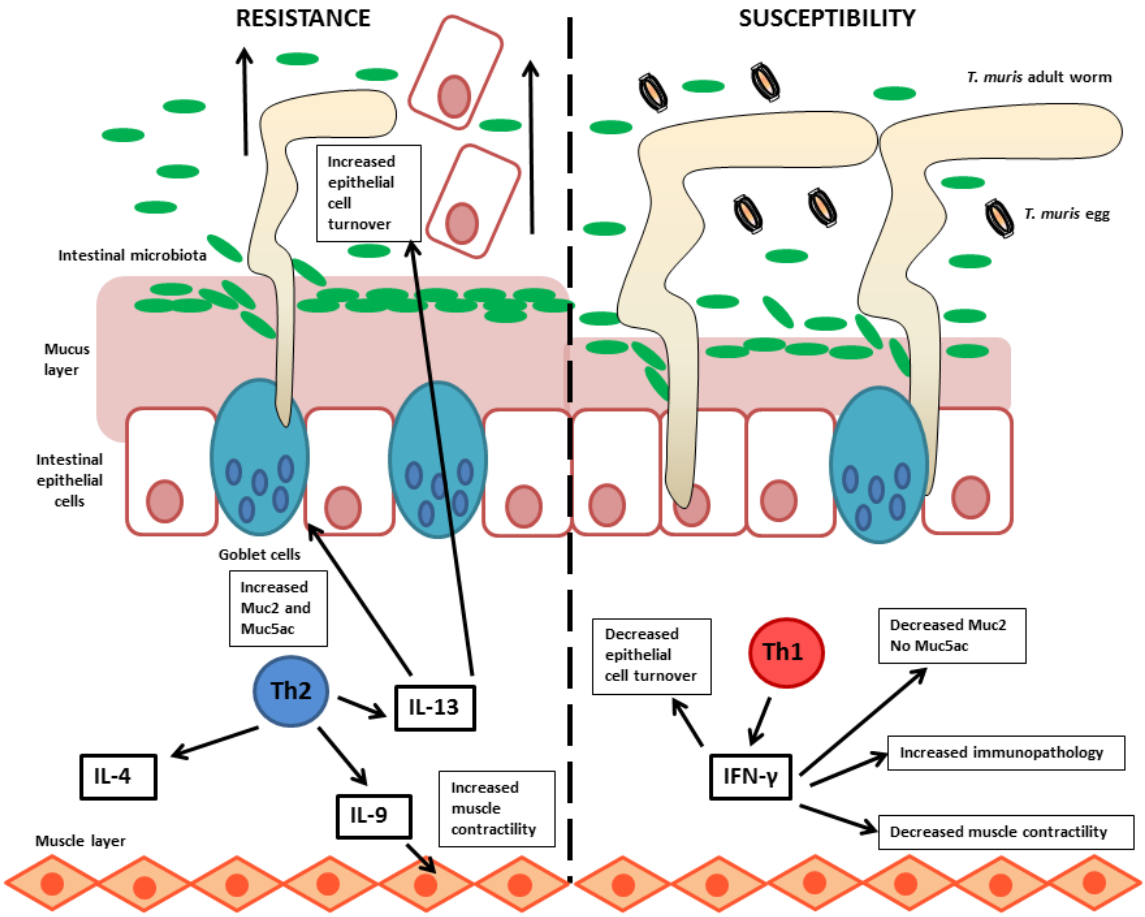

Figure 1.8 Immune responses generated against *Trichuris muris* in resistant and susceptible hosts. With the resistant phenotype, a Th2 response is induced characterised by the cytokines IL-4, IL-13 and IL-9. Increased epithelial cell turnover and increased production of Muc2 and Muc5ac is controlled by IL-13. These effector mechanisms act to displace the parasites from the intestinal epithelium, together with increased muscle hypercontractility controlled by IL-9. On the other hand, susceptibility is caused by a Th1 response where effector mechanisms are dampened due to IFN-γ production.

1.6.3.1. The Th1 response

Susceptibility is associated with Th1 responses including the production of IFN-γ, as well as IL-12 and IL-18, at high levels (Fig. 1.8). Decreasing levels of these cytokines leads to a switch from susceptible to a resistant phenotype (Cliffe and Grencis, 2004). IL-18 depletes levels of Th2 cytokines, IL-4 and IL-13, suggesting it can directly down regulate Th2 responses and promote Th1 (Helmby *et al.,* 2001). It has been suggested that *T. muris* can potentiate Th1 responses by producing an IFN-γ like molecule to prevent expulsion and benefit its own survival within the host (Grencis and Entwistle, 1997). Host gender has also been shown to influence susceptibility to infection. Studies using male and female BALB/c IL-4 KO mice demonstrated that males succumb to chronic infection, whereas females can mount a resistant Th2 response. Administration of soluble IL-13 receptors (which block IL-13 activity) to female mice caused them to revert to a susceptible phenotype. This is thought to be due to female hormones promoting a Th2 response, suggesting that IL-13 is responsible for parasite clearance in BALB/c IL-4 KO mice (Bancroft *et al.,* 2000). Genetic background influences susceptibility to *T. muris* infection with different outbred and inbred strains of mouse varying in their ability to expel the parasite. For example, AKR mice mount a Th1 response to a high dose challenge leading to chronic infection, whereas BALB/c and C57BL/6 mice generate a resistant Th2 response triggering several effector mechanisms enabling worm expulsion (Cliffe and Grencis, 2004). Infective dose can also affect resistance as low dose infections, i.e. less than 20 eggs, in usually resistant mice generate a Th1 susceptible response and parasites are not expelled (Bancroft *et al.,* 1994). However, high doses in this background are expelled.

1.6.3.2. The Th2 response

The resistant phenotype is typified by a Th2 response (Fig. 1.8). This is shown in BALB/c mice, which have a resistant genetic background and can clear high dose infections by day 20 p.i. Resistance is associated with Th2-type cytokines; IL-4, IL-13 and IL-9. Both IL-4 and IL-13 play key roles in the expulsion of worms, as mice lacking these cytokines fail to mount an effective immune response against infection (Cliffe and Grencis, 2004). Studies have also indicated a function for IL-9 during early infection, as adoptive transfer of IL-9 producing T cells to mice with a susceptible phenotype causes greater worm expulsion (Faulkner *et al.,* 1998). Recently, other cytokines have been implicated in facilitating the development of a protective immune response during early infection. IL-25 and IL-33 can stimulate innate lymphoid cells to produce Th2-type cytokines aiding worm expulsion (Humphreys *et al.,* 2008; Saenz *et al.,* 2010).

Th2 cytokines mediate worm expulsion through the induction of several effector mechanisms shown in figure 1.8. Chronically infected mice show crypt cell hyperplasia, known to be controlled by Th1 cytokines, such as IFN-γ (Cliffe *et al.,* 2007). However, this is not seen in the intestinal tracts of resistant mice as the Th2 cytokine IL-13 activates an increased rate of epithelial cell turnover. However, increasing IFN-γ and CXCL10 causes decreased epithelial cell turnover. Known as the 'epithelial escalator', this mechanism involves the proliferation and movement of epithelial cells from the bottom of the crypt where the larval forms of *T. muris* burrow, encouraging worm expulsion into the lumen. This is only effective up to day 14 p.i. when *T. muris* are present at the bottom of epithelial crypts. After this, the parasite undergoes two more moults whilst moving up the crypt axis and the 'epithelial escalator' is no longer effective at facilitating worm expulsion (Cliffe *et al.,* 2005). This expulsion mechanism has recently been shown to be influenced by the lysine methyltransferase, SETD7. Mice lacking the SETD7 gene are more resistant to infection with *T. muris* due to altered epithelial cell turnover, and this occurs independently of the host adaptive immune system (Oudhoff *et al.,* 2016).

During infection, goblet cell hyperplasia is observed in both resistant and susceptible mice (Artis *et al.,* 2004; Klementowicz *et al.,* 2012). However, the mucins produced by goblet cells vary between these two phenotypes. An up-regulation of Muc2 is detected and Muc5ac, a mucin normally present in airways and stomach, is seen in the intestine of resistant mice prior to worm expulsion (Hasnain et al. 2011). IL-13 can enhance the expression of Muc5ac causing mucus to thicken, possibly hindering parasite attachment. Mice deficient in these two mucins show delayed or inhibited parasite expulsion even with a strong Th2 response (Hasnain *et al.,* 2011; Hasnain *et al.,* 2011a).

In addition, increased muscle contractility within the intestinal tract mediated by IL-9 is thought to be a further effector mechanism to promote worm expulsion. Indeed, blocking IL-9 causes decreased smooth muscle contractility and a lack of worm expulsion (Khan *et al.,* 2003). Therefore, these Th2 effector mechanisms create a hostile environment through the generation of inflammatory responses in the intestine that damage the parasite and force it from its niche.

1.6.3.3. B cells and antibodies

The role of other immune cells in resistance, such as B cells, has also been studied. Different classes of parasite-specific antibody have been detected in resistant and susceptible mice with increased IgG1 and IgG2a, respectively (Koyama and Ito, 2000). Mice lacking B cells, μMT mice, are susceptible to *T. muris* infection suggesting a role for B cells and antibody in worm expulsion (Blackwell and Else,

2001). However SCID mice, which lack B and T cells, transferred with CD4+ T cells can successfully expel worms without the need for B cells, questioning the importance of these cells for resistance (Else and Grencis, 1996).

1.6.3.4. Immune regulation

Chronic infections generate considerable immunopathology as a result of strong Th1 responses. In order to prevent overt pathology, the host immune system can modulate parasite-induced pathology using various host regulatory molecules. IL-10 is thought to modulate pathogenesis with an important role in promoting Th2 responses and maintaining the intestinal mucosal barrier. Mice that lack this cytokine are susceptible to infection and develop fatal intestinal pathology, but those treated with broad-spectrum antibiotics show enhanced survival suggesting a role for IL-10 in the prevention of opportunistic bacterial infections that can contribute to increased mortality (Schopf *et al.,* 2002).

Foxp3+ Treg cells are known to limit inflammation and regulate immune responses, and would therefore be beneficial during parasite infection. However, during *T. muris* infection there is a significant decrease in the proportion of Foxp3+ Treg cells in the intestinal tract (Holm *et al.,* 2015; Houlden *et al.,* 2015). Other studies have shown that Foxp3+ Tregs do not play a key role in the expulsion of worms as depletion or adoptive transfer of cells did not impact worm burden (Worthington *et al.,* 2013). Reduction in Treg cell numbers can promote a stronger Th2 response since Treg cells limit expansion of this T cell subset, although this has varying consequences for the host depending on the time post infection (Tian *et al.,* 2011; Sawant *et al.,* 2014). Conversely, different laboratory isolates of *T. muris* can induce different Treg cell responses. Infection with the S (Sobreda) isolate causes an increase in Foxp3+ Tregs in the intestine, compared to the E (Edinburgh) isolate which is more commonly used. Altering the function or abundance of these cells causes an increase in intestinal pathology suggesting that the S isolate can induce Tregs to dampen inflammation and promote its own survival (D'Elia *et al.,* 2009).

1.6.3.5. Innate lymphoid cells

Certain innate cell populations can produce Th2 cytokines in response to IL-25 and IL-33, and therefore promote protective responses early in infection. This includes type 2 ILCs (ILC2s), which can produce IL-13 and can be found in the intestine. Consequently, mice that cannot produce IL-25 are susceptible to infection due to reduced Th2 responses and altered mucin production. Addition of these cells reverses this phenotype and promotes a resistant Th2 response, resulting in a decreased worm burden (Saenz *et al.,* 2010; Grencis *et al.,* 2014). IL-13 producing ILC2s have

been shown to expand under conditions where vitamin A is lacking, consequently promoting a resistant phenotype. These cells maintain function and IL-13 production during micronutrient deficiency and *T. muris* infection, conditions commonly seen together in humans, by instead using fatty acid metabolism as their primary energy source (Wilhelm *et al.,* 2016; Spencer *et al.,* 2014). As a result, these cells can respond to changes in nutrients to protect the intestinal barrier.

1.7. Interplay between the intestinal microbiota and macrofauna

The intestinal microbiota and macrofauna (parasites) have evolved together over millions of years with their host, aiding development and maturation of the immune system. However, there is a distinct lack of parasitic disease in the developed world, which has coincided with an increase in allergy and autoimmune disease (Bancroft *et al.,* 2012). This is thought to be related to the 'hygiene hypothesis' where bacterial antigens, and now parasitic helminth infection, during childhood can direct immune responses to tolerate environmental antigens (Wold, 1998). For instance, parasitic worms induce IgE production in the intestinal tract to promote tolerance to environmental antigens and the intestinal microbiota (Fumagalli *et al.,* 2009; Clemente *et al.,* 2012).

The growth and pathogenesis of certain intestinal parasites within the mammalian intestinal tract are affected by the host microbiota. This is seen with the parasite, *Entamoeba histolytica*, which resides in the large intestine and depends on the intestinal microbiota to cause symptomatic infections (Phillips and Wolfe, 1959). Interactions between the parasite and pathogenic strains of *Escherichia coli* and *Shigella dysenteriae* occur via a surface lectin on *E. histolytica* and this promotes growth and virulence by altering parasite gene expression (Mendoza-Macías *et al.,* 2009; Galván-Moroyoqui *et al.,* 2008; Padilla-Vaca *et al.,* 1999). *Giardia*, an extracellular protozoan parasite known to colonise the small intestine, grows slower in the presence of *Lactobacilli in vitro* and treatment of animal models with these bacteria as a probiotic reduces the severity and duration of infection (Pérez *et al.,* 2001; Goyal & Shukla 2013; Humen *et al.,* 2005). However, *Giardia* also interacts with certain members of the intestinal microbiota promoting their ability to become opportunistic pathogens via altered bacterial gene expression (Gerbaba *et al.,* 2015). Parasite infection is also accompanied by increased bacterial growth, mucosal adherence and infiltration after tight junction damage (Chen *et al.,* 2013). This highlights the varied host-microbe-parasite interactions that can occur within the intestinal tract and that organisms should not be studied in isolation, but together with their surrounding ecosystem.

Recent studies have shown that infection with GI nematodes can cause significant alterations to the host intestinal microbiota. *Heligomosomoides polygyrus*, a small intestinal murine roundworm, causes changes to the ileal microbiota and increases bacterial abundance (Walk *et al.,* 2010). This is accompanied by an increase in *Lactobacillaceae* species in the small intestine and an outgrowth of *Enterobacteria* and *Clostridiales* in the caecum independently of the IL-4/-13 – Signal transducer and activator of transcription 6 (STAT6) signalling axis (Reynolds *et al.,* 2014; Rausch *et al.,* 2013; Zaiss *et al.,* 2015). The increase in *Lactobacilli* is linked to a greater susceptibility to infection, with greater parasite load and an enrichment of Foxp3+ Treg cells. Addition of these bacteria to the drinking water of resistant animals increases Treg cell numbers and parasite burden, demonstrating the parasite's ability to manipulate its environment to promote and sustain infection within its host (Reynolds *et al.,* 2014). Furthermore, the microbiota alterations caused by *H. polygyrus* infection resulted in changes to the concentrations of SCFAs in the caecum. Since the parasite infects the small intestine, these effects are not local. Consequent increases in caecal butyrate concentrations reduced allergic asthma via the SCFA receptor, GPR41, indicating that helminth infection and its impact on the intestinal microbiota can have far reaching consequences for host health (Zaiss *et al.,* 2015).

1.8. Bacterial colonisation of nematodes

As with mammalian hosts, smaller organisms, such as nematodes, can also harbour single bacterial endosymbionts or more complex microbiotas. One of the most noted examples of endosymbiosis, where both organisms benefit, is between filarial worms and the intracellular bacterial genus *Wolbachia*. Filarial nematodes such as *Brugia malayi*, responsible for lymphatic filariasis, rely on *Wolbachia* for normal development and long term survival within the host, as treatment with antibiotics hinders larval and embryonic development (reviewed by Taylor *et al.,* 2005). This has led to the use of antibiotics as an effective way to treat filarial disease in human patients, with the potential to treat other parasitic diseases using this strategy (Taylor, Makunde, *et al.,* 2005). Furthermore, genome analysis of this endosymbiont has shown that *Wolbachia* harbours genes and metabolic pathways that are lacking in its host, indicating that these bacteria provide metabolites promoting the mutualistic relationship (Foster *et al.,* 2005).

Some nematodes use bacteria as a food source and are consequently associated with diverse communities within their intestinal tracts. The majority of this research has so far focussed on environmental free-living or parasitic nematodes and their

microbiotas. *Pristionchus* species are often found in association with beetles and harbour a diverse intestinal microbiota, that is mostly dominated by Proteobacteria (Rae *et al.,* 2008). Certain bacteria derived from their natural habitats can impact nematode reproduction and survival, and these worms have developed strategies to discriminate and avoid these detrimental species (Rae *et al.,* 2008). Another free-living nematode, *Acrobeloides maximus*, which also feeds on bacteria, is associated with a conserved microbiota that is also enriched for Proteobacteria. The authors suggest that this relationship is mutualistic so that the nematode benefits from colonisation resistance against potential pathogens, and also assistance for the breakdown of other ingested bacteria (Baquiran *et al.,* 2013).

Caenorhabditis elegans is a model organism for many areas of research and is traditionally used as an axenic culture (bacteria free) or as a monoxenic culture with a single laboratory strain of *E. coli*. In its natural environment, *C. elegans* is free-living soil nematode and can be found living in decaying matter; habitats rich in bacteria. Recent work has characterised the microbiota associated with this bacterivore when isolated from soil. *C. elegans* worms select for a diverse core microbiota enriched for Proteobacterial families, specifically the *Enterobacteriaceae* and *Pseudomonadaceae*, and this is distinct to the soil microbiota they are recovered from (Berg *et al.,* 2016; Dirksen *et al.,* 2016). This microbiota is functionally important and promotes population growth under stressful conditions, such as high temperature and variable osmolarity, and certain members can inhibit growth of fungal and bacterial pathogens (Dirksen *et al.,* 2016; Montalvo-Katz *et al.,* 2013). Further studies have identified specific bacteria that can promote *C. elegans* viability, for example*, Lactobacilli* can extend the lifespan of worms by increasing resistance to oxidative stress (Nakagawa *et al.,* 2016). Furthermore, infection with the pathogen *Bacillus nematocida* B16, which is lethal to *C. elegans*, can induce changes to the worm microbiota, indicating that the worm microbiota is influenced by infection as mammalian microbiotas are (Niu *et al.,* 2016).

The potential microbiotas associated with pathogenic nematodes that can infect a mammalian host have not been fully investigated. Analysis has been performed on *H. polygyrus* L3 larvae and adult worms, although surface sterilisation was not undertaken. As a result, the bacterial communities identified are likely to contain adherent bacteria and may explain why the adult worm microbiotas isolated are very similar to its ileal environment. However, L3 larvae presented a unique microbiota that is distinct from its host, although these worms were not isolated from the intestinal tract but were instead cultured on plates prior to infection (Walk *et al.,* 2010). Further work is needed to properly characterise the internal microbiota of this parasite but

demonstrates the potential presence of a diverse microbiota within pathogenic organisms.

1.9. *T. muris* and the host intestinal microbiota

As previously mentioned, *T. muris* relies on components of the host intestinal microbiota to trigger hatching and initiate infection in the caecum and colon of infected mice (Hayes *et al.,* 2010). Larval stages consequently burrow into the intestinal epithelia causing a breach of the mucosal barrier, allowing bacteria access to the underlying host immune cells (Bancroft *et al.,* 2012). The parasite is therefore in intimate association with the surrounding bacterial communities that share the same intestinal niche.

Recent studies have shown that infection with *Trichuris* species causes alterations to the intestinal microbiota of a range of mammalian hosts. Studies using the pig whipworm, *T. suis*, identified significant changes in the proximal colon microbiota of infected pigs. These alterations are worm burden dependent and specifically impact the abundance of Proteobacteria and Deferribacteres at day 21 p.i. This consequently affects the metabolic potential of the intestinal microbiota so that carbohydrate metabolism and lysine biosynthesis are reduced (Li *et al.,* 2012; Wu *et al.,* 2012). This indicates that the microbiota of infected individuals is impaired in its ability to breakdown dietary carbohydrates and this may be of benefit to the worm. Increasing fermentable carbohydrates in the diet of *T. suis*-infected pigs has been shown to cause early expulsion and reduced growth of established worms in the intestinal tract (Thomsen *et al.,* 2005). Similarly, significant alterations to the intestinal microbiotas of *T. muris* infected C57BL/6 mice also impacts the metabolites detected within stool samples. These microbiota changes are characterised by a decrease in bacterial diversity, decreases in *Prevotella* and *Parabacteroides* and an increase in the abundance of *Lactobacilli* (Holm *et al.,* 2015; Houlden *et al.,* 2015). In agreement with the data shown in pigs, *T. muris* infection reduces the amount of dietary carbohydrate breakdown products detected in the large intestine, indicating that the ability of the microbiota to breakdown these nutrients is impaired (Houlden *et al.,* 2015). Further to this, infection results in a reduction of Foxp3+ Tregs in the intestine, contrary to what has been described with other helminth infections (Holm *et al.,* 2015; Houlden *et al.,* 2015). Together, these changes may be induced by *Trichuris* species in order to manipulate the intestinal environment, alter metabolite levels and modulate the host immune system facilitating persistence in infected individuals.

Studies looking at the impact of helminth infection on the human intestinal microbiota have produced varying results. *T. trichiura* infection has been shown to cause no change to the host intestinal microbiota, whereas another study presented conflicting

results where infection significantly increased bacterial diversity and altered the bacterial abundance of specific genera (Cooper *et al.,* 2013; Lee *et al.,* 2014). These differences are likely to be due to numerous variables commonly associated with human studies, for example, differences in diet, worm burden, the presence of multiple helminth infections and other microbial infections, genetics and sample processing. The results from these studies must therefore be approached with caution as specific effects of a certain helminth species will not be easy to dissect. However, they do present data demonstrating the impact of multiple helminths on the host intestinal microbiota in natural infections.

It is clear that *Trichuris* species have the ability to manipulate their host and local intestinal environment to promote their survival. As a result, these worms could be used to treat intestinal inflammatory disorders and this is in part controlled by the host intestinal microbiota. As previously described, IBD causes dysbiosis and a similar disease, idiopathic chronic diarrhoea (ICD), can be used as a model in macaques. Infection with *T. trichiura* reduced symptoms associated with ICD and promoted an increase in microbiota diversity and a decrease in the attachment of bacteria to the intestinal mucosa, restoring it nearer to 'healthy' levels (Broadhurst *et al.,* 2012). Mice deficient in the gene encoding NOD2 are also used as a model for studying IBD, and colonisation with *Bacteroides vulgatus* induced further inflammation and intestinal abnormalities. However, infection with *T. muris* reduced these symptoms through a shift in the abundance of specific bacteria. In particular, a decrease in *B. vulgatus* and an increase in the *Clostridiales*. The expansion of these bacteria is associated with an increased Th2 response after helminth infection, and they are thought to protect against inflammation and act as 'defensive symbionts' (Ramanan *et al.,* 2016).

In summary, it is evident that there are intimate associations between nematodes and bacterial communities throughout nature. This includes the bacteria that reside in the external environment and also within worms as an endosymbiont or microbiota. These relationships are of particular interest in parasitic organisms and their potential importance for pathogenesis. The intimate association between *Trichuris* species and the host microbiota that share the same intestinal niche has consequences for the host, parasite and microbiota. However, these consequences have not been fully investigated.

1.10. Aims and objectives

The aim of this study is to gain a greater understanding of the relationship between the mouse whipworm, *T. muris*, and the intestinal microbiota of its host. Further to this, the study will focus on the internal microbiota of *T. muris* for the first time and the

consequences this has for the parasite and its host. These aims will be achieved by the following objectives;

1. To investigate the impact of worm burden and the host adaptive immune system on *T. muris*-induced alterations to the host microbiota, using high and low dose infections in C57BL/6 and immunodeficient (SCID) mice.
2. To determine the impact of infection on caecal SCFA concentrations.
3. To characterise the internal microbiota of adult *T. muris* and its relationship to its host's intestinal microbiota using molecular methods including DGGE, qPCR and FISH.
4. To determine the importance of the *T. muris* microbiota for parasite viability *in vitro* and *in vivo* using germ-free mice.

Chapter 2

Materials and methods

2.1 Bacterial strains, media and growth conditions

Escherichia coli strain PK1162 (Hayes *et al.,* 2010), with green fluorescent protein (*gfp*) encoded on the chromosome, was routinely grown overnight in Luria-Bertani (LB) broth (containing 1% tryptone (w/v), 0.5% yeast extract (w/v) and 1% NaCl (w/v)) at 37°C and shaking at 200 revolutions per minute (rpm). For growth on plates, 1.5% agar (w/v) was added. For faecal sampling of germ free (GF) mice, 3% (w/v) tryptone soya broth (TSB) with an additional 1.5% agar was used.

2.2 Reagents

Chemicals and primer oligonucleotides were purchased from Sigma unless stated otherwise. For sterilisation of chemicals, either autoclaving (121°C and 15 psi for 20 min) or filter sterilisation using 0.22 µm filters (Millipore) was used. Tissue culture media, including RPMI 1640 + L-glutamine, and antibiotics were purchased from Invitrogen unless otherwise stated.

2.3 Animals

2.3.1 Strains and maintenance

Male C57BL/6, AKR (Harlan Olac, UK) and female or male C.B17 SCID and Rag2 KO mice (homebred) were housed in ventilated cages in the University of Manchester animal facilities. Mice were housed in groups of 5 with diagnostic ear punches to identify individuals. For each experiment, mice were from the same batch to control for between batch differences in the murine intestinal microbiota. Mice were housed in the facility for 2 weeks prior to an experiment's start date to allow acclimatisation to new conditions, and kept at 22°C ± 1°C, 65% humidity with a 12 h light-dark cycle and had free access to food and water. All animal procedures were performed under the regulations of the Home Office Scientific Procedures Act (1986).

GF C57BL/6 mice were housed in the Manchester Gnotobiotic Facility (MGF) in the University of Manchester animal facilities. Health status of GF animals was confirmed when euthanising animals, using faecal pellets collected from the lower digestive tract under aseptic conditions. Faecal pellets were also collected from control specific pathogen free (SPF) animals and incubated in 500 µl sterile PBS at 4°C for 2 h. After vortexing tubes well, 100 µl of each sample was plated onto TSB agar plates and incubated for 18 h at 37°C, 0% CO_2. In all experiments, mice were infected at 6-8 weeks old by oral gavage and euthanised in accordance with Home Office regulations.

2.3.2 Administration of treatments

To prevent expulsion of a high dose *Trichuris* infection in C57BL/6 mice, 0.3 µg of recombinant IL-12 (rIL-12; Peprotech, USA) was given in 0.2 ml sterile PBS per mouse. This was administered by intraperitoneal (i.p.) injection on day 7, 9, 12, 14 and 16 p.i. (Bancroft *et al.,* 1997).

For oral antibiotic treatment, a combination of metronidazole (10 mg/ml; Acros Organics), neomycin (10 mg/ml), ampicillin (10 mg/ml) and vancomycin (5 mg/ml) was made up in sterile H_2O and filter sterilised (Reikvam *et al.,* 2011). Infected mice (C57BL/6 or Rag2 KO) were treated every morning by oral gavage for 8 days when worms were at the L2 larval or adult stage. For i.p. treatment, metronidazole (5 mg/ml; Acros Organics), neomycin (3 mg/ml), ampicillin (2.5 mg/ml) and vancomycin (2 mg/ml) (veterinary guideline doses) was given in 0.2 ml H_2O every other day for 2 weeks when worms were at the L2 larval or adult stage. Mice were then sacrificed at the end of treatment or until worms had reached adulthood.

To clear worm infections, mebendazole treatment was given. A dose of 50 mg/kg was used per mouse in 0.2 ml by oral gavage. Efficacy of antihelmintic treatment was confirmed by negative faecal egg counts around 7 day post treatment (see 2.5.2), together with worm burdens at the end of the experiment.

2.4 Trichuris muris

2.4.1 Maintenance of parasite

For all experiments, the Edinburgh (E) strain of *Trichuris muris* was used. *T. muris* was maintained in susceptible mice (SCID) as a high dose infection (~ 200 embryonated eggs via oral gavage). At day 42 post infection (p.i.), the caecum and colon were removed and dissected longitudinally. After washing with PBS to remove caecal contents, the caecum and colon were placed in RPMI 1640 supplemented with 100 U/ml penicillin and 100 µg/ml streptomycin. Worms were carefully removed and placed in 4 ml media in a 6 well culture plate (Corning Inc, UK) for incubation at 37°C in 100% humidity for 4 h. Media was collected after this time for excretory/secretory (E/S) antigen preparation (as described in 2.4.2) and replaced with fresh media for overnight incubation, when it was collected the next day. The collected media was centrifuged at 2000 g for 10 min to pellet eggs. The supernatant was removed and used for E/S preparation and eggs were resuspended in ultra-pure distilled H_2O. After filtering the egg suspension with a 100 µm cell strainer (Fisher Scientific), eggs were stored in a tissue culture flask at RT in the dark. This allowed eggs to embryonate for 6-8 weeks before being stored at 4°C ready for use.

2.4.2 Excretory/secretory (E/S) antigen preparation

Media collected after 4 h and overnight incubation of adult *T. muris* was centrifuged at 2000 g for 30 min and dialysed into 5 L of PBS, which was changed 3 times over 24 h. The protein concentration was determined using a ND-1000 apparatus (NanoDrop). E/S was filter sterilised and stored in aliquots at -20°C. Overnight E/S was consequently used for antibody specific ELISA at 5 µg/ml (section 2.12).

2.4.3 Preparation of sterile eggs and larvae

For surface sterilisation, embryonated eggs in H_2O were pelleted by centrifugation at 13,000 g for 5 min. The supernatant was removed and 1 ml sterile H_2O was added to resuspend the eggs. In a 6 well culture plate, the eggs were added to an additional 3 ml sterile H_2O and 2 ml 96% v/v sodium hypochlorite for 5 min at 37°C, 5% CO_2 to remove any surface contaminants. Eggs were washed with RPMI 1640 twice and incubated in fresh media at 37°C, 5% CO_2.

To produce sterile L1 larvae, 2 ml embryonated eggs in H_2O were pelleted by centrifugation at 13,000 g for 5 min and resuspended in 1 ml sterile H_2O. In a 6 well culture plate, eggs were added to an additional 3 ml sterile H_2O and 2 ml 96% v/v sodium hypochlorite for 2 h at 37°C, 5% CO_2 to dissolve the two polar egg opercula. Eggs were washed with media twice and incubated in 4 ml media at 37°C, 5% CO_2 for 5 days until hatched. L1 larvae were maintained for several weeks by the removal of 500 µl media and replacement with fresh RPMI 1640 every 3 days.

2.4.4 Infection

For a high dose infection, ~200 embryonated eggs in 200 µl were given by oral gavage per mouse. Stock eggs were pelleted by centrifugation at 14,000 g for 5 min, the supernatant removed and the eggs resuspended in 15 ml H_2O. This aliquot of eggs was then diluted to the correct concentration of approximately 80 eggs per 50 µl H_2O. For a low dose infection, 20 embryonated eggs were individually counted under 5 x objective, selected and suspended in 200 µl H_2O for administration by oral gavage.

GF animals were infected with sterile eggs or L1 larvae, as described above in section 2.4.2, using sterile disposable 1 ml syringes (BD Plastipak) and sterile disposable plastic oral gavage needles under sterile conditions. A higher number of eggs and larvae (~500) were given to GF mice to account for poor hatching rates due to a lack of microbiota, and passage of L1 larvae through the stomach.

2.4.5 *In vitro* maintenance of adult *T. muris*

After removal from the intestinal tract, adult worms were washed in RPMI 1640 supplemented with 100 U/ml penicillin and 100 µg/ml streptomycin. Worms were transferred to a 6 well plate where each well contained 10-20 worms in 4 ml RPMI 1640 and plates were incubated at 37°C, 5% CO_2.

2.5 Sample collection

2.5.1 Quantification of worm burdens

The colon and caecum were removed and dissected longitudinally. Caecal contents were removed as described below (section 2.5.2) and remaining faeces were carefully washed out using RPMI 1640 supplemented with 100 U/ml penicillin and 100 µg/ml streptomycin. Adult worms and fourth stage larvae were removed individually, whereas other larval stages were removed by scraping the caecal tissue using curved tipped forceps. For isolation of live L2 larvae, caecum and colon were cut into small sections after washing and incubated with 0.9% w/v NaCl at 37ºC for 2 h, with occasional shaking every 20 min. The digested caecum and colon were then passed through a sieve, keeping the flow through containing L2 larvae in a petri dish for counting. All worms were counted under a binocular dissecting microscope (Leica, UK). Worms were kept in RPMI 1640 on a heat mat at 37°C until all worms had been counted. Worms were also frozen at -20°C for bacterial community analysis or fixed in 4% w/v paraformaldehyde (PFA) for 24 h at room temperature (RT) for histology. To quantify worm size, female worms were fixed and mounted onto glass microscope slides. Photos were taken using an upright confocal microscope at the same objective and the length of the worm posterior was measured in ImageJ.

2.5.2 Stool and caecal content collection

Stools were collected from naïve and infected mice weekly. Individual mice were placed into plastic beakers cleaned with 70% v/v EtOH and ~2 pellets per mouse were collected into 1.5 ml tubes. For caecal contents, the large intestine was removed and dissected longitudinally. The contents of the caecum were removed using sterile forceps and transferred into 1.5 ml tubes. All samples were stored at -20°C.

For faecal egg counts, stools were collected (~2 pellets per mouse), weighed and 1 ml H_2O was added. After vortexing well, 1 ml saturated NaCl (100 g NaCl in 280 ml H_2O) was added and vortexed again. A McMaster chamber was filled with 800 µl of the suspension and kept at RT until eggs were visible at the top of the chamber. Eggs were then counted

in the gridded sections and counts per gram of faeces were calculated with the following equation:

((volume of water + volume of salt + grams of faeces) / (grams of faeces x 0.15)) x mean eggs per chamber

For pH measurements using stool samples, ~0.05g stool pellets were added to 1 ml distilled H_2O and incubated at RT for 30 min. Samples were vortexed well and centrifuged at 16,000 g for 1 min. The resulting supernatant was then transferred to a 6 well plate and pH was measured using an Extech PH100 ExStik pH meter (Extech, USA). Each sample was measured three times and three samples were used per treatment or group.

2.5.3 Serum collection

Blood was collected post mortem using a plastic pipette. Blood was left to clot for 20 min at RT and spun at 16,000 g for 10 min. The serum was collected and stored at -20°C.

2.5.4 Gut tissue collection

Tissue for RNA extraction was taken prior to the dissection of the caecum and colon. Caecal tips (~5 mm tissue) were removed and placed in 1 ml TRIzol reagent (Life Technologies) for storage at -80°C. For histology, caecal tips were fixed in 10% neutral buffered formalin (NBF; 10% formaldehyde in PBS) overnight, and then stored in 70% EtOH until processing.

2.6 Histology

2.6.1 Histological processing

PFA-fixed worms were processed using a method described by Carleton *et al.,* (1980) with slight adaptations. Worms were cut into segments, re-fixed in PFA for 5 h before transfer to 70% v/v EtOH. Samples were then dehydrated through an EtOH gradient of 90% and 100% and kept in 100% EtOH overnight. Cedar wood oil was used as a clearing agent for 2 h and repeated 3 times. Residual cedar wood oil was removed by 15 min incubation in xylene (Fisher Scientific). Samples were then impregnated with V5 (RAL) wax (Fisher Scientific) for 30 min and 45 min at 60°C, followed by a further 45 min under vacuum.

For caecal tissue, NBF fixed samples were processed overnight using a Microm STP 120 Spin Tissue Processor (Fisher Scientific) using the programme shown below in Table 2.1. Processed material was embedded in wax blocks and cooled to -7°C using a Tissue-Tek® III Cryo Console (Sakura), before 5 µm sections were cut using a Microm HM325

microtome (Thermo Scientific). Sections were mounted on slides using warm sterile H_2O and dried overnight at 37°C. Sections were dewaxed twice in citroclear (TCS Biosciences) for 30 min and rehydrated through a decreasing EtOH gradient.

Step	Time
70% v/v EtOH	7 h
90% v/v EtOH	45 min
95% v/v EtOH	45 min
100% v/v EtOH	45 min (x 3)
Xylene	30 min (x 3)
Paraffin wax	1 h (x 2)

Table 2.1 Tissue processing protocol

2.6.2 Fluorescence *in situ* hybridisation (FISH)

To visualise the *T. muris* microbiota or host microbiota, the 16S rRNA probe EUB338 (5'-GCTGCCTCCCGTAGGAGT-3') was used for all FISH experiments. EUB338 was synthesised commercially and double labelled with the fluorophore Cy3 at both the 5' and 3' ends (excitation wavelength, 555 nm; emission wavelength, 570 nm). The complimentary sense sequence (NONEUB338; 5'-ACTCCTACGGGAGGCAGC-3') was used as a negative control probe and was also double labelled.

A positive control using an overnight culture of PK1162 was prepared by incubating with 100% v/v EtOH at a ratio of 1:1 for 3 h at RT, before being centrifuged at 14,000 g for 1 min. The remaining pellet was resuspended in 1% (w/v) PBS and 100% (v/v) EtOH at a 1:1 ratio.

Hybridisation was performed using 100 pmol/ml of Cy3 labelled probe in a probe buffer (30% v/v formamide, 0.9 M NaCl, 20 mM Tris/HCl (pH 7.4) and 0.1% w/v SDS) to cover sections. After incubation in a humid chamber at 46°C for 2 h, slides were washed in pre-warmed hybridisation buffer (0.9 M NaCl, 20 mM Tris/HCl (pH 7.4) and 0.1% w/v SDS) and incubated in the buffer for 15 min at 48°C. Slides were submerged in 4°C sterile H_2O for 2 s. Slides with caecal tip sections were subjected to a further incubation with DAPI (4′,6-diamidino-2-phenylindole) at 0.5 µg/ml in PBS for 20 min in the dark at RT. After washing with PBS, 0.1% w/v Sudan Black B (SBB) was prepared in 70% v/v EtOH and applied to all sections for 10 min at RT. Slides were then washed in PBS twice and immediately dried. Slides were mounted with mowiol mounting medium, sealed with coverslips and kept in the dark at 4°C until microscopy.

2.6.3 Fluorescence microscopy

Images were collected on an Olympus BX51 upright microscope using 60x or 100x objectives and captured using a Coolsnap ES camera (Photometrics) through Metavue Software (Molecular Devices). Specific band pass filter sets for Cy3, DAPI, *gfp* or brightfield were used to prevent bleed through from one channel to the next. Images were then processed and analysed using ImageJ (Abramoff *et al.,* 2004).

2.7 Bacterial community profiling

2.7.1 Sterilisation of *T. muris* adult worms

To remove external contaminants, adult *T. muris* worms were surface sterilised in 3% v/v sodium hypochlorite for 10 min followed by 5 washes in sterile H_2O. Sterility was confirmed by PCR on the final wash as described in section 2.7.3.

2.7.2 DNA extraction

2.7.2.1 *T. muris* and caecal content

DNA was extracted using methods previously described by Griffiths *et al.,* 2000 with some minor modifications. Briefly, samples were suspended in 500 µl BBCTAB buffer (120 mM K_2PO_4 buffer (pH 8.0); 5% hexadecyltrimethylammonium bromide (CTAB); 0.45 M NaCl) in a lysing matrix E-tube (Bio-101), followed by the addition of 500 µl of phenol-chloroform-isoamyl alcohol (25:24:1) (pH 8.0). Samples were homogenised by bead beating twice using a Fastprep^{TM} FP120 bead beating system (Bio-101) for 30 s at 5,500 rpm, with an ice step in between, to extract DNA. Cell debris was then pelleted by centrifugation (14,000 g) for 5 min at 4°C and the top aqueous layer collected and washed with chloroform-isoamyl alcohol (24:1). Samples were re-spun at 14,000 g for 5 min at 4°C. The top aqueous layer was collected and DNA precipitated using 2 volumes of 30% PEG (30% w/v polyethylene glycol 6000, 1.6 M NaCl) overnight at 4°C. After incubation, DNA was pelleted by centrifugation (14,000 g) at 4°C for 10 min. DNA was subjected to an ice cold 70% v/v EtOH wash and the remaining pellet allowed to air dry, before being resuspended in 50 µl H_2O for caecal contents or 20 µl for *T. muris*.

2.7.2.2 Stool samples

DNA was extracted from individual faecal pellets using the QIAmp Fast DNA Stool Mini Kit (Qiagen) following the manufacturer's instructions with some alterations. To each pellet, 1 ml InhibitEX buffer was added and vortexed until the stool was fully homogenised. Samples were incubated at 95°C for 30 min to lyse bacterial cells and separate inhibitory substances from DNA, followed by a brief vortex and centrifugation at 13,000 g for 1 min. To digest any proteins present, 30 µl Proteinase K was added to 400 µl supernatant and

400 µl buffer AL and vortexed. After incubation at 70°C for 10 min, 400 µl 100% EtOH was added to the solution and vortexed. The lysate was applied to the provided QIAmp spin columns, centrifuged for 1 min and the column was placed into a new collection tube. This was repeated until the total volume of lysate was loaded onto the column. The column was then washed with 500 µl of the first provided wash buffer (buffer AW1) and centrifuged for 1 min. This was repeated with the second wash buffer (buffer AW2) and centrifuged for 3 min. The provided eluting buffer (buffer ATE) was applied to the column at a volume of 100 µl for 5 min at RT. The column was then centrifuged to elute the DNA. DNA was stored at -20°C.

2.7.3 Polymerase chain reaction (PCR)

Reactions were carried out in 50 µl volumes made up with additional H_2O using the protocol listed in table 2.2 below in a Techne TC-4000 thermal cycler (Bibby Scientific). A negative control, where H_2O replaced the template DNA in the PCR reaction mix, was included for every PCR run to avoid the possibility of false-positive results, as well as a positive control using *E. coli* strain PK1162 genomic DNA to ensure the PCR worked. A full list of primers used for PCR in this study is given in Table 2.3.

Template DNA	1 µl		95°C	5 min
Primers (Sigma)	1 pmol	30 cycles	95°C	1 min denaturing
dNTP's (Bioline)	0.2 µM		55°C	2 min annealing
PCR + Mg buffer (Roche)	1 x		72°C	1 min extension
Bovine serum albumin (BSA) (New England Biolabs)	5 µg		72°C	10 min
Taq DNA Polymerase (Roche)	2.5 U		10°C	Hold

Table 2.2 PCR reaction mix and cycles used

2.7.4 Agarose gel electrophoresis

Agarose gel electrophoresis was performed as described by Sambrook & Russell (2001). Briefly, 1% (w/v) agarose in TAE buffer (0.5 M Tris. 5.7% acetic acid, 10 mM EDTA pH 8) was melted by heating in a microwave for 1 min on full power. Ethidium bromide (0.1 µg ml^{-1}) was added to the gel, which was then poured into an EPS 200 gel chamber (Pharma Biotech) and left to solidify with a comb placed at the top of the chamber. Samples were added to 5x DNA loading buffer (Bioline) to make a final 1x solution and loaded into the wells alongside Hyperladder I markers (Bioline) to indicate molecular weights. Samples

were electrophoresed at 110 V in TAE buffer for 40 min and visualised with an ultraviolet (UV) light transilluminator (UVItec UVIpro silver).

Primer name	Sequence (5' – 3')	Use	Reference
341F-GC	CGCCCGCCGCGCGCGGC GGGCGGGGCGGGGGCAC GGGGGGCCTACGGGAGG CAGCAG	Amplify 16S rRNA gene variable V3 region with 518R; contains GC clamp for DGGE.	(Muyzer *et al.,* 1993)
518R	ATTACCGCGGCTGCTGG	Amplify 16S rRNA gene variable V3 region with 341F-GC.	(Muyzer *et al.,* 1993)
27F	AGAGTTTGATCCTGGCTCA G	Amplify full length 16S rRNA gene with 1492R.	(Lane, 1991)
1369F	CGGTGAATACGTTCYCGG	Forward primer for qPCR with 1492R.	(Suzuki *et al.,* 2000)
1492R	GGTTACCTTGTTACGACTT	Amplify full length 16S rRNA gene with 27F. Reverse primer for qPCR with 1369F.	(Lane, 1991; Suzuki *et al.,* 2000)

Table 2.3 16S rRNA gene primers used within this study

2.7.5 Quantification of DNA

The concentration of DNA was measured by applying 1 µl of sample to a ND-1000 apparatus (NanoDrop). For more accurate readings, a Qubit Fluorometer and Qubit dsDNA HS Assay Kit (both Invitrogen) were used according to manufacturer's instructions. A working solution was prepared by diluting the Qubit reagent in the provided buffer (v/v, 1:200) so that there was 200 µl working solution per standard and sample. Standards were prepared by adding 190 µl of working solution to 10 µl of each provided standard. For samples, 199 µl of working solution was added to 1 µl of each sample. All tubes were vortexed and incubated at RT for 2 min. The concentration of DNA was then measured in the Qubit Fluorometer.

2.7.6 Purification of PCR products

PCR products were purified using a MinElute PCR Purification Kit (Qiagen) according to manufacturer's instructions. Briefly, the PCR products were mixed with the provided binding buffer (5:1) and applied to spin columns. After centrifugation (13,000 g, 1 min) to bind DNA fragments to the column membrane, the columns were washed with 750 µl ethanol-containing wash buffer and the DNA eluted in 20 µl H_2O.

2.7.7 Denaturing gradient gel electrophoresis (DGGE)

DGGE was used to separate PCR products of the amplified 16S rRNA gene, using primers 341F-GC and 518R, by their DNA denaturation point using a polyacrylamide gel with a linearly increasing gradient of DNA denaturants. This was performed using a DCode Universal Mutation Detection System (Bio-Rad) as previously described by Muyzer *et al*. 1993. Purified PCR products at a concentration of 150 ng were run down a 10% acrylamide gel (10% acrylamide (Fisher Scientific), 1% TAE) containing a gradient of 30% denaturant (12% deionised formamide, 2.1 M urea) and 70% denaturant (24% deionised formamide, 4.2 M urea) increasing in the direction of electrophoresis. An additional 0.09% ammonium persulphate and 0.009% N,N,N',N'-tetramethylethylenediamine (TEMED, Biorad) were added to polymerise the gel. Electrophoresis was performed at 60°C in a circulating tank (Biorad) in 1x TAE (40 mM Tris base, 20 mM sodium acetate, 1.0 mM EDTA (pH 7.4)) for 16 h at 63 V. The gels were stained with 20 ml 1x Sybr gold solution (Molecular Probes) for 30 min, washed with H_2O and destained for 10 min, before being viewed by UV transillumination (UVItec) and photographed.

2.7.8 DGGE analysis

Bacterial community profiles were analysed using PhoretixTM 1D Advanced Gel Analysis software (Ver. 11.2, Nonlinear Dynamics Ltd). This allowed bands of similar migration to be identified and a binary matrix of presence/absence to be created for sample comparison. RStudio (Ver. 0.97.312, RStudio, Inc) was used for non-metric multidimensional scaling (NMDS) using the Vegan and Ecodist packages. The binary matrix generated in PhoretixTM 1D software was used to calculate Bray-Curtis dissimilarity, to quantify the compositional differences between treatments/groups. The resulting dissimilarity matrix was plotted using NMDS, which substitutes the distance data with ranks so that pairwise dissimilarity between samples is presented in low dimensional space. Figures are plotted in arbitrary two dimensional space, with the axis representing a scale for Euclidian distance between samples centred on zero. Stress values indicated the quality of fit of the data, where values less than 0.2 are a good fit. RStudio was also used to perform a permutational ANOVA (PERMANOVA, Adonis function in RStudio), which

does not require any assumptions about the distribution of the data, on the dissimilarity matrix to calculate P values between groups. P values were adjusted to account for multiple comparisons using the p.adjust method, which is based on the Bonferroni correction method, in RStudio.

2.7.9 Quantitative PCR (qPCR) for absolute abundance

Bacterial abundance was determined by qPCR using the Applied Biosystems StepOnePlus Real-Time PCR System (Applied Biosystems) using the primers 1369F and 1492R listed in Table 2.3. For qPCR standards, DNA was extracted from an overnight culture of *E. coli* PK1162 as described in section 2.7.2.1. PCR was performed using primers 27F and 1492R as described in section 2.7.3. The consequent PCR products were purified with the MinElute PCR Purification kit (Qiagen), quantified with a Qubit (Invitrogen) and the copy number calculated:

$$((\text{template concentration (ng/µl)} \times 10^{-9}) / \text{Mw (daltons)}) \times 6.022 \times 10^{23} \text{ (Avogadro's constant)}$$

Serial dilutions were performed and 10^7 – 10^2 copies of DNA were used in triplicate for the standard curve. *T. muris* or caecal DNA was diluted to standardise qPCRs and a control PCR was performed with primers 27F and 1492R to ensure DNA was of sufficient quality. Each reaction contained 1 ng DNA, 0.2 µM forward primer, 0.2 µM reverse primer, 1 unit of SYBR Green Master Mix (Fisher Scientific) and H_2O in a final volume of 20 µl. The PCR programme is detailed in table 2.4 below. Each sample was run in triplicate and five different *T. muris* adults were used for each age group. Results were expressed as the total copy number of bacterial 16S rRNA genes per sample by multiplying by the total DNA concentration in each sample.

Initial denaturation (Holding stage)	95°C	20 s	
Denaturing	95°C	3 s	
Annealing	60°C	30 s	40 cycles
Read plate			
Melt curve	95°C	15 s	
	60°C (+ 0.3°C)	1 min	
	95°C	15 s	

Table 2.4 Cycling conditions for qPCR and melt curve analysis

2.7.10 Illumina 16S sequencing

2.7.10.1 Library preparation

gDNA extracted from caecal contents and stool samples was used to prepare libraries using the 16S metagenomic sequencing library preparation protocol provided by Illumina. Briefly, the V3 and V4 regions of the 16S rRNA gene were amplified using the protocol detailed in Table 2.5 and the following primers with overhang adapters attached to produce a fragment of ~550 b.p;

16S Amplicon PCR Forward Primer =
5'-TCGTCGGCAGCGTCAGATGTGTATAAGAGACAGCCTACGGGNGGCWGCAG-3'

16S Amplicon PCR Reverse Primer =
5'-GTCTCGTGGGCTCGGAGATGTGTATAAGAGACAGGACTACHVGGGTATCTAATCC-3'

Microbial DNA (5 ng/µl)	2.5 µl		95°C	5 min
Forward primer (1 µM)	5 µl		95°C	30 s denaturing
Reverse primer (1 µM)	5 µl		55°C	30 s annealing
2x KAPA HiFi HotStart ReadyMix (KAPA Biosystems)	12.5 µl	25 cycles	72°C	30 s extension
Total	25 µl		72°C	5 min
			4°C	Hold

Table 2.5 Amplicon PCR protocol

Resulting amplicons were purified to remove free primers and primer dimer species using AMPure XP beads (Beckman Coulter Genomics). Firstly, beads were vortexed for 30 s, 20 µl was added to each sample and then incubated for 5 min at RT. Samples were then placed on a magnetic stand (Dynal, Norway) for 2 min and the clear supernatant removed. To wash, 200 µl of freshly prepared 80% EtOH was added and incubated for 30 s on the magnetic stand. The supernatant was removed and a further wash step repeated. Excess EtOH was removed and the beads left to dry on the magnetic stand for 10 min. The beads were then resuspended in 52.5 µl 10 mM Tris pH 8.5 and incubated at RT for 5 min. The tubes were then placed on the magnetic stand for 2 min and 50 µl of the clear supernatant was transferred to a fresh tube for the next step of library preparation.

For pooling of different samples, an index PCR was performed to attach dual indices and Illumina sequencing adapters using the Nextera XT Index Kit (Illumina). The protocol is detailed in Table 2.6 and used 5 µl of DNA from the previous step resulting in a final library of ~ 630 b.p The purification step using AMPure XP beads was repeated using 56 µl of beads per sample. In the final step, beads were resuspended in 27.5 µl 10 mM Tris pH 8.5 and 20 µl of the cleared supernatant was transferred to a new tube.

DNA	5 µl		95°C	3 min
Nextera XT index primer 1	5 µl		95°C	30 s denaturing
Nextera XT index primer 2	5 µl		55°C	30 s annealing
2x KAPA HiFi HotStart ReadyMix	25 µl	8 cycles	72°C	30 s extension
PCR grade water (Fisher Scientific)	10 µl		72°C	5 min
Total	50 µl		4°C	Hold

Table 2.6 Index PCR protocol

The final libraries were quantified using a Qubit Fluorometer and Qubit dsDNA HS Assay Kit (both Invitrogen) as detailed in 2.4.5. DNA concentration in mM was calculated using the following equation:

$$\frac{\text{(concentration in ng/µl)}}{\text{(660 g/mol x 600)}} \times 10^6 = \text{concentration in nM}$$

The final libraries were diluted to 4 nM using 10 mM Tris pH 8.5. Libraries with unique indices were then pooled using 5 µl of each library.

2.7.10.2 Sequencing

Libraries were sent to Genomic Technologies at the University of Manchester for paired end MiSeq sequencing (Illumina). Briefly, 5 µl of pooled final DNA libraries were denatured using 5 µl 0.2 N NaOH, vortexed and centrifuged at 280 g for 1 min. To produce ssDNA, samples were incubated for 5 min at RT and then diluted with 990 µl pre-chilled hybridisation buffer (HT1; Illumina) to produce 20 pM denatured library in 1 mM NaOH. For loading, libraries were diluted to 4 pM and kept on ice until needed.

A PhiX library is included as a control for Illumina sequencing runs. To prepare, the PhiX library (Illumina) was denatured using 0.2 N NaCl and diluted from 10 nM to the same concentration as the amplicon library i.e. 4 pM. The PhiX control (30 µl) was then mixed with 570 µl of the amplicon library and heated at 96°C for 2 min to heat denature. The tubes were then inverted to mix and immediately placed in an ice-water bath for 5 min. The library was then loaded onto the MiSeq flow cell (Illumina) for sequencing.

2.7.10.3 Data analysis

Samples were separated based on their indices and sequences were paired generating a total of 5,503,328 paired-end reads. Sequences were then quality trimmed to q20 (quality score of 20), which determines the estimated probability that a base is incorrect in a sequence using the following equation: Q (quality score) = $-10\log_{10}(e)$, and a read length of 300 resulting in a total of 4,540,649 sequences. Samples were also chimera checked and samples with a cluster of less than 4 sequences were removed using scripts in

Quantitative Insights into Microbial Ecology (QIIME). Operational taxonomic units (OTUs) were picked at the 97% sequence similarity level and taxonomy identified using a 16S rRNA gene database (Greengenes database release Feb 2011; http://greengenes.lbl.gov) and QIIME open reference OTU picking scripts (Caporaso *et al.,* 2010). The resulting file was then rarefied to the lowest sequence depth of 56,450 sequences using QIIME to produce a rarefied OTU table (See appendix; Table A). Generation of rarefaction curves and analysis of Shannon diversity was performed in QIIME.

2.8 *In vitro* antibiotic treatment

To remove any surface contaminants, *T. muris* adults were washed in RPMI 1640 supplemented with 100 U/ml penicillin and 100 µg/ml streptomycin (all Invitrogen, UK) and L1 larvae were prepared as detailed in section 2.4.3. Worms were incubated in RPMI 1640, with or without antibiotics, in groups of 3 adult worms per well or ~50 L1 larvae per well, with 3 repeats for each. Antibiotics used and their final concentrations were as follows; metronidazole (0.5 mg/ml; Acros Organics), ampicillin (0.5 mg/ml), vancomycin (0.25 mg/ml) and neomycin (0.5 mg/ml). Motility was scored every 24 h until 96 h using a motility scale that has been previously described (Stepek *et al.,* 2006). Scoring ranged from 0 to 3; 0 = dead, 1 = very low motility only at one end, 2 = low motility that is less than controls, 3 = normal motility. L1 larvae were scored as % alive compared to controls every 24 h until 96 h.

2.9 *T. muris* and bacteria co-culture

Adult stage *T. muris* were incubated overnight in 4 ml RPMI 1640 and 1 ml of an overnight bacterial culture of *E. coli* PK1162 at 37°C, 5% CO_2. Worms were then washed in RPMI 1640 supplemented with 100 U/ml penicillin and 100 µg/ml streptomycin to remove external bacteria. *T. muris* were then fixed in 4% PFA overnight at 4°C and processed for FISH.

2.10 Genome analysis

The *T. muris* and *T. trichiura* genomes were annotated with functions and KEGG (Kyoto Encyclopaedia of Genes and Genomes; http://www.genome.jp/kegg/) pathway maps were reconstructed using KAAS (KEGG Automatic Annotation Server; http://www.genome.jp/keg/kaas/). Genomes were uploaded in multi-FASTA format and

compared with all organisms in KEGG. Pathways were then analysed for key missing pathways.

2.11 Quantification of short-chain fatty acids (SCFAs)

2.11.1 Sample preparation

Standards were prepared for each SCFA in 1ml H_2O in triplicate to create standard curves; 0.5 mM, 1 mM, 5 mM and 10 mM sodium butyrate (Acros Organics), sodium propionate and sodium acetate (both Fisher Scientific). Adult *T. muris* or L1 larvae were incubated in RPMI 1640 overnight and media samples were collected in 1 ml aliquots. Caecal contents were collected, 1 ml H_2O added and vortexed well. For controls, RPMI 1640 only and RPMI 1640 plus 5 mM SCFAs were prepared. To acidify the samples, 0.5% phosphoric acid was added to each sample, vortexed well and centrifuged at 16000 g for 1 min to pellet any debris. The supernatant (~1 ml) was then extracted with 0.9 ml ethyl acetate containing 0.1% sec-butylbenzene as the internal standard. Samples were vortexed well and centrifuged at 16000 g for 1 min. The top aqueous layer was removed, dried over $MgSO_4$ and filtered into an autosampler vial (Fisher Scientific) ready for analysis.

2.11.2 Gas chromatography-mass spectrometry (GC-MS)

The GC-MS system consisted of an Agilent Technologies 7890A GC fitted with a DB-WAX column (30 m; 0.32 mm; 0.25 µm film thickness; JW Scientific) and coupled to an Agilent 5977A mass selective detector (MSD). The injector temperature was 240°C with a split ratio of 10:1 and an injection volume of 1 µl. The carrier gas was helium with a flow rate of 1 ml/min and a pressure of 5.5 psi. The column temperature began at 40°C, increased to 80°C at 10°C/min, to 180°C at 15°C/min, and finally to 220°C at 20ºC/min with a hold for 2 min. Total time was 15.7 min and solvent delay was set to 3.5 min. The detector was operated in electron impact ionisation mode, scanning 30 – 250 *m/z* range. The temperature of the ion source was 230°C, quadrupole was 150°C and interface was 280°C. SCFAs were identified based on the retention time of standards (butyrate 9.5 min, acetate 8 min, propionate 8.5 min) and using NIST/EPA/NIH 11 mass spectral library. The mass spectra fragmentation patterns of unknown SCFAs were entered into the above library for identification.

2.12 Parasite specific IgG1 and IgG2a antibody ELISA

Overnight *T. muris* E/S was used to coat 96 well flat-bottomed plates (Immunlon4, Thermo Lifesciences, UK) at 5 µg/ml diluted in 0.05 M carbonate bicarbonate buffer (pH 9.6) using 50 µl per well. Plates were incubated overnight at 4°C and then washed 5 times with PBS-T (PBS, 0.05% w/v Tween 20) using a plate washer (SKAN Washer 400, Molecular Devices, USA). To block any non-specific binding, 100 µl blocking buffer (PBS-T, 3% bovine serum albumin (BSA)) was added to each well and plates were incubated for 1 h at RT then washed 5 times in PBS-T as before. Serum was serially diluted in PBS-T from a 1/20 to a 1/2560 dilution and 50 µl of diluted sera was added to each well, before incubating the plates for 90 min at RT. After washing with PBS-T 5 times, 50 µl/well of either biotinylated rat anti-mouse antibodies IgG1 (Serotec, UK) or IgG2a (BD Biosciences, Oxford, UK) diluted in PBS-T (1:500 or 1:1000, respectively) were added to the plates. Plates were incubated for 60 min at RT and then washed with PBS-T 5 times. Streptavidin-peroxidase (SA-POD, Roche Diagnostics Ltd, West Sussex, UK) was diluted in PBS-T (1:1000) and 75 µl/well was added for 1 h at RT. After another wash step, 100 µl/ well of ABTS substrate (10% 2,2-azino (3-ethyl benzthiazoline – 6-sulphuric acid) in 0.045 M citrate buffer) was added to the plates and left to develop in the dark at RT. The plates were read at 405 nm, with reference of 490 nm on a Dynex MRX11 microplate reader (Dynex Technologies).

2.13 Quantification of gene expression in caecal tissue

2.13.1 RNA extraction

Caecal tips in 1 ml TRIzol reagent (Life Technologies) were defrosted and transferred into Lysing Matrix D 2 ml tubes (MP Biomedicals). Samples were homogenised in a Fastprep FP120 bead beating system (Bio-101) 3 times for 30 s at 5,500 rpm, with an ice step in between, and incubated at RT for 5 min. To each sample, 0.2 ml of chloroform (Fisher Scientific) was added and tubes were shaken vigorously for 15 s, incubated for 2 min at RT and centrifuged at 12,000 g for 15 min at 4°C. The upper aqueous phase was transferred into a new RNase-free tube and mixed with 0.5 ml isopropanol (Fisher Scientific). After incubation at RT for 10 min, the samples were centrifuged at 12,000 g for 10 min at 4°C. The supernatant was removed and the remaining RNA pellet was washed with 1 ml 75% EtOH by vortexing briefly and centrifuging at 7500 g for 4 min at 4°C. This wash step was repeated and the RNA pellet allowed to air dry for 10 min at RT. The RNA pellet was resuspended in 20 µl RNase-free H_2O and incubated for 10 min at 55°C. The RNA quality was measured using a Nanodrop ND-1000 spectrophotometer at an absorbance of 260 nm to ensure 260/280 ratios were between 1.8 and 2.0. RNA quantity was calculated using the following equation:

$$RNA\ (\mu g\ ml^{-1}) = A_{260} \times 40$$

If the samples were not of sufficient quality, they were reprecipitated using 3 M sodium acetate (pH 5.2) and 2 volumes of 100% EtOH. After incubation at -80°C for 1 h, samples were centrifuged at 12,000 g for 20 min at 4°C and the supernatant removed. RNA pellets were resuspended in 20 µl RNase-free H_2O, incubated for 10 min at 55°C and re-quantified using a Nanodrop. Samples were stored at -80°C.

2.13.2 cDNA creation

RNA was reverse transcribed using the Quantitect Reverse Transcription Kit (Qiagen) according to the manufacturer's instructions. Briefly, 1 µg RNA was transferred to an RNase free microtube containing a final concentration of 1 x gDNA wipeout buffer and RNase free H_2O to a volume of 14 µl. Tubes were incubated for 2 min at 42°C then stored on ice. The total volume of the gDNA elimination reaction was then added to 1 µl Quantiscript reverse transcriptase, 1 x reverse transcription buffer and 1 µl primer mix in a total of 20 µl. Tubes were incubated at 42°C for 15 min followed by 3 min at 95°C. cDNA was quantified by measuring absorbance at 260 nm on a Nanodrop, then stored at -20°C until RT-PCR.

2.13.3 qPCR for relative gene expression

qRT-PCR was performed using the Applied Biosystems StepOnePlus Real-Time PCR System (Applied Biosystems) using the primers for host target genes listed in Table 2.7. Standard curves were created using a ten-fold dilution series of pooled cDNA to test the efficiency of each primer set (87 – 102%). β-actin was included as the reference gene to normalise data for differences in cDNA levels, as its expression is unchanged during Trichuris infection and is a well used reference gene in related studies (Forman *et al*., 2012). Each reaction contained 1 ng cDNA, 0.2 µM forward primer, 0.2 µM reverse primer, 1 unit of SYBR Green Master Mix (Fisher Scientific) and H_2O in a final volume of 20 µl. The PCR programme is detailed in table 2.4. Each sample was run in triplicate and there were five animals per experimental group. Technical replicates were initially averaged for each animal, and then an average was taken for each treatment group. No-RT (reverse transcription) controls were included (RNA only) for each sample to ensure there was no gDNA contamination. Results were calculated using the Pfaffl method, which takes into account variable primer efficiencies, to calculate the fold change in relative gene expression over naïve controls using the following equation, where R = relative gene expression, E = primer efficiency and Ct = Ct value:

$$R = \frac{(E_{target})^{\Delta Ct\ target\ (naive\ control - sample)}}{(E_{B-actin})^{\Delta Ct\ B-actin\ (naive\ control - sample)}}$$

Primer name	Sequence (5' – 3')	Reference
β actin-F	GTGGGCCGCTCTAGGCACCAA	(Forman *et al.,* 2012)
β actin-R	CTCTTTGATGTCACGCACGATTTC	(Forman *et al.,* 2012)
MCT1-F	CGCGAGACACACATAACGATAC	This study
MCT1-R	AAGGCTCCGACTAACACTGC	This study
SLC5A8-F	CTGCCGAGGTCTACCGTTTT	This study
SLC5A8-R	AGGATTGTGCCACAGAGACG	This study

Table 2.7 Primers for qRT-PCR using host caecal tissue

2.14 Statistics and graphing

Non-parametric multi-dimensional scaling (NMDS) statistical analysis of all sequencing and the community compositional analysis were undertaken in R statistical package. All graphs were produced and statistics performed using GraphPad Prism 6 software (GraphPad Software, Inc). An unpaired Mann-Whitney U test was used for comparisons between two groups with a 95% confidence interval where data was not normally distributed, unless otherwise stated. Where an ANOVA has been used, data was normally distributed. For Groups were considered significantly different if the P value was less than 0.05 (*) with further annotation if groups were <0.01 (**) and <0.001 (***).

Chapter 3

The impact of *T. muris* infection on the host intestinal microbiota

3.1 Introduction

Certain GI parasites can induce significant changes to the composition of the host intestinal microbiota. Several studies have shown that the nematode, *H. polygyrus*, that infects the small intestine can cause shifts in the microbiota locally in the ileum but also downstream in the caecum, away from the site of infection (Rausch *et al.,* 2013; Zaiss *et al.,* 2015). These changes are characterised by increases in *Lactobacillaceae* in the ileum, as well as increases in *Enterobacteriaceae* and *Bacteroides* in the caecum of wild type mice (Rausch *et al.,* 2013; Reynolds *et al.,* 2014; Walk *et al.,* 2010; Zaiss *et al.,* 2015). The increase in *Lactobacillaceae* has been associated with an increased Treg cell response and helminth colonisation, therefore promoting infection (Reynolds *et al.,* 2014). Furthermore, these infection-induced alterations to the microbiota have been shown to be independent of the IL-4/-13 – STAT6 pathway (Rausch *et al.,* 2013), which is important for Th2 driven worm expulsion.

The altered caecal microbiota of *H. polygyrus*-infected mice had an increased ability to produce SCFAs, specifically butyrate (Zaiss *et al.,* 2015). Butyrate is a product of bacterial fermentation and has critical importance in the mediation of intestinal homeostasis and inflammatory responses, inducing the differentiation of Treg cells (Furusawa *et al.,* 2013). Thus, the helminth-induced increase in butyrate was associated with reduced allergic inflammation in the lungs and an increased Treg population mediated by the SCFA receptor GPR41 (Zaiss *et al.,* 2015). Intestinal epithelial cells can also use this SCFA as an energy source, taking it up from the intestinal lumen via diffusion or by transporters such as monocarboxylate transporter 1 (MCT-1) and sodium-coupled monocarboxylate transporter 1 (SLC5A8), whose expression is induced by butyrate itself (Borthakur *et al.,* 2008; Miyauchi *et al.,* 2004; Thangaraju *et al.,* 2008; Thibault *et al.,* 2007).

Trichuris species can also cause significant restructuring of the intestinal bacterial communities in various mammalian hosts (Broadhurst *et al.,* 2012; Holm *et al.,* 2015; Houlden *et al.,* 2015; Li *et al.,* 2012; Wu *et al.,* 2012). Specifically, *T. muris* infection causes a significant reduction in bacterial diversity and also proportional changes in certain bacterial groups. These include a decrease in *Prevotella* and *Parabacteroides*, and an increase in the *Lactobacillaceae* and the Proteobacteria phylum (Holm *et al.,* 2015; Houlden *et al.,* 2015). These changes were accompanied by alterations to host immune responses, with significant decreases in the abundance of FoxP3+ CD4+ Treg cells in the lamina propria of the large intestine, and the metabolic capabilities of the intestinal microbiota (Holm *et al.,* 2015; Houlden *et al.,* 2015). Studies using the pig whipworm, *T. suis*, have shown significant worm burden dependent changes to the colonic microbiota, including an increased abundance of Proteobacteria, which is also seen in mice. This was

also accompanied by changes in the metabolic potential of the intestinal microbiota (Li *et al.,* 2012; Wu *et al.,* 2012).

So far murine microbiota studies have used low intensity *T. muris* infections. It is not known, however, if increasing *T. muris* numbers affects the compositional changes in the host microbiota, and if this caecal dwelling helminth can alter the concentrations of SCFAs locally in the intestinal tract. In addition, the cause of these microbiota changes is yet to be identified. Therefore, this study investigated the impact of *T. muris* worm burden on the composition of the host intestinal microbiota, and SCFA concentrations, in wild type and immunodeficient mice.

Aims

- To determine whether *T. muris* induced changes to the host intestinal microbiota are dose dependent.
- To investigate the impact of infection on SCFA concentrations in the caecum.
- To determine the involvement of the host adaptive immune system in host microbiota changes using immunodeficient SCID mice.
- To define the compositional changes that occur in the host intestinal microbiota during a high dose infection.

3.2 Results

3.2.1 *T. muris* induced changes to the host intestinal microbiota are dose and time dependent

It has previously been shown that chronic low dose infection with *T. muris* in C57BL/6 mice induces significant changes to the host intestinal microbiota. These changes occur from day 20 p.i. and become more distinct over time (Holm *et al.,* 2015; Houlden *et al.,* 2015). To determine the impact of worm burden, wild type (WT) C57BL/6 mice were infected with a high (~ 200) and a low (~ 20) dose of *T. muris* embryonated eggs. As C57BL/6 mice are naturally resistant to *T. muris* infections, recombinant interleukin-12 (rIL-12) can be administered to promote a Th1 response and therefore establish a chronic high-level infection (Bancroft *et al.,* 1997). rIL-12 was given by i.p. injection from day 7 p.i. for two weeks, every second day, to low (N = 4) and high dose (N = 4) infected mice, as well as a group of naïve animals (N = 4) to account for possible rIL-12 effects on the intestinal microbiota. A fourth naïve group was given PBS following the same treatment schedule as an additional control group (N = 4).

Stool samples were collected weekly from day 0 until the experiment was concluded at day 42 p.i., and worm burdens were also assessed at this point. Figure 3.1 shows that the rIL-12 treatment successfully allowed a high-level infection to reach chronicity in WT mice. However, the circled mouse in the high dose group had a worm burden of 6, reflecting the counts seen in the low dose infected group. This mouse is referred to as HD3 throughout this chapter.

For microbiota analysis, DNA was extracted from stool samples and analysed by 16S rRNA DGGE and NMDS. For each time point, shown as days post infection (d p.i.), samples were compared to day 0 as a baseline (Fig. 3.2). At days 7 and 14 p.i., all samples clustered together on the NMDS plot and there was no significant difference between any groups (Fig. 3.2B). However, in line with previous studies, by day 21 p.i. high dose samples began to show a different banding pattern by DGGE (Fig. 3.2A) and cluster away from all other groups on the NMDS plot, with HD3 clustering with naïve and low dose samples. By day 35 p.i., both low dose and high dose groups cluster separately and are significantly different from all naïve samples and each other ($P < 0.04$). At the final time point (day 42 p.i.), this was still true with HD3 clustered more towards naïve and low dose samples as expected. This also shows that there was no cage effect and that the intestinal microbiota associated with a high dose infection was not transferred between mice of the same cage during the course of the experiment. Furthermore, at no time point was there a significant difference between naïve PBS and rIL-12 treated mice indicating that rIL-12 does not cause changes to the host intestinal microbiota. This was also true for naïve samples and all day 0 samples, suggesting that bacterial communities associated

with naïve mice were fairly stable over time. Overall this indicates that infection with *T. muris* causes significant changes to the host intestinal microbiota in WT mice, and that this is both time and dose dependent, with higher worm burdens causing greater changes.

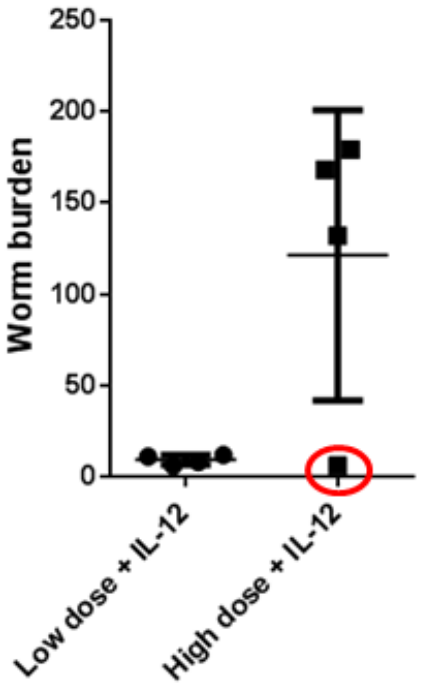

Figure 3.1 Worm burdens in C57BL/6 mice treated with rIL-12. Low dose mice were infected with ~20 embryonated *T. muris* eggs and high dose were given ~200 eggs via oral gavage. The numbers of adult worms in the large intestine were counted at day 42 p.i. Points represent individual mice and the circled point represents a mouse with a worm burden of 6 in the high dose group (HD3). Values represent mean +/- SEM.

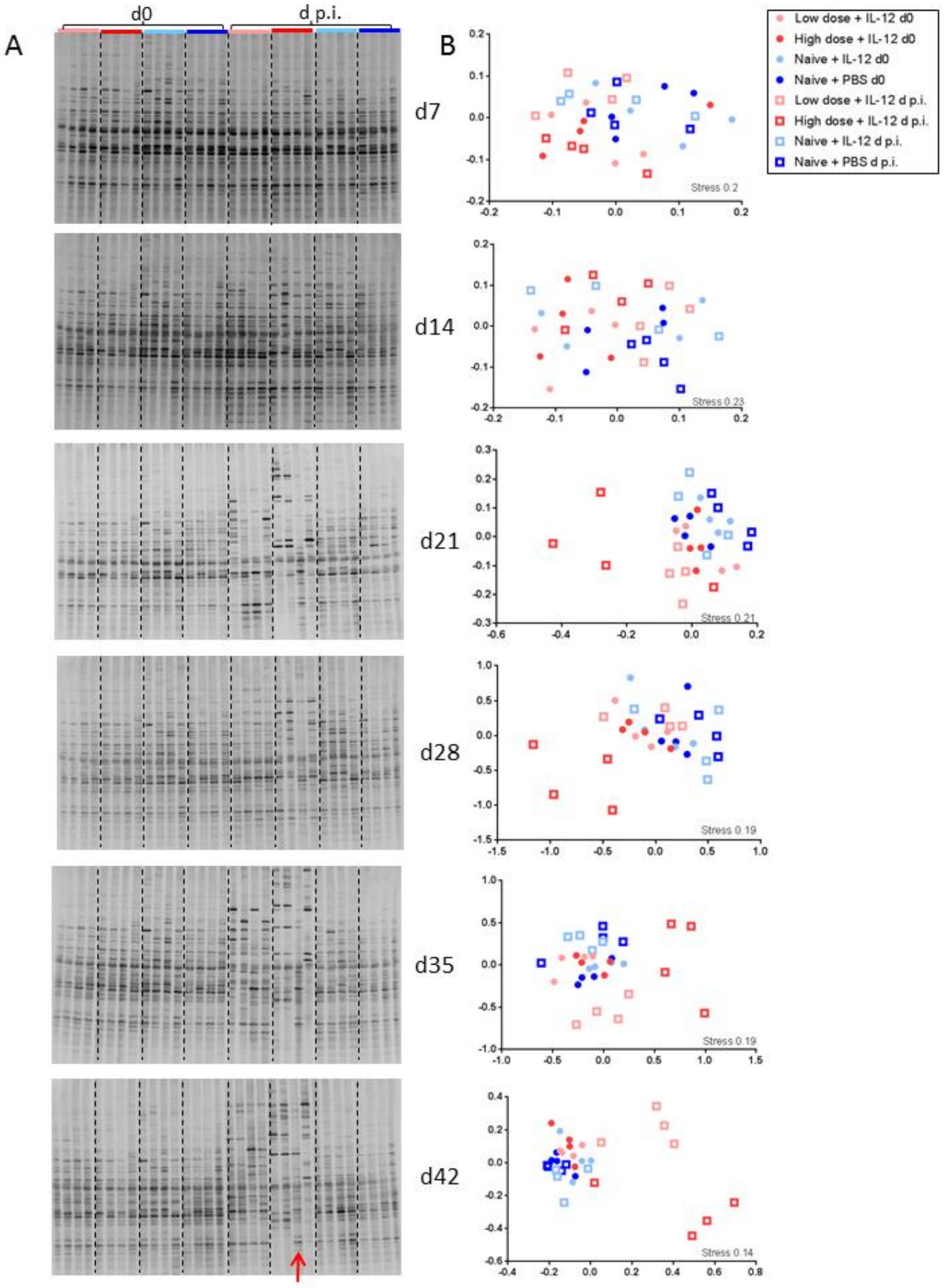
A
d0
d p.i.
B
d7
d14
d21
d28
d35
d42
Low dose + IL-12 d0
High dose + IL-12 d0
Naive + IL-12 d0
Naive + PBS d0
Low dose + IL-12 d p.i.
High dose + IL-12 d p.i.
Naive + IL-12 d p.i.
Naive + PBS d p.i.
Stress 0.2
Stress 0.23
Stress 0.21
Stress 0.19
Stress 0.19
Stress 0.14

Figure 3.2 DGGE and NMDS analysis of stool samples from C57BL/6 mice infected with a low (~ 20 eggs) or a high (~200 eggs) dose of *T. muris*, and naïve control mice, over time. Infected mice and one group of naïve mice were treated with rIL-12 for 2 weeks to ensure the high number of worms were not expelled. Stools were collected weekly; DNA was extracted and consequently used for 16S rRNA DGGE analysis. (**A**) DGGE analysis comparing the intestinal microbiota at day 0 (d0), which are technical replicates between gels for all day 0 groups and biological replicates within groups (N = 4 per group), and the intestinal microbiota days post infection (d p.i.), which ranges from day 7 (d7) to day 42 (d42) when the experiment ended, which includes biological replicates within groups only. The red arrow indicates the individual with a low dose worm burden in the high dose group (HD3). (**B**) The corresponding NMDS plots where each point represents an individual mouse with the axis scale for Euclidian distance between samples centred on zero. Stress indicates the quality of fit of the data (<0.2 is a good fit). P values were calculated by permutational ANOVA (PERMANOVA) on the NMDS distance matrix and corrected for multiple comparisons.

3.2.2 High dose infections induce significant changes to the composition of the host intestinal microbiota

To identify specific changes in the composition of the intestinal microbiota as a result of infection, day 42 p.i. stool samples from low dose, high dose and naïve IL-12 treated mice were subjected to 16S rRNA gene Illumina sequencing (N = 3 per group, excluding HD3). Libraries were constructed for samples 1, 2 and 4 from each group by amplifying the V3 and V4 regions of the 16S rRNA gene and attaching unique indices to each sample. This generated 2,747,421 paired-end reads, which was reduced to an average of 1,013,905 sequences per sample after low quality or short reads were removed. Sequences were clustered at 97% identity to produce operational taxonomic units (OTUs). Rarefaction curves showed that all samples were sequenced to an appropriate depth with all curves plateauing (Fig. 3.3). Furthermore, it is clear from figure 3.3 that naïve samples (blue) have a higher number of unique OTUs, compared to infected samples (pink). This indicates that infection with *T. muris* reduced the number of species present in the intestinal microbiota and that a higher worm burden reduced this further. Using Good's coverage estimate, the depth of sequencing was estimated for each sample with between 100 and 99.99% of OTUs sequenced. A rarefied OTU table was then created to the lowest sequencing depth (56,450 sequences) using Quantitative Insights into Microbial Ecology (QIIME) scripts (See table A, Appendices).

Using the rarefied OTU table, NMDS analysis was performed and each group clustered separately ($P < 0.05$; Fig. 3.4). Samples within groups did not cluster tightly indicating a level of variation between samples of the same group (beta diversity) as shown previously (Holm *et al.,* 2015; Houlden *et al.,* 2015). Average bacterial community proportions were

also compared between naïve, and low and high dose infected samples at different taxonomic ranks (Fig. 3.5). At the phyla level, Bacteroidetes, Firmicutes and Proteobacteria dominated in all three groups. As expected, alterations were detected with low dose infection. However, these changes were more pronounced in high dose infection samples, with a decrease in Firmicutes and an increase in Bacteroidetes, Proteobacteria and Verrucomicrobia (Fig. 3.5A). Further proportional changes are shown at different taxonomic levels in figure 3.5. Shannon diversity was also assessed for total bacteria between groups. As previously shown, low dose *T. muris* infection reduced bacterial diversity, and this was further reduced with a high dose infection (Fig. 3.6A; P = 0.04) (Holm *et al.,* 2015; Houlden *et al.,* 2015).

At the family level several shifts in proportions were evident as a result of infection (Fig. 3.5D). Unlike previous work by Houlden *et al.,* there was a decrease in *Rikenellaceae* (phyla, Bacteroidetes) from 4.9% in naïve animals to 2.7% in low dose, which was further decreased to 0.2% in a high dose infection. However, in agreement with this work, reductions in *Prevotella* (phyla, Bacteroidetes) were also seen with low dose infection in this study, where in 2 out of 3 samples it was below detection levels (Houlden *et al.,* 2015). Moreover, increases in *Lachnospiraceae* (phyla, Firmicutes) were detected in both low and high dose infected individuals from 1.8% in naïve animals to 7.6% and 10.7%, respectively. A striking increase in the *Bacteroidaceae* (phyla, Bacteroidetes) was evident as a result of high dose infection, with levels of 42.9% compared to 1.3% in naïve and 5% in low dose individuals. Conversely, there was a pronounced reduction with infection in the Bacteroidetes family S24-7, a prevalent murine commensal, which decreased from 47.1% in naïve mice to 45% in low dose and only 12.8% in high dose mice. This was accompanied by a significant reduction in the Shannon diversity of the phyla Bacteroidetes (Fig. 3.6B). This suggests that the increase in proportions of the Bacteroidetes phyla was likely the result of *Bacteroidaceae* outgrowth rather than an increase in a wide range of species. *T. muris* infection-induced reductions in members of the Firmicutes phyla were also identified including a tenfold reduction in *Clostridiales* (phyla, Firmicutes) from 20.5% in naïve, 17.2% in low dose and only 2.6% in high dose samples. *Ruminococcaceae* (phyla, Firmicutes) also decreased from 10.6% in naïve to only 2.7% in high dose samples. This was further mirrored by a significant reduction in the Shannon diversity of Firmicutes (Fig. 3.6C, P = 0.04). Interestingly, there was a significant increase in Proteobacterial diversity as a result of high dose infection (Fig. 3.6D; P = 0.04), unlike low dose infection, which did not induce a significant change (P = 0.8). This is in keeping with the two fold increase in proportions of Proteobacteria as a result of high dose infection (Fig. 3.5A). Furthermore, the *Enterobacteriaceae* (phyla, Proteobacteria) was only detected in high dose infection samples (6.1%) indicating numbers below

detection in naïve and low dose samples, and an expansion of this family as a result of an increased worm burden.

Overall, these data show that high dose infections and therefore increased worm burden resulted in various microbiota alterations, specifically increases in the *Bacteroidaceae* and *Enterobacteriaceae* families.

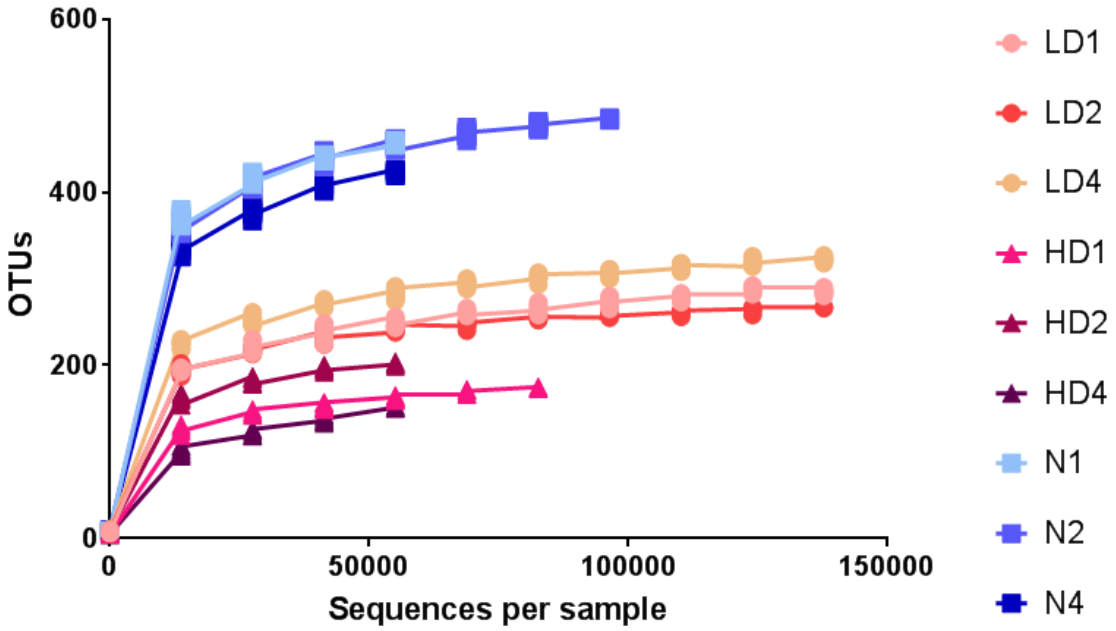

Figure 3.3 Rarefaction curves indicating the sequencing depth of C57BL/6 samples. Samples 1, 2 and 4 from each group (naïve (N), low dose (LD) and high dose (HD)) were used for Illumina sequencing. The number of OTUs at 97% sequence similarity were identified in each group and plotted against the number of sequences per sample.

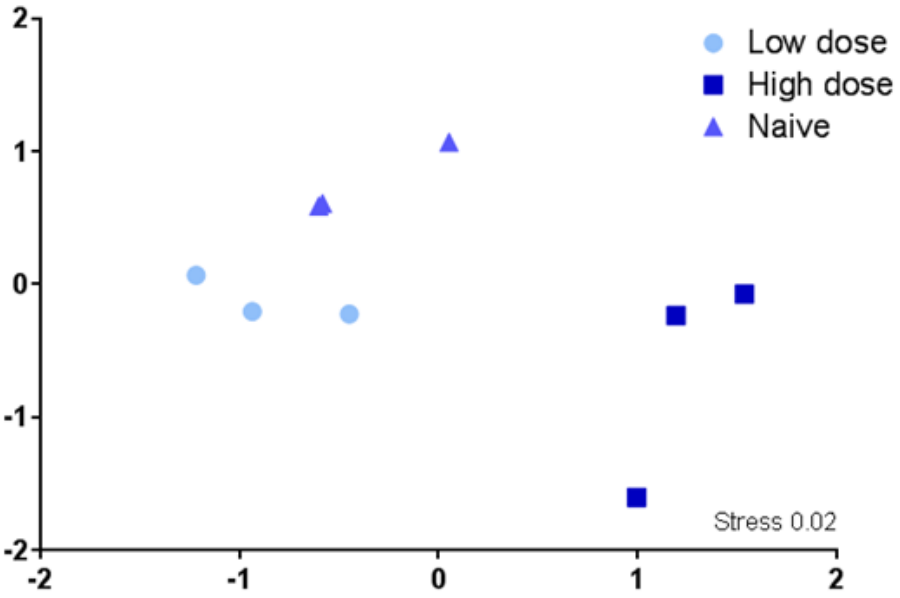

Figure 3.4 NMDS analysis of sequenced C57BL/6 day 42 p.i. stool samples. Each point represents an individual mouse with the axis scale for Euclidian distance between samples centred on zero. Stress indicates the quality of fit of the data (<0.2 is a good fit).

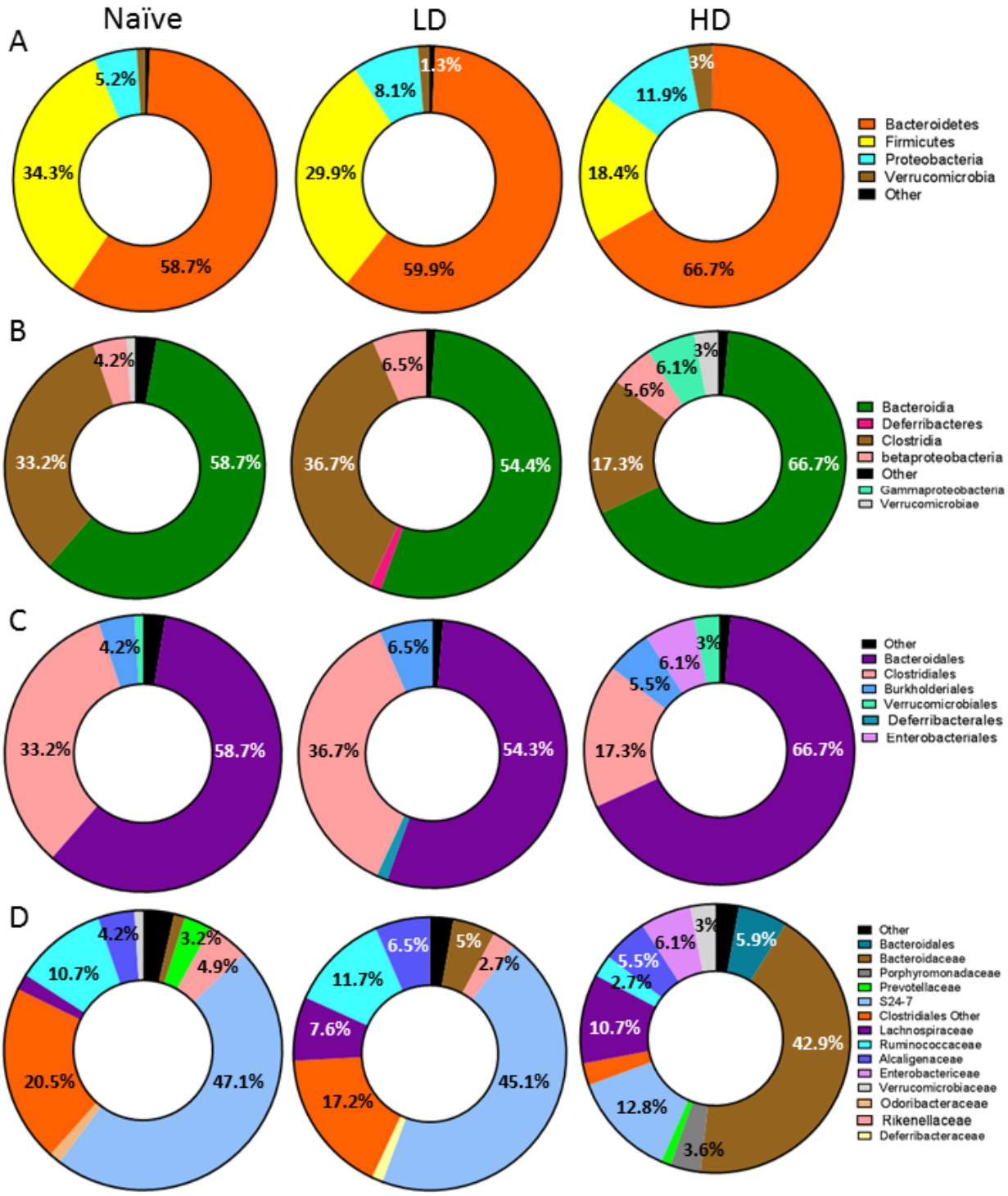

Figure 3.5 Comparison of the proportional changes that occur in the intestinal microbiota of low and high dose *T. muris* infected C57BL/6 mice, compared to naïve controls, by 16S Illumina sequencing of stool samples at day 42 p.i. The rarefied OTU table was used to compare proportions shown in % between naïve, low dose (LD) and high dose (HD) samples at different levels; (**A**) phylum, (**B**) class, (**C**) order and (**D**) family. Groups less than 1% were pooled into 'Other'. A full list of proportional changes can be found in Table B in the suppled appendix.

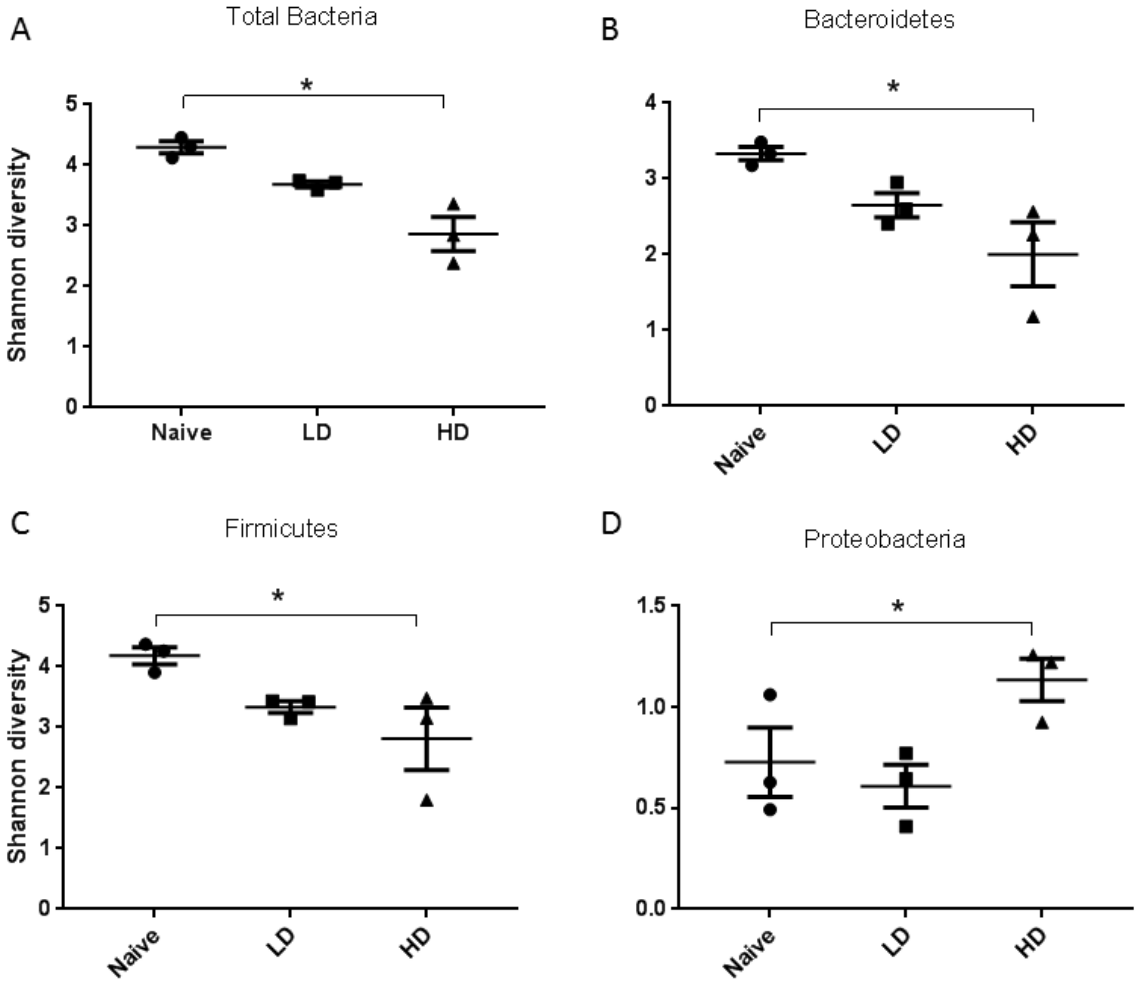

Figure 3.6 Shannon diversity of intestinal microbiota at day 42 p.i. in C57BL/6 stool samples. Differences in bacterial alpha diversity were determined from the rarefied OTU table in QIIME between naïve, and low dose (LD) and high dose (HD) infected samples, for (**A**) total bacteria, (**B**) Bacteroidetes, (**C**) Firmicutes, and (**D**) Proteobacteria. Values represent mean +/- SEM. * indicates significance ($P < 0.04$) as calculated by ANOVA with TukeyHSD tests.

3.2.3 *T. muris* infection disturbs the spatial organisation of the intestinal microbiota

Although it is clear that infection with *T. muris* causes distinct alterations to the composition of the host intestinal microbiota, little is known about the spatial organisation of these bacteria in the intestinal tract. *Trichuris* species have an unusual niche and reside within syncitial tunnels in the host epithelial cell layer, breaching the mucosal barrier. It is therefore likely that the breakdown of the inner mucosal layer, which under 'normal' conditions is largely sterile, will result in changes to the distribution of bacteria and therefore the relationship between host and microbiota in this intestinal niche (Johansson *et al.,* 2008).

To investigate this, caecal tips were collected at day 42 p.i. from C57BL/6 mice described previously in this chapter for comparison between naïve, and low and high dose infected individuals. Tissue was fixed in NBF overnight, processed and embedded in wax blocks for sectioning. Sections were used for Fluorescence *in situ* hybridisation (FISH) analysis using a universal 16S rRNA gene Cy3 labelled probe that hybridises to most bacteria. DAPI was also used to stain nuclei, allowing visualisation of the intestinal epithelial cell layer.

In naïve animals, treated with rIL-12 or PBS, there was a clear separation between bacteria (red) and the epithelial cell layer (blue), which is most likely due to the mucosal layer (Fig. 3.7C-D). However, figure 3.7A shows that a low dose *T. muris* infection reduced the separation between bacteria and host epithelium. Bacteria (red) were present within the caecal crypts allowing direct contact between them and the intestinal epithelial cell layer. Increased crypt elongation was also evident and is commonly associated with *T. muris* infection (Artis *et al.,* 1999; Cliffe *et al.,* 2005, 2007). The intimate association between microbiota and host epithelium was seen in all low dose samples, including HD3, which had a low level worm burden but was housed in the high dose group. Individuals with a high worm burden displayed a similar phenotype with bacteria present deep within the intestinal crypts (Fig. 3.7B). The white arrow indicates the presence of a *T. muris* adult worm, and it is evident that there was an increase in bacteria within the crypts directly surrounding the worm compared to those further away. This suggests that the presence of *T. muris* adult worms within the intestinal epithelial layer triggers the movement of bacteria deep within the crypts, allowing an intimate association between host, microbiota and parasite.

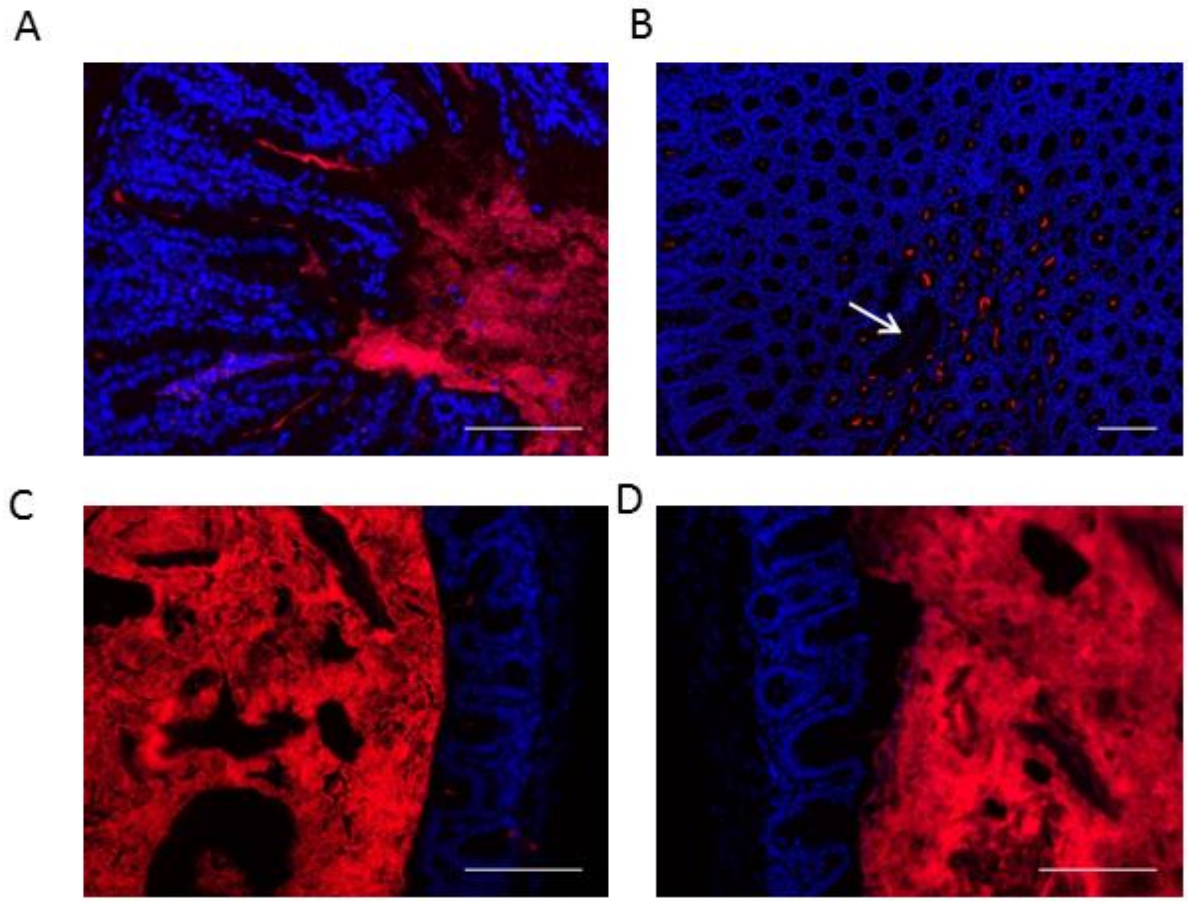

Figure 3.7 FISH analysis of the spatial organisation of the host intestinal microbiota with *T. muris* infection. Caecal tips from (**A**) low dose + IL-12, (**B**) high dose + IL-12, (**C**) naïve + IL-12, and (**D**) naïve + PBS treated mice were fixed in NBF at day 42 p.i., processed and sections were used for FISH with a Cy3 labelled 16S universal rRNA gene probe (red) and DAPI (blue). Arrow indicates the presence of an adult *T. muris* worm. Scale bars, 100 µm.

3.2.4 Infection reduces concentrations of the SCFA butyrate in the caecum

Infection of the small intestine with the helminth parasite, *H. polygyrus*, causes a significant increase in the concentrations of the SCFA butyrate in caecal contents (Zaiss *et al.,* 2015). To investigate the impact of *T. muris* infection on local caecal SCFA concentrations, caecal contents were collected from the C57BL/6 mice used in previous sections of this chapter. Samples were weighed, emulsified in acidified water and extracted with ethyl acetate for GC-MS. Concentrations were quantified using standard curves of the SCFAs butyrate, acetate and propionate (Fig. 3.8).

Figure 3.9 shows that SCFA concentrations within the naïve and rIL-12 treated caeca were dominated by acetate followed by butyrate and propionate, reflecting previous studies, with rIL-12 treatment having no significant impact (Zaiss *et al.,* 2015). However, infection with *T. muris* caused a significant reduction in the levels of butyrate in caecal contents compared to both naïve groups. This was seen for low dose infections where concentrations decreased to half of naïve levels (~ 5 mmol/g), whereas in high dose infections these concentrations dropped even further to ~ 1 mmol/g (Fig. 3.9A). Conversely, acetate was unaffected by infection and reflected naïve concentrations (Fig. 3.9B). This was also true for propionate in low dose infections, although there was a slight decrease with high level infections but this was not significant (Fig. 3.9C). Total SCFA concentrations were not significantly altered by infection but again a slight decrease was seen with high dose infections, although this was not significantly different to naïve control levels (Fig.3.9D).

To determine if *T. muris* must be present within the caecum to cause these changes, SCFA concentrations were measured in the caecal contents of C57BL/6 mice that had been cleared of a low dose *T. muris* infection at day 35 p.i. using mebendazole (LD – Meb). At this point, *T. muris* are at the adult stage and have caused significant alterations to the host intestinal microbiota. Previous work has shown that clearance of *T. muris* infection with mebendazole causes host intestinal bacterial communities to recover towards naïve status, although there is a window of 2-3 weeks where the communities are not fully recovered (Houlden *et al.,* 2015). This window was exploited and mice were sacrificed two weeks after treatment at day 49 p.i. to ensure any residual mebendazole had been cleared, but host intestinal microbiota were not yet recovered to naïve status. Faecal egg counts were used to confirm the success of mebendazole treatment. Caecal contents were collected from low dose mebendazole treated (LD – Meb; N = 6), low dose infected (LD – X; N = 5), naïve (Naïve – X; N = 7) and naïve mebendazole treated (Naïve – Meb; N = 6) mice at day 49 p.i. GC-MS was performed on all samples and concentrations of SCFAs were quantified. Infection and mebendazole treatment did not cause a significant impact on acetate and total SCFA concentrations in caecal contents

(Fig. 3.10B and D). As shown before, figure 3.10A demonstrates the significant reduction in butyrate concentrations as a result of low dose infection (P = 0.02). Importantly, the removal of worms from the lower intestinal tract by mebendazole treatment caused a significant increase in butyrate concentrations (P = 0.006). This was also seen for propionate, where infection caused a significant reduction (P = 0.005) and clearance of worms returned levels back to naïve status (Fig. 3.10C). This indicates that removal of *T. muris* from its intestinal niche causes an increase in butyrate and recovery towards naïve levels.

To see if the reduction in butyrate concentrations during infection is due to an increased uptake of butyrate from the intestinal lumen by intestinal epithelial cells, the gene expression levels of butyrate transporters, MCT-1 and SLC5A8, were measured by qRT-PCR. Caecal tips were collected at day 49 p.i. and placed in TRIzol for RNA extraction. RNA was then reversed transcribed and the resulting cDNA was used for qPCR. Gene expression levels of the housekeeping gene β-actin were also measured to control for variance between samples. Results were calculated using the Pfaffl method which takes into account differences in efficiency between primer sets and expresses gene expression levels as fold change over naïve levels (Naïve – X samples). Figure 3.11 shows that during *T. muris* infection, expression of the transporters MCT-1 and SLC5A8 were downregulated. These levels were significantly different to naïve (Naïve – X) and naïve mebendazole treated (Naïve – Meb) controls (P = 0.02). However, the removal of *T. muris* worms and consequent increase in butyrate levels was accompanied by an increase in MCT-1 and SLC5A8 expression in caecal tissue. These levels did not reach that of naïve samples but for MCT-1 they were significantly increased from infected samples (P = 0.009; Fig. 3.11A). Therefore the decrease in transporters reflects the decrease in caecal butyrate concentrations.

Moreover, stool samples were also collected at day 49 p.i. to perform DGGE and NMDS analysis on the bacterial communities within the intestinal tract of all animals. Figure 3.12 shows that mebendazole treatment did not cause significant alterations to the intestinal microbiota (P = 0.1). As expected, infection with *T. muris* caused a significant difference compared to naïve samples (P = 0.003). However, the intestinal microbiota of individuals that had been cleared of their infection was different to all other groups (P = 0.003). This indicates that removal of worms from the lower intestinal tract resulted in a shift in bacterial communities after two weeks that is not yet similar to naïve animals, but also different to the infected host microbiota. This therefore suggests that the reduction in butyrate seen with infection is dependent on the presence of the worm, and potentially associated with *T. muris*-induced microbiota changes.

Since worm burden has a clear impact on the host intestinal microbiota, and alterations to these bacterial communities in turn impacts butyrate production, the effect of worm burden on caecal butyrate concentrations was investigated. Butyrate measurements on C57BL/6 low dose infected and naïve caecal contents were collated, together with worm counts, and a linear regression was performed (Fig. 3.13A). This showed a significant negative correlation between the number of worms and the concentration of butyrate within the caecum, where increasing worm burden leads to decreased butyrate production ($P = 0.0007$). High dose measurements were not included in this instance, although the linear regression was still significant with their inclusion ($P = 0.048$). This was to allow the prediction of a worm count threshold where butyrate levels diminish. Butyrate concentrations decreased to below 1 mmol/g after ~ 13 worms, and regression analysis predicted that after ~17 worms butyrate levels decrease further. The linear regression analysis was repeated with low dose samples only to determine if the correlation remained without the inclusion of the many naïve samples. As a result, the negative correlation remained although it was no longer significant ($R^2 = 0.39$, $P = 0.0527$). The addition of more data points, especially at varying worm burdens, may give a greater insight into the association between butyrate concentrations and infection intensity.

Overall these data indicate that infection with *T. muris* causes a significant reduction in the ability of the host intestinal microbiota to produce butyrate, which is dependent on worm burden and associated microbiota changes, and subsequently reduces the expression of butyrate transporters by host intestinal epithelial cells.

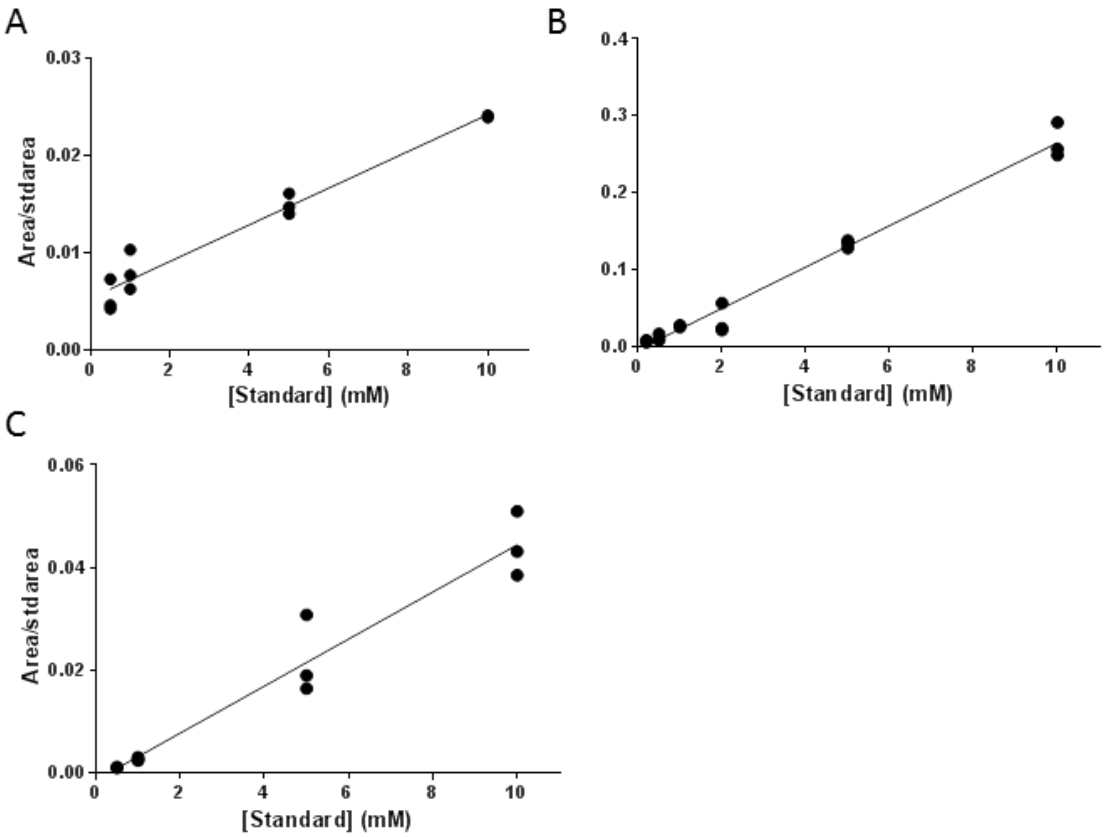

Figure 3.8 Standard curves for quantifying concentrations of SCFAs by GC-MS. Known concentrations of each SCFA were dissolved in H_2O and an internal standard added. The peak areas of each SCFA was divided by the peak area of the internal standard, and plotted against SCFA concentration to create a standard curve; (**A**) Sodium acetate, (**B**) sodium butyrate, (**C**) sodium propionate.

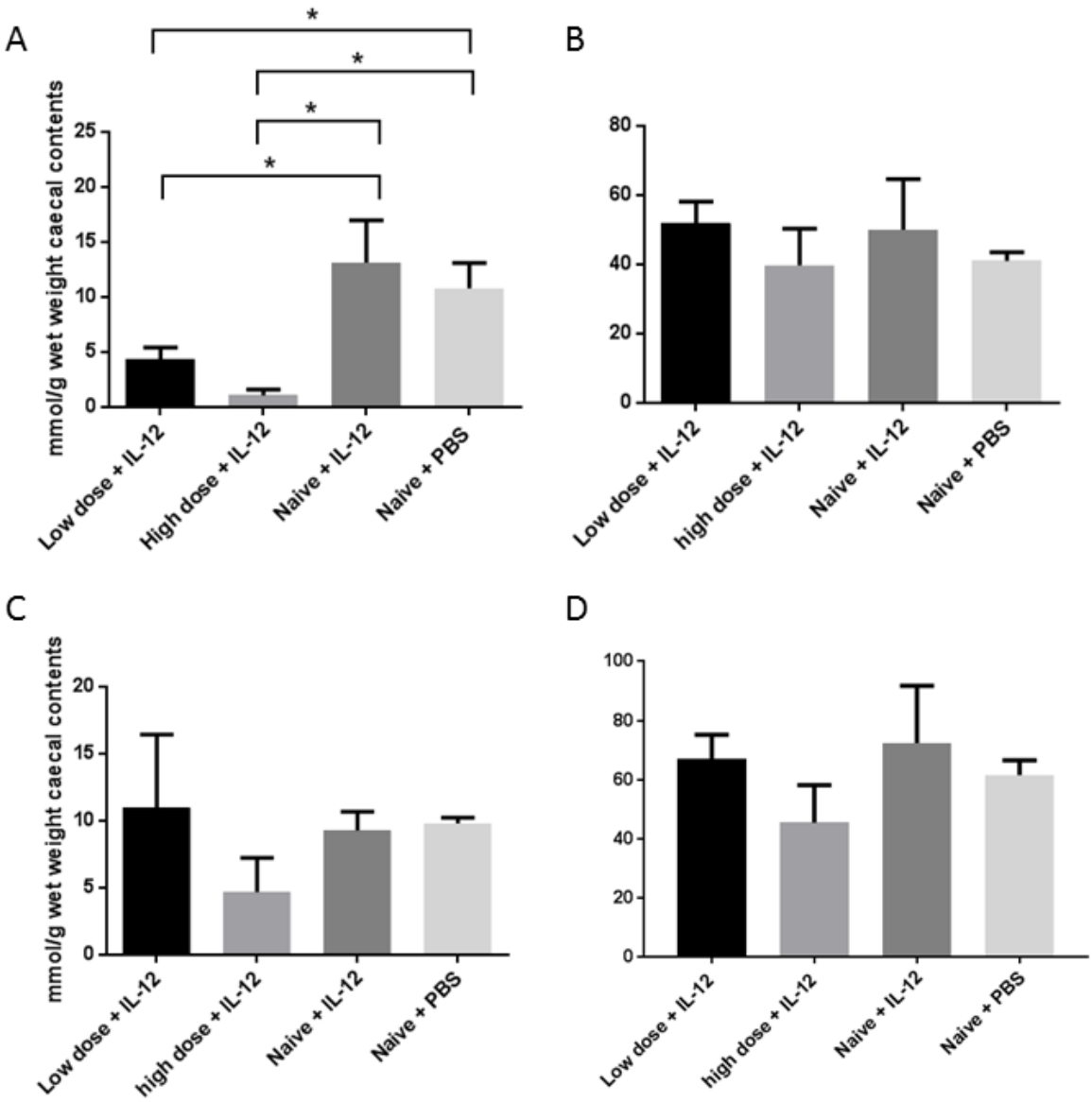

Figure 3.9 SCFA concentrations in the caecal contents of C57BL/6 mice infected with *T. muris* compared to naïve controls. Caecal contents were collected at day 42 p.i. from low and high dose infected and naïve mice (N = 4 per group), and used for GC-MS analysis. Concentrations of SCFAs were calculated using standard curves and expressed as mmol per gram of wet caecal contents. Two technical replicates were performed per sample. These values were averaged, and then the average of the biological replicates, i.e. caecal contents from 4 mice, was plotted. (**A**) Butyrate, (**B**) Acetate, (**C**) Propionate, (**D**) Total SCFAs. Values represent mean +/- SEM. * indicates significance ($P < 0.05$) as calculated by Mann Whitney U tests between treatments.

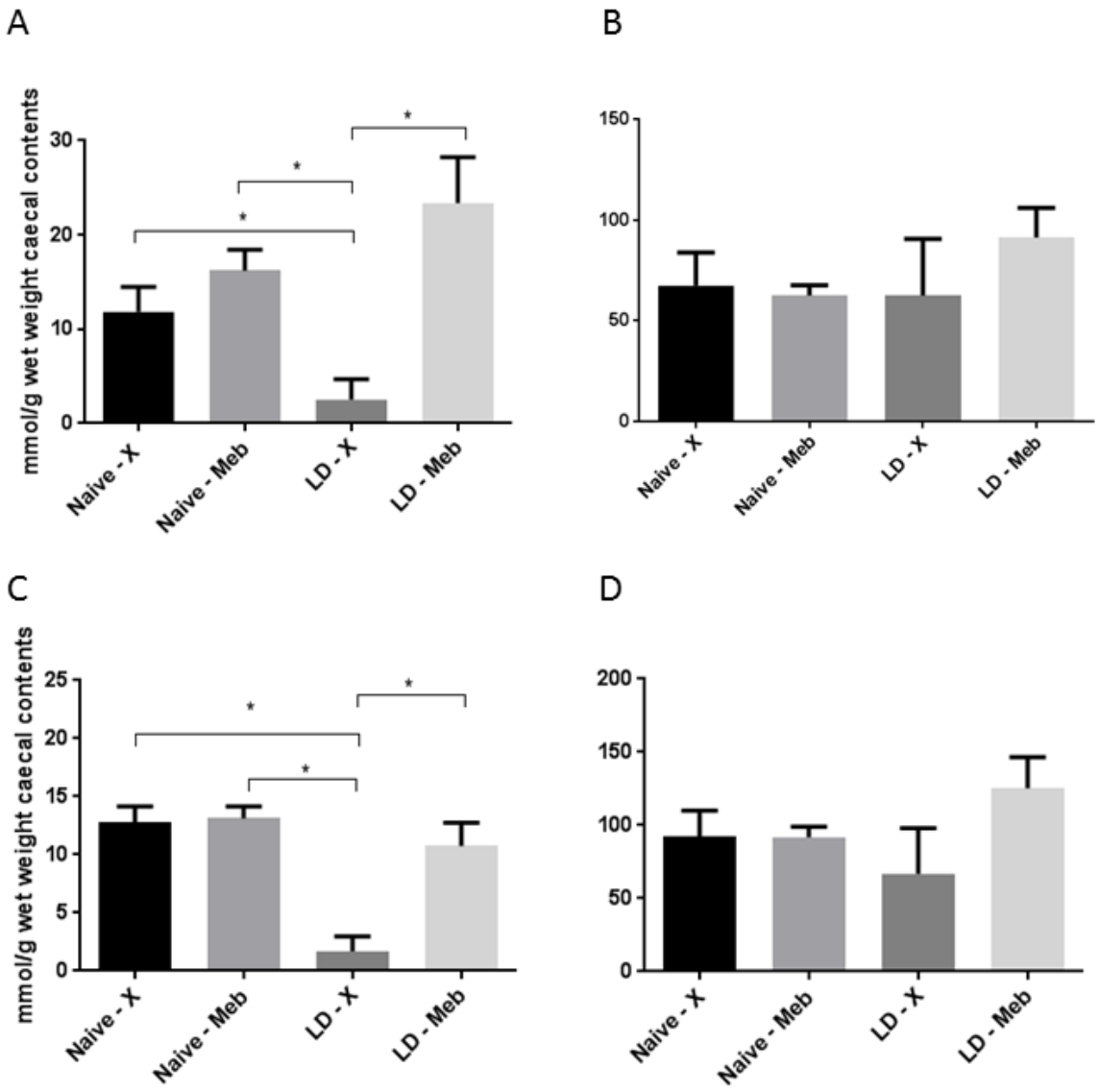

Figure 3.10 SCFA concentrations in caecal contents of C57BL/6 mice infected with a low dose of *T. muris* or after clearance of worms by mebendazole treatment at day 49 p.i. Caecal contents were collected from naïve (naïve – X), naïve mebendazole treated (Naïve – Meb), low dose (LD - X) infected and low dose mebendazole treated (LD – Meb) mice (N = 5-6) at day 49 p.i. (2 weeks after mebendazole treatment) and analysed by GC-MS. Two technical replicates were performed per sample. These values were averaged, and then the average of the biological replicates, i.e. caecal contents from 5/6 mice, was plotted. (**A**) Butyrate, (**B**) Acetate, (**C**) Propionate, (**D**) Total SCFAs. Concentrations of SCFAs were calculated using standard curves and expressed as mmol per gram of wet caecal contents. Values represent mean +/- SEM. * indicates significance ($P < 0.02$) as calculated by Mann Whitney U tests between treatments.

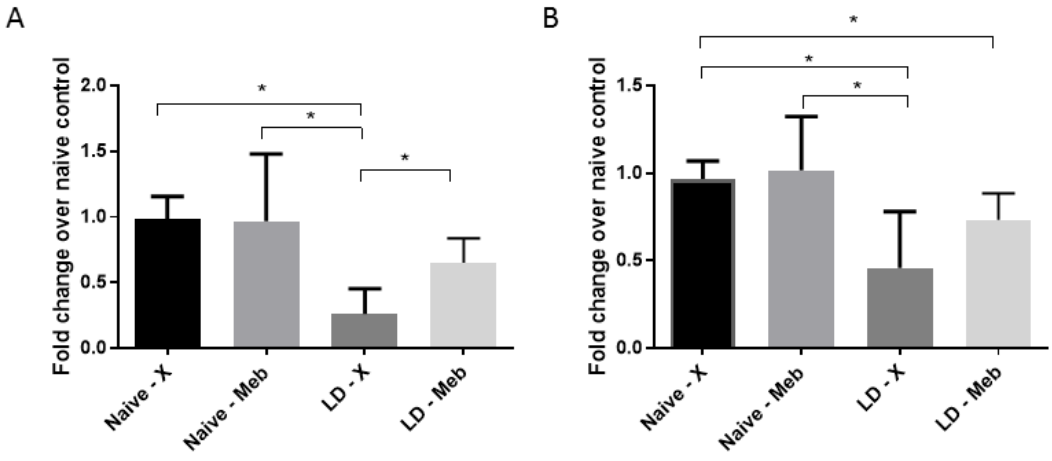

Figure 3.11 Gene expression of butyrate transporters in C57BL/6 host caecal tissue at day 49 p.i. Caecal tissue was collected from naïve (naïve – X), naïve mebendazole treated (naïve – meb), low dose (LD - X) infected and low dose mebendazole treated (LD – Meb) mice (N = 5-6) at day 49 p.i. RNA was extracted, reverse transcribed and gene expression levels of the butyrate transporters (**A**) MCT-1 and (**B**) SLC5A8 were quantified by qRT-PCR using 4 techinical replicates for each primer set for each animal (N = 5-6). β-actin was used to standardise numbers and results were calculated using the Pfaffl method. Results are shown as the fold change over naïve levels (Naïve – X). Values represent mean +/- SEM. * indicates significance ($P < 0.02$) as calculated by Mann Whitney U tests as data was not normally distributed.

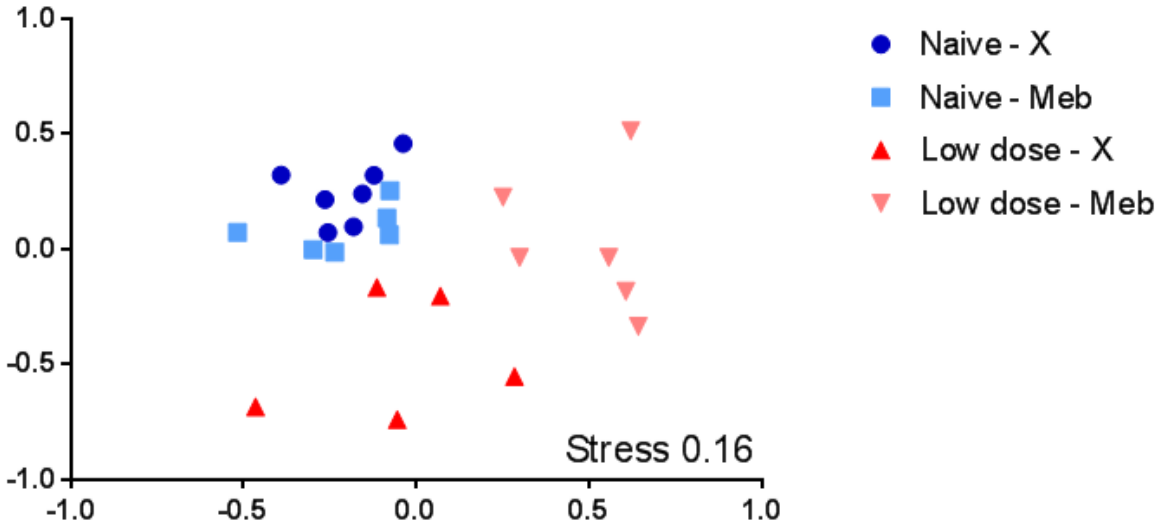

Figure 3.12 NMDS analysis of the intestinal microbiota of C57BL/6 mice at day 49 p.i. using stool samples 14 days after mebendazole treatment. Stools were collected from naïve (naïve – X), naïve mebendazole treated (naïve – meb), low dose (LD - X) infected and low dose mebendazole treated (LD – Meb) mice (N = 5-6) at day 49 p.i., 14 days after mebendazole treatment. DNA was extracted and analysed by 16S rRNA DGGE and NMDS. Each point represents an individual mouse (biological replicates) with the axis scale for Euclidian distance between samples centred on zero. Stress indicates the quality of fit of the data (<0.2 is a good fit). P values were calculated by permutational ANOVA (PERMANOVA) on the NMDS distance matrix and corrected for multiple comparisons.

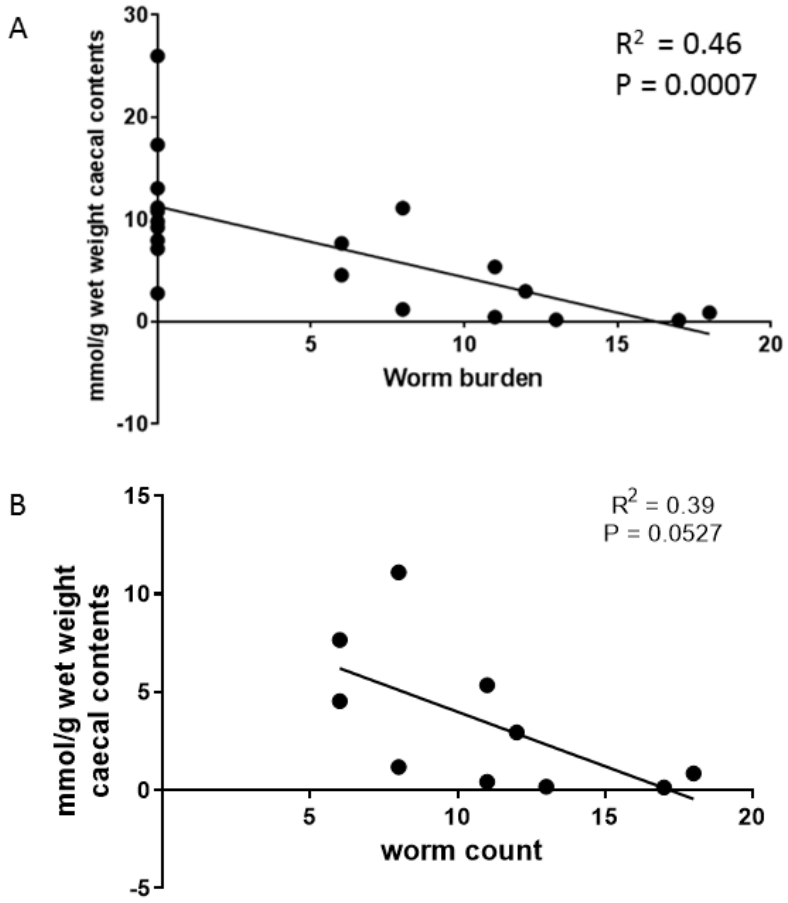

Figure 3.13 Relationship between caecal butyrate concentrations and worm burden in *T. muris* infected and naïve C57BL/6 mice. (**A**) All GC-MS and worm burden data quantifying butyrate levels in caecal contents from naïve C57BL/6 mice (N = 11) or C57BL/6 mice infected with a low dose of *T. muris* (N = 10) was collated. Linear regression analysis showed a significant negative correlation where R^2= 0.46 and P = 0.0007. (**B**) The linear regression analysis was repeated with low dose samples only to determine if the correlation remained without the many naïve samples. The negative correlation remained although it was no longer significant (R^2 = 0.39, P = 0.0527).

3.2.5 *T. muris* induced dysbiosis occurs independently of the host adaptive immune system

It is clear that *T. muris* infection results in significant alterations to the host intestinal microbiota that are worm burden dependent. However, the cause of these alterations is unknown. To determine the influence of the host adaptive immune system, SCID mice, which lack functional B and T cells, were infected with a low and high dose of *T. muris*. This is a susceptible mouse strain so additional treatment was not needed to allow the high dose infection to reach chronicity, as shown by the worm counts in figure 3.14.

Stool samples were collected weekly from both infected groups, and a naïve control group (N = 5 per group). DNA was extracted and bacterial community analysis was performed by 16S rRNA DGGE and NMDS. Figure 3.15 shows the shifts in bacterial communities over time from days 7 – 35 p.i. compared to day 0 as a baseline. By day 21 p.i., as seen in C57BL/6 mice, differences were detected in low and high dose infected samples compared to naïve and day 0 samples (Fig. 3.15, P = 0.01). This became greater over time with time points from day 42 to 56 p.i (Fig. 3.16). At day 42 p.i. high dose samples were very tightly clustered away from all other points, so that the remaining points cluster on top of each other. The NMDS analysis was therefore repeated without the high dose day 42 p.i. samples to reveal the associations between the remaining points. As a result, low dose samples began to cluster further from the naïve samples, which became more evident at days 49 and 56 p.i (P = 0.01) (Fig. 3.16). All high dose samples produced a very similar, conserved banding pattern with reduced diversity that was strikingly different to naïve and low dose samples. Furthermore, one low dose sample repeatedly clustered away from the other low dose samples. This sample is indicated by the red arrow on the DGGE plot in figure 3.16 and produced a banding pattern that was more similar to that of a high dose sample. The worm count for this individual was 18 *T. muris*, technically a low dose although higher than other samples in the same group, supporting previous links between increasing worm burden and intestinal microbiota alterations. Caecal contents were also used for DGGE and NMDS analysis, and bacterial communities looked very similar to those present in the stool samples at day 56 p.i. highlighting the significant difference between all groups (P = 0.03). Therefore these data show that worm burden and time dependent *T. muris* induced alterations to the host intestinal microbiota occur independently of the host adaptive immune system.

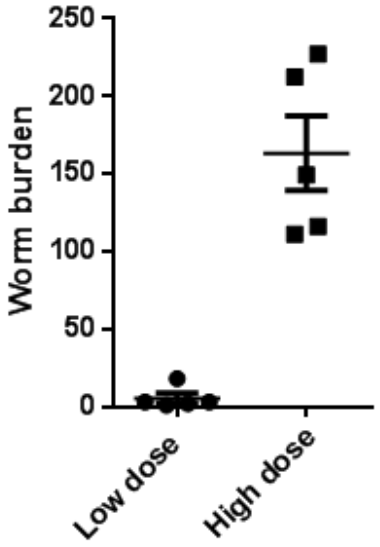

Figure 3.14 Worm burdens in SCID mice at day 56 p.i. Low dose mice were infected with ~20 embryonated *T. muris* eggs and high dose were given ~200 eggs via oral gavage. The numbers of adult worms in the large intestine were counted at day 56 p.i. Values represent mean +/- SEM.

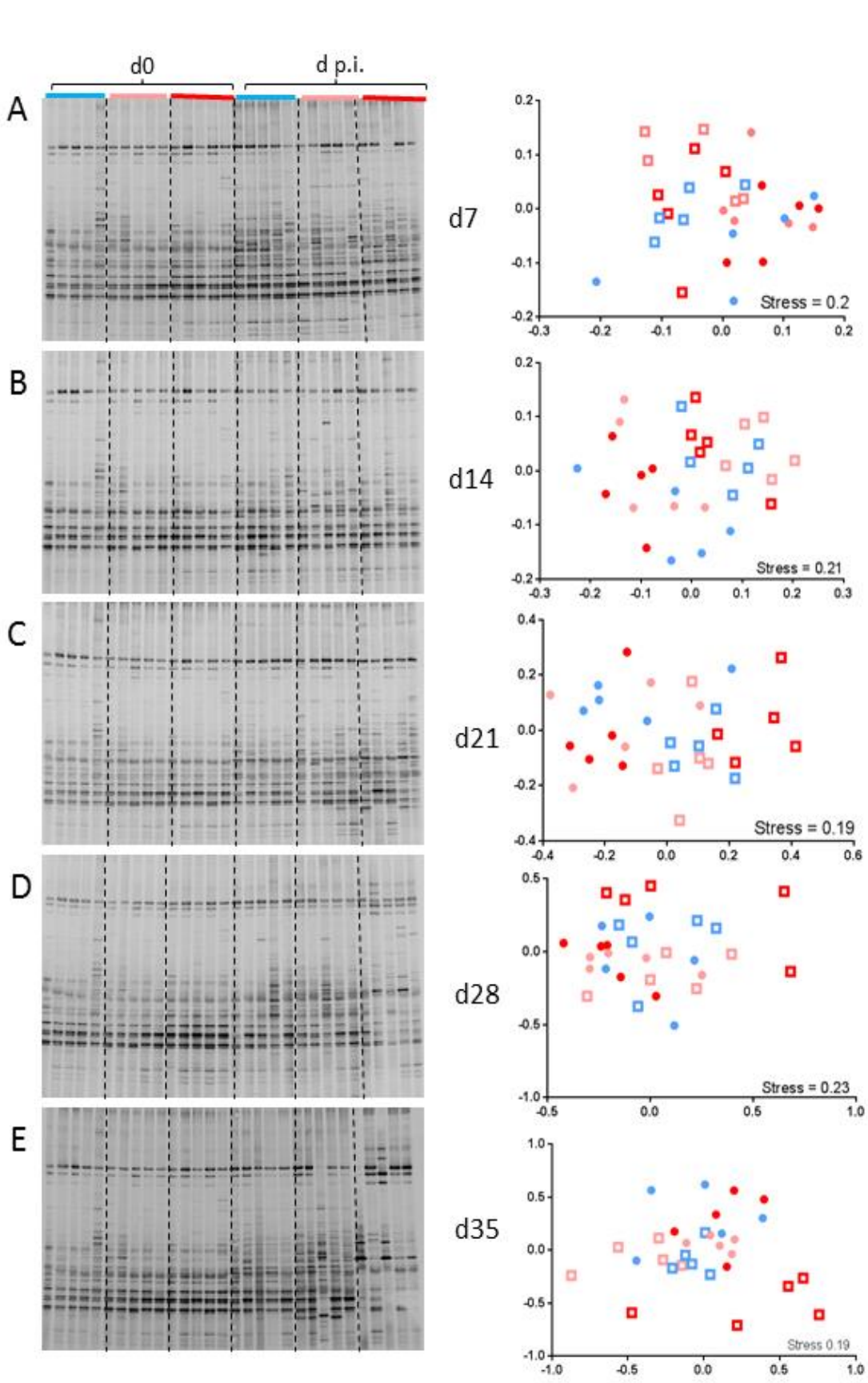
d0
d p.i.
A
B
C
D
E
d7
d14
d21
d28
d35
Stress = 0.2
Stress = 0.21
Stress = 0.19
Stress = 0.23
Stress 0.19
Naive d0
Low dose d0
High dose d0
Naive d p.i.
Low dose d p.i.
High dose d p.i.

Figure 3.15 DGGE and NMDS analysis of stool samples from SCID mice infected with a low (~ 20 eggs) or a high (~200 eggs) dose of *T. muris*, and naïve control mice, from day 0 to day 35. Stools were collected weekly; DNA was extracted and consequently used for 16S rRNA DGGE analysis. (**A**) DGGE analysis comparing the intestinal microbiota at day 0 (d0), which are technical replicates between gels for all day 0 groups and biological replicates within groups (N = 5 per group), and the intestinal microbiota days post infection (d p.i.), which ranges from day 7 (d7) to day 35 (d35), which includes biological replicates within groups only. (**B**) The corresponding NMDS plots where each point represents an individual mouse with the axis scale for Euclidian distance between samples centred on zero. Stress indicates the quality of fit of the data (<0.2 is a good fit). Time points d42 – d56 are shown in figure 3.16. P values were calculated by permutational ANOVA (PERMANOVA) on the NMDS distance matrix and corrected for multiple comparisons.

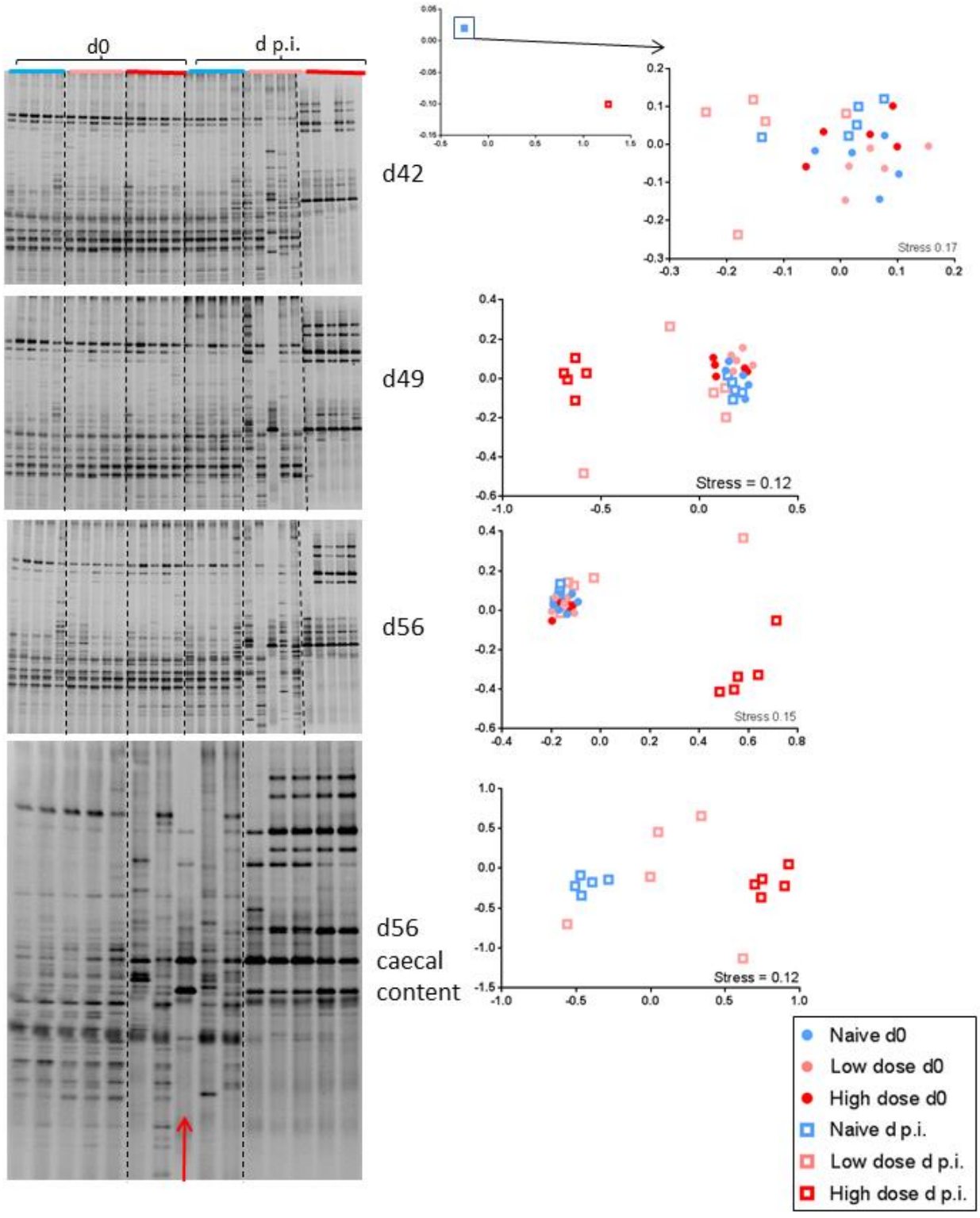

Figure 3.16 DGGE and NMDS analysis of stool samples from SCID mice infected with a low (~ 20 eggs) or a high (~200 eggs) dose of *T. muris*, and naïve control mice, from day 42 to 56, and caecal contents at day 56. Stools were collected weekly and caecal content was collected on the final day of the experiment (day 56). DNA was extracted and consequently used for 16S rRNA DGGE analysis. (**A**) DGGE analysis comparing the intestinal microbiota at day 0 (d0), which are technical replicates between gels for all day 0 groups and biological replicates within groups (N = 5 per group), and the intestinal microbiota days post infection (d p.i.), which ranges from day 42 (d42) to day 56 (d56), which includes biological replicates within groups only.

DGGE analysis was also performed on caecal contents at d56. The red arrow indicates the individual with a worm count of 18 that has an intestinal microbiota more similar to that associated with the high dose group. (**B**) The corresponding NMDS plots where each point represents an individual mouse with the axis scale for Euclidian distance between samples centred on zero. Stress indicates the quality of fit of the data (<0.2 is a good fit). The NMDS for day 42 has been enlarged on the right and excludes high dose data at day 42 to allow analysis of individual points. Time points d7 – d35 are shown in figure 3.15. P values were calculated by permutational ANOVA (PERMANOVA) on the NMDS distance matrix and corrected for multiple comparisons.

3.2.6 High dose *T. muris* infection selects for an increase in specific bacterial families independently of the adaptive immune system

From the DGGE and NMDS analysis, it was clear that a high dose infection in a SCID mouse resulted in a conserved microbiota with a marked reduced number of bands or species compared to naïve and low dose microbiotas. Therefore, to identify what these conserved bacterial species were and to determine changes in the composition of the intestinal microbiota as a result of high dose *T. muris* infection, day 56 p.i. caecal contents from low dose, high dose and naïve mice were subjected to 16S rRNA gene Illumina sequencing (N = 3 per group).

Libraries were generated for samples 2, 4 and 5 from each group as described previously for C57BL/6 samples. This produced 2,755,907 paired-end reads, which was reduced to an average of 1,875,709 sequences per sample. Analysis was performed on the rarefied OTU table (Table A, Appendices). Rarefaction curves indicated that all samples were sequenced to an appropriate depth with all curves plateauing (Fig. 3.17). This also showed that high dose samples had a decreased number of unique OTUs (blue), whereas low dose and naïve samples (pink) had similar species richness and a higher number of unique OTUs (Fig. 3.17).

As before, NMDS analysis was performed on sequenced samples (Fig. 3.18). This indicated that high dose samples were very different to both low dose and naïve samples ($P < 0.05$). However, two low dose samples clustered with naïve samples and they were not significantly different (Fig. 3.18). As high dose samples cluster so tightly, this suggests that beta diversity is very low for these samples with a high level of similarity between samples. However, low dose samples are not clustered tightly indicating a higher beta diversity, as shown by previous studies (Holm *et al.,* 2015; Houlden *et al.,* 2015). Average bacterial community proportions were also compared between naïve, low dose and high dose infected samples at different taxonomic ranks using the rarefied OTU table (Fig. 3.19). Comparisons between the C57BL/6 data set and the SCID data set must be approached with caution due to differences in the naïve intestinal microbiotas, a result of

genetic background, and also differences in days post infection and sampling site (Friswell *et al.,* 2010; Gu *et al.,* 2013). Nevertheless, at the phylum level, microbiota alterations due to high dose *T. muris* infection followed a similar trend to C57BL/6 mice with increased Bacteroidetes and Proteobacteria but a reduction in the proportion of Firmicutes (Fig. 3.19A). In naïve SCID samples, the Firmicutes dominated, in particular, *Clostridiales* (family unspecified), *Lachnospiraceae* and *Ruminococcaceae* families, making up an average of 89.7% of sequences. This was also seen in low dose samples, with infection causing little variation in the proportions of the three major phyla and at lower taxa levels. Additionally, low dose infection had no impact on overall Shannon diversity compared to naïve samples (P = 0.9), whereas high dose infection caused a dramatic reduction and was significantly different to both naïve (P = 0.00006) and low dose (P = 0.0001) samples (Fig. 3.20A).

High dose infection caused a dramatic increase in the phylum Bacteroidetes; four times higher than proportions seen with low dose infection and naïve samples. This increase can be explained by the enrichment of the *Bacteroidaceae* family, which consequently resulted in a striking reduction in Bacteroidetes Shannon diversity (Fig. 3.19D and 3.20B). This was also seen in C57BL/6 high dose samples (Figs. 3.5 – 3.6). Furthermore, although there was a reduction in the proportion of Firmicutes with high dose infection, the composition within this phylum at lower taxa levels had undergone restructuring compared to naïve and low dose samples. There was a striking outgrowth of the *Lactobacillales* order, which accounted for 50.4% of total sequences, in particular the *Lactobacillaceae* family (32.9%). This was accompanied by a tenfold reduction in the *Lachnospiraceae* family and an even greater reduction in other *Clostridiales* families (Fig. 3.19C-D). This was reflected by the reduction in Firmicutes Shannon diversity as a result of high dose infection (Fig. 3.20C). Moreover, at the family level there was a small increase in *Lactobacillaceae* in low dose samples to 1.4% from 0.2% in naïve samples, but other *Clostridiales* families still dominated (54.4%) (Fig. 3.19D).

As seen with high dose C57BL/6 samples, there was an expansion in Proteobacteria; five times more than naïve and low dose samples. This related to the 3.8% increase in *Enterobacteriaceae*, which was undetectable in naïve and low dose samples. Proteobacterial Shannon diversity, however, significantly decreased (P = 0.0001; Fig. 3.20D). Conversely, diversity increased in low dose samples, which was likely to be related to several small proportional increases in Proteobacterial families such as *Anaeroplasmataceae* (Fig. 3.19D).

Overall, a high level *T. muris* infection in an immunodeficient background resulted in restructuring of the intestinal microbiota. In particular, the outgrowth of the *Lactobacillales* order and the *Bacteroidaceae* family, which consequently reduced Firmicutes,

Bacteroidetes and overall bacterial Shannon diversity. Further to this, an increase in *Enterobacteriaceae* proportions was also detected with high level infection, as seen previously in stool samples taken from high dose infected C57BL/6 wild type mice. This indicates that these changes occur independently of the adaptive immune system, and can therefore driven by a different factor(s).

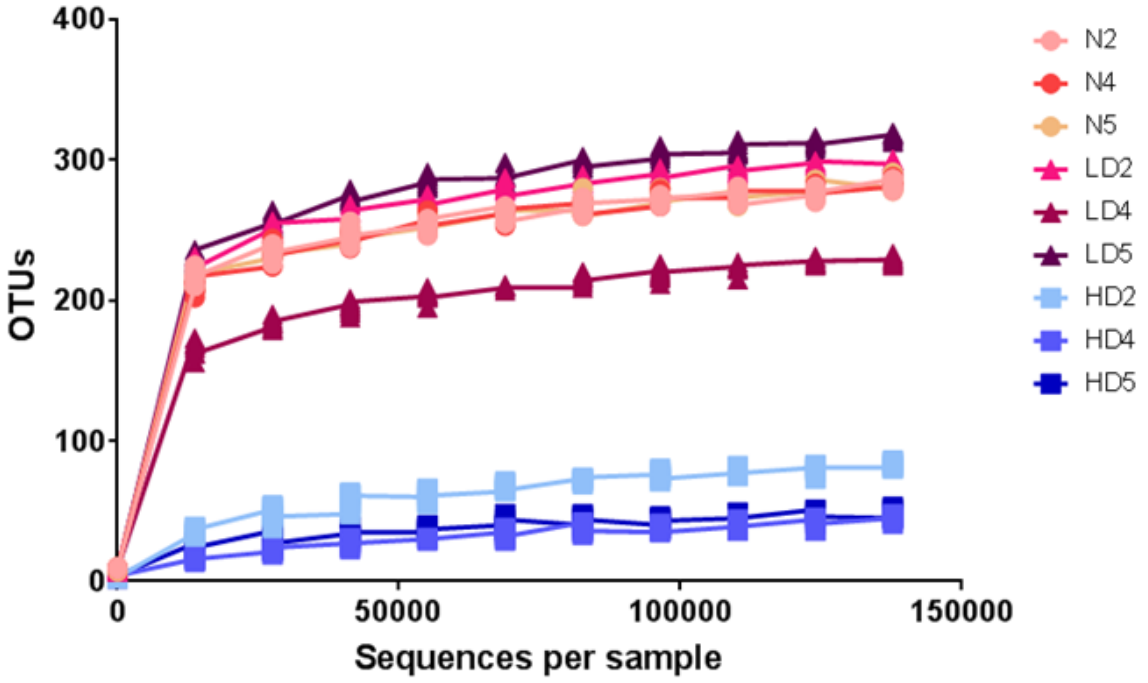

Figure 3.17 Rarefaction curves indicating the sequencing depth of SCID samples. Samples 2, 4 and 5 from each group (naïve, low dose and high dose) were used for Illumina sequencing. The number of OTUs at 97% sequence similarity were identified in each group and plotted against the number of sequences per sample.

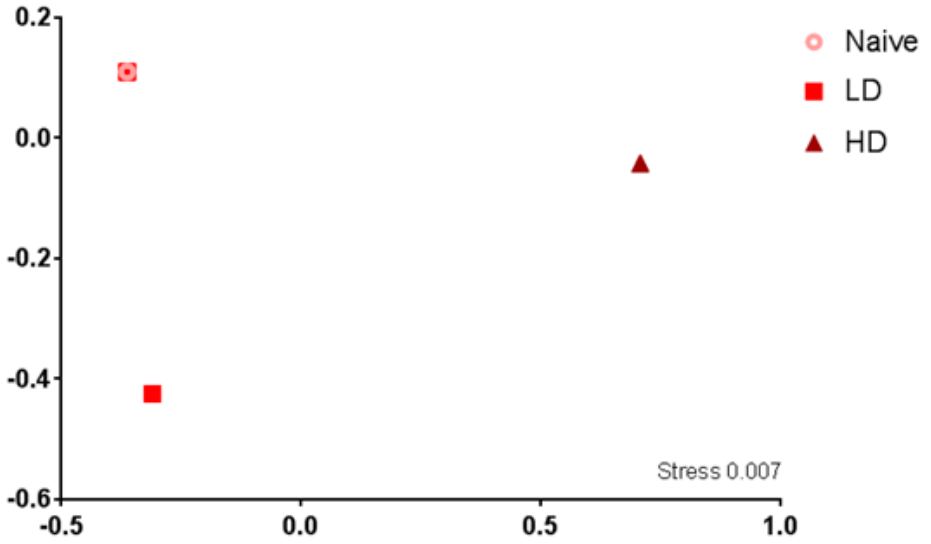

Figure 3.18 NMDS analysis of sequenced SCID day 56 p.i. caecal samples. Each point represents an individual mouse with the axis scale for Euclidian distance between samples centred on zero. Stress indicates the quality of fit of the data (<0.2 is a good fit).

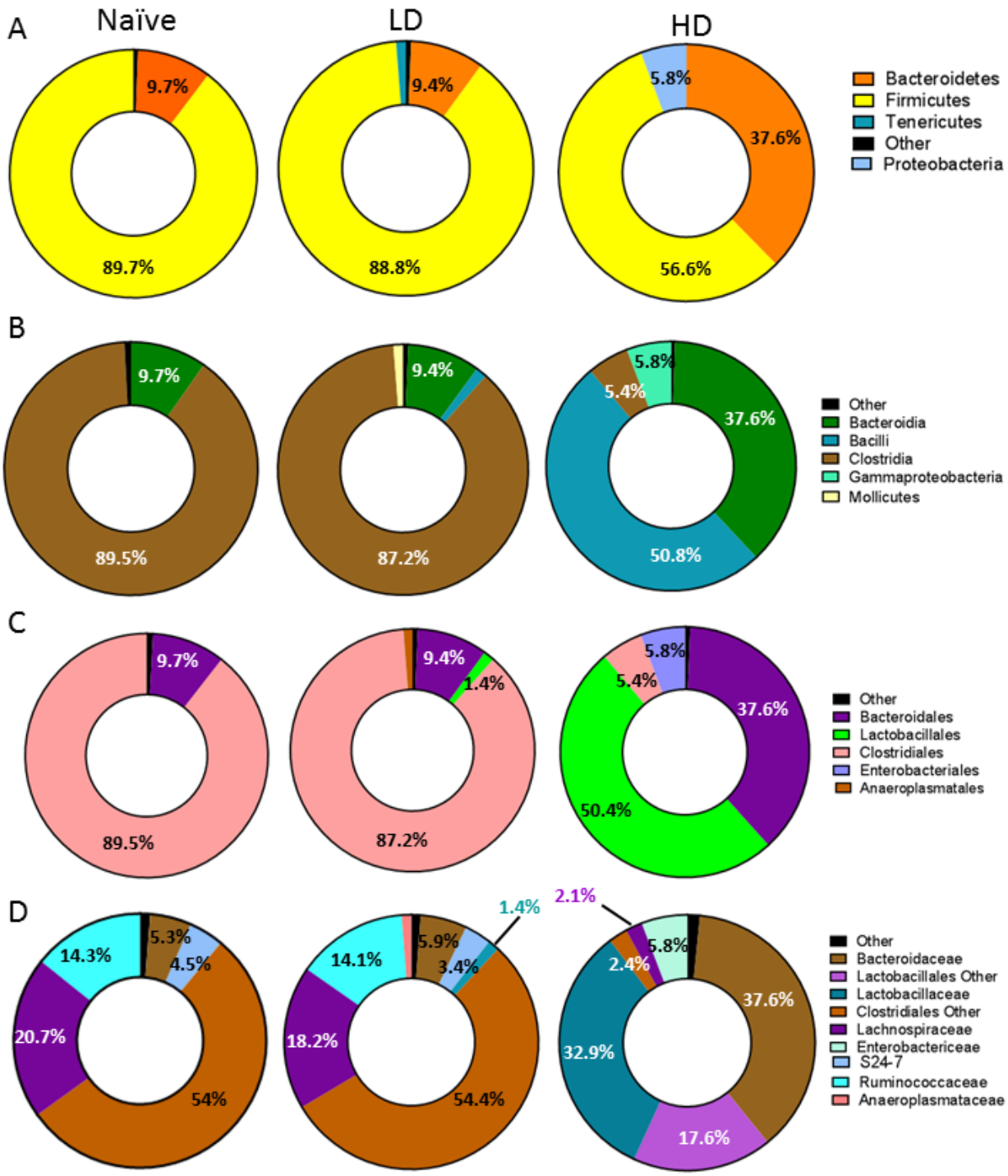

Figure 3.19 Comparison of the proportional changes that occur in the intestinal microbiota of low and high dose *T. muris* infected SCID, compared to naïve controls, by 16S Illumina sequencing of caecal contents at day 56 p.i. The rarefied OTU table was used to compare proportions shown in % between naïve, low dose (LD) and high dose (HD) samples at different levels; (**A**) phylum, (**B**) class, (**C**) order and (**D**) family. Groups less than 1% were pooled into 'Other'. A full list of proportional changes can be found in table B in the supplied appendix.

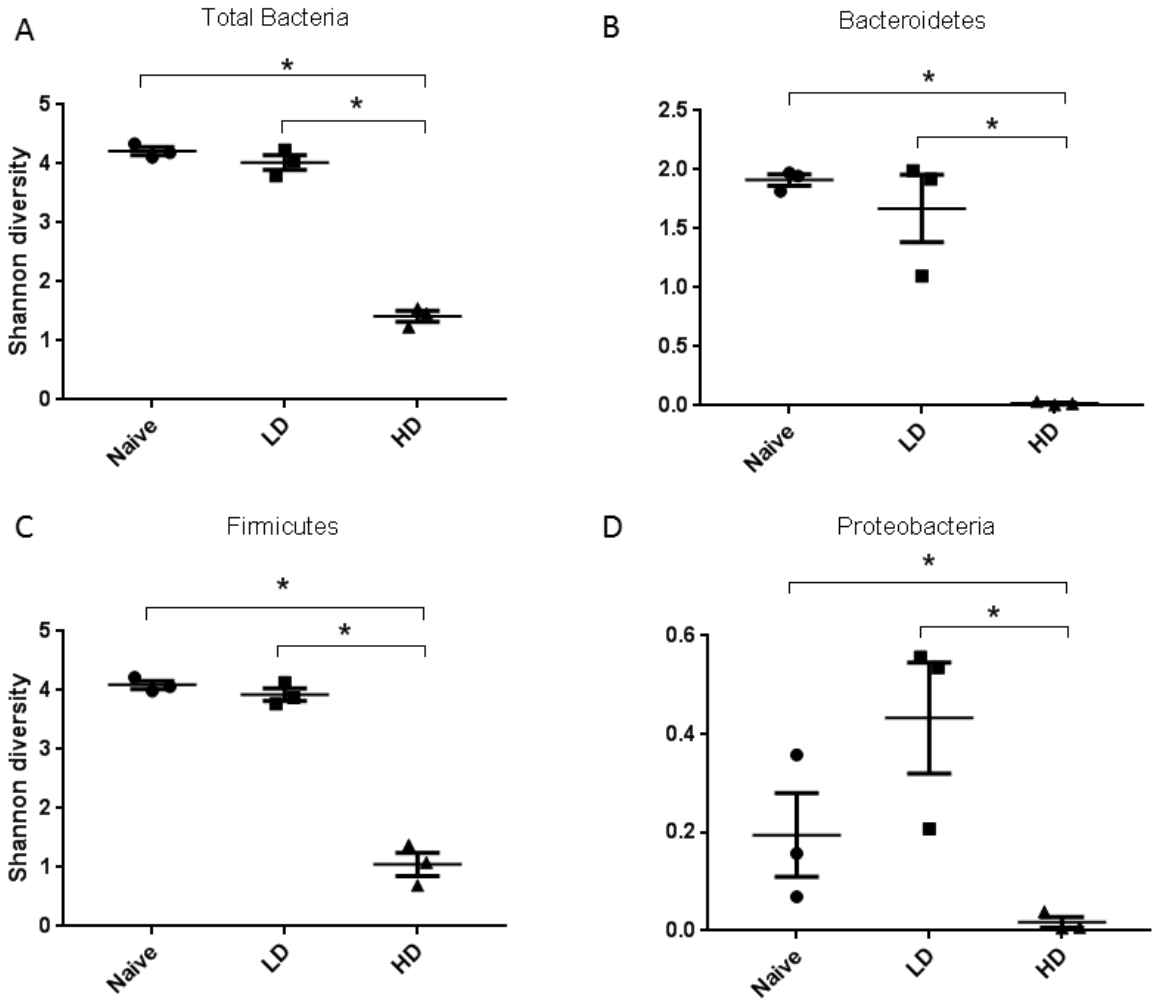

Figure 3.20 Shannon diversity of intestinal microbiota at day 56 p.i. in SCID caecal samples. Differences in bacterial alpha diversity were determined from the rarefied OTU table in QIIME between naïve, and low and high dose infected samples, for (**A**) total bacteria, (**B**) Bacteroidetes, (**C**) Firmicutes, and (**D**) Proteobacteria. Values represent mean +/- SEM. * indicates significance ($P < 0.0001$) as calculated by ANOVA with TukeyHSD tests.

3.2.7 High dose infection in SCID mice results in a more acidic intestinal environment

To determine if the shift in bacterial communities as a result of high dose infection impacted intestinal pH, stools collected at day 56 p.i., from the same SCID mice that had caecal contents sequenced, were used for pH measurements. Stools were added to dH_2O, vortexed well and centrifuged. The resulting supernatant was used for pH measurements using a flat head pH probe. Three measurements were taken for each sample, using three samples per group and these averages were plotted. Figure 3.20 shows that with a high level infection of *T. muris*, there is a significant drop in stool pH compared to naïve and low dose samples, with low level infection having no impact on pH. This may be due to the enrichment of lactic acid producing *Lactobacillales* in high dose infected SCID mice, reducing the pH within the intestinal tract.

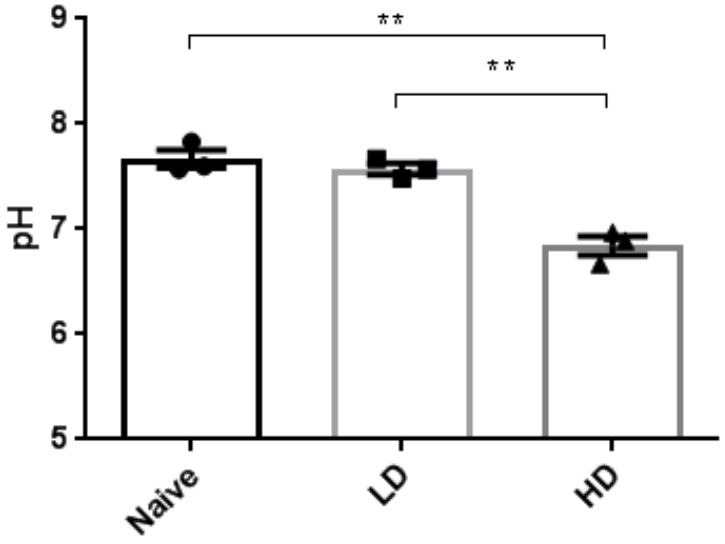

Figure 3.21 pH of day 56 p.i. stool samples from SCID mice infected with a high and low dose of *T. muris* compared to naïve animals. Stools were emulsified in water, centrifuged and the pH of the remaining supernatant was measured using a flat surface pH electrode. Each point represents 3 repeat readings (technical replicates) per individual mouse (N = 3; biological replicates). Values represent mean +/- SEM. ** indicates significance (P < 0.002).

3.3 Discussion

It is known that parasitic nematodes which inhabit the GI tract of their host can induce significant alterations to the host intestinal microbiota. This is true for *T. muris*, and other *Trichuris* species, as shown in wild type C57BL/6 mice with low dose infection. This chapter presents data using high dose infections in both C57BL/6 and immunodeficient SCID mice, demonstrating the impact on microbiota composition and spatial organisation, as well as caecal SCFA concentrations as a result of *T. muris* infection for the first time.

3.3.1 *T. muris* infection causes significant alterations to the intestinal microbiota that are dose dependent in C57BL/6 mice

As shown previously, C57BL/6 mice infected with a low dose of *T. muris* embryonated eggs have an intestinal microbiota that is significantly different to that of naïve mice. This was characterised by slight shifts in bacterial proportions including an increase in Proteobacteria, a loss of *Prevotella*, and a significant decrease in overall diversity and species richness (Holm *et al.,* 2015; Houlden *et al.,* 2015). Decreased bacterial diversity is also seen in IBD patients and therefore may be a result of inflammation (Sartor and Mazmanian, 2012). Furthermore, in agreement with previous studies, an increase in the *Deferribacteraceae* family, specifically the *Mucispirillum* species, was seen in low dose samples (Houlden *et al.,* 2015; Li *et al.,* 2012). These bacteria inhabit the mucus layer of the intestinal tract and therefore may thrive as a result of the altered mucus production, and disruption of the mucin layer that occurs during chronic *T. muris* infection (Hasnain *et al.,* 2012; Robertson *et al.,* 2005). Nonetheless, Holm *et al.* describe an increased abundance of Firmicutes and decreased Bacteroidetes with infection. Conversely, this study identified the opposite, although these changes were small and not significant, with low dose samples clustering more closely with naïve samples than high dose samples (Fig. 3.4). These differences may be due to several variables, for example, different sampling days (day 35 vs day 42), variations in diet and housing conditions, differences in sequencing depth and differences in worm burden. Although both studies used a low dose of ~20 *T. muris* embryonated eggs, the resulting worm burden can vary. It is evident from data presented in this chapter that low dose samples can cause a spectrum of changes in the host intestinal microbiota and resulting butyrate concentrations, and this must be considered for future work.

Moreover, microbiota changes are exacerbated with an increased worm burden during high dose infection, with a reduction in total bacterial diversity and species richness. These effects are also highly conserved as shown by the DGGE analysis, where high dose samples have a very similar banding pattern and therefore cluster together on the NMDS plot. This is not seen with low dose infection, where banding patterns are variable and beta diversity is high (Holm *et al.,* 2015; Houlden *et al.,* 2015). This again may be due

to a maximum number of worms acting as a threshold for microbiota changes, where numbers below this cause variable changes but once past the threshold, changes are highly conserved. As a result, analysis of the intestinal microbiota associated with high dose infections may give us greater insight into what bacterial species are selected for in the changed environment of the caecum following *T. muris* infection.

A high worm burden caused an enrichment of bacterial families associated with inflammation. Notably, an increase in the phyla Bacteroidetes was seen but there was significant restructuring of bacterial groups at lower taxa levels, reducing Bacteroidetes Shannon diversity. This included a significant loss of S24-7 and an increase in the family *Bacteroidaceae*, specifically the genera *Bacteroides*. Increases in the *Bacteroidaceae* are linked to a shorter GI transit time, which may also be seen during *Trichuris* infection due to symptoms of diarrhoea (Kashyap *et al.,* 2013). Furthermore, this family are increased in an inflamed gut, for example during Crohn's disease (Swidsinski *et al.,* 2002). This is likely due to their ability to use a wide range of substrates for metabolism and they are highly tolerant to oxygen exposure, enabling them to survive the changing intestinal environment as a result of *T. muris* infection (Rocha *et al.,* 2003).

Interestingly, a rise in *Enterobacteriaceae* proportions was only seen in high dose samples, increasing Proteobacterial Shannon diversity. Like the *Bacteroidaceae*, increases in this bacterial family are associated with a range of inflammatory disorders and are found to be enriched in mouse models of IBD (Earley *et al.,* 2015; Garrett *et al.,* 2010; Lupp *et al.,* 2007). During a high dose infection, there are hundreds of adult worms present in the murine lower intestinal tract and consequently the epithelial surface is severely disrupted and is accompanied by increased inflammation. This could result in fewer attachment sites for the intestinal microbiota and therefore reduced colonisation resistance against potential pathogens. Members of the *Enterobactericeae* found in the intestine can act as opportunistic pathogens, such as *Escherichia coli*, *Salmonella* and *Shigella,* and can rapidly colonise the intestinal epithelial cell surface. Therefore the environmental changes induced by a high worm burden are likely to select for bacteria that can adapt and survive in these inflammatory conditions.

Another bacterial family that increases in high dose samples, but not low dose, is the *Verrucomicrobia*. The genus *Akkermansia* is responsible for this increase and contains a single species, *Akkermansia muciniphila*. This is a mucin degrading commensal that has been associated with increased intestinal inflammation (Ganesh *et al.,* 2013). Similarly to *Mucispirillum*, these bacteria are likely to adapt to the changing intestinal environment during infection, especially the altered mucin production. Excessive mucin degradation by this bacterium may facilitate invasion of the epithelium by *T. muris*, increase inflammation and promote the interaction between the host epithelial cell layer and microbiota. This

study has also shown that bacteria can colonise the intestinal crypts during *T. muris* infection. This may be aided by the breakdown of the mucin layer by these bacteria promoting a more intimate association between the microbiota, host epithelial cell layer and the host immune system.

3.3.2 Infection causes a worm burden dependent reduction in caecal butyrate and butyrate transporter levels

Work using the helminth *H. polygyrus* has identified an increase in butyrate within the caecum as a result of infection-induced microbiota alterations. However, this parasite resides in the small intestine, a site distinct to the caecum, so changes identified will be the result of a downstream effect. On the other hand, *T. muris* infects the caecum and colon of its host and so is in close association with this microbiota. Here it has been shown that *T. muris* infection causes a significant decrease in caecal butyrate concentrations in both low and high dose infected animals. This decrease is worm burden dependent, where numbers greater than 15 cause a significant decline in butyrate concentrations in the caecum. Further to this, the decrease also reflects the reduction in butyrate transporters and the reduction in Treg cells associated with *T. muris* infection, as their expression is controlled by butyrate (Holm *et al.,* 2015; Houlden *et al.,* 2015). A reduction in butyrate transporters indicates a reduction in butyrate uptake by intestinal epithelial cells, which use this SCFA as an energy source. This reduction is also seen with intestinal inflammation and conditions such as IBD (Thibault *et al.,* 2007). This can result in host cells becoming metabolically stressed, which can increase bacterial translocation across the intestinal epithelial cell layer. Addition of butyrate can restore barrier function and reduce bacterial translocation (Lewis *et al.,* 2010). Since *T. muris* infection reduces butyrate concentrations and bacteria can colonise the intestinal crypts, therefore in close association with the intestinal epithelial cell layer, it is likely that there is increased bacterial translocation. This would be exacerbated by the burrowing of *T. muris* into the mucosal layer facilitating the movement of bacteria. Altogether this will have implications for immune responses to infection.

Removal of *T. muris* by mebendazole treatment caused butyrate concentrations and consequently butyrate transporter levels to increase. DGGE and NMDS analysis showed that the microbiota of the treated mice was significantly different to both naïve and infected mice. As a result, the microbiota induced during infection was not sustained and removal of the worm caused the microbiota to begin to recover to naïve status. Therefore, the increase in butyrate could be a result of the altered microbiota and an increase in butyrate-producing bacteria. In the infected intestine, there was a great reduction in the abundance of the *Clostridiales* order, known for their ability to synthesise butyrate, and

may explain the reduction in butyrate concentrations (Vital *et al.,* 2014). These bacteria may be enriched after the removal of worms from the intestine and thus increase butyrate levels. However, many other bacteria encode genes for the biosynthesis of butyrate, including the *Lachnospiraceae*, which are increased with high dose infection (Meehan and Beiko, 2014; Vital *et al.,* 2014). It could be that *T. muris* infection also alters the transcriptome of the microbiota, so that bacterial gene expression for butyrate production is decreased. Further work must be done to determine whether it is changes to the microbiota that cause a reduction in butyrate or if it is a worm specific effect. After removal of the worm by mebendazole, GC-MS measurements were not taken until 14 days later. This time scale could be reduced to minimise microbiota recovery and to capture butyrate concentrations that correspond to the infected microbiota.

Infection is also associated with an increase in the *Bacteroidaceae* family, specifically the genus *Bacteroides*. These bacteria utilise ammonia as their primary nitrogen source in the intestinal tract, which is also the main excretory product of many nematodes (Lee 1965; Yamamoto *et al.,* 1984). During a high level infection when there are hundreds of worms in the caecum and colon, ammonia concentrations are likely to increase substantially. As a result, there will be an increased pool of nitrogen for use by the *Bacteroides*, but not the Firmicutes including *Clostridium* species, which preferentially use free amino acids and peptides. Thus, the altered intestinal environment will select for an increase in *Bacteroides*. Furthermore, *Bacteroides* species generate amino acids from ammonia and also SCFAs (Allison *et al.,* 1984; Fischbach & Sonnenburg 2011). This may further explain the reduction in butyrate concentrations seen with *T. muris* infection, due to an increase in the abundance of bacteria that use these metabolites to produce amino acids.

Moreover, studies have shown a link between increasing SCFA concentrations and decreasing *Enterobacteriaceae* abundance. SCFAs have a bacteriostatic effect on these pathogenic bacteria minimising their ability to colonise the intestinal tract (Byrne and Dankert 1979; Lee and Gemmell 1972; van Der Wielen *et al.,* 2000). During a high level *T. muris* infection, intestinal homeostasis is perturbed with a decrease in butyrate and also an increased abundance of *Enterobacteriaceae*. Therefore, it is likely that the bacterial restructuring in response to *T. muris* infection, which includes the loss of *Clostridiales*, results in a reduction of antimicrobial butyrate and this allows an expansion of opportunistic *Enterobacteriaceae* species.

3.3.3 *T. muris* infection causes an enrichment of *Enterobacteriaceae* in the intestinal tract independently of the host adaptive immune system

High dose infection of SCID mice, which lack an adaptive immune system, caused significant alterations to the host intestinal microbiota. Low dose infection caused very slight changes with small shifts in the *Mollicutes* and *Bacilli* classes. This may be due to the lower worm burden seen with the sequenced samples (< 5 adult worms) compared to those seen in the C57BL/6 experiment (> 6 worms). Again, this highlights the sensitivity of the microbiota to worm numbers and the existence of a worm burden threshold for significant microbiota changes and consequent butyrate concentrations. Nevertheless, high dose infection was accompanied by a reduction in bacterial diversity and species richness, as seen in wild type mice. This indicates that microbiota changes occur independently of the host adaptive immune system. Infection with *H. polygyrus* has also been shown to induce microbiota alterations independently of the IL-4/13-STAT6 signalling pathway (Rausch *et al.,* 2013). In both cases, these changes must be induced by an alternative factor, such as the physical presence of the parasite itself and its secretions or the innate immune system.

As mentioned previously, high dose infection of C57BL/6 mice with *T. muris* caused an increase in *Enterobacteriaceae* in the faecal microbiota at day 42 p.i. High dose infection of SCID mice also selected for an increased abundance of these bacteria in the caecal microbiota at day 56 p.i. These changes were accompanied by a decrease in Firmicutes, particularly the *Clostridiales*, and a reduction in Firmicutes Shannon diversity, independently of the adaptive immune system. IBD and intestinal inflammation are commonly linked to a reduction in diversity and abundance of obligate anaerobes, such as the Firmicutes, and an increase in facultative anaerobes such as the *Enterobacteriaceae* (Frank *et al.,* 2007; Lupp *et al.,* 2007; Manichanh *et al.,* 2006).

The intestinal tract is typically anaerobic with low oxygen concentrations at the epithelium. This results in the formation of an oxygen gradient so that the intestinal lumen is dominated by obligate anaerobes, such as the Firmicutes and Bacteroidetes. Facultative anaerobes including the *Enterobacteriaceae* preferentially colonise the mucosal layer, and are absent or at low abundance in the lumen (Albenberg *et al.,* 2014; Swidsinski *et al.,* 2002). This may therefore explain why the *Enterobactericeae* were absent from naïve and low dose samples for both strains of mouse. High dose infections promote the outgrowth of this family and are therefore detected in the intestinal lumen. Interestingly, *T. trichiura* infection in macaques showed that infection resulted in reduced bacterial attachment (Broadhurst *et al.,* 2012). As the *Enterobacteriaceae* are usually found attached to the mucosal layer, *T. muris* infection may promote their detachment and subsequent detection in the luminal contents of the caecum and faeces (Swidsinski *et al.,* 2002).

The host inflammatory response to infection can increase oxygen concentrations in the intestinal tract causing dysanaerobiosis (Rigottier-Gois, 2013). A recent study has shown that inflammation caused by *Salmonella* infection results in a decrease in *Clostridia*, which in turn depletes butyrate concentrations in the intestinal tract (Rivera-Chávez *et al.,* 2016). This is similar to the changes seen in this study with high dose *T. muris* infections. During intestinal homeostasis, butyrate is transported into host intestinal epithelial cells for oxidation and subsequent use as an energy source. This uses high concentrations of oxygen and causes the intestinal epithelium to become hypoxic (< 1% O_2). Reduced butyrate concentrations, as seen with *Salmonella* and *T. muris* infection, can cause intestinal epithelial cells to ferment glucose as an alternative energy source (Kelly *et al.,* 2015; Rivera-Chávez *et al.,* 2016). The lack of oxidation consequently increases oxygen concentrations within the intestinal epithelium and also the lumen (Espey, 2013). Increased oxygen concentrations throughout the intestinal tract, and not just at the epithelial surface, would select for and increase the abundance of bacteria that are able to use oxygen for respiration, i.e. facultative anaerobes. This could therefore explain the increase in *Enterobacteriaceae* within the intestinal tract of mice infected with a high dose of *T. muris*, independently of the adaptive immune system. Furthermore, butyrate is a strong inhibitor of IFN-γ signalling in the intestinal tract and susceptibility to *T. muris* infection is characterised by and dependent on this cytokine (Else *et al.,* 1994; Klampfer *et al.,* 2003). A decrease in butyrate-producing bacteria, such as the *Clostridiales*, and consequently lower butyrate concentrations would therefore be beneficial to *T. muris* to prevent its expulsion from the intestine of its host.

Oxidative burst caused by the release of reactive oxygen species can also contribute to the changing intestinal environment and this has been linked to IBD pathology (Zhu and Li, 2012). Reactive oxygen and nitrogen species can react with luminal compounds to produce respiratory electron acceptors that can be used by *Enterobacteriaceae* species, such as *Salmonella*, giving them a selective advantage over other bacterial species (Winter *et al.,* 2010). Other innate immune responses should also be investigated, including the production of antimicrobial peptides, some of which have been associated with *T. muris* infection. An increase in angiogenin 4 (Ang4) production is seen in the large intestine during *T. muris* infection, but is most noticeable in resistant strains. Therefore it is unlikely that levels will be significantly increased in susceptible SCID mice to cause significant alterations to the host microbiota (Forman *et al.,* 2012). Furthermore, antimicrobial levels were also analysed during *H. polygyrus* infection with no increases in expression compared to naïve controls (Rausch *et al.,* 2013).

3.3.4 An enrichment of *Lactobacillales* and decreased intestinal pH occurs in high dose infections in an immunodeficient mouse

A significant expansion of the *Lactobacillales* order was detected making up over half the caecal microbiota of high dose infected SCID mice, with 32.9% explained by an increase in the *Lactobacillaceae* family. A small increase was detected in low dose infected mice (1.3%), but was not seen in any wild type mice or naïve SCID mice. An increase in the family *Lactobacillaceae* was also identified in the faeces and caecal content of *T. muris* low dose infected wild type mice (Holm *et al.,* 2015). These bacteria are also facultative anaerobes and will therefore thrive in an increasingly oxygenated intestinal tract, as discussed above. Furthermore, as lactic acid bacteria (LAB), members of this group produce lactic acid as an end product of carbohydrate metabolism (Walter, 2008). An increased production of lactic acid by the intestinal microbiota could explain the reduction in pH seen with high dose infection. Since SCFA concentrations decrease, in the case of butyrate and propionate, or are unchanged as for acetate, it is unlikely that the reduction in pH is associated with these acids. These bacteria are also acid-tolerant so would be able to colonise the intestine with a lower pH in the absence of more sensitive bacteria (Walter, 2008). Furthermore, *Lactobacillus* species have been shown to increase host susceptibility to helminth infection, in particular, *L. casei* treatment of B10Br mice has been found to increase *T. muris* worm burden (Dea-Ayuela *et al.,* 2008; Reynolds *et al.,* 2014). Therefore, *T. muris* may select for these bacteria in order to promote its own infection within the intestinal tract.

Summary

- *T. muris* infection causes dose dependent alterations to the host intestinal microbiota in wild type and immunodeficient hosts, resulting in decreased bacterial diversity and species richness.
- The microbiota colonise intestinal crypts during *T. muris* infection.
- *T. muris* infection results in a significant decrease in caecal butyrate concentrations and butyrate transporter gene expression by host intestinal epithelial cells, which is worm burden dependent.
- High dose infections are associated with increases in specific bacterial families including the *Bacteroidaceae*, *Enterobacteriaceae* and *Verrucomicrobiaceae* in wild type mice.
- Increases in bacterial groups associated with inflammation are selected for during high dose infection of wild type and SCID mice.

- Increased worm burden in SCID mice selects for an increase in facultative anaerobes such as the *Enterobacteriaceae*, independently of the adaptive immune system.
- High dose infection in an immunodeficient animal causes an outgrowth of the *Lactobacillales* order and a decrease in pH.

Chapter 4

Defining the intestinal microbiota of the parasitic helminth *T. muris*

4.1 Introduction

Many organisms that have an intestinal tract are colonised by complex bacterial communities that are important for their health. This is not restricted to larger, more complex organisms but smaller, parasitic organisms, which also have an intestinal tract, can harbour a diverse microbiota. Free-living non-pathogenic parasites such as *C. elegans* and *Acrobeloides maximus*, that consume bacteria as a food source, have core intestinal microbiotas dominated by Proteobacterial families. For both nematodes, their microbiotas were distinct to the soil communities they were isolated from, indicating a host-dependent process to select for a specific core microbiota, independently of the environmental diversity (Baquiran *et al.,* 2013; Berg *et al.,* 2016; Dirksen *et al.,* 2016).

However, whether medically relevant nematode pathogens that infect the same niche as the resident microbiota also carry a diverse bacterial community has not been fully investigated. Although the intracellular bacterial genus *Wolbachia* has been detected in its filarial parasitic host, these bacteria are vertically transmitted and are typically found in the hypodermal cells of the lateral cords and female reproductive organs. This endosymbiont is important for the fitness of the parasite but exists in isolation, unlike the diverse communities present in the intestinal tract of many organisms (Taylor *et al.,* 2005a).

The location of *T. muris* within the crypts of the caecum and colon results in an intimate association with the complex intestinal microbiota of the host. Previous work has revealed that *T. muris* depends on the host intestinal microbiota for hatching and successful establishment within the intestinal tract (Hayes *et al.,* 2010). Furthermore, subsequent infection induces restructuring of the bacterial communities present in the host intestinal tract and therefore alters its metabolic potential (Holm *et al.,* 2015; Houlden *et al.,* 2015).

The recent evidence demonstrating the close relationship between *T. muris* and its host's intestinal microbiota, together with the existence of parasite-microbiota interactions in nature, led to the investigation into whether *T. muris* harbours its own internal microbiota, promoting its long term survival in the host.

Aims

The aim of this chapter was to investigate whether *T. muris* adults harbour an internal microbiota.

This was achieved through the following objectives;

1. Develop a method to surface sterilise adult *T. muris* worms for internal microbiota analysis.
2. Analyse the internal microbiota of adult *T. muris* using molecular methods and compare to the intestinal microbiota of its host.

3. Is there an impact of parasite gender or the naïve intestinal microbiota of the host on the *T. muris* internal microbiota?
4. Determine the localisation of this microbiota within adult worms.

4.2 Results

4.2.1 Surface sterilisation of adult *T. muris* allows analysis of the internal microbiota

To determine if the GI parasite *T. muris* has an internal microbiota, any surface contaminants had to first be removed to ensure analysis did not include any adherent bacteria or their DNA. Adult *T. muris* worms were harvested from chronically infected C57BL/6 mice at day 42 p.i. and treated with 3% sodium hypochlorite for 10 minutes followed by five washes with sterile H_2O. Previous work had shown that bleaching for this amount of time resulted in efficient surface sterilisation without degradation of the parasites (A. Houlden, personal communication). To confirm this, the final two washes from 8 sterilised *T. muris* worms were centrifuged at 13,000 g for 5 min, the supernatant removed and pellets resuspended in 20 µl sterile water. To detect any bacterial contaminants, 10 µl of each wash was used for PCR with universal 16S rRNA gene primers (See Table 2.3, Materials and Methods) and analysed on a 1% agarose gel. Figure 4.1A shows that no bacterial DNA was detected in any of the samples (lanes 1 – 16; 2 washes from each worm), apart from the unbleached worm (lane UB), therefore suggesting that bleaching for 10 minutes successfully sterilised the parasites. This consequently prevents any interference with the analysis of the *T. muris* internal microbiota.

To ensure that the lack of amplification seen was not due to an inhibitory effect of residual bleach, the five washes were used for PCR with 16S rRNA primers again but with additional *E. coli* gDNA. Figure 4.1B shows that the first wash post-bleaching (lanes A1, B1 and C1) inhibited the PCR reaction but the consequent four washes did not contain inhibitory levels of sodium hypochlorite. Therefore for all future analysis, 10 minutes bleaching with 3% sodium hypochlorite followed by 5 washes in H_2O was used.

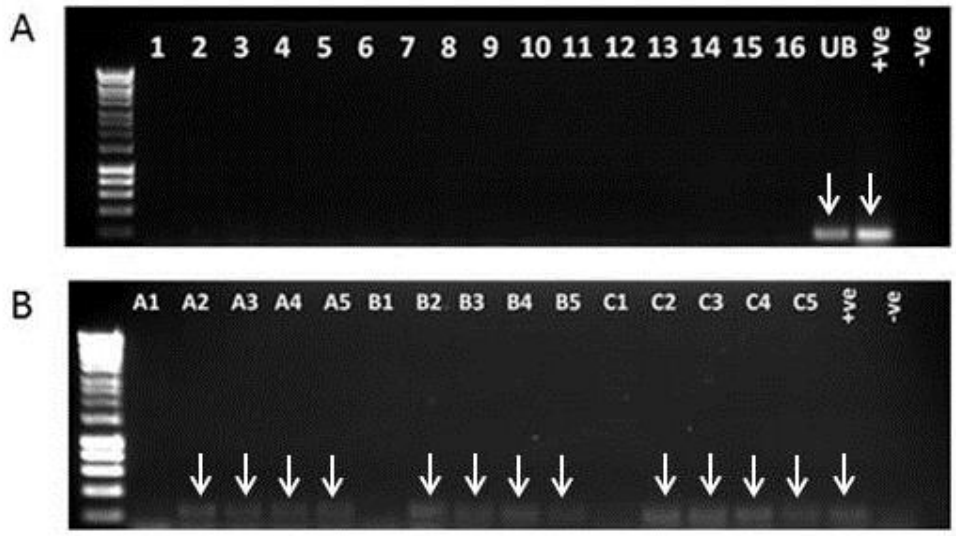

Figure 4.1 Bleaching with 3% sodium hypochlorite followed by 5 washes with sterile H_2O results in successful surface sterilisation of adult *T. muris* worms. (**A**) The final two washes of 8 surface sterilised adult *T. muris* worms isolated from C57BL/6 mice were used for PCR analysis with universal 16S rRNA gene primers (lanes 1 – 16). Lane UB is a wash from an unbleached *T. muris* adult worm. (**B**) Five H_2O washes (1 – 5) from 3 surface sterilised *T. muris* adult worms (A, B and C), spiked with *E. coli* gDNA, and were used for PCR analysis to detect any inhibitory levels of sodium hypochlorite. Lane +ve is *E. coli* genomic DNA as a positive control and –ve is H_2O as a negative control. White arrows indicate positive bands.

4.2.2 The *T. muris* microbiota is conserved and is significantly different to its host's microbiota

In order to analyse the *T. muris* internal microbiota and the caecal microbiota of its host, C57BL/6 mice were chronically infected with ~20 *T. muris* embryonated eggs (n=4; B1 – B4) and compared to a naïve control group (n=3; A1 – A3) (Fig. 4.2). Caecal contents were collected at day 42 p.i. from naïve and infected mice. Three male and three female adult worms were also isolated from each of the infected mice and surface sterilised as described previously. DNA was extracted from all caecal and worm samples and the universal 16S rRNA gene was amplified by PCR. The resulting PCR products were visualised by DGGE. Figure 4.2 shows that *T. muris* infection causes significant changes to the host intestinal microbiota and that the worm microbiota shows a consistent banding pattern, which is different to both naïve and infected host intestinal microbiotas.

NMDS analysis of the DGGE data demonstrated a distinct clustering of *T. muris* samples away from host intestinal samples (naïve and infected), and also confirmed a clear shift in bacterial communities as a result of infection (Fig 4.3A). Further analysis using PERMANOVA on the NMDS distance matrix (Adonis function in vegan package R), showed significant differences between the *T. muris* microbiota and the microbiotas of the naïve host, the environment the worm initially infects ($P = 0.0004$), and the infected host, the environment the worm resides within ($P = 0.00005$) (Fig 4.3C).

Figure 4.3B is an enlarged NMDS plot of the boxed area on figure 4.3A, showing male and female *T. muris* worms only. To determine if the microbiota varied due to worm gender, PERMANOVA analysis was also performed on this NMDS distance matrix comparing male and female worms only (Fig 4.3B and D). There was no significant difference between the worm microbiotas ($P = 0.8$) with samples clustering closely. Additionally, although worms were isolated from different hosts, they remain clustered indicating that the microbiota is conserved between worms, regardless of gender or individual host.

As bleaching removes any external bacteria, the bacterial communities detected must represent an internal *T. muris* microbiota. Furthermore, embryonated eggs used to infect the mice are sterile shown by PCR analysis with 16S rRNA gene primers (A. Houlden, personal communication) so *T. muris* must gain this microbiota after hatching within the caecum and colon and selecting its microbiota from the naïve host.

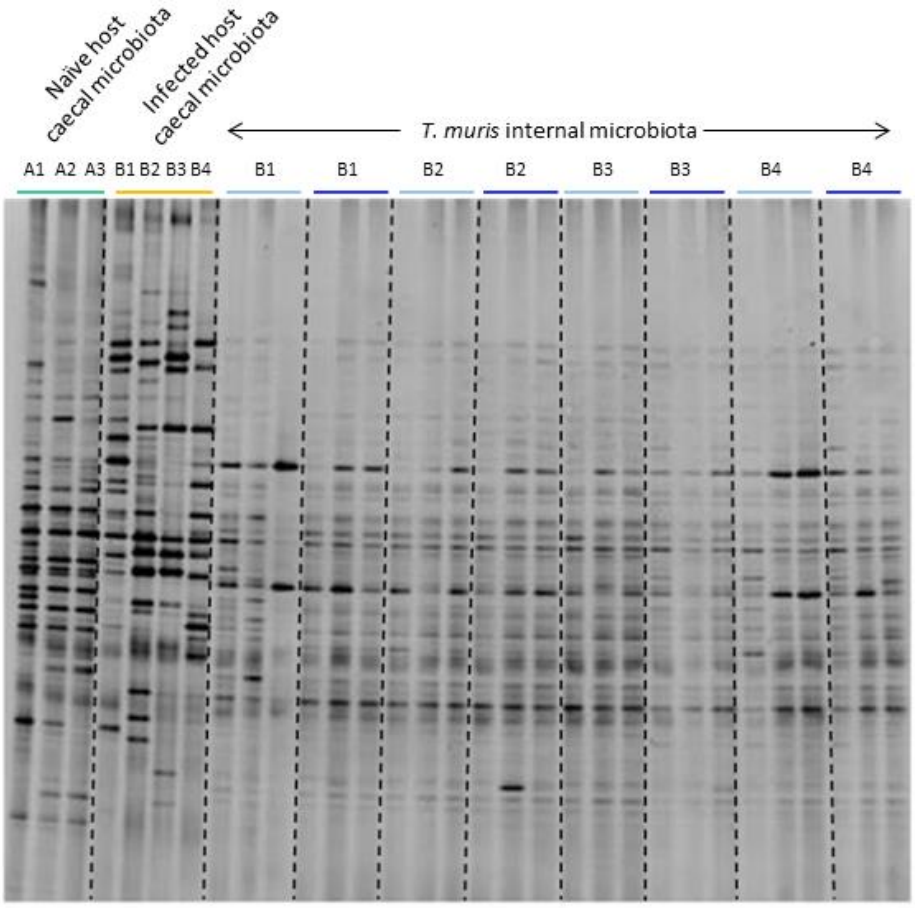

Figure 4.2 DGGE analysis of the microbiotas associated with *T. muris* and its host. Caecal contents from 3 naïve C57BL/6 mice (A1 – A3) (green) and 4 infected C57BL/6 mice (B1 – B4) (orange), together with 3 male (pale blue) and 3 female (dark blue) adult *T. muris* from each infected mouse. Samples were subjected to DNA extraction, PCR using primers specific for the 16S rRNA gene and DGGE analysis, where each band represents a bacterial species.

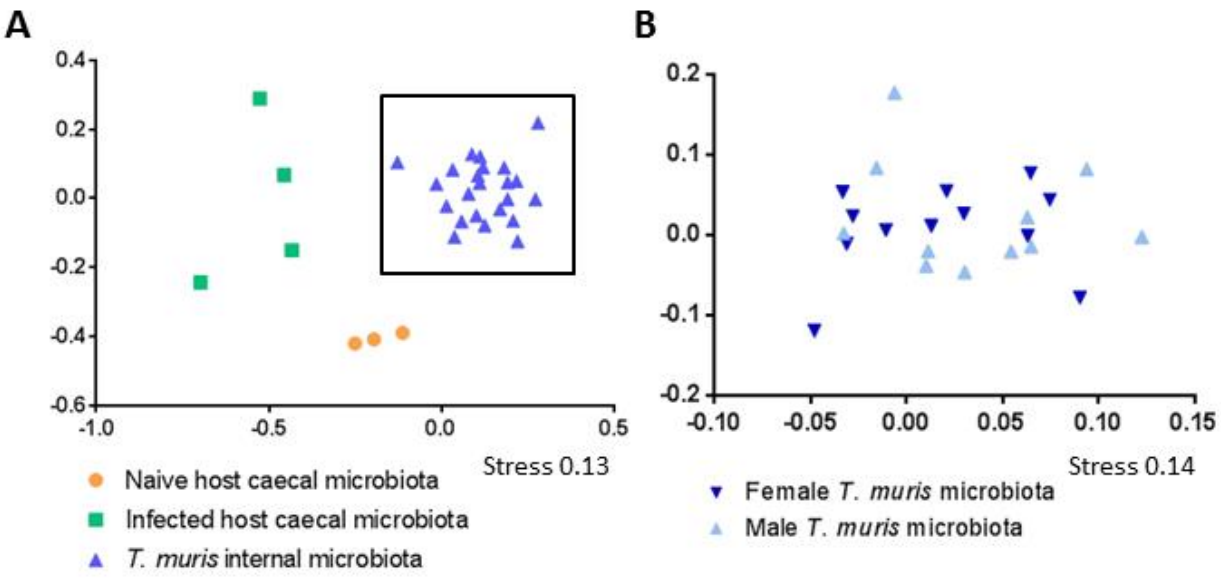

C

	Infected host caecal microbiota	*T. muris* microbiota
Naïve host caecal microbiota	**0.03 ***	**0.0004 *****
Infected host caecal microbiota	-	**0.00005 *****

D

	Female *T. muris* microbiota
Male *T. muris* microbiota	0.8

Figure 4.3 NMDS analysis of bacterial communities in naïve and infected host caecal contents, and within *T. muris* worms, by 16S rRNA gene DGGE. (**A**) NMDS plot of naïve (orange circles) and infected caecal microbiotas (green squares), and *T. muris* internal microbiotas (purple triangles) at day 42 p.i. Each point represents an individual mouse or *T. muris* adult worm with the axis scale for Euclidian distance between samples centred on zero. Stress indicates the quality of fit of the data (<0.2 is a good fit). (**B**) Samples represent the boxed *T. muris* samples in (A) and the impact of worm gender is compared with dark blue triangles representing female *T. muris* and pale blue triangles for males. Each point represents an individual *T. muris* adult worm. (**C** and **D**) RStudio was also used to perform a permutational ANOVA (PERMANOVA, Adonis function in RStudio), which does not require any assumptions about the distribution of the data, on the dissimilarity matrix to calculate P values between groups. P values were adjusted to account for multiple comparisons using the p.adjust method, which is based on the Bonferroni correction method, in RStudio. * indicates significance <0.05 and ***<0.001.

4.2.3 *T. muris* maintains a conserved microbiota regardless of the host intestinal microbiota

Although the data suggests strong selection by *T. muris* for a microbiota that is shared between worms, it is not clear whether this is dependent on the hatching environment, i.e. the initial intestinal microbiota of its host. Previous work was undertaken using worms isolated from one strain of mouse, and therefore a similar hatching environment (the naïve intestinal microbiota). To address this, inbred genetically distinct mouse strains including two immune-deficient strains, Rag2 KO and SCID, were infected with a high (~200 eggs) dose of *T. muris*, and C57BL/6 and another group of SCID mice were given a low (~20 eggs) dose. It has been shown previously that these mice have distinct intestinal microbiotas (Friswell *et al.,* 2010; Thoene-Reineke *et al.,* 2014) and that differences in infective dose can result in different host microbiota alterations in mice of the same genetic background and batch (Chapter 3). To ensure that the mice also showed the same distinct intestinal microbiotas, 16S rRNA PCR followed by DGGE analysis was performed using stool samples from naïve mice of each strain (N = 5 per group). Figure 4.4 shows how each host strain had a different naïve intestinal microbiota, with each group clustering separately. These differences are significant as shown by PERMANOVA analysis on the NMDS distance matrix, where the intestinal microbiotas of SCID mice and C57BL/6 mice were strikingly different (P = 0.00003). This has been shown previously (Friswell *et al.,* 2010) and confirms the impact of genetic background and immune-deficiency on the composition of the intestinal microbiota.

Once adult worms were present in the caecum and colon (from day 32 p.i.), caecal contents and worms were harvested for bacterial community analysis. Critically, the microbiota of *T. muris* isolated from each host strain was remarkably similar (no significant difference; Fig 4.5B) and was also distinct from its host's intestinal microbiota, suggesting that *T. muris* must select for a specific conserved microbiota irrespective of the bacterial community it hatches and lives within.

To determine the number of bacteria that are typically found in the *T. muris* microbiota and to see if this varies over time, DNA was extracted from surface sterilised worms isolated at day 42 and 91 p.i. from C57BL/6 mice (n = 5; 1 worm per mouse). The DNA was then used for qPCR with universal 16S rRNA gene primers to quantify the gene copy number per worm, allowing an estimation of bacterial abundance. At day 42 p.i. worms harbour around 5×10^4 bacteria. This number stays constant as the worm ages within the host as day 91 worms had similar levels (Fig. 4.6). This suggests that the parasite is maintaining its microbiota over time as it ages perhaps to benefit its survival within its host.

A

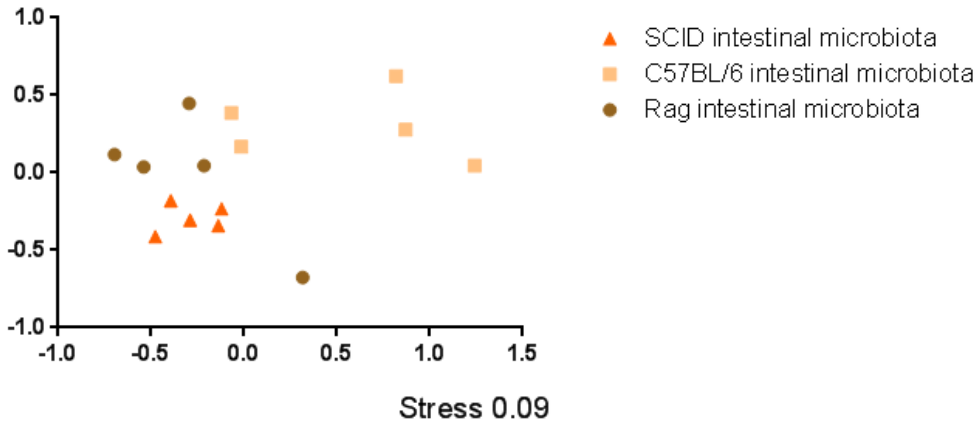

B

	SCID intestinal microbiota	C57BL/6 intestinal microbiota
Rag intestinal microbiota	**0.01 ***	**0.02 ***
SCID intestinal microbiota	-	**0.00003 *****

Figure 4.4 NMDS analysis of bacterial communities in naïve stools from different strains of mouse by 16S rRNA DGGE. (**A**) NMDS plot of intestinal microbiotas from C57BL/6, Rag2 KO and SCID mice (N=5 per group). Each point represents an individual mouse with the axis scale for Euclidian distance between samples centred on zero. Stress indicates the quality of fit of the data (<0.2 is a good fit). (**B**) RStudio was also used to perform a permutational ANOVA (PERMANOVA, Adonis function in RStudio), which does not require any assumptions about the distribution of the data, on the dissimilarity matrix to calculate P values between groups. P values were adjusted to account for multiple comparisons using the p.adjust method, which is based on the Bonferroni correction method, in RStudio. * indicates significance <0.05, ***<0.001.

A

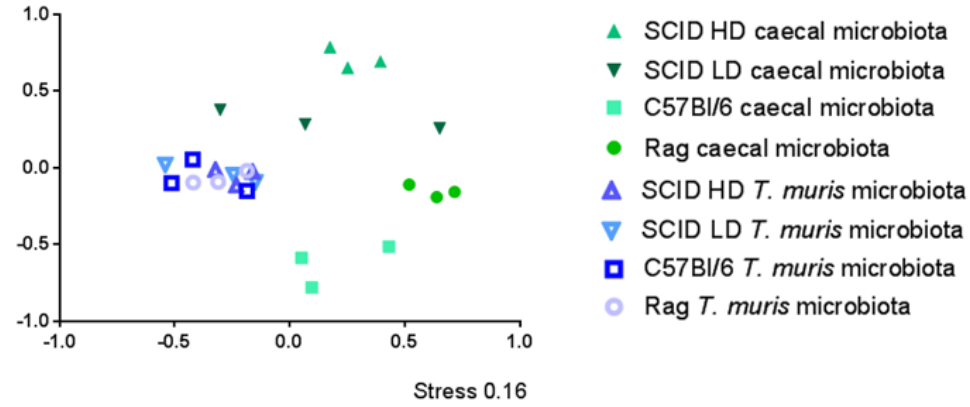

Stress 0.16

B

	Rag *T. muris* microbiota	C57BL/6 *T. muris* microbiota	SCID LD *T. muris* microbiota	SCID HD *T. muris* microbiota	Rag caecal microbiota	C57BL/6 caecal microbiota	SCID LD caecal microbiota
SCID HD caecal microbiota	0.04 *	0.00008 ***	0.04 *	0.00008 ***	0.04 *	0.04 *	0.00008 ***
SCID LD caecal microbiota	0.04 *	0.00008 ***	0.04 *	0.00008 ***	0.00008 ***	0.04 *	-
C57BL/6 caecal microbiota	0.04 *	0.04 *	0.04 *	0.04 *	0.00008 ***	-	-
Rag caecal microbiota	0.04 *	0.00008 ***	0.00008 ***	0.04 *	-	-	-
SCID HD *T. muris* microbiota	0.448	0.622	0.828	-	-	-	-
SCID LD *T. muris* microbiota	0.313	0.585	-	-	-	-	-
C57BL/6 *T. muris* microbiota	0.255	-	-	-	-	-	-

Figure 4.5 NMDS analysis of the caecal microbiota from different strains of mice infected with *T. muris*, and the microbiota of their infecting worms, by 16S rRNA DGGE. (**A**) NMDS plot of caecal microbiotas associated with SCID mice given both a low dose (LD; ~20 eggs) and a high dose (HD; ~200 eggs) at day 56 p.i., Rag2 KO mice given a high dose at day 42 p.i., and C57BL/6 mice given a low dose at day 42 p.i. The microbiotas of *T. muris* worms isolated from each mouse are also plotted. Each point represents an individual *T. muris* adult worm or individual mouse with the axis scale for Euclidian distance between samples centred on zero. Stress indicates the quality of fit of the data (<0.2 is a good fit). (**B**) RStudio was also used to perform a permutational ANOVA (PERMANOVA, Adonis function in RStudio), which does not require any assumptions about the distribution of the data, on the dissimilarity matrix to calculate P values between groups. P values were adjusted to account for multiple comparisons using the p.adjust method, which is based on the Bonferroni correction method, in RStudio. * indicates significance. Pale blue shading indicates no significant difference.

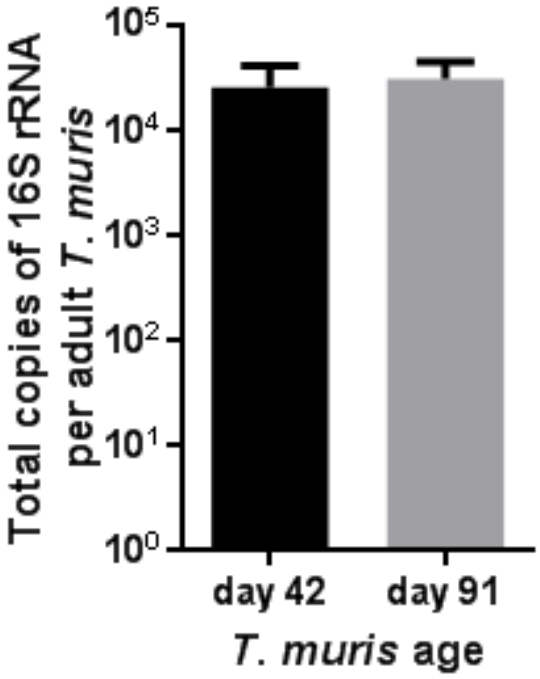

Figure 4.6 Bacterial abundance within an adult *T. muris* worm over time. DNA was extracted from adult worms isolated from C57BL/6 mice at day 42 p.i. and day 91 p.i. (n = 5 per time point; 1 worm per mouse) and used for qPCR with universal 16S rRNA gene primers. The total copy number of the 16S rRNA gene per worm was calculated inferring the bacterial load. Values represent mean +/- SEM.

4.2.4 The *T. muris* microbiota is located within the parasite intestinal tract

To determine where the complex microbiota isolated from adult *T. muris* worms was located, SCID and AKR mice were infected with a high dose (~ 200 embryonated eggs) of *T. muris* and harvested at day 42 p.i. Worms were processed for histological analysis using a method by Carleton *et al.,* (1980) with revisions, due to the *Trichuris* impermeable and tough cuticle making traditional methods ineffective. This method involved cutting worms into segments to assist penetration of fixative and used cedarwood oil as a clearing agent, as it hardens tissues gently and is therefore useful for already hard or dense samples. However, it acts slowly so longer incubations are required compared to traditional clearants, and it becomes difficult to remove from tissues. As a consequence treatment was followed by a short incubation in xylene to allow successful infiltration of wax. A final wax incubation under vacuum was included to allow complete impregnation of tissues with wax. Worms were embedded as bundles, cut into 5 µm sections and used for FISH. A Cy3 double labelled 16S rRNA gene probe, EUB338, that targets most *Bacteria* (3' binding positions 338 – 355) was hybridised to sections of adult *T. muris* for 2 h in a probe buffer. To reduce autofluorescence, sections were treated with Sudan black B (SBB) allowing better detection of the *T. muris* microbiota.

Analysis of sections with a fluorescent microscope detected signals within the intestinal tracts of worms (Fig. 4.7) and signals were not identified elsewhere within the worm. Consecutive sections were also hybridised with a double labelled Cy3 probe complementary to EUB338 (NON338) to control for non-specific binding, and no fluorescence was detected (Fig 4.8). This indicated the presence of an intestinal microbiota within the intestinal tracts of adult *T. muris* worms.

As previously mentioned, *T. muris* must gain its microbiota from the bacterial communities that inhabit the naïve murine intestinal tract. Although *Trichuris* eggs are exposed to unsterile environments, such as soil, during its life cycle, they will not hatch. Hatching only occurs in the presence of intestinal bacteria at 37°C and the parasite is protected by a dense outer shell (Hayes *et al.,* 2010; Preston and Jenkins, 1985). Therefore no hatching will occur outside of the host and there is no free-living form of this parasite outside of the lower intestinal tract, where the first bacteria they encounter is the intestinal microbiota. To investigate the uptake of bacteria by *T. muris* during infection, adult worms were isolated from AKR mice infected with a high dose and incubated with *gfp* - expressing *E. coli* overnight. After washing with media containing antibiotics to remove any surface adherent bacteria, worms were processed for sectioning as previously described and hybridised with the EUB338 probe. Figure 4.9 shows the clear localisation of ingested *gfp E.coli* (Fig. 4.9C; green) with the red resident microbiota (Fig. 4.9D; red) in the nematode intestinal

tract, shown as yellow in figure 4.9D. This demonstrates that *T. muris* can ingest bacteria from their environment and that these bacteria are able to colonise the intestinal tract.

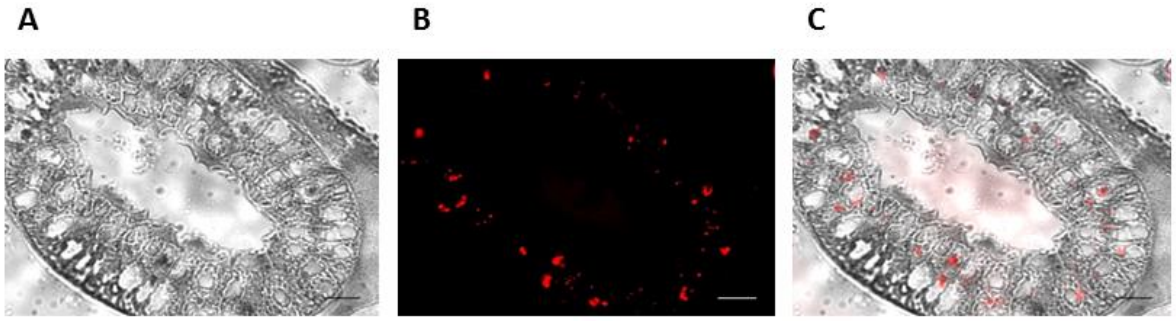

Figure 4.7 Detection of the *T. muris* microbiota within the nematode intestinal tract. FISH was performed on cross-sections of an adult *T. muris* intestinal tract hybridised with a Cy3 labelled 16S universal rRNA gene probe for 2 hours (100X). (**A**) Light-field image; (**B**) Cy3 fluorescence image (red); (**C**) combined image. Scale bars, 10 µm.

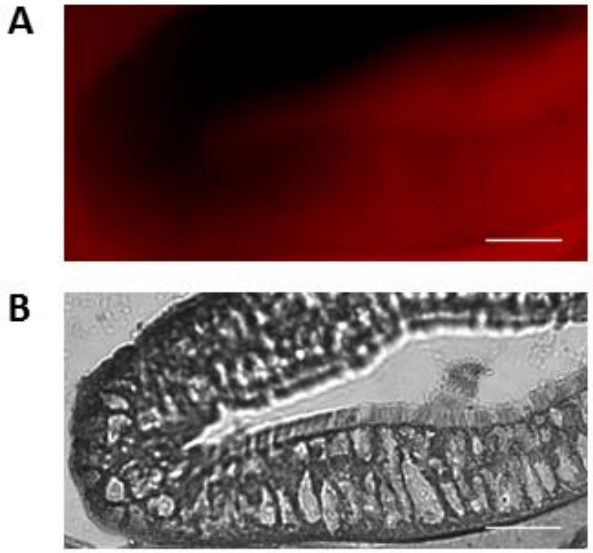

Figure 4.8 No fluorescence is detected using a control Cy3 labelled probe on sections of adult *T. muris* intestinal tracts. Sections were treated the same as those with the 16S rRNA gene probe (EUB338) but instead using a complementary probe (NON338) to control for non-specific binding, and imaged using the (**A**) Cy3 and (**B**) light-field channels (100X). Scale bars, 10 µm.

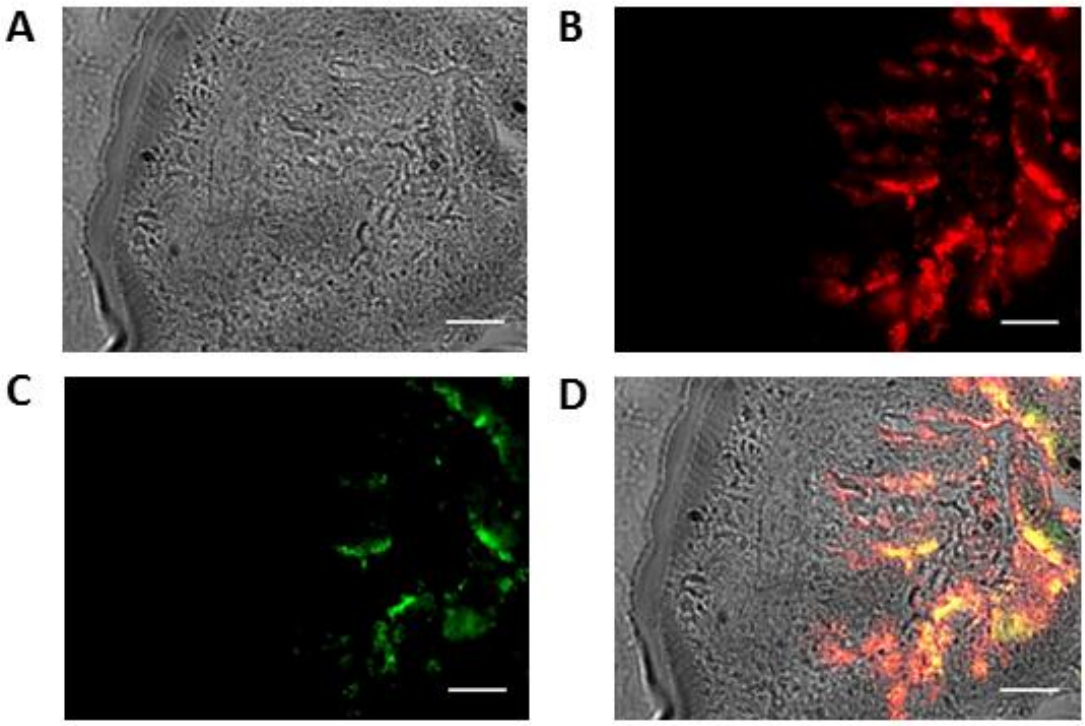

Figure 4.9 Adult *T. muris* worms are able to ingest bacteria from their environment, which then localise with their resident microbiota in the nematode intestinal tract. Live *T. muris* adults were incubated overnight with *gfp*-expressing *E.coli* (green), washed in RPMI supplemented with penicillin/streptomycin solution to remove any adherent bacteria, and processed for sectioning and FISH with a 16S universal Cy3 probe (red; 60X). (**A**) Light-field, (**B**) Cy3 (bacteria), (**C**) *gfp* (ingested *E. coli*), (**D**) combined image (yellow represents the ingested *E. coli* and red represents the resident microbiota). Scale bars, 10 µm.

4.3 Discussion

Although the existence of intestinal microbiotas in related environmental, free-living nematodes such as *C. elegans* have been described, the data presented in this chapter is the first evidence of a complex bacterial community within the intestinal tract of a medically relevant pathogen, that infects the mammalian intestinal tract (Baquiran *et al.,* 2013; Dirksen *et al.,* 2016).

4.3.1 Sodium hypochlorite successfully surface sterilises adult *T. muris*

To ensure the bacterial communities being studied were in fact internal and not artefacts of adherent bacteria, a method to ensure successful surface sterilisation was vital. Studies using *C. elegans* used several washing steps with either gentamycin or media with added Triton X-100 to remove bacteria from the nematode surface (Berg *et al.,* 2016; Dirksen *et al.,* 2016). Although this will remove the majority of bacteria, it is likely that some microbes will remain adherent as confirmed by Dirksen *et al*. Microbial DNA will also not be removed by antibiotic treatment and will be detected by the sensitive 16S rRNA gene primers used in these studies. As a result this may give false insights into the internal microbiota of these nematodes. We therefore used a more rigorous treatment to fully remove any traces of bacteria and their DNA that could interfere with the molecular analysis of the internal microbiota. Previous work had demonstrated that 10 minute incubation in diluted 3% sodium hypochlorite effectively removed any surface contamination from *T. muris* adult worms, shown by PCR with 16S rRNA gene primers. To confirm that this was reproducible, several adult worms were subjected to the sterilisation process of bleaching followed by 5 washes in sterile H_2O. PCR primers for the 16S rRNA gene failed to amplify any bacterial DNA from these washes confirming the effectiveness of this method. These washes also ensured that any residual sodium hypochlorite was removed preventing inhibition of the PCR and false negative results. Together these data indicated that this method was rigorous enough to use for the rest of the study.

Adult stages of *T. muris* are protected by a tough outer cuticle, which remains intact after bleaching with sodium hypochlorite for 10 minutes. However, attempts to sterilise larval stages (L2-L4) of *T. muris* were unsuccessful, which included sodium hypochlorite, UV light treatment and chemical treatments such as Microsol, Triton X-100 and lysozyme at various concentrations. During larval stages, this protective cuticle is different to that of adults and consequently larvae either did not survive or were not successfully sterilised by the methods tested. As a result, further work is needed to develop a sterilisation strategy as it is important to know if younger stages of the nematode have a microbiota and if it is different to that of an adult *T. muris* worm. It is well known that age can impact the intestinal microbiota of mice and humans, and that the microbiota of different developmental stages of *C. elegans* varies, so we would expect to see differences

(Claesson *et al.,* 2012; Dirksen *et al.,* 2016; Langille *et al.,* 2014; Mariat *et al.,* 2009). Different microbial species may be selected for by the worm throughout its life cycle as it develops within the host and as its physiology changes, due to changes metabolic and nutritional requirements, and knowing this would give us further insight into the host-parasite-microbiota interaction.

4.3.2 *T. muris* adult worms have a diverse, core microbiota different to their host

From the DGGE analysis it is clear that the *T. muris* microbiota is not restricted to a small number of bacterial species but is extremely complex, and is different to that of its naïve and infected mammalian host. This was supported by 454 pyrosequencing data that was performed alongside this study, showing increased overall diversity in the *T. muris* microbiota compared to both caecal microbiotas (A. Houlden, personal communication). There was a clear, consistent DGGE banding pattern for all *T. muris* worms, which resulted in close clustering on NMDS plots. As such, there was no significant difference between male and female *T. muris* suggesting no impact of gender on the composition of the microbiota. Further to this, worms from different inbred strains of mouse had strikingly similar microbiotas that also clustered closely on NMDS plots. The naïve intestinal microbiotas of these mice were compositionally significantly different and infection with *T. muris* also induced significantly different changes. This indicates that *T. muris* selects for a specific conserved microbiota independently of the host-microbiota diversity that surrounds it. This was again supported by sequencing data that showed the existence of a core microbiota of 36 species in all *T. muris* worms. It may be that there are various selective pressures at play within the nematode digestive tract, different to that of the mammalian host intestinal tract, so that some species are unable to persist. The metabolic needs of the parasite will also be different to that of its host and therefore selection will depend on what *T. muris* needs for its own fitness and survival within the host. The existence of a core microbiota has also been described in *C. elegans*, where nematodes select for very similar microbiotas irrespective of the bacterial communities they were isolated from, for example soil and decomposing plant material. However, differences in microbiotas were evident between *C. elegans* and related species, *C. remanei* and *C. briggsae*. It may be that we would see differences between the *T. muris* microbiota and that of related species, including the human whipworm, *T. trichiura*. Future work would be necessary to determine the presence of a microbiota within *T. trichiura* and how it differs to *T. muris*, which is particularly important considering its use as a model for Trichuriasis in humans.

4.3.3 *T. muris* gains its intestinal microbiota from the host it infects

As embryonated *T. muris* eggs are sterile, the parasite must gain its microbiota from the host intestinal microbiota it infects. The lower intestinal tract is one of the, if not the most, densely populated habitats on earth and as a result *T. muris* larvae are exposed to huge numbers of bacteria. Here we have shown that adult worms are capable of ingesting bacteria and that these bacteria are able to localise within the intestinal tract with the resident microbiota. Pinpointing when *T. muris* are first colonised would be an interesting but challenging observation, especially as surface sterilisation of larval stages has not yet been successful and unlike *C. elegans*, *T. muris* does not have any free-living stages of its lifecycle and will not develop past an L1 stage larvae outside of a host intestinal tract *in vitro*.

Moreover, detection of bacteria within the intestinal tract suggests a potential nutritional importance for this microbiota, either providing metabolites that the worm cannot make itself, or aiding the breakdown of ingested food, as our own microbiota do for us. This has been investigated further in Chapter 5.

Summary

- *T. muris* adult worms can be treated with 3% sodium hypochlorite for 10 minutes to remove bacteria and their DNA from their surface.
- A diverse, core microbiota can be identified in adult *T. muris*, which is not dependent on gender or the intestinal microbiota of their host.
- The *T. muris* microbiota is significantly different to the naïve and infected intestinal microbiota of its host.
- Adult worms have an intestinal microbiota and are able to ingest bacteria from their environment.

Chapter 5

The *T. muris* microbiota is important for parasite viability

5.1 Introduction

The intestinal microbiota is extremely important for the health of mammalian hosts, aiding the development of the host immune system, providing defence against pathogenic microbes and increasing the metabolic potential of the host intestinal tract. Removal of the intestinal microbiota by antibiotic treatment, or the use of GF mice, results in an enlarged caecum, reduced Peyer's patches and small spleens. Gene expression is also altered resulting in an overall transformed intestinal environment (Reikvam *et al.,* 2011; Round and Mazmanian, 2009). Although a reduced or absent intestinal microbiota clearly impacts host health, it is not a requisite for host survival, and this is likely to be the case for other organisms that harbour diverse microbial communities.

Other animals, such as insects, have developed associations with bacteria and many can be colonised by single symbionts or complex communities. These bacteria have important roles for insect fitness, including the provision of additional nutrients such as amino acids, protecting against pathogens and their toxins, producing signalling compounds and digesting environmental products such as lignocellulose (Engel and Moran, 2013). This is also true for parasitic organisms, where commensals promote physiological development and reproduction, provide nutrients and have antimicrobial properties. Filarial nematodes, such as *B. malayi*, can be colonised by the intracellular endosymbiont *Wolbachia*, which is important for parasite fitness. Tetracycline and related antibiotics are effective against the order of alpha-Proteobacteria, *Rickettsiales*, which includes *Wolbachia*, and treatment can have anti-filarial activity. This is only seen in filarial parasites that harbour the endosymbiont and no effect has been documented in related parasites that do not, such as *Acanthocheilonema viteae* (Hoerauf *et al.,* 1999). Removal of *Wolbachia* by antibiotics in various *Wolbachia*-dependent filarial nematodes resulted in a wide range of phenotypes including reduced motility and viability, decreased microfilarial release, inhibition of larval development and prevented moulting in L3/L4 stages (Hoerauf *et al.,* 2003, 1999; Rao and Weil, 2002; Rao *et al.,* 2002). Furthermore, sequencing of the *B. malayi* and *Wolbachia* genomes has given great insight into their mutualistic association and how each benefits. *B. malayi* has lost several important pathways that are present in the genome of *Wolbachia*, for example purine and pyrimidine de novo synthesis and heme biosynthesis indicating that the bacterial endosymbiont can provide these additional nutrients necessary for nematode health. The loss of biosynthetic pathways is not isolated to filarial nematodes and their endosymbiont, but is also evident in other parasitic organisms. Several amino acid biosynthetic pathways are absent in parasites (Payne and Loomis, 2006). Many of these organisms live in nutrient rich environments within host cells and it is therefore likely that they have evolved with their host and have consequently lost unnecessary pathways. In addition, the free-living nematode *C. elegans* cannot make the amino acid arginine and lacks the enzymes needed to synthesise heme and the

signalling molecule nitric oxide itself. It therefore relies on its associated microbiota to provide additional metabolic functions. Together these highlight the evolutionary relationships between nematodes, their host and microbiota throughout nature and the adaptations that occur as a result.

Since *T. muris* selects for a diverse microbiota that is conserved between worms, it is likely to be necessary for the fitness of the parasite and potentially promote its long term survival within the host. The location of the microbiota within the intestinal tract of *T. muris* suggests nutritional importance but it may also have a wider impact on worm processes, as our own microbiota does. Thus, the purpose of this chapter was to determine the importance of the *T. muris* intestinal microbiota for parasite fitness.

Aims

- To determine if certain bacterial groups or the entire microbiota are essential for parasite fitness using antibiotic treatments *in vitro.*
- To test whether the *T. muris* microbiota can provide particular metabolites for use by the adult worm.
- To investigate the importance of the parasite microbiota for survival within the host *in vivo*.

5.2 Results

5.2.1 Selective depletion of bacterial groups had no significant impact on parasite fitness

To determine the importance of the various bacterial members that make up the *T. muris* microbiota, adult worms were incubated with different antibiotic treatments to selectively deplete certain phyla or groups. Clindamycin was used to target the dominant phyla Bacteroidetes and Firmicutes, but not Proteobacteria (Fig. 5.1A), whereas gentamicin was used to deplete Proteobacteria and some Firmicutes, but not Bacteroidetes (Fig. 5.1B). Gram positive bacteria were removed using vancomycin (Fig. 5.1C), and Gram negative bacteria using ciprofloxacin (Fig. 5.1D). The fitness of adult *T. muris* worms was then monitored using a motility scoring system described by Silbereisen *et al.,* (2011) every 24 hours for 5 days. For all treatments, overall motility was not significantly different from control worms not exposed to antibiotics (Fig. 5.1). During vancomycin treatment, treated worms were significantly less motile than controls after 72 hours (Fig. 5.1C). However, this was the only time point that was significantly different indicating that overall, removal of Gram positive bacteria does not impact parasite fitness. Altogether, these data suggest that of the particular groups targeted here, none are essential for parasite fitness, but it is instead likely that the entire microbiota is necessary for health.

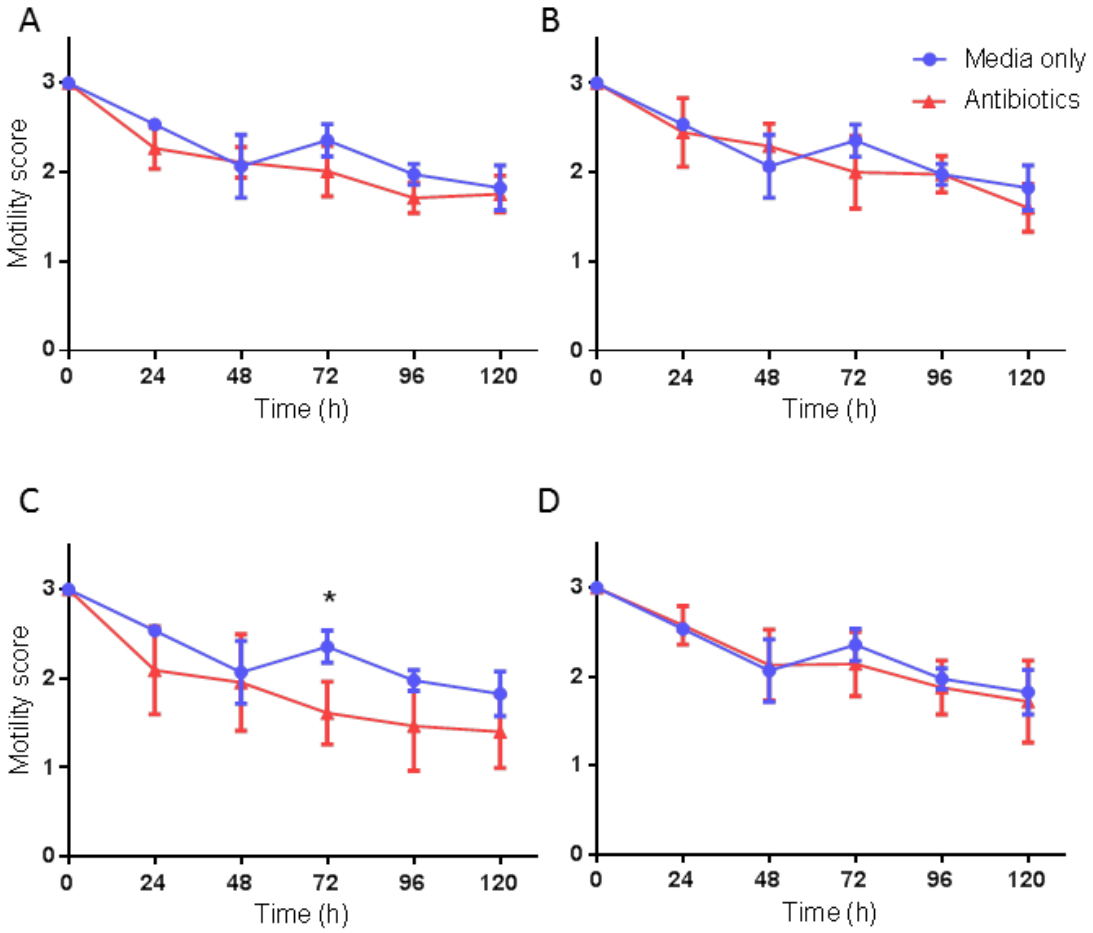

Figure 5.1 Motility scores for adult *T. muris* worms treated with different antibiotics to selectively deplete bacterial groups. Adult *T. muris* worms were incubated for 5 days with an antibiotic treatment (red triangles) and compared to worms incubated in media only as a negative control (blue circles) (N = 3 adult worms per well with 3 wells per treatment). Motility scoring was performed every 24 hours where 3 = normal motility, 2 = low motility (less than controls), 1 = very low motility/just at one end, 0 = no motility/dead. The average motility score per well was taken and then the average of 3 wells per treatment was plotted for each timepoint. (**A**) Clindamycin; (**B**) gentamicin; (**C**) vancomycin; (**D**) ciprofloxacin. Values represent mean +/- SEM and * indicates significance ($P<0.05$) as calculated by unpaired t-tests at each timepoint.

5.2.2 Antibiotic treatment to deplete the *T. muris* microbiota fully resulted in a significant decline in parasite fitness

Since selective removal of *T. muris* microbiota members did not significantly impact parasite fitness, a combination of antibiotics was used to target the entire microbiota. The use of metronidazole, vancomycin, ampicillin and neomycin (MVAN) is often used in mice to deplete the majority of their intestinal microbiota (Reikvam *et al*., 2011). We therefore used this treatment to deplete the microbiota of *T. muris* adult worms *in vitro* for 5 days with motility scoring every 24 hours as before. Figure 5.2 shows that MVAN antibiotic treatment significantly reduced the motility and therefore fitness of the parasites over time compared to controls (P = 0.0001), and resulted in the death of all parasites after 5 days. This indicates that *T. muris* needs its complete intestinal microbiota for its fitness *in vitro.*

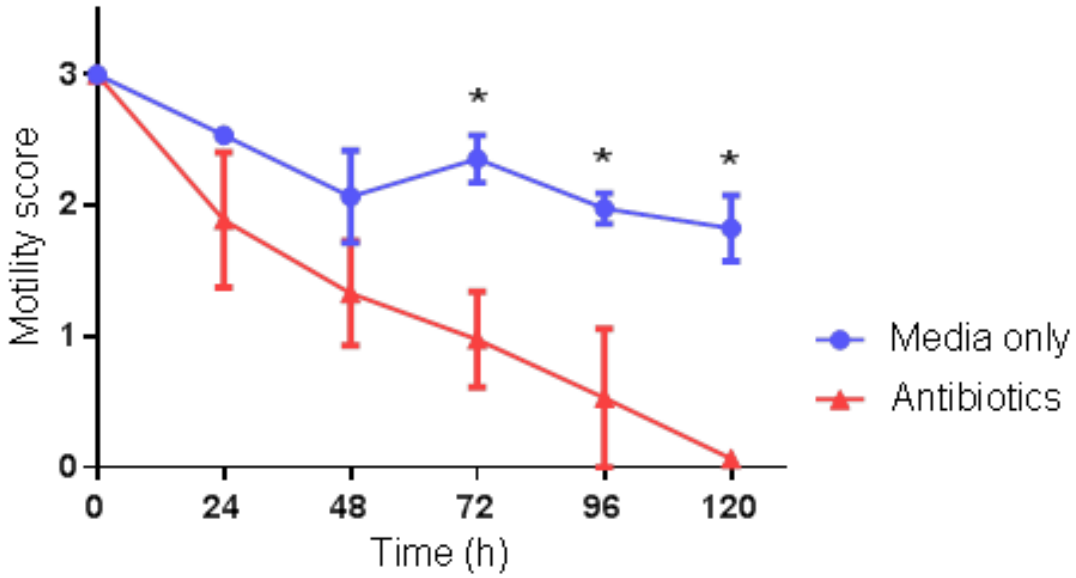

Figure 5.2 Motility scores for adult *T. muris* worms treated with antibiotics to fully deplete their intestinal microbiota. Adult *T. muris* worms (N = 3 adult worms per well with 3 wells per treatment) were incubated for 5 days with an antibiotic treatment of metronidazole, vancomycin, ampicillin and neomycin (red triangles) and compared to worms incubated in media only as a negative control (blue circles). Motility scoring was performed every 24 hours where 3 = normal motility, 2 = low motility (less than controls), 1 = very low motility/just at one end, 0 = no motility/dead. The average motility score per well was taken and then the average of 3 wells per treatment was plotted for each timepoint. Values represent mean +/- SEM and * indicates significance (P<0.0001) as calculated by unpaired t-tests at each timepoint.

5.2.3 Reduction in parasite fitness was not an anthelmintic result of the antibiotic treatment

To ensure that the reduction in viability that we saw with MVAN treatment was due to the removal of the *T. muris* microbiota and not an anthelmintic effect on the parasite itself, the same treatment was used on sterile L1 *T. muris* larvae. As larvae at this stage are microscopic, motility scoring was not suitable. Instead, the number of live (moving) and dead (not moving) larvae were counted and the percentage of live L1 larvae was calculated. Figure 5.3 shows that there was no significant difference in survival between antibiotic treated and media only control L1 larvae over time. This suggests that MVAN antibiotic treatment does not have an anthelmintic effect on *T. muris*, and that it is the presence of a microbiota within adult stages that is important for their fitness.

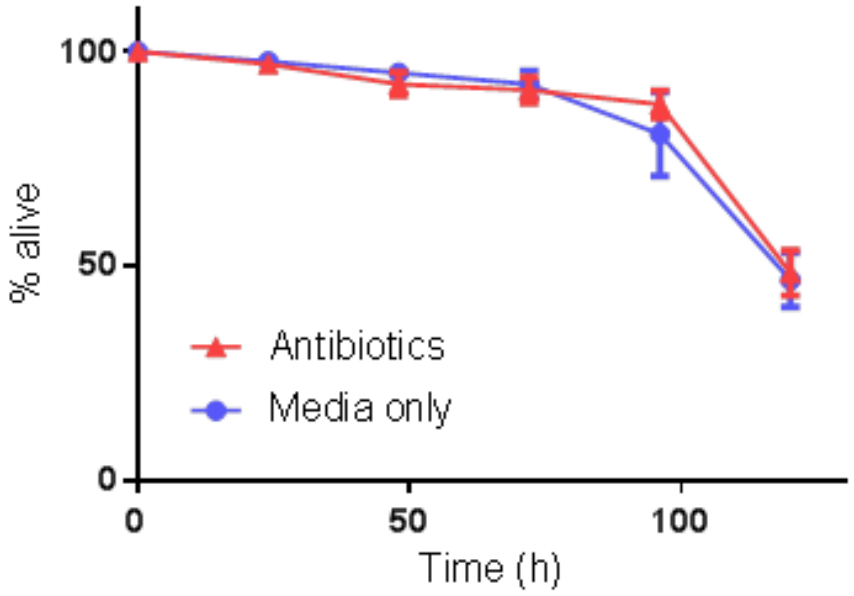

Figure 5.3 Survival of L1 *T. muris* larvae after treatment with MNAV antibiotics. Sterile L1 *T. muris* larvae (N = ~ 50 per well, 3 wells per treatment) were incubated with the same antibiotic treatment used for adult worms for 5 days. The percentage of larvae that were alive in each well was calculated every 24 hours, averaged and compared to untreated controls kept in media only. Values represent mean +/- SEM as calculated by unpaired t-tests at each timepoint.

5.2.4 *In vivo* oral antibiotic treatment did not significantly reduce worm burdens in wild type or immunodeficient mice at L2 and L4 larval stages

To test whether antibiotic treatment impacts parasite fitness and therefore the ability to infect its host *in vivo*, mice were treated with MVAN antibiotics by oral gavage. Infected mice were treated daily with the following combination in final volume of 0.2 ml; metronidazole (10 mg/ml), vancomycin (5 mg/ml), ampicillin (10 mg/ml) and neomycin (10 mg/ml). This cocktail of antibiotics is a popular way of depleting cultivable members of the host intestinal microbiota to mimic a GF animal. Treatment causes a significant drop in microbial density and diversity but complete eradication of the microbiota does not occur (Hill *et al.,* 2010; Reikvam *et al.,* 2011).

Wild type C57BL/6 mice were infected with a low dose (~ 20 embryonated eggs) and given 8 days of antibiotic treatment when worms were at the L2 larval stage (day 14 p.i., N = 5) or the adult stage (day 35 p.i., N = 5). It is well known that *T. muris* susceptibility to anthelmintic drugs changes throughout the life cycle as the worm develops and therefore we included two different parasite stages to determine the impact of antibiotic treatment on parasite fitness (Wimmersberger *et al.,* 2013). Worm counts were performed on the last day of treatment, and caecal contents and adult worms were taken for bacterial community analysis.

Figure 5.4A-B indicates that oral antibiotic treatment does not significantly reduce worm burdens in C57BL/6 mice at the L2 (P = 0.5) or adult stage (P = 0.4). DGGE and NMDS analysis of the intestinal microbiotas of the host and adult stage *T. muris* showed that antibiotic treatment significantly altered the host caecal microbiota (P = 0.01), with a decrease in diversity shown by the reduced number of bands, compared to untreated infected mice (Fig 5.4C-E). *T. muris* isolated from treated and untreated control mice had very similar microbiotas (P = 0.5) suggesting that the antibiotic treatment did not affect the parasite in its intestinal niche. Further to this, two samples within the antibiotic treated host microbiotas showed a greater reduction in diversity compared to others in the same group. This implies that the antibiotic treatment may have been less effective in certain animals and may explain why *T. muris* were unaffected by the treatment. Nevertheless, these data suggest that oral antibiotic treatment of the host does not impact the ability of *T. muris* to survive *in vivo*.

This was repeated in an immunodeficient mouse model (Rag2 KO) using a high dose (~200 embryonated eggs) to eliminate the influence of the host adaptive immune response and examine if a higher infective dose allowed a clearer affect to be identified. However, there was no significant decrease in the worm burden of antibiotic treated mice compared to untreated controls at the L2 larval stage (P = 0.7). At the adult stage there

was a slight reduction in worm burden of antibiotic treated mice, although this was not significant (P = 0.056).

Caecal contents and adult *T. muris* were harvested and used for DGGE and NMDS analysis. Antibiotic treatment again caused significant alterations to the host caecal microbiota (Fig 5.5C-E) with a striking reduction in the number of bands and therefore diversity. Unlike adult *T. muris* isolated from C57BL/6 antibiotic treated mice, those from treated Rag2 KO mice had a significantly different intestinal microbiota when compared to those from untreated mice (Fig 5.5C-E, P = 0.02). These worms still maintained the majority of their microbiota although several bands conserved in untreated worms were missing, shown in figure 5.5C highlighted by the green bracket, and may explain why they are shown as significantly different by NMDS and PERMANOVA analysis. The antibiotic induced alterations in host caecal microbiota are more pronounced in all Rag2 KO mice used, compared to C57BL/6 mice where only two saw similar reductions (Fig 5.4). This suggests that dramatic reductions in the diversity of host caecal bacterial communities are needed to impact the infecting *T. muris* adult worms, and oral antibiotic treatment may not successfully reach the intestinal niche of the worm inside the intestinal epithelial cells of its host.

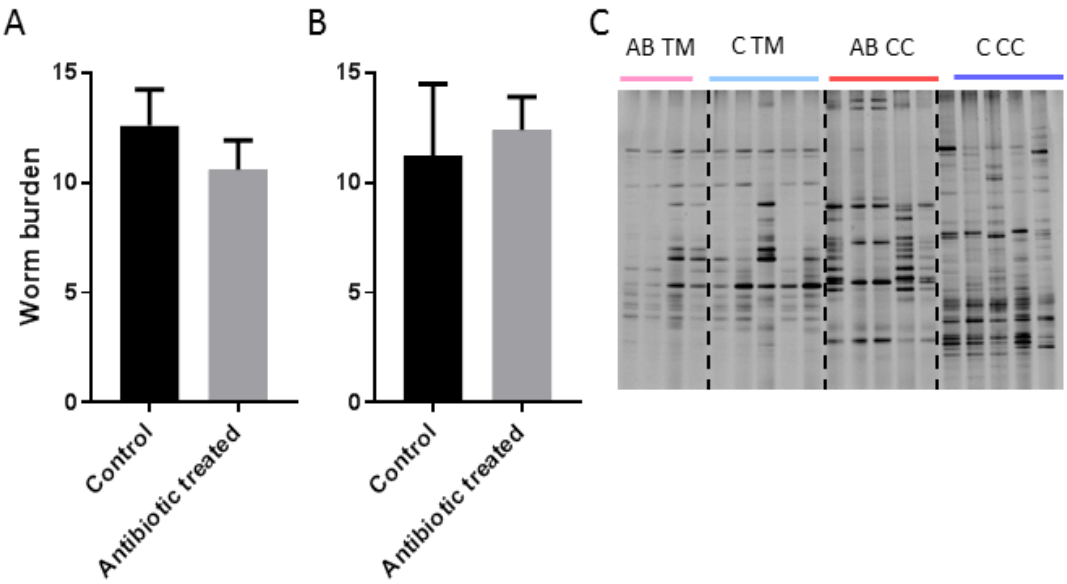

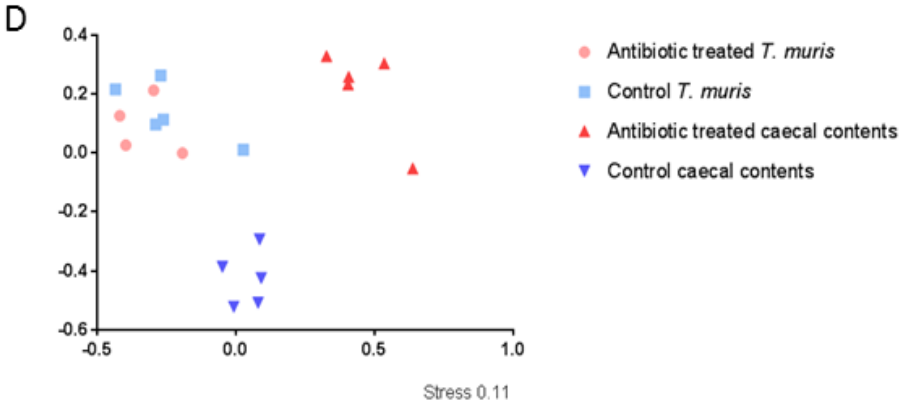

E

	C CC	AB TM	C TM
AB CC	**0.01** *	**0.01** *	**0.01** *
C CC	-	**0.01** *	**0.01** *
AB TM	-	-	0.5

Figure 5.4 Oral antibiotic treatment of C57BL/6 mice infected with a low dose of *T. muris* at the L2 larval or adult stage had no impact on worm burden, and significantly altered the intestinal microbiota of the host but not *T. muris* adult worms. Infected mice were treated for 8 days via oral gavage with metronidazole (10 mg/ml), vancomycin (5 mg/ml), ampicillin (10 mg/ml) and neomycin (10 mg/ml) (MVAN) when *T. muris* was at the (**A**) L2 larval stage (N = 5, day 14 p.i., P = 0.5), or (**B**) adult stage (N = 5, day 35 p.i., P = 0.4). Values represent mean worm burden +/- SEM. (**C**) DGGE analysis of bacterial communities from caecal contents of antibiotic treated (AB CC) and control (C CC) *T. muris* infected mice and *T. muris* isolated from antibiotic treated (AB TM) and control (C TM) mice. Biological replicates only. (**D**) NMDS plot of DGGE data where each point represents an individual *T. muris* adult worm or individual mouse with the axis scale for Euclidian distance between samples centred on zero. Stress indicates the quality of fit of the data (<0.2 is a

good fit). (**E**) Permutational ANOVA (PERMANOVA, Adonis function in RStudio) was performed, which does not require any assumptions about the distribution of the data, on the dissimilarity matrix to calculate P values between groups. P values were adjusted to account for multiple comparisons using the p.adjust method, which is based on the Bonferroni correction method, in RStudio. * indicates significance.

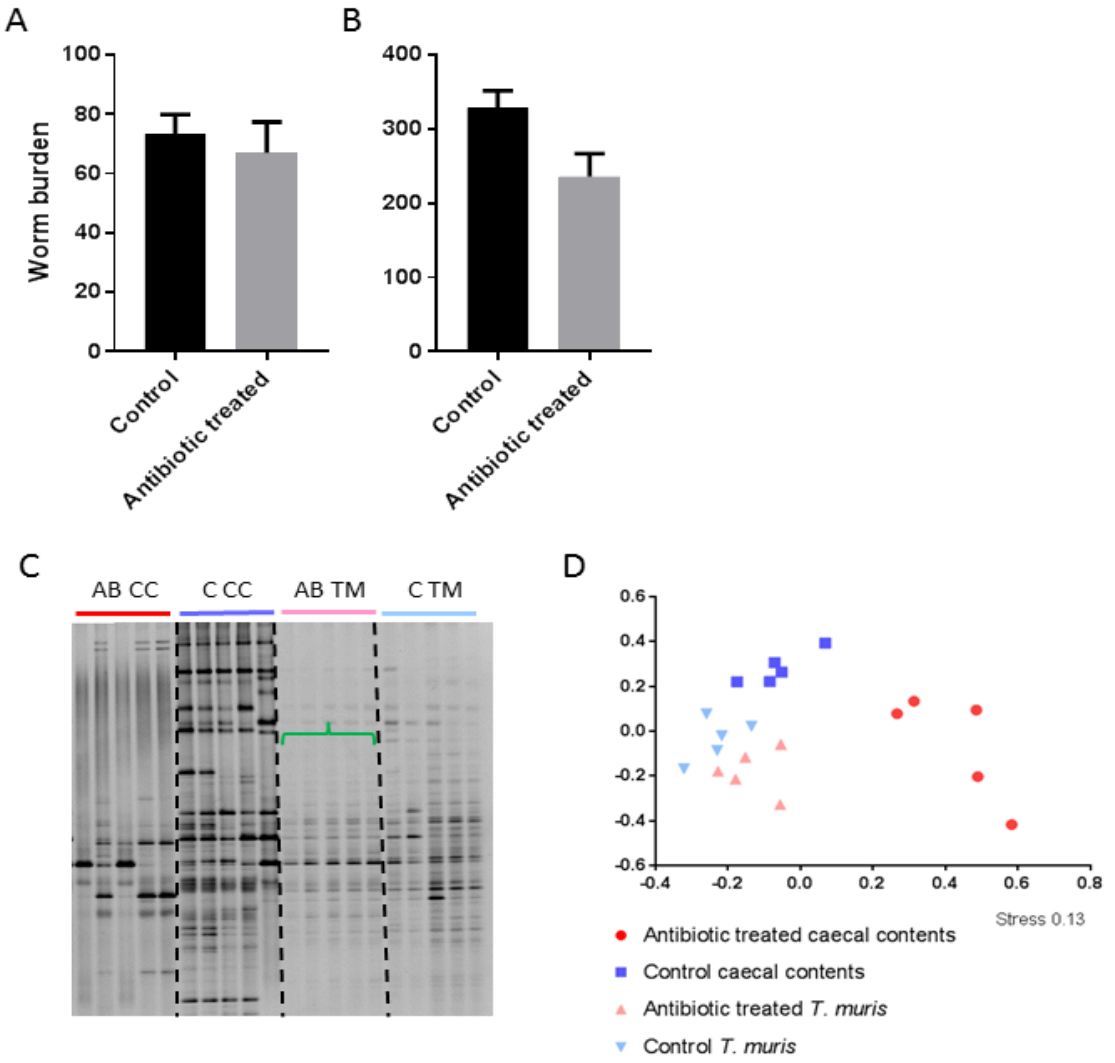

E

	C CC	AB TM	C TM
AB CC	**0.01** *	**0.01** *	**0.01** *
C CC	-	**0.01** *	**0.01** *
AB TM	-	-	**0.02** *

Figure 5.5 Oral antibiotic treatment of Rag2 KO mice infected with a high dose of *T. muris* at the L2 larval or adult stage had no impact on worm burden, but significantly altered the intestinal microbiota of L4 *T. muris* worms and the host. Infected mice were treated for 8 days via oral gavage with metronidazole (10 mg/ml), vancomycin (5 mg/ml), ampicillin (10 mg/ml) and neomycin (10 mg/ml) (MVAN) when *T. muris* was at the (**A**) L2 larval stage (N -= 5, day 14 p.i., P = 0.7), or (**B**) adult stage (N = 5, day 35 p.i., P = 0.056). Values represent mean worm burden +/- SEM. (**C**) DGGE analysis of bacterial communities from caecal contents of antibiotic treated (AB CC) and control (C CC) *T. muris* infected mice and *T. muris* isolated from antibiotic treated (AB TM) and control (C TM) mice. The green bracket highlights the loss of bands in *T. muris* isolated from antibiotic treated mice. (**D**) NMDS plot of DGGE data where each point represents an individual *T. muris* adult worm or individual mouse with the axis scale for Euclidian distance between samples centred on zero. Stress indicates the quality of fit of the data (<0.2 is a good fit).

(**E**) Permutational ANOVA (PERMANOVA, Adonis function in RStudio) was performed, which does not require any assumptions about the distribution of the data, on the dissimilarity matrix to calculate P values between groups. P values were adjusted to account for multiple comparisons using the p.adjust method, which is based on the Bonferroni correction method, in RStudio. * indicates significance.

5.2.5 Intraperitoneal antibiotic treatment had a variable impact on worm burden in immunodeficient mice

T. muris burrows within caecal epithelial cells after hatching and remains in intimate contact with the host for the duration of infection. Therefore for antibiotics to be taken up by the parasite at high concentrations they must be absorbed from the lumen of the intestinal tract by the host epithelial cell layer. Studies have shown that absorption of some antibiotics is poor when administered orally, particularly neomycin and vancomycin (Kunin *et al*. 1960; S. Rao *et al*. 2011). As a result, it is likely that the antibiotic mixture given orally did not fully penetrate the host intestinal epithelial cells and was not taken up by the parasite at the doses given. Therefore we administered the same antibiotic mixture via i.p. injection at a slightly lower dosage to prevent systemic toxicity; metronidazole (5 mg/ml), vancomycin (2 mg/ml), ampicillin (2.5 mg/ml) and neomycin (3 mg/ml).

Rag2 KO mice infected with a high dose (~300 embryonated eggs) were used again to eliminate the involvement of the adaptive immune system and enable the use of a high dose infection. Antibiotic treatment was administered when *T. muris* were either at the L2 stage (day 14 p.i.) or adult stage (day 59 p.i.) for 2 weeks, every other day. For adult worms, worm burdens were assessed on the last day of antibiotic treatment and there was no significant difference in worm burden after antibiotic treatment compared to untreated controls (P = 0.4) (Fig 5.6A). DGGE analysis of the host caecal microbiotas showed a reduction in the number of bands with antibiotic treatment, although not a complete removal of the microbiota, and separate clustering of host caecal microbiotas on the NMDS plot (Fig. 5.6B-C). Calculation of P values from the NMDS plot was not possible in this case due to the small sample number of control mice (N = 2), as at least 3 samples are needed. This was consequently taken into consideration for the rest of the study. The intestinal microbiotas of isolated adult *T. muris* worms were also analysed by DGGE and plotted using NMDS. One worm from each treatment group looked very different to others analysed, but overall there was no obvious difference in microbiota composition with treated and control worms clustering together (Fig. 5.6B-C).

Mice that were treated when infected with L2 stage larvae were not sacrificed until worms had matured to the adult stage (day 35 p.i.) to allow analysis of the *T. muris* microbiota. When worm burdens were assessed, there was a significant decrease in worm burden in

antibiotic treated mice compared to controls (Fig 5.7A, P = 0.04). Analysis of the host caecal microbiota revealed a significant difference as a result of antibiotic treatment (P = 0.003), even after a period of recovery where antibiotics were not administered. However, compared to figure 5.6B where microbiota analysis occurred on the final day of antibiotic treatment, it is clear that after a week the caecal microbiota begins to recover with more bands appearing on the DGGE gel. NMDS analysis of the intestinal microbiotas of *T. muris* isolated from treated and control mice showed no significant difference (P = 0.2) suggesting that this antibiotic treatment had not affected the bacterial communities within the remaining worms (Fig. 5.7B-D). Worms affected by the treatment would have been expelled by the mice, and it is possible that their microbiotas will have been altered. To determine if the fitness of the remaining worms had been affected by antibiotic treatment, worms from treated and control mice were assessed for motility, size and fecundity. The motility of worms cultured in RPMI with and without antibiotics *in vitro* was scored as described before. Both sets of worms followed similar trends with good motility in media only. Antibiotic treatment *in vitro* caused a significant reduction in motility for both groups of worms suggesting no difference in parasite fitness between treatments (Fig. 5.8A). As mice were treated when *T. muris* were at the L2 larval stage but were not harvested until day 35 p.i., worms were assessed for any reduction in growth that may have occurred during moults from L2 through to adult stages. Females (N = 50 worms per mouse, 4 mice) were used due to their larger size, fixed and mounted onto microscope slides for imaging. The resulting images, taken at the same objective, were then analysed in ImageJ. The posterior end of female worms from antibiotic treated and control mice were measured and showed no significant difference in size (P = 0.7) (Fig. 5.8B). However, worms isolated from one antibiotic treated mouse were similar in size to control worms (~3.7 mm); whereas worms from two other treated mice measured an average of 3.2 mm. Therefore treatment could potentially inhibit normal development of *T. muris* worms resulting in growth stunting, although these results were inconclusive.

Moreover, antibiotic treatment of filarial nematodes, which results in the removal of the endosymbiont *Wolbachia*, has been shown to impact the fertility of these parasites (Hoerauf *et al.,* 2003; Rao *et al.,* 2002; Smith and Rajan, 2000). To see if antibiotic treatment of the host impacted female *T. muris* fecundity, stools were collected at day 35 p.i. for faecal egg counts. Stools were emulsified in water and added to saturated NaCl, which causes eggs to float to the surface allowing quantification of numbers. Eggs per gram of faeces were calculated and there was no significant difference between treated and control animals (P = 0.057) (Fig. 5.8C). Nonetheless, counts within treatments were very variable with control mice having between 3.1×10^4 and 1.1×10^5 eggs per gram of faeces. Antibiotic treated mice had counts that were more reproducible between individuals (between 2.4×10^4 and 6×10^4). Again, this suggests that antibiotic treatment

of the host could potentially impact the fertility of infecting female parasites although the results are not significant.

The antibiotic treatment of Rag2 KO mice infected with L2 *T. muris* larvae was repeated, as well as mice infected with L1 stage larvae. Mice were again treated using i.p. injection for 14 days, every other day, and left until worms had matured to adult stage (day 35 p.i.). Worm burdens were assessed and no significant difference was seen when antibiotics were given at the L1 stage ($P = 0.7$) or L2 stage ($P = 0.69$) compared to untreated controls (Fig. 5.9). This indicates that antibiotic treatment of the murine host to deplete the host caecal and *T. muris* microbiotas gives inconsistent results in terms of worm burden and parasite fitness. This could be due to the many variables at play including host microbiota response to antibiotic treatment, life cycle stage of the parasite, initial worm burden, absorption of antibiotics by the host and therefore access of antibiotics to the parasite.

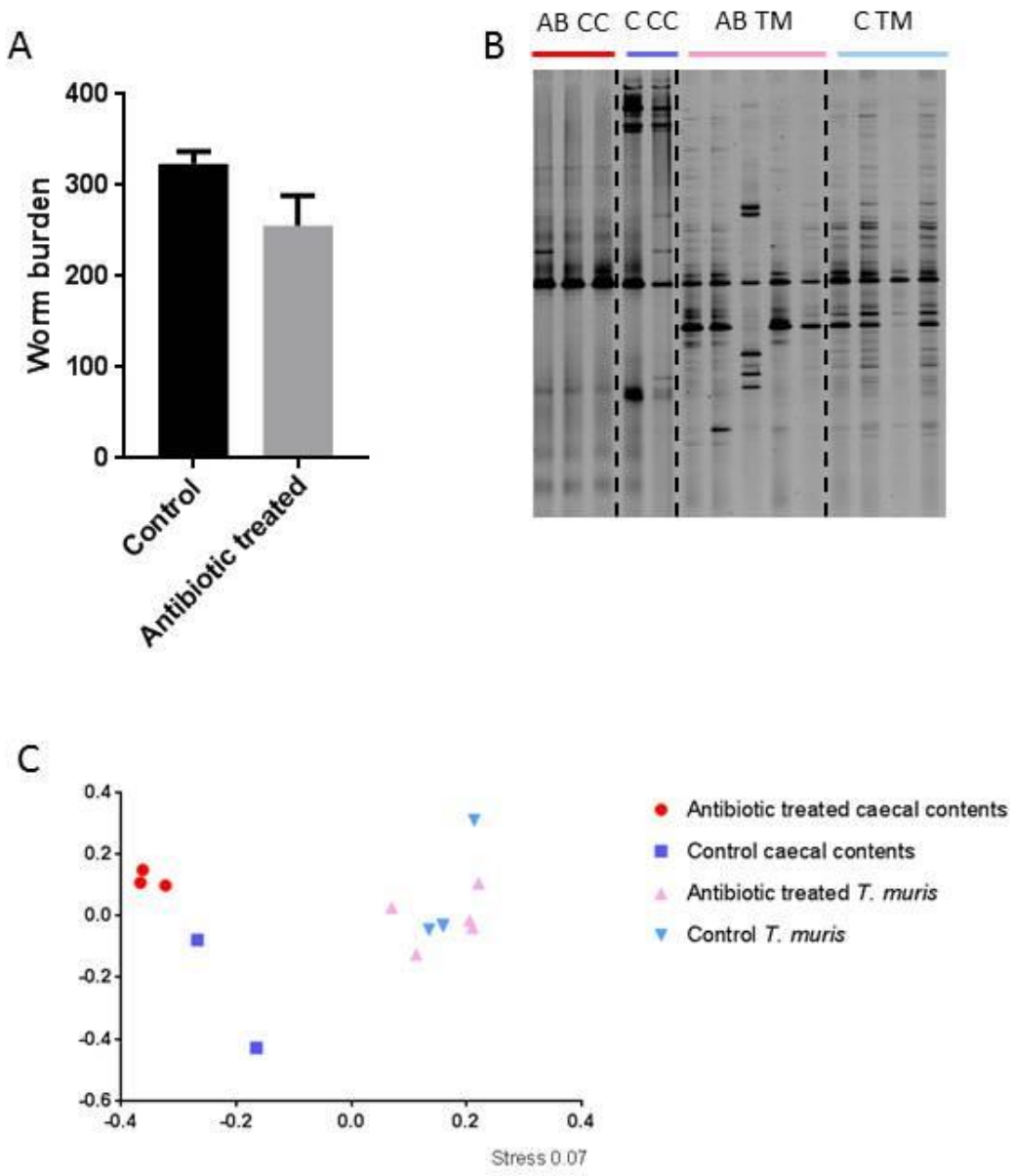

Figure 5.6 Rag2 KO mice infected with a high dose of *T. muris* adult worms and treated with a cocktail of antibiotics via intraperitoneal (i.p.) injection saw no significant decrease in worm burden compared to untreated, infected controls. Infected mice were treated for 2 weeks, every other day, via i.p. injection using metronidazole (5 mg/ml), vancomycin (2 mg/ml), ampicillin (2.5 mg/ml) and neomycin (3 mg/ml) (MVAN) when *T. muris* were adults (N = 2-3, day 59 p.i.). (**A**) Worm burdens were assessed on the last day of treatment (day 73 p.i.). Values represent mean worm burden +/- SEM. (**B**) DGGE analysis of bacterial communities from caecal contents of antibiotic treated (AB CC) and control (C CC) *T. muris* infected mice and *T. muris* isolated from antibiotic treated (AB TM) and control (C TM) mice. (**D**) NMDS plot of DGGE data where each point represents an individual *T. muris* adult worm or individual mouse with the axis scale for Euclidian distance between samples centred on zero. Stress indicates the quality of fit of the data (<0.2 is a good fit).

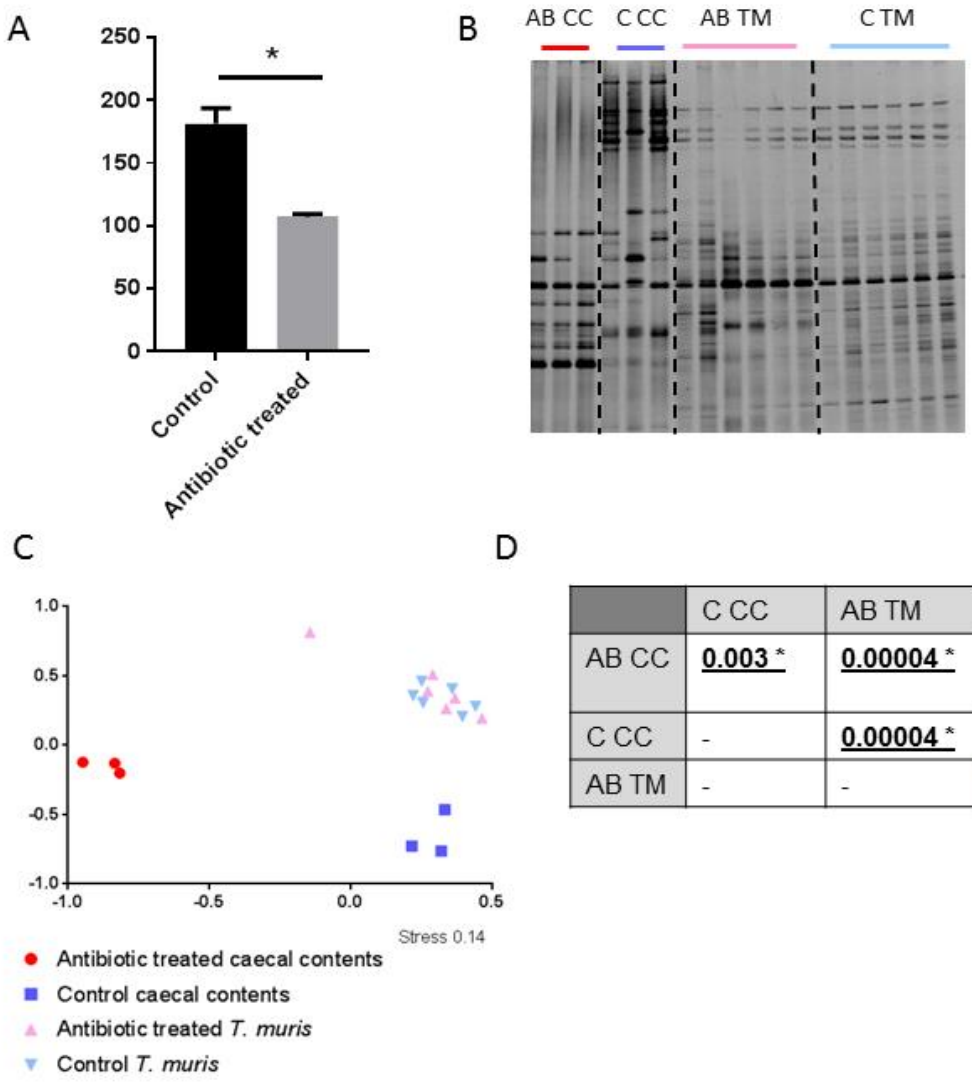

	C CC	AB TM	C TM
AB CC	**0.003** *	**0.00004** *	**0.02** *
C CC	-	**0.00004** *	**0.00004** *
AB TM	-	-	0.2

Figure 5.7 Rag2 KO mice infected with a high dose of *T. muris* at the L2 larval stage treated with a cocktail of antibiotics via i.p. injection saw a significant decrease in worm burden compared to untreated, infected controls, but no alteration in *T. muris* microbiota was detected in surviving worms. Infected mice were treated for 2 weeks, every other day, via i.p. injection using metronidazole (5 mg/ml), vancomycin (2 mg/ml), ampicillin (2.5 mg/ml) and neomycin (3 mg/ml) (MVAN) when *T. muris* were L2 larvae (N = 3, day 14 p.i.). (**A**) Worm burdens were assessed when *T. muris* reached adulthood (day 35 p.i.). Values represent mean worm burden +/- SEM. * indicates significance (P = 0.04). (**B**) DGGE analysis of bacterial communities from caecal contents of antibiotic treated (AB CC) and control (C CC) T. *muris* infected mice and *T. muris* isolated from antibiotic treated (AB TM) and control (C TM) mice. (**D**) NMDS plot of DGGE data where each point represents an individual *T. muris* adult worm or individual mouse with the axis scale for Euclidian distance between samples centred on zero. Stress indicates the quality of fit of the data (<0.2 is a good fit). (**D**) Permutational ANOVA (PERMANOVA, Adonis function in RStudio) was performed, which does not require any assumptions about the distribution of the data, on the dissimilarity matrix to calculate P values between groups. P values were adjusted to account for multiple comparisons using the p.adjust method, which is based on the Bonferroni correction method, in RStudio. * indicates significance

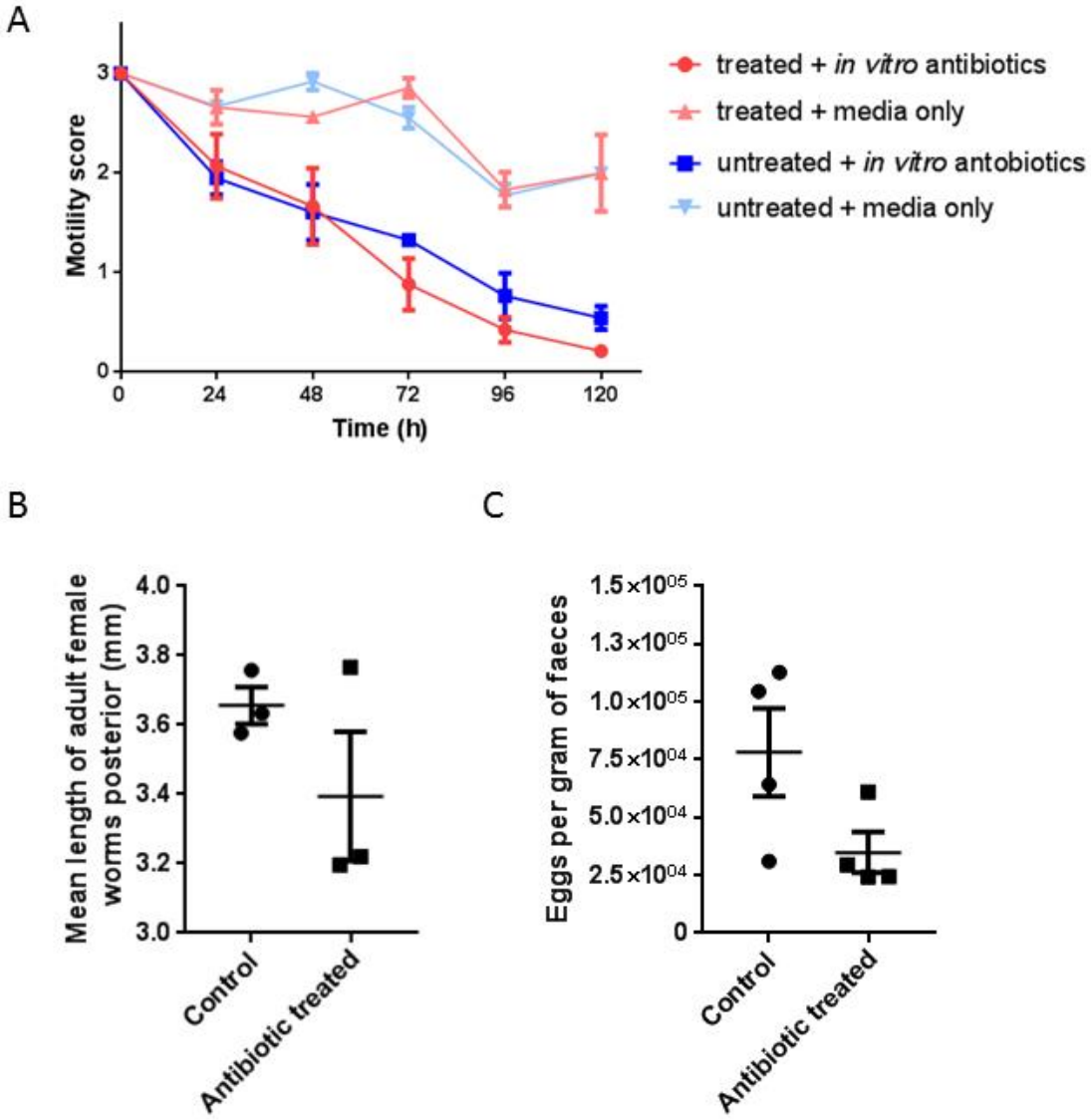

Figure 5.8 Surviving worms from Rag2 KO mice infected with a high dose of *T. muris* worms treated with antibiotics at the L2 larval stage showed no significant difference in motility, size or fecundity compared to untreated controls. (**A**) Adult worms isolated from i.p. treated and control mice were cultured in media with or without antibiotics (MVAN; N = 3 adult worms per well with 3 wells per treatment) for 5 days at 37°C, 5% CO_2. Motility was scored every 24 h where 3 = normal motility, 2 = low motility (less than controls), 1 = very low motility/just at one end, 0 = no motility/dead. The average motility score per well was taken and then the average of 3 wells per treatment was plotted for each timepoint. (**B**) Female worms were fixed (N = 50 per mouse, 3 mice) and mounted onto glass microscope slides, photos were taken using an upright confocal microscope at the same objective and the length of the worm posterior was measured in ImageJ. The average worm length per mouse was plotted. P = 0.7 as calculated by Mann Whitney U test. (**C**) Stools were collected from treated and untreated mice (N = 2 stools per mouse, 4 mice), weighed and added to saturated NaCl for faecal egg counts (P = 0.057 as calculated by Mann Whitney U test). The average egg count per mouse was plotted. Values represent mean +/- SEM.

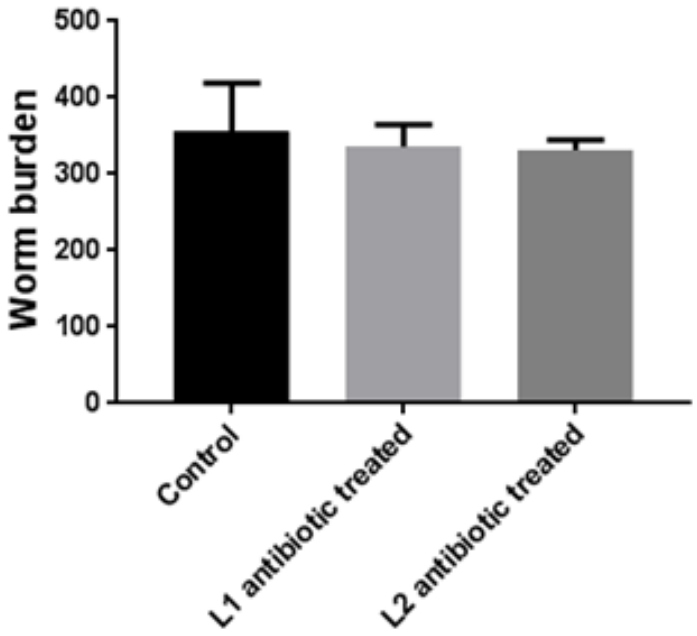

Figure 5.9 Intraperitoneal antibiotic treatment of Rag2 KO mice infected with L2 stage *T. muris* larvae was repeated, and also at the L1 larval stage, and no significant reduction in worm burden was seen. Infected mice were treated for 2 weeks, every other day, via i.p. injection using metronidazole (5 mg/ml), vancomycin (2 mg/ml), ampicillin (2.5 mg/ml) and neomycin (3 mg/ml) (MVAN) when *T. muris* were L1 larvae (day 3 p.i.) or L2 larvae (day 14 p.i.). Worm burdens were assessed when *T. muris* reached adulthood (day 35 p.i.). Values represent mean worm burden +/- SEM.

5.2.6 Infection of germ free animals did not result in a productive *T. muris* infection

We have previously shown that *T. muris* embryonated eggs are internally sterile and therefore L1 larvae hatched aseptically *in vitro* from these eggs are also sterile. As a result, surface sterilised embryonated eggs and aseptically hatched L1 *T. muris* larvae were used for infections in GF mice. This was to determine the importance of the host microbiota, and consequently the parasite microbiota selected from its host, for successful *T. muris* infection and survival *in vivo*.

For infections, a greater number of eggs and larvae (~ 500 per mouse in 0.2 ml sterile RPMI 1640 media) were used to account for poor hatching rates in the absence of a microbiota and also L1 larval passage through the stomach and small intestine, as they lack a protective outer layer. WT C57BL/6 specific pathogen free (SPF) mice were also infected with identical samples to control for poor egg hatching or potential reduced infectivity when using L1 larvae.

After infection using sterile plastic gavage needles under aseptic conditions, worm burdens were assessed at day 14 p.i. when *T. muris* were at the L2 larval stage. Figure 5.10 illustrates the striking reduction in infectivity of GF mice compared to their WT counterparts when using both eggs ($P < 0.004$) and L1 larvae ($P < 0.01$). Although very few worms were recovered from GF mice infected with a high dose of *T. muris* eggs, previous work had shown that certain *in vitro* cell lines were able to induce *T. muris* egg hatching, although at poorer rates compared to bacterial cells, so minimal hatching was expected to occur within the GF intestinal tract (K. Hayes, personal communication). No worms were recovered from GF mice infected with L1 larvae, even though WT mice had a mean worm burden of 67. This indicates that a host microbiota is important for a productive *T. muris* infection to occur.

Furthermore, after day 14 p.i. resistant hosts begin to expel their worms when infected with a high dose of *T. muris*. To account for this, a group of GF and WT mice were also given a low dose (~25) of *T. muris* L1 larvae to allow worms to progress to adulthood without expulsion, and to test if this is possible in the absence of host and parasite microbiotas. Unfortunately the low dose used in this instance was not high enough to allow successful infection of the host, and at day 34 p.i. only one adult worm was recovered from a WT animal. Therefore although L1 larvae can be used to infect, higher numbers are needed when considering they are more fragile than eggs and will become damaged on passage to the lower intestinal tract.

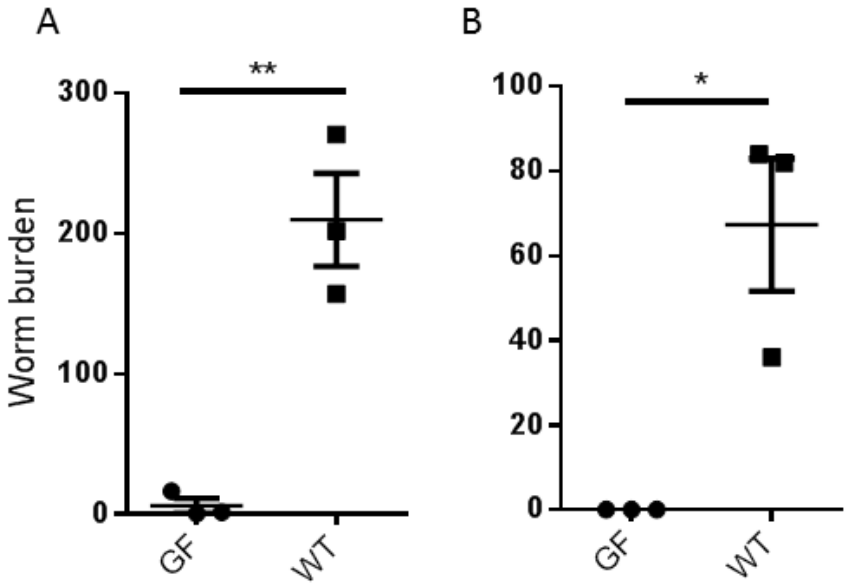

Figure 5.10 Worm burdens for *T. muris* infection of germ free animals at day 14 p.i. compared to control animals. GF and SPF WT animals were infected with a high dose (~500) sterile *T. muris* (**A**) embryonated eggs, *P < 0.004 or (**B**) L1 larvae, **P < 0.01. Points represent worm burden for individual animals plus mean worm burden +/- SEM.

5.2.7 The *T. muris* genome was lacking several pathways for key metabolites

Parasites that have bacterial symbionts, either as a microbiota or a single species, often benefit from additional metabolic processes performed by these bacteria. As a result, many parasites have lost important pathways from their genomes, which are instead provided by their commensals. To see if this is true for *T. muris* and its microbiota, the genome of *T. muris* was annotated using Kyoto Encyclopaedia of Genes and Genomes (KEGG) and pathway maps were reconstructed using KEGG Automatic Annotation Server (KAAS). Pathway maps were then analysed for missing key pathways and genes, and the main findings are summarised in Table 5.1.

The ability to make many essential amino acids is predicted to be missing from the *T. muris* genome including isoleucine, leucine, valine, phenylalanine, tryptophan, lysine and histidine, which is true for all animals. However, pathways for additional amino acids, such as arginine and tyrosine, were also missing. Pathways for synthesising vitamins including thiamine and biotin were absent. The enzyme nitric oxide synthase, necessary for the production of nitric oxide, was missing and is an important signalling molecule in multicellular organisms. *T. muris* was also unable to synthesise heme, an important cofactor for many biological processes, and butyrate, a bacterially derived metabolite important for intestinal homeostasis and host health, where all genes for both pathways were absent (Figure 5.11 and 5.12).

Metabolite	KEGG map number	Incomplete pathway/genes missing
Heme	00860	All genes missing
Butyrate	00650	All genes missing
Arginine	00220, 00330, 01230	All genes missing
Tyrosine	00130, 00350, 00360, 00400, 00730, 01230	Only has final enzyme
Nitric oxide	00910, 00330	All genes missing
Biotin	00780	All genes missing
Thiamine (vitamin B1)	00730	Incomplete pathway

Table 5.1 Main pathways and genes missing from the *T. muris* genome. Pathways were mapped to the *T. muris* genome and missing genes were identified. Metabolites are listed where a complete pathway or the majority of the pathway was absent from the genome, and therefore unlikely to be produced by *T. muris* itself.

5.2.8 Addition of missing metabolites did not reduce the impact of antibiotic treatment

The majority of metabolites listed in Table 5.1 are found in RPMI 1640, the media used for culturing *T. muris in vitro*. Since culturing worms in this media with antibiotics caused reduced motility and resulted in death, it is unlikely that these metabolites are enough to sustain the worm after the removal of its microbiota. Heme and butyrate are not components of this media and cannot be synthesised by *T. muris*. Therefore these metabolites were added to media at different concentrations, with and without antibiotics, to determine their importance for worm fitness.

The conserved pathway for heme metabolism involves seven enzymes, with two sets being interchangeable (HemF/HemN and HemY/HemG). All of these are missing from the *T. muris* genome, as well as the human whipworm, *T. trichiura*, genome (Fig 5.11A). *C. elegans*, together with other free-living and parasitic worms, have also lost the ability to synthesise heme but need heme for health, with 20 µM of hemin chloride being optimum for *C. elegans* growth and reproduction (Rao *et al.,* 2005). Hemin chloride was therefore added at concentrations of 4 µM and 20 µM to culture media (RPMI 1640), with and without antibiotics. Figure 5.11B shows that addition of hemin chloride at either concentration did not rescue worm fitness when incubated in antibiotics. These worms showed the same decline in motility as antibiotic only worms. In fact, hemin chloride at a concentration of 20 µM reduced the motility of worms without the addition of antibiotics. This suggests that this concentration of hemin chloride, although optimal for *C. elegans*, is actually toxic for *T. muris* adult worms. Motility levels of adult worms cultured with antibiotics and additional 4 µM hemin chloride did not result in 100% death of worms after 120 h, as seen with antibiotics only and 20 µM hemin chloride treated worms. It is possible that heme is needed by the worm at low levels, but this compound alone cannot promote *T. muris* survival in the absence of a microbiota.

Butyrate is also not present in RPMI 1640 media but again genes for its biosynthesis are missing from the *T. muris* genome (Fig. 5.12A). Sodium butyrate has been shown to extend the lifespan of the nematode *C. elegans* (Edwards *et al.,* 2014; Gao *et al.,* 2014). Culturing adult *T. muris* with sodium butyrate at two different concentrations (2 mM and 4 mM) saw similar results to the heme addition described above. The addition of butyrate did not significantly increase motility compared to media only controls, and when antibiotics were added there was no significant effect of the butyrate to prevent a reduction in worm fitness (Fig. 5.12B). In mammals, butyrate can be taken up by cells via transporters such as MCT-1 and SLC5A8, or it can act via receptors including GPR41, GPR43 and GPR109A (reviewed in den Besten *et al*. 2013). To determine if nematodes such as *C. elegans* and *T. muris* can use butyrate, BLAST analysis of their genomes was performed for protein homologues of the above transporters and receptors. *C. elegans*

returned significantly similar sequences ranging from ~ 20 – 30% identity for all three receptors and the transporter SLC5A8, although there were no similar homologues found for the transporter MCT-1. BLAST analysis was repeated using the *T. muris* genome and no significant sequence similarity was found for any of the transporters or receptors, suggesting that *T. muris* cannot respond to or use butyrate, supporting the data shown in figure 5.12. As *T. muris* selects for a diverse microbiota and several pathways are absent from its genome, it is unlikely that one or a select few metabolites are responsible for its fitness.

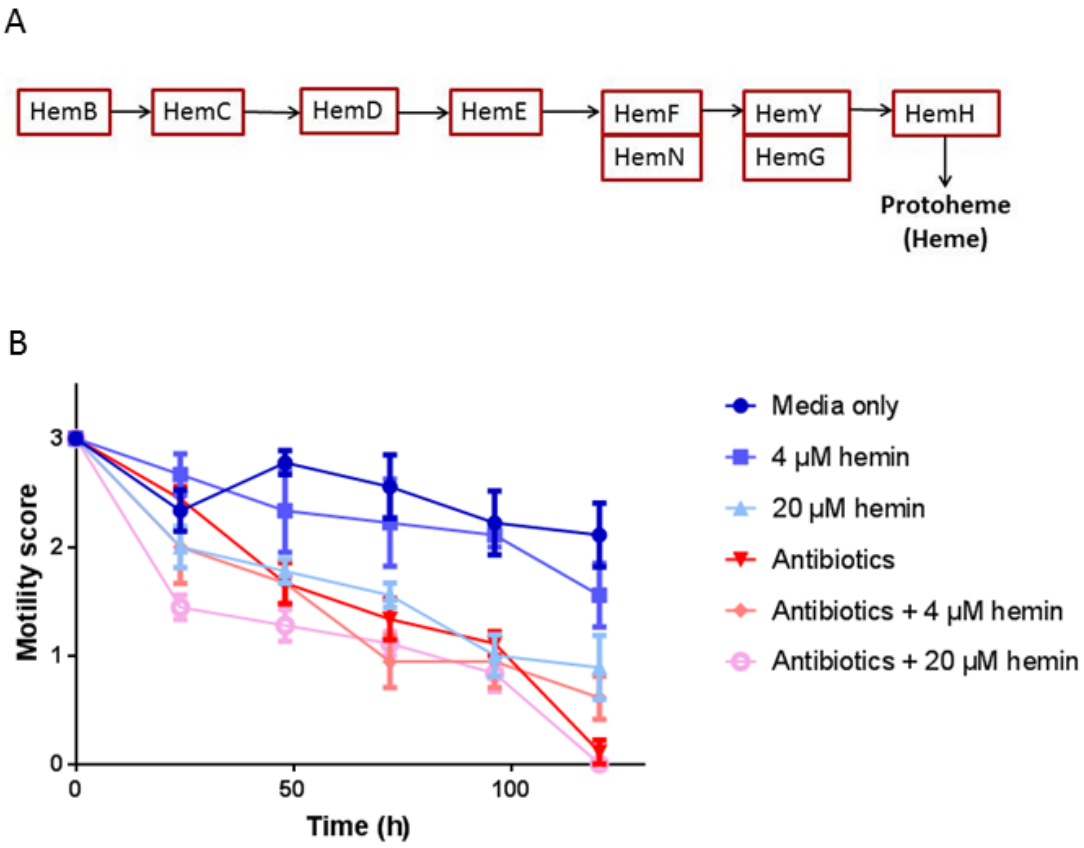

Figure 5.11 Pathway for heme biosynthesis is missing from the *T. muris* genome and addition of hemin chloride to *T. muris in vitro* culture does not reduce the impact of antibiotic treatment. (**A**) All enzymes in this pathway are absent from the genome and therefore heme is not produced via this pathway. Figure modified from KEGG map 00860, porphyrin and chlorophyll metabolism. (**B**) Adult *T. muris* worms (N = 3 per well, 3 wells per treatment) were incubated for 5 days with an antibiotic treatment of MVAN (red triangles) and additional hemin chloride at 4 µM (pink diamonds) or 20 µM (pale pink circles), and compared to worms incubated in media only (navy blue circles), with additional hemin chloride at 4 µM (purple squares) or 20 µM (pale blue triangles) as negative controls. Motility scoring was performed every 24 hours where 3 = normal motility, 2 = low motility (less than controls), 1 = very low motility/just at one end, 0 = no motility/dead. The average motility score per well was taken and then the average of 3 wells per treatment was plotted for each timepoint. Values represent mean +/- SEM.

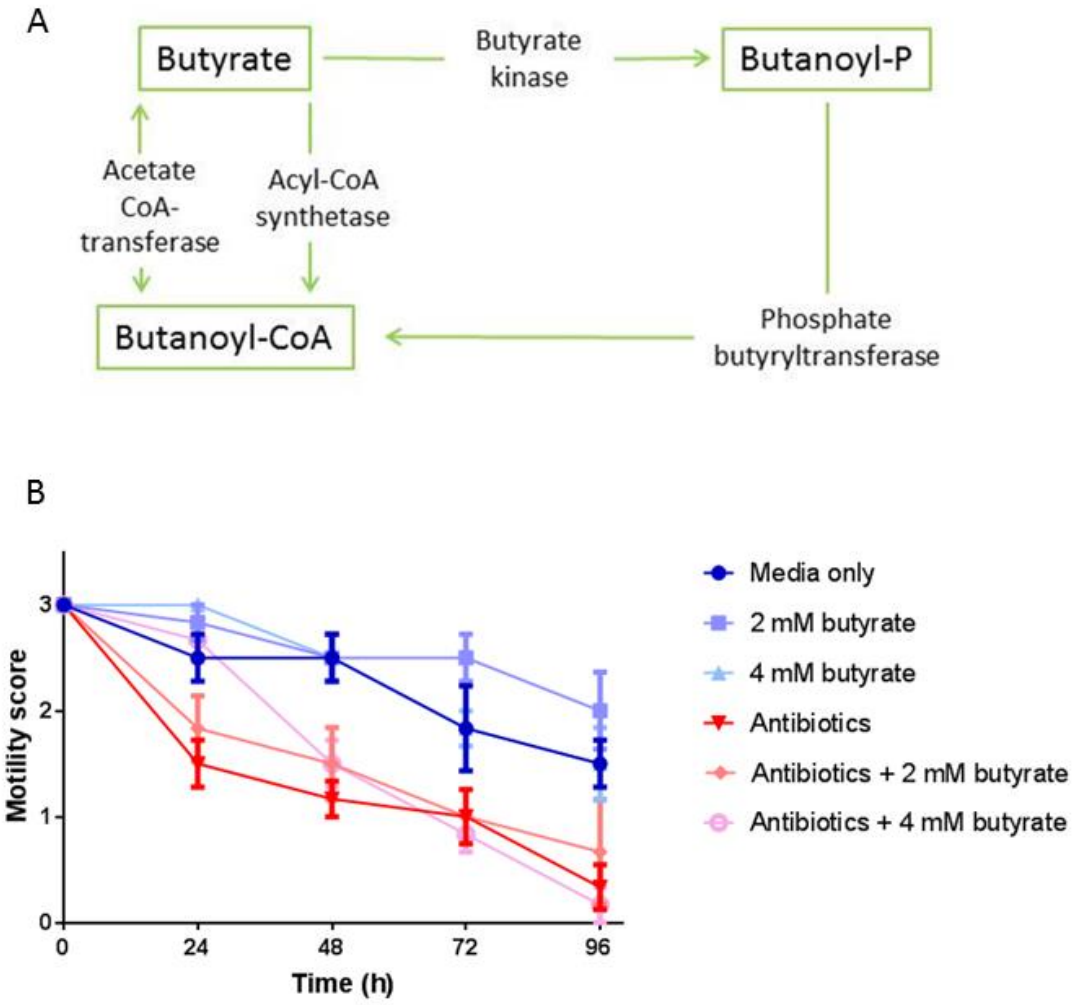

Figure 5.12 Pathway for butyrate synthesis is missing from the *T. muris* genome and addition of sodium butyrate to *T. muris in vitro* culture does not reduce the impact of antibiotic treatment. (**A**) Above enzymes are not present in the genome and therefore boxed metabolites, including butyrate, are not formed via this pathway. Figure modified from KEGG map 00650, butanoate metabolism. (**B**) Adult *T. muris* worms (N = 3 per well, 3 wells per treatment) were incubated for 5 days with an antibiotic treatment of MVAN (red triangles) and additional 2 mM (pink diamonds) or 4 mM (pale pink circles) sodium butyrate. These treatments were compared to worms incubated in media only (navy blue circles), with additional sodium butyrate at 2 mM (purple squares) or 4 mM (pale blue triangles) as negative controls. Motility scoring was performed every 24 hours where 3 = normal motility, 2 = low motility (less than controls), 1 = very low motility/just at one end, 0 = no motility/dead. The average motility score per well was taken and then the average of 3 wells per treatment was plotted for each timepoint. Values represent mean +/- SEM.

5.2.9 The *T. muris* microbiota were able to produce SCFAs including butyrate

The data presented in Chapter 3 has shown that *T. muris* infection causes a significant decrease in butyrate concentrations in host caecal contents, which returns to naïve levels upon clearance of worms. This chapter has also demonstrated that *T. muris* does not have the pathways necessary for butyrate biosynthesis encoded in its genome (Fig. 5.12A). It is well known that butyrate is a product of the bacterial fermentation of complex polysaccharides in the colon. This SCFA plays a critical role for host health in maintaining intestinal homeostasis and regulating inflammatory responses (Segain *et al.,* 2000).

To determine whether members of the *T. muris* microbiota can produce butyrate, adult worms were isolated from SCID mice infected with a high dose (~200) of embryonated eggs, washed with media containing antibiotics, and incubated in 4 ml RPMI 1640 media for 24 h at 37°C, 5% CO_2 (N = 100 worms per well from 3 mice, 6 wells in total). The resulting spent media was then analysed for the presence of butyrate, and other SCFAs including acetate and propionate, in 1 ml aliquots by GC-MS. To quantify the concentrations of SCFAs, particularly butyrate, standard curves were generated (see Chapter 3, section 3.2.4) (Figs. 3.8 and 5.13). To ensure butyrate was not present in any media used, RPMI 1640 only samples were also tested and no SCFAs were detected at any point (Fig 5.13B). Interestingly, SCFAs could be detected in media analysed after incubation with adult worms for 24 h, with butyrate, acetate and propionate detected in all samples analysed. Furthermore, other fatty acids including pentanoic acid and hexanoic acid, also not present in RPMI 1640 media were detected (Fig 5.13C).

Although genome analysis demonstrated that *T. muris* could not synthesise butyrate (Fig. 5.12), an alternative, previously undescribed pathway in these worms could not be ruled out. Therefore to determine the source of butyrate in the cultures, whether it was parasite or parasite-microbiota derived, sterile L1 larvae (N = 100 per well, 3 wells in total) were incubated in 2 ml RPMI media and the same conditions as adult worms for 24 h. The spent media was analysed for the presence of SCFAs and no butyrate was detected. However, low concentrations of acetate were detected as this fatty acid is a known excretory product of many parasitic helminths (Fig. 5.13D) (Tielens *et al.,* 2010). This suggests that should there have been any butyrate present, detection limits were sensitive enough to identify it.

Adult worms were harvested from the low dose (~20 worms) infected C57BL/6 mice used in Chapter 3 for SCFA analysis of caecal contents (N = 5 mice, 2 technical replicates for each). The live worms were treated as previously described and incubated for 24 h in 2 ml media (~ 8 per well), which was then collected in 1 ml aliquots for extraction and analysis by GC-MS. All three SCFAs were detected in media analysed (Fig. 5.14). The main SCFA detected was acetate (~2 mM/ml media), which was an expected result due to it being an

excretory product of parasitic helminths, although not previously shown for *T. muris*, and butyrate was detected at concentrations of ~ 0.5 mM/ml media in all samples. However, propionate was only detected in two samples at very low concentrations of ~ 0.1 mM/ml, with three having no propionate or concentrations below the detection limit (Fig. 5.14). Using these numbers together with the number of worms used, the average amount of butyrate produced per worm by their microbiota over a 24 h period *in vitro* could be estimated at 0.16 mM. As a result, these data show that members of the *T. muris* microbiota are capable of producing SCFAs including butyrate and that the worm can excrete these fatty acids into its local environment. Since *T. muris* lacks any butyrate transporter or receptor homologues and addition of butyrate to *in vitro* culture does not significantly improve worm fitness, it is unlikely that the butyrate produced by its own microbiota is used by the worm to promote its own fitness, but is alternatively excreted to influence its local environment within the host intestine.

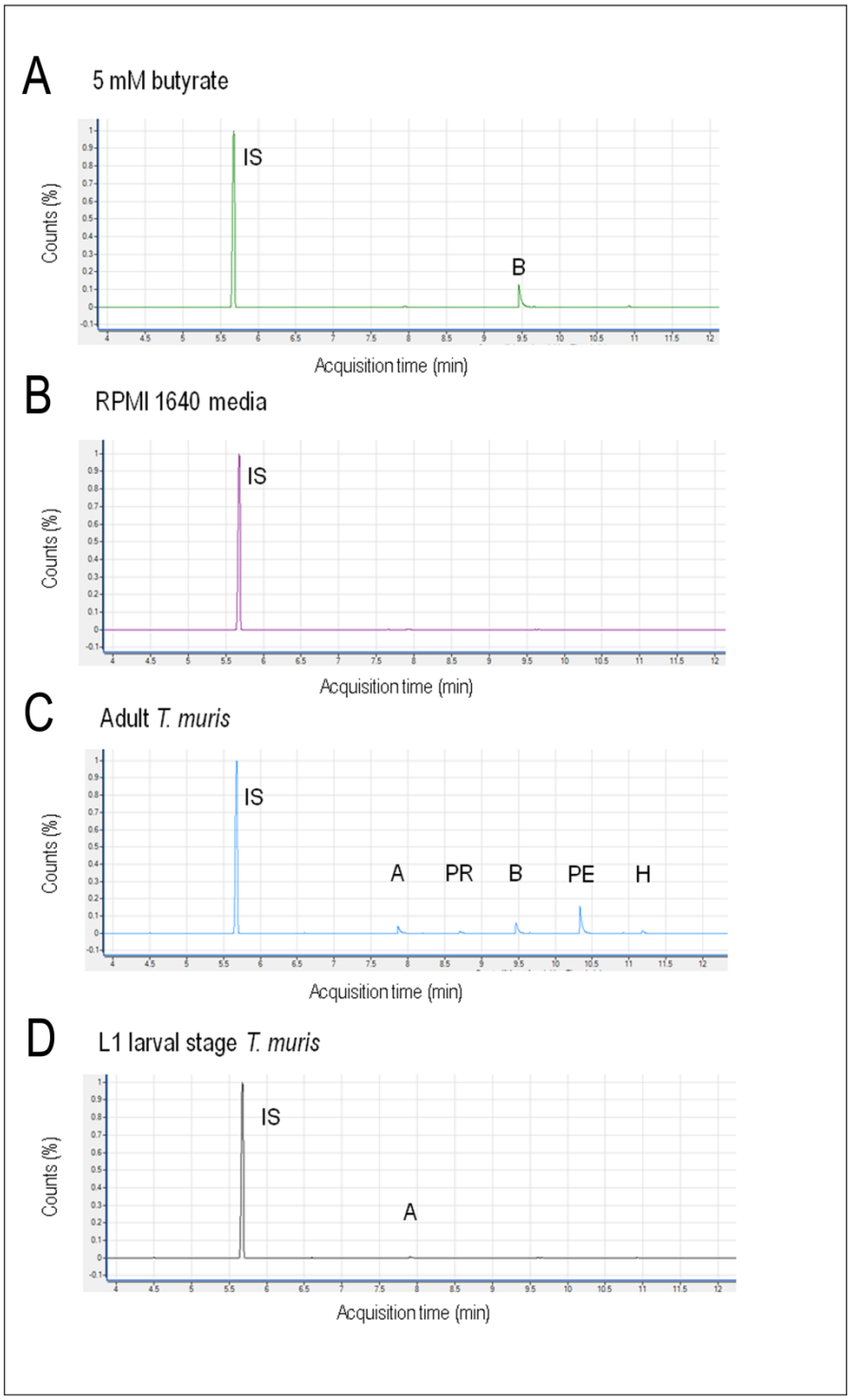

Figure 5.13 Mass spectra of adult stage and L1 larval stage *T. muris* excretions *in vitro*. Worms were incubated in RPMI 1640 overnight and spent media was analysed by GC-MS to detect butyrate and other fatty acids (3 technical replicates per sample, 3 samples per group). (**A**) 5 mM butyrate standard, (**B**) RPMI 1640 media, (**C**) adult *T. muris* (~100 worms), (**D**) sterile L1 larval stage *T. muris* (~100 larvae). IS = internal standard, B = butyrate, A = acetate, PR = propionate, PE = pentanoic acid, H = hexanoic acid.

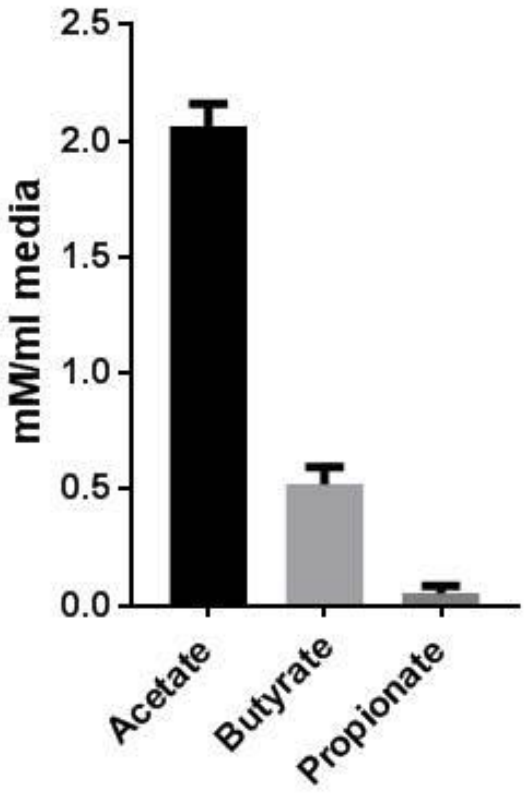

Figure 5.14 Quantification of SCFAs excreted by adult *T. muris* worms *in vitro*. C57BL/6 mice (N = 5) were infected with a low dose (~20 embryonated eggs) of *T. muris,* and worms were harvested at day 42 p.i. Worms were immediately transferred into RPMI 1640 media in a 6 well plate (1 well per mouse) after washing and incubated at 37°C, 5% CO_2 overnight. The spent media was then collected in 1 ml aliquots (2 ml per well) and extracted for GC-MS analysis. Concentrations of SCFAs were calculated using standard curves and expressed as mmol per ml media. Two technical replicates were averaged for each sample (5 samples) and then the mean concentration of 5 samples was plotted. Values represent mean +/- SEM as calculated by paired t-test (data was normally distributed).

5.3 Discussion

The importance of the intestinal microbiota for host fitness has been shown in various organisms including metazoan parasites, insects and mammals. The data presented in this chapter shows that *T. muris* requires its complex intestinal microbiota for its fitness *in vitro* and to establish a productive infection within its mammalian host. Furthermore, the T. *muris* microbiota produces butyrate, which cannot be used by the worm, but is excreted by the parasite and is likely used by the host.

5.3.1 Removal of the *T. muris* intestinal microbiota by *in vitro* antibiotic treatment reduces parasite fitness

Antibiotic treatment using a cocktail of metronidazole, neomycin, vancomycin and ampicillin is reliably used in mice to cause a dramatic reduction in the total number of bacteria, a loss of diversity and a shift in community composition in the murine microbiota. This significantly impacts immune development and responses through the reduction in antimicrobial production, cytokine expression and overall suppressed immune response, thus influencing host fitness (Willing *et al.,* 2011). To deplete the majority of the *T. muris* microbiota, a combination of broad-spectrum antibiotics was used. More specific antibiotics were also used to target certain groups of bacteria, for example Gram negative species. Motility scoring is routinely used *in vitro* to determine the effectiveness of anthelmintic drugs as a read out for parasite fitness. When targeting specific groups of bacteria with antibiotics, there was no significant reduction in the motility of adult *T. muris,* and therefore no observable impact on parasite fitness. Due to the diverse nature of the *T. muris* microbiota, it is highly likely that there is a significant level of functional redundancy, as seen with the murine and human intestinal microbiotas (Ley *et al.,* 2006a). Many bacteria will be able to provide the same functions so that the overall fitness of the host is not significantly reduced by the loss of a specific bacterial group. However, when targeting the microbiota as a whole, there was a striking reduction in parasite motility *in vitro* compared to untreated controls that resulted in death after 120 h. This indicates that *T. muris* adults require a complete microbiota for optimum fitness.

To rule out a possible anthelmintic effect of the antibiotic treatment, L1 *T. muris* larvae were exposed to the same treatment *in vitro*. As described before, embryonated eggs can be hatched in aseptic conditions to produce sterile L1 larvae. Therefore these larvae can be used to test whether the antibiotic treatment used causes a decline in parasite fitness due to a parasite specific effect or due to the removal of the associated parasite microbiota. Using an assay described by Wimmersberger *et al.,* (2013), the percentage of live L1 larvae was calculated every 24 h. At this stage of the life cycle, L1s are too small for the same motility scoring used for adults. As a result, larvae were scored as either alive (moving) or dead (not moving). Both untreated and treated larvae followed the same

trend and no reduction in viability was seen as a result of antibiotics. This indicates that sterile L1 larvae were unaffected by antibiotic treatment due to their lack of microbiota. At this stage they do not need a microbiota, as aseptically hatched L1s can survive for ~ 2 weeks *in vitro* with RPMI 1640 media and therefore it is likely that at this stage they can access all their essential nutrients from this media. However, these larvae do not survive beyond this time and they cannot develop further. It may be that *T. muris* needs its complete intestinal microbiota during the first stage of its life cycle for development into further larval stages. The addition of bacteria, such as *E. coli*, fails to trigger potential development, as does culture in a defined and enriched axenic media used for *C. elegans* development *in vitro* (modified *C. elegans* habitation and reproduction medium (mCeHR)). Although both nematode worms, they colonise distinct habitats and are likely to have very different requirements and developmental triggers, so this media may lack an essential component for *T. muris* survival or development. Nevertheless, it could be that *T. muris* selects for its microbiota between the L1 and L2 larval stages allowing development and growth within the intestinal tract of its host. Further work must be done to determine the stage at which the microbiota is gained and also what the triggers for development are. If these triggers could be used *in vitro*, it would be extremely useful for further work, i.e. mono-colonisation of *T. muris* worms allowing identification of important species and what exactly is provided by the microbiota for its fitness in the host. Furthermore, it is possible that the antibiotic cocktail that we have used here is effective against adult stages and not L1s due to differences in developmental stage. However, it is well known that larval stages of *Trichuris* are more susceptible to several anthelmintic treatments compared to adult stages (Wimmersberger *et al.,* 2013). Therefore it is unlikely that in this case adults were more sensitive than larvae. This can instead be explained by a dependence on the presence of a microbiota in adult worms, which L1s have not yet obtained.

5.3.2 Antibiotic treatment *in vivo* targets the *T. muris* microbiota with variable success

As antibiotic treatment *in vitro* causes a significant decline in parasite fitness, this was also tested *in vivo* to determine if removal of the microbiota prevented the worm from surviving within its murine host. Therefore worm burdens were used as a measure of survival within the host and compared to untreated control animals. Caecal contents and adult worms were also subjected to microbiota analysis by DGGE and NMDS. Initially, C57BL/6 mice were infected with a low dose of *T. muris* eggs with antibiotic treatment given by oral gavage when worms were at the L2 or adult stage. Oral antibiotic treatment of mice using MVAN reduced the number of bacterial species detected in the host caecal contents by DGGE, as expected. However, there was no alteration to the *T. muris* microbiota and no reduction in worm burden at either time point. This was also performed in an

immunodeficient Rag2 KO mouse model to eliminate the involvement of the host adaptive immune response in potential expulsion, and also allow the study of a high dose infection. Although there was again no reduction in worm burden in these mice, microbiota analysis revealed a more striking reduction in the host caecal microbiota as a result of antibiotics, and a significant difference between *T. muris* isolated from treated and untreated mice. Looking at the DGGE banding patterns produced by the host caecal contents from antibiotic treated C57BL/6 mice, it is clear that not all of the mice responded to the treatment as effectively. There were still a large number of bands and therefore not a substantial reduction in microbiota diversity and abundance. It could be that there were issues when gavaging the animals so that the full dose of antibiotics was not given or that the antibiotic solution was less concentrated on certain days. This suggests that as the host caecal contents were not fully depleted, it is unlikely that the worm microbiota had been affected. This is supported by the reduction in bands in the *T. muris* microbiota of worms isolated from treated Rag2 KO mice with dramatic alterations to their caecal microbiotas, although this did not induce parasite death or expulsion from the host. A longer treatment schedule may have been needed to see an effect on worm burden but long term treatment can impact the heath of the murine host and ultimately result in death.

Antibiotics given orally are not always efficiently absorbed in the host intestinal tract. Neomycin and vancomycin are poorly absorbed and therefore it is likely that they will not target the parasite's intestinal niche; the intestinal epithelial cell layer (Kunin *et al*. 1960; S. Rao *et al*. 2011). Consequently, we treated Rag2 KO mice with adult or L2 worms via i.p. injection to allow antibiotics to penetrate the cells surrounding *T. muris* in the intestinal tract. There was no significant difference in adult worm burden, even though the host caecal microbiota was dramatically altered by treatment. However, there was a significant reduction in worm burden when mice were treated with antibiotics when *T. muris* were at the L2 larval stage. As mentioned previously, larval stages of *T. muris* are more susceptible to anthelmintic treatments so this may explain why we see a reduction with L2 stages but not adults, which are more established within the host (Wimmersberger *et al.,* 2013). To allow analysis of the *T. muris* microbiota, these mice were not sacrificed until the worms had developed into adults; 1 week after the last antibiotic treatment. As a result, the host caecal microbiota had begun to recover with an increase in bacterial diversity. Furthermore, adult worms that had not been expelled from the treated host had a similar microbiota and motility scores to those from untreated control mice. This indicates that these remaining worms were unaffected by the antibiotic treatment and that maybe why they had not been removed from the host. In addition, further fitness tests were performed on the remaining worms to support this. No significant difference was seen in worm length, motility or female fecundity between treated and control worms. However, looking at the data more closely revealed a potential impact of antibiotic

treatment on worm fitness, but because the data is so variable it is not a significant reduction.

To see if the reduction in worm burden seen with L2 stage *T. muris* in an antibiotic treated Rag2 KO mouse model was reproducible, a further experiment was performed including an additional time point using L1 larval stage *T. muris* to determine if there would be a greater impact of treatment on younger larval stages. Conversely, there was no reduction in worm burden for either time point. Altogether these data suggest that this method of treating the host with antibiotics in order to deplete the *T. muris* microbiota is inconsistent and this is likely to be due to several variables, particularly when using *in vivo* models. This may be due to slight differences in antibiotic dose over time, and previous studies have also shown that the antibiotic treatment used does not completely sterilise the host intestinal tract, which in turn will target the *T. muris* microbiota incompletely (Croswell *et al.,* 2009). Furthermore, it is known that the effectiveness of antibiotic treatment can differ between individuals due to variation in absorption. This can be affected by intestinal transit time and intestinal motility, which also is affected by *Trichuris* infection with increased muscle contractility (Khan *et al.,* 2003). The pH of the absorption site also impacts permeability and uptake, as well as the presence or absence of drug metabolising bacteria (Parsons, 1977). These factors may have resulted in inadequate absorption of antibiotics from the intestinal lumen into the intestinal epithelial cell layer, limiting the parasites' exposure to the treatment. In addition, there may be certain life cycle stages that are more susceptible to treatment and consequently more dependent on their microbiota for survival and development within the intestinal niche. Worm burden may also be an important factor to consider with variation between experiments. A certain degree of variation is expected for high dose infections as egg counts are estimates. In this study, worm burdens in control animals ranged from ~300 to ~100 worms. A high worm burden may dilute the effect of antibiotic treatment or cause greater worm induced changes in the intestinal environment, reducing the impact of antibiotic treatment. Therefore, these data indicate that antibiotic treatment of the host results in variable outcomes for worm survival *in vivo* and that an intact host intestinal microbiota is not necessary for the survival of *T. muris* once established in the host.

5.3.3 *T. muris* requires a microbiota to establish a productive infection in germ free mice

The intestinal microbiota is essential for the hatching of *T. muris* eggs both *in vitro* and *in vivo*, allowing subsequent infection (Hayes *et al.,* 2010). This chapter has demonstrated that the *T. muris* microbiota is important for parasite fitness *in vitro*, but whether it is necessary *in vivo* for fitness and successful infection is unclear. As eggs are sterile and aseptically hatched L1 larvae are also sterile, both can be used to infect GF mice. As a result, infecting *T. muris* are not exposed to any bacteria within the host intestinal tract

and therefore will not have a microbiota themselves. Previous work has shown that certain cell lines are able to induce *T. muris* egg hatching *in vitro*, although not to the same level as bacterial hatching, so some hatching was expected within the GF caecum and colon (K. Hayes, personal communication). For infection of GF animals, both surface sterilised embryonated eggs and aseptically hatched L1 larvae were used. To account for reduced hatching rates and to ensure enough larvae reached the lower intestinal tract after passage through the stomach, higher numbers were used to infect (~ 500 eggs or larvae).

Previous work using GF animals has shown that an intestinal microbiota is necessary for some intestinal parasites to establish infection and cause pathology. The protozoan parasite, *Entamoeba histolytica*, cannot establish infection in GF guinea pigs, whereas *Giardia lamblia* can multiply within the intestinal tract but fails to cause any pathology in the absence of an intestinal microbiota (Phillips and Wolfe, 1959; Torres *et al.,* 1992). This study shows that GF mice given a high dose of *T. muris* L1 larvae fail to establish infection, with no worms recovered, which was significantly lower than worm burdens in WT SPF control animals given the same dose. When eggs were used, very few worms were recovered from one germ free animal with no worms in the other GF animals. However, control animals had a considerable worm burden as expected, where ~200 worms were recovered when eggs were used to infect and ~80 when L1 larvae were used. This indicates that *T. muris* requires its host to have an intestinal microbiota to establish a productive infection in the intestinal tract of its host.

5.3.4 The *T. muris* genome lacks several important biosynthetic pathways

The mammalian intestinal microbiota provides various metabolites that cannot be synthesised by the host itself. This is also true for nematodes that live in close association with their host or in high nutrient environments, and that possess a microbiota themselves. Many organisms have lost biosynthetic pathways as a result of this, for example pathways for the metabolism of certain amino acids and vitamins (Cabreiro and Gems, 2013; Payne and Loomis, 2006). Availability of the sequenced *T. muris* genome allowed the presence or absence of certain biosynthetic pathways to be identified and if they are potentially provided by its intestinal microbiota, thus explaining why removal or lack of a microbiota impacts the parasite's fitness (Foth *et al.,* 2014). This analysis highlighted many missing or incomplete pathways, with the main findings summarised in table 5.1. As with all animals, *T. muris* cannot synthesise key amino acids. Since this worm lives in close association with the host intestinal epithelial cell layer, there will be a constant source of amino acids and proteins available to it. It could be that the intestinal microbiota enables the worm to use these nutrients or provide enzymes for their breakdown and consequent absorption in the parasite intestinal tract. Thiamine and biotin are vitamins that again cannot be synthesised by many organisms, so dependence is on either dietary uptake or

production by the intestinal microbiota. RPMI 1640 media used to culture the worms *in vitro* contains all of these amino acids and vitamins, and as antibiotic treatment in this media resulted in death, it is unlikely that these nutrients are enough to sustain the worm without a microbiota.

Furthermore, bacterially derived nitric oxide has been shown to promote survival in the free-living nematode, *C. elegans*, which lacks its own nitric oxide synthase to produce this important signalling molecule (Gusarov *et al.,* 2013). Genome analysis showed that *T. muris* also lacks this enzyme. It is possible that members of the *T. muris* microbiota are able to produce this signalling molecule, which could also promote the survival of this nematode.

Heme is an important cofactor for many proteins and biological processes. *T. muris* lacks the entire conserved biosynthetic pathway needed to make heme. This has also been identified in other worms such a *C. elegans* and *B. malayi*, which both harbour bacterial symbionts (Foster *et al.,* 2005; Rao *et al.,* 2005; Severance *et al.,* 2010). These worms possess hemoproteins and therefore need heme to function in biological processes. Heme can be acquired from the diet and in the case of *B. malayi,* can be supplied by its bacterial endosymbiont, *Wolbachia* (Foster *et al.,* 2005). The availability of genome sequences for other organisms allowed the presence or absence of the heme biosynthesis pathway to be determined. This analysis showed that the majority of nematodes, including related *Trichuris* species, *Trichinella spiralis*, lack the entire pathway. This suggests that *T. muris* gains its heme either through its diet of host cell debris or through supplementation by its own intestinal microbiota. However, addition of hemin chloride, the oxidised version of heme, to culture media did not promote the survival of *T. muris in vitro* and even had damaging effects at a concentration of 20 µM. Furthermore, lower concentrations did not prevent the reduction in fitness caused by antibiotic treatment. It is therefore likely that low concentrations of heme are needed by the worm. Overall, it is unlikely that a single metabolite will suffice for *T. muris* survival, rather it is the complete microbiota and therefore a combination of nutrients and metabolites that are necessary for *T. muris* fitness.

5.3.5 The *T. muris* intestinal microbiota produces butyrate excreted by adult worms

Butyrate is a microbial metabolite that promotes intestinal homeostasis. We have shown previously in Chapter 3 that *T. muris* infection significantly reduces the concentrations of butyrate found in caecal contents of the host, which is likely a result of the restructuring of bacterial communities in the caecum. Genome analysis indicated that *T. muris* lacks the genes comprising the butyrate biosynthesis pathway, which is not surprising given that

this SCFA is a product of bacterial fermentation. To see if members of the *T. muris* microbiota could produce this important modulatory compound, the excretions of adult worms kept in media for 24 h were analysed by GC-MS for the presence of SCFAs, particularly butyrate. Acetate was expected to be detected as the biosynthetic pathway for its formation was identified in the analysis of the *T. muris* genome and it is a known excretory product of helminths, although this has not yet been confirmed for *T. muris* (Tielens *et al.,* 2010). This showed that adult worms can produce butyrate, as well as propionate and acetate. This was repeated with sterile L1 larvae and only acetate was detected in the media after 24 h. As a result, the data indicates that *T. muris* can produce acetate as an excretory product but it is the microbiota of the parasite that is producing butyrate, which is then excreted by the worm into its environment.

To determine if *T. muris* can use the butyrate derived from its own microbiota, adult worms were incubated in media with additional sodium butyrate with and without antibiotics. However, additional butyrate had no impact on worm fitness. Butyrate is used by mammalian hosts in the intestinal tract via transporters and receptors on the intestinal epithelial cell surface (Cresci *et al.,* 2010). The *T. muris* genome was analysed for the presence of protein homologues to these receptors and transporters but none were identified. It has been shown that *C. elegans* actually benefits from the addition of sodium butyrate to its culture media and analysis of its genome identified some similarity to mammalian butyrate receptors and one butyrate transporter, supporting this study. These data suggest that although its microbiota produces butyrate, *T. muris* does not use this SCFA for its own biological processes and overall fitness. Since butyrate is actually excreted from the worm, this indicates that it may instead impact the local environment surrounding the worm, i.e. host intestinal epithelial cells and the host intestinal microbiota, potentially manipulating its surroundings for survival in the host.

Summary

- *T. muris* requires its complete intestinal microbiota for survival *in vitro*.
- Antibiotic treatment of the murine host has a variable impact on the *T. muris* microbiota and consequently parasite fitness.
- *T. muris* requires its host to have an intestinal microbiota for a productive infection.
- Several important biosynthetic pathways are absent from the *T. muris* genome but addition of missing metabolites does not prevent the reduction in fitness caused by antibiotic treatment.
- The *T. muris* microbiota can produce SCFAs including butyrate, which are excreted by the worm.

Chapter 6

Summary discussion

The impact of intestinal helminth infection on host immune responses is well documented. Studies are now questioning the impact on the bacterial communities that live in close association with these metazoan pathogens, and the consequences for host health. Low level *T. muris* infections in WT mice have confirmed that this parasite can induce significant changes to the composition and diversity of the host intestinal microbiota (Holm *et al.,* 2015; Houlden *et al.,* 2015). This is associated with changes in Treg populations and metabolite levels in the intestinal tract, therefore affecting host health (Houlden *et al.,* 2015). This thesis has demonstrated for the first time that *T. muris*, a pathogen of mammalian hosts, selected for a diverse and conserved intestinal microbiota that is important for its viability. Further analyses of the changes that occur within the murine host intestinal microbiota as a result of *T. muris* infection have also been investigated. This included the influence of worm burden, the host adaptive immune system and the repercussions for intestinal homeostasis, such as altered butyrate concentrations and the spatial organisation of the microbiota. Together these strategies employed by the parasite may promote its long term survival in the chronically infected host.

6.1 *T. muris* selects for a diverse, core microbiota from its host that is important for its viability

The intestinal microbiotas of certain free-living, non-pathogenic nematodes, such as *C. elegans*, have been characterised and are distinct from the soil microbiota they inhabit (Berg *et al.,* 2016; Dirksen *et al.,* 2016). However, research into microbiotas associated with medically relevant, parasitic nematodes is limited to *H. polygyrus* and this study lacked evidence of adequate surface sterilisation prior to analysis of the internal parasite microbiota (Walk *et al.,* 2010). This is an important step to ensure that the bacterial communities being studied are part of an internal microbiota, and not an artefact of adherent surface bacteria. Chapter 4 in this thesis describes an effective protocol using sodium hypochlorite to surface sterilise adult *T. muris* worms prior to DNA extraction and analysis of the internal microbiota by 16S rRNA gene PCR and DGGE. This method could be used for other pathogenic nematodes that infect a wide range of mammalian hosts, specifically adult stages that can withstand the bleaching method without disintegration. Development of a surface sterilisation protocol for earlier lifecycle stages is critical for future work, including the characterisation of the microbiota associated with larval stages. This will reveal whether the microbiota associated with adult worms is conserved throughout the nematode lifecycle, or if it changes with nematode development and the varying requirements of the worm. Additionally, it is not known at what stage *T. muris* gains its microbiota and how it takes up these bacteria. It is likely that this occurs after hatching and just before the L1 larvae penetrate the intestinal epithelial cell layer. At this point, L1 larvae are exposed to the bacteria present in the densely populated caecum, whereas at later points during the lifecycle the worms are embedded in the intestinal

epithelial cell layer. The data in this thesis indicates that the parasite selects for a specific set of bacteria regardless of the host microbiota they hatch and reside within, and these bacteria are likely to be functionally important. Uptake of these bacteria is likely to occur via the mouth for transport to the intestinal tract, since incubation of adult *T. muris* with *gfp*-expressing *E. coli* results in co-localisation of ingested bacteria with the resident microbiota. This experiment should be repeated with younger lifecycle stages, such as L2 larvae, although attempts to use L1 larvae were unsuccessful.

The lack of a *T. muris* microbiota either by *in vitro* antibiotic treatment or infection into GF mice results in reduced viability or an unproductive infection, respectively, indicating its importance for the parasite. However, more work must be done to determine the functions of the microbiota and how they benefit the parasite. Genome analysis has highlighted several pathways that are incomplete in the *T. muris* genome, although it is not known if the end products are needed by the parasite for its fitness. This has been performed for the filarial nematode, *B. malayi*, and its endosymbiont *Wolbachia*, using genome sequencing *(*Foster *et al.,* 2005). Analysis of the *T. muris* microbiota transcriptome, together with the existing *T. muris* genome and transcriptome (Foth *et al.,* 2014), may give a greater insight into what genes are expressed within the worm, and how this may differ to the gene expression within the host intestinal tract. The mammalian host and nematode worm are likely to have different requirements from their microbiotas and this is supported by the distinct microbiotas selected by each. Identification of important bacterial species or genes may give a greater insight into what the worm needs when living within the host and may potentially reveal pathways that are not required by the host, therefore revealing potential novel drug targets.

6.2 High level *T. muris* infection may give a greater insight into what factor(s) cause microbiota alterations

Previous studies analysing the impact of *T. muris* infection on the host intestinal microbiota have used a low level chronic infection in C57BL/6 mice as a model (Holm *et al.,* 2015; Houlden *et al.,* 2015). In this thesis, high level infection was used to determine the impact of worm burden on these changes in both C57BL/6 mice and immunodeficient SCID mice. High level infections caused an increased abundance in the *Bacteroidaceae* and *Enterobacteriaceae*, independently of the host adaptive immune response. An increase in the *Lactobacillaceae* was also observed only in immunodeficient mice, although this increase has also been noted in C57BL/6 mice previously (Holm *et al.,* 2015). The changes identified with a high level infection are more pronounced and are an amplified version of the shifts identified with low level infection. As a result, the use of an infective high dose may be useful for future studies to effectively dissect the changes that

occur and to identify the potential mechanisms behind these changes. Infective doses used in the laboratory vary drastically between a low dose (~ 20 eggs) and a high dose (~ 200 eggs). Further work could be performed to determine the impact of worm burdens that lie between these two extremes on the host intestinal microbiota, as well as trickle infection, i.e. repeated low dose infection, that is more representative of natural infections.

Data presented in Chapter 3 of this thesis using immunodeficient (SCID) mice suggests that the host adaptive immune system is not the main driving factor behind the microbiota changes associated with *T. muris* infection. It is also clear that increasing worm numbers increases the extent of changes to the microbiota, with striking shifts being identified with high level infection. As worm numbers increase, the intestinal environment will be drastically altered. For example, the intestinal epithelial cell and mucosal barriers will be severely disrupted so that bacteria that reside in the mucosal layer will be disturbed. This resulted in increased association with intestinal crypts, as shown by FISH on sections of caecal tissue in Chapter 3, potentially altered immune responses including antimicrobial release and reactive oxygen species, and increased excretory products from the parasites including waste products and their excretory/secretory (E/S) products.

E/S from *T. suis* has been shown to have antibacterial properties (Abner *et al.,* 2001) and *T. muris* E/S has been shown to alter bacterial growth (A. Bancroft, personal communication). One possibility is that during a high level infection, increased excretion of E/S products into the intestinal lumen can impact specific bacterial groups causing their decrease, whereas other groups may be resistant allowing their enrichment within the intestinal tract. Furthermore, microbiota changes are time dependent and occur when *T. muris* develops from L3 larvae to an L4 larvae at around day 20 p.i. At this point the worms are moving up the intestinal crypts, increasing in size and are present in the intestinal lumen. This will result in increasing damage to intestinal epithelial cell layer and also increased interactions with the luminal microbiota. The composition of the host intestinal microbiota stays fairly constant after day 35 when worms reach adulthood. After this time there is no further nematode development and it could be that the developing worm causes gradual microbiota changes over time as it moults and moves up the intestinal crypts. This could also be accompanied by an increase in excretory products or antigens that cause the defined altered microbiota. Additionally, *T. muris* E/S contains many serine proteases which aid the breakdown of mucus, further altering the intestinal barrier (Hasnain *et al.,* 2012). This will facilitate the colonisation of the intestinal crypts and will likely have an impact on the host immune response. Additional work could use antibodies specific to the mucins, Muc2 and Muc5ac, to determine if the mucus layer is responsible for the separation between host and microbiota in naïve samples and what happens to this protective layer and its association with the microbiota during *T. muris* infection. Probes specific for certain bacterial groups could also be used, particularly those

that are enriched during infection, for example the *Enterobacteriaceae* and *Bacteroidaceae*. This would give an insight into their location within the intestinal tract and potential invasion of the intestinal crypts.

The microbiota alterations seen with *T. muris* infection, particularly those associated with high level infection, reflect those described in individuals with IBD and intestinal inflammation. These changes also occur in an immunodeficient mouse model indicating that the innate immune system could be responsible. Further work is needed to establish the immune environment in the intestinal tract of SCID mice infected with both a low and high dose of *T. muris*, including cell populations, cytokine levels and antimicrobial levels.

Another factor that could be fuelling the microbiota restructuring during infection is the altered metabolism within the intestinal tract, of both the bacteria and the host. The 16S amplicon sequencing data can be used to infer the metabolic pathways expressed by the bacteria present using PICRUSt software. This is not accurate as it uses known genomes of detected bacteria to predict potential gene expression. Therefore, other 'omics techniques, such a metabolomics and transcriptomics, should also be used. However, the above software could highlight potential metabolic changes as a result of infection. Low level infection does not significantly impact the potential expression of these pathways (A. Houlden, personal communication). Since microbiota changes associated with a high level infection are more defined, PICRUSt analysis may highlight more obvious changes in bacterial metabolism that could not be detected with a low level infection.

Overall, the microbiota alterations detected during *T. muris* infection could be a combined effect of all of these factors.

6.3 Infection impacts butyrate concentrations in the caecum

This thesis has demonstrated that infection with *T. muris* decreases the concentration of butyrate locally in the caecum of its host in a worm burden dependent manner. As microbiota alterations are also affected by worm burden, and butyrate is a product of bacterial fermentation, it is likely that the changes in butyrate are a direct result of infection-induced microbiota alterations. Infection caused a significant reduction in the proportion of *Clostridiales* in the intestinal tract, but an increase in the *Lachnospiraceae*. Both of these bacterial groups are known for their butyrate producing abilities, however, there are other bacteria that can potentially metabolise these SCFAs, including the Bacteroidetes, and these bacteria increased with infection. Analysis of the genes expressed by the microbiota altered by infection, compared to the naïve microbiota, would give a useful insight into the abilities of these bacterial communities to synthesise butyrate and help determine if the reduction in butyrate is a result of an altered microbiota. Furthermore, both low and high level infections caused significant reductions in caecal

butyrate concentrations, indicating that if the microbiota alterations are responsible, then a small but significant shift in proportions can have a substantial impact, which is again exacerbated by a high level infection. Additionally, clearance of infection caused butyrate concentrations to increase, and this was mirrored by an increase in the gene expression of butyrate transporters. However, the removal of worms also caused the host intestinal microbiota to alter so that it was significantly different to both naïve and infected microbiotas. This experiment should be repeated so that caecal butyrate concentrations are analysed when the intestinal microbiota is still representative of an infected host. Therefore, samples should be collected a day or two post mebendazole treatment to ensure that this is possible. This would give a greater insight into whether it is actually the altered microbiota as a result of infection that is causing the decrease in butyrate, or whether it is dependent on the physical presence of the worm.

As discussed previously in Chapter 3, the reduction in butyrate may be a result of shifts in bacterial proportions induced by changes in the inflammatory environment and levels of metabolites, thus altering the oxygen concentrations within the intestinal tract and selecting for bacteria capable of surviving in these conditions. It could therefore be hypothesised, as depicted in figure 6.1, that inflammation induced by a high worm burden, via the innate immune system, causes an altered intestinal environment that selects for a reduction in the *Clostridiales* order. This may be accompanied by an increase in nematode waste products, such as ammonia, which are then used by the *Bacteroidaceae* selecting for an increase in this bacterial family and a further loss of the *Clostridiales*, which are unable to use this as a nitrogen source. The loss of butyrate-producing bacteria and an increase in *Bacteroidaceae* species, which use SCFAs for amino acid production, results in a reduction in luminal butyrate and butyrate transporters. This causes a shift from butyrate oxidation to glucose fermentation as the primary energy source for intestinal epithelial cells, increasing epithelial oxygenation. As a result, there is increasing selection for facultative anaerobes, such as the *Enterobacteriaceae* and decreasing butyrate concentrations. This consequently promotes IFN-γ mediated immune responses, which can be inhibited by butyrate. Butyrate also causes an increase in mucus production, including Muc5ac, which is seen in resistant hosts, so reducing butyrate and consequently levels of this protective mucus would be beneficial for *T. muris* survival in the host. Higher oxygen concentrations may also be beneficial for the worm itself, which already inhabits an intestinal niche with increased oxygenation compared to the intestinal lumen. Production of butyrate by the worm microbiota and secretion by the worm could potentially act to compensate and limit the reduction in butyrate in its local environment to maintain a level of intestinal homeostasis, and prevent severe pathology by increasing inflammation that could damage the worm itself. Even with a high dose of *T. muris*, infection does not result in morbidity and as a parasite *T. muris* will want to maintain the health of its host for

an extended period of time. Therefore, selection for a parasite microbiota that is capable of making butyrate would promote the long term survival of *T. muris* within the chronically infected individual.

However, further work needs to be done to test this hypothesis. For example, techniques should also be employed to measure oxygen concentrations within the host intestinal tract to compare naïve and infected samples, and determine if increases in epithelial oxygenation could cause the microbiota alterations associated with *T. muris* infection. Furthermore, addition of sodium butyrate via oral gavage to *T. muris* infected mice could determine whether the reduction in butyrate seen is important for maintaining infection levels; does increasing butyrate concentration impact worm burden or worm viability? Work using *T. suis* in pigs has shown that a diet high in fermentable carbohydrates, the substrate for bacterial fermentation and production of butyrate, promotes early expulsion (Thomsen *et al.,* 2005). This diet could be implemented in mice to determine the impact on *T. muris* infection. However, as the *T. muris* microbiota produces butyrate it may be unlikely that this SCFA can impact on worm viability since addition of butyrate to culture media did not affect *T. muris* motility *in vitro*. Instead, it may be that increasing the substrate for SCFA production in the diet or addition of butyrate may result in an increased selection for bacteria that can use these substrates, for example the Clostridiales, and cause a shift in microbial populations back towards naïve status. The shift in the host intestinal microbiota back to naïve status may cause the intestinal niche to become less favourable for the worm due to altered metabolites. Decreasing the concentration of butyrate is likely to have an impact on the host immune response promoting the long term survival of *T. muris* in its host. SCFA measurements need to be performed on the caecal contents of SCID infected mice to determine if reductions in butyrate occur in an immunodeficient host independently of the host adaptive immune system.

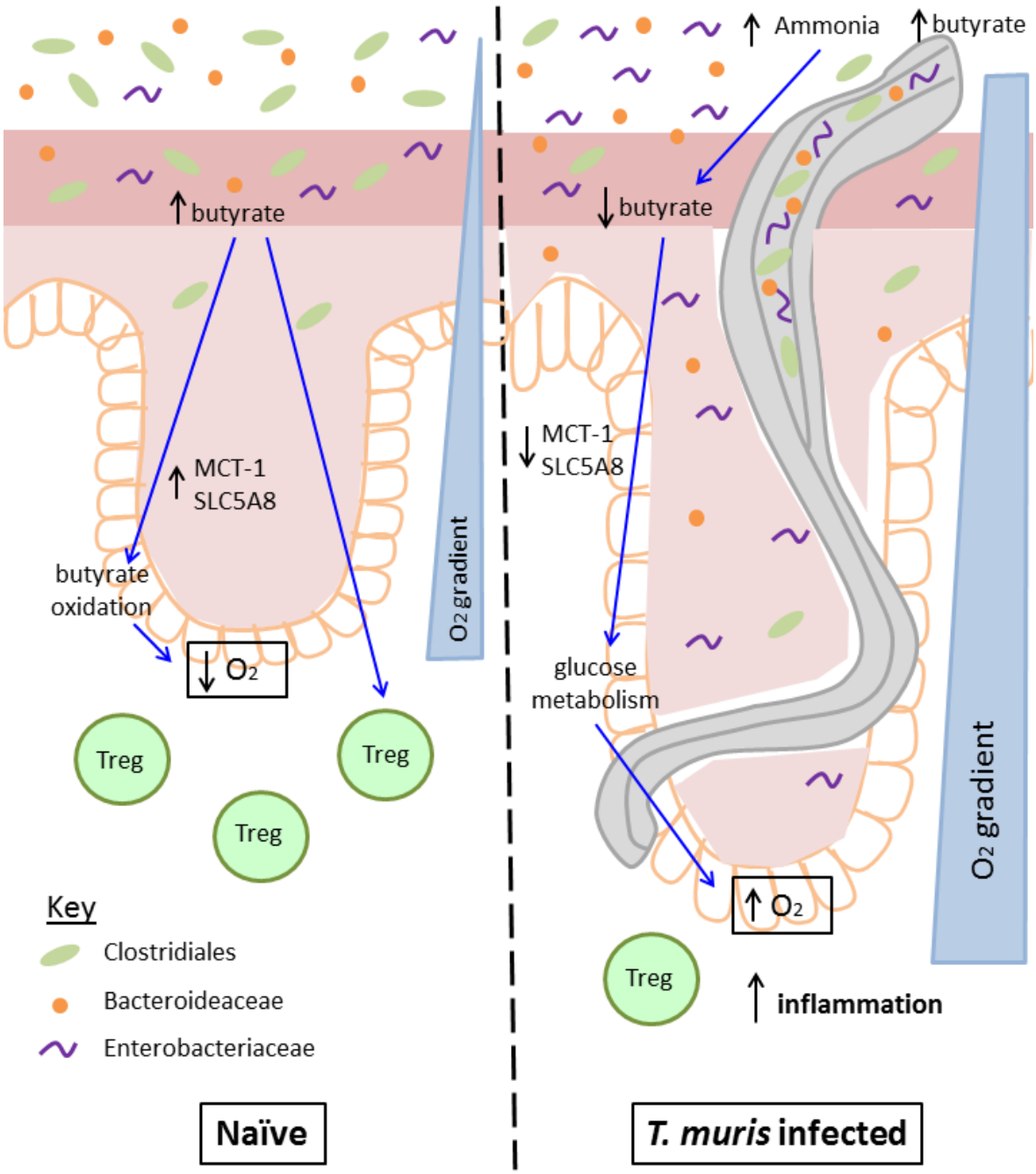

Figure 6.1 Hypothetical interactions between host, parasite and microbiotas in the caecum and colon during *T. muris* infection. Inflammation induced by *T. muris* infection and increased bacterial colonisation of the intestinal crypts, via the innate immune system, causes an altered intestinal environment characterises by a reduction in the *Clostridiales* (green) order. Nematode waste products, such as ammonia, will increase and can be used by the *Bacteroidaceae* (orange), which increase in abundance. The *Bacteroidaceae* can also use SCFAs for amino acid production, which results in a reduction in luminal butyrate, butyrate transporters (MCT-1 and SLC5A8) and Treg cells. This causes intestinal epithelial cells to use glucose fermentation instead of butyrate oxidation as their primary energy source, increasing oxygen levels. As a result, there is increasing selection for facultative anaerobes, such as the *Enterobacteriaceae* (purple). Low butyrate levels can also promote IFN-γ mediated immune responses. Production of butyrate by the worm microbiota and secretion by the worm in its local environment could potentially act to compensate for the reduction in butyrate to maintain a certain level of intestinal homeostasis.

6.4 Concluding remarks

Together, the ability of *T. muris* to select for a diverse, core intestinal microbiota whilst causing significant alterations to the host intestinal microbiota it resides within, could act as survival strategies to promote its long term survival within the chronically infected individual. As other intestinal parasitic helminths also live in close association with the host intestinal microbiota and cause significant alterations, these strategies may be conserved throughout nature. This has consequences for future studies of host-pathogen interactions and requires an additional factor, the parasite microbiota, to be acknowledged for further dissection of the complex interactions between host, pathogen and microbiota all interacting within a dynamic ecosystem.

References

Abner, S.R., Parthasarathy, G., Hill, D.E., Mansfield, L.S., 2001. Trichuris suis: detection of antibacterial activity in excretory-secretory products from adults. Exp. Parasitol. 99, 26–36.

Abramoff, M.D., Magalhães, P.J., Ram, S.J., 2004. Image processing with ImageJ. Biophotonics Int.

Adessi, C., Matton, G., Ayala, G., Turcatti, G., Mermod, J.J., Mayer, P., Kawashima, E., 2000. Solid phase DNA amplification: characterisation of primer attachment and amplification mechanisms. Nucleic Acids Res. 28, E87.

Albenberg, L., Esipova, T. V, Judge, C.P., Bittinger, K., Chen, J., Laughlin, A., Grunberg, S., Baldassano, R.N., Lewis, J.D., Li, H., Thom, S.R., Bushman, F.D., Vinogradov, S.A., Wu, G.D., 2014. Correlation between intraluminal oxygen gradient and radial partitioning of intestinal microbiota. Gastroenterology 147, 1055–63.e8.

Allison, M., Baetz, A., Wiegel, J., 1984. Alternative pathways for biosynthesis of leucine and other amino acids in Bacteroides ruminicola and Bacteroides fragilis. - PubMed - NCBI. Appl. Environ. Microbiol. 48, 1111–1117.

Amann, R.I., Ludwig, W., Schleifer, K.H., 1995. Phylogenetic identification and in situ detection of individual microbial cells without cultivation. Microbiol. Rev. 59, 143–69.

Andoh, A., Kuzuoka, H., Tsujikawa, T., Nakamura, S., Hirai, F., Suzuki, Y., Matsui, T., Fujiyama, Y., Matsumoto, T., 2012. Multicenter analysis of fecal microbiota profiles in Japanese patients with Crohn's disease. J. Gastroenterol. 47, 1298–307.

Ardissone, A.N., de la Cruz, D.M., Davis-Richardson, A.G., Rechcigl, K.T., Li, N., Drew, J.C., Murgas-Torrazza, R., Sharma, R., Hudak, M.L., Triplett, E.W., Neu, J., 2014. Meconium Microbiome Analysis Identifies Bacteria Correlated with Premature Birth. PLoS One 9, e90784.

Artis, D., Potten, C.S., Else, K.J., Finkelman, F.D., Grencis, R.K., 1999. Trichuris muris: host intestinal epithelial cell hyperproliferation during chronic infection is regulated by interferon-gamma. Exp. Parasitol. 92, 144–53.

Artis, D., Wang, M.L., Keilbaugh, S.A., He, W., Brenes, M., Swain, G.P., Knight, P.A., Donaldson, D.D., Lazar, M.A., Miller, H.R.P., Schad, G.A., Scott, P., Wu, G.D., 2004. RELMbeta/FIZZ2 is a goblet cell-specific immune-effector molecule in the gastrointestinal tract. Proc. Natl. Acad. Sci. U. S. A. 101, 13596–600.

Atuma, C., Strugala, V., Allen, A., Holm, L., 2001. The adherent gastrointestinal mucus gel layer: thickness and physical state in vivo. Am. J. Physiol. Gastrointest. Liver Physiol. 280, G922-9.

Bäckhed, F., Ding, H., Wang, T., Hooper, L. V, Koh, G.Y., Nagy, A., Semenkovich, C.F., Gordon, J.I., 2004. The gut microbiota as an environmental factor that regulates fat storage. Proc. Natl. Acad. Sci. U. S. A. 101, 15718–23.

Bäckhed, F., Fraser, C.M., Ringel, Y., Sanders, M.E., Sartor, R.B., Sherman, P.M., Versalovic, J., Young, V., Finlay, B.B., 2012. Defining a healthy human gut microbiome: current concepts, future directions, and clinical applications. Cell Host Microbe 12, 611–22.

Bancroft, A.J., Else, K.J., Sypek, J.P., Grencis, R.K., 1997. Interleukin-12 promotes a chronic intestinal nematode infection. Eur. J. Immunol. 27, 866–70.

Bancroft, A.J., Hayes, K.S., Grencis, R.K., 2012. Life on the edge: the balance between macrofauna, microflora and host immunity. Trends Parasitol. 28, 93–8. doi:10.1016/j.pt.2011.12.001

Baquiran, J.-P., Thater, B., Sedky, S., De Ley, P., Crowley, D., Orwin, P.M., 2013. Culture-Independent Investigation of the Microbiome Associated with the Nematode Acrobeloides maximus. PLoS One 8, e67425.

Bauer, H., Horowitz, R.E., Levenson, S.M., Popper, H., 1963. The response of the lymphatic tissue to the microbial flora. Studies on germfree mice. Am. J. Pathol. 42, 471–83.

Belkaid, Y., Hand, T.W., 2014. Role of the microbiota in immunity and inflammation. Cell 157, 121–141.

Bentley, D.R., Balasubramanian, S., Swerdlow, H.P., Smith, G.P., Milton, J., Brown, C.G., Hall, K.P., Evers, D.J., Barnes, C.L., Bignell, H.R., *et al.*, 2008. Accurate whole human genome sequencing using reversible terminator chemistry. Nature 456, 53–9. doi:10.1038/nature07517

Berg, M., Stenuit, B., Ho, J., Wang, A., Parke, C., Knight, M., Alvarez-Cohen, L., Shapira, M., 2016. Assembly of the Caenorhabditis elegans gut microbiota from diverse soil microbial environments. ISME J.

Blackwell, N.M., Else, K.J., 2001. B cells and antibodies are required for resistance to the parasitic gastrointestinal nematode Trichuris muris. Infect. Immun. 69, 3860–8.

Borthakur, A., Saksena, S., Gill, R.K., Alrefai, W.A., Ramaswamy, K., Dudeja, P.K., 2008. Regulation of monocarboxylate transporter 1 (MCT1) promoter by butyrate in human intestinal epithelial cells: involvement of NF-kappaB pathway. J. Cell. Biochem. 103, 1452–63.

Broadhurst, M.J., Ardeshir, A., Kanwar, B., Mirpuri, J., Gundra, U.M., Leung, J.M., Wiens, K.E., Vujkovic-Cvijin, I., Kim, C.C., Yarovinsky, F., Lerche, N.W., McCune, J.M., Loke, P., 2012. Therapeutic helminth infection of macaques with idiopathic chronic diarrhea alters the inflammatory signature and mucosal microbiota of the colon. PLoS Pathog. 8, e1003000.

Byrne, B.M., Dankert, J., 1979. Volatile fatty acids and aerobic flora in the gastrointestinal tract of mice under various conditions. Infect. Immun. 23, 559–563.

Cabreiro, F., Gems, D., 2013. Worms need microbes too: Microbiota, health and aging in caenorhabditis elegans. EMBO Mol. Med. 5, 1300–1310.

Caporaso, J.G., Kuczynski, J., Stombaugh, J., Bittinger, K., Bushman, F.D., Costello, E.K., Fierer, N., Peña, A.G., Goodrich, J.K., Gordon, J.I., Huttley, G.A., Kelley, S.T., Knights, D., Koenig, J.E., Ley, R.E., Lozupone, C.A., McDonald, D., Muegge, B.D., Pirrung, M., Reeder, J., Sevinsky, J.R., Turnbaugh, P.J., Walters, W.A., Widmann, J., Yatsunenko, T., Zaneveld, J., Knight, R., 2010. QIIME allows analysis of high-throughput community sequencing data. Nat. Methods 7, 335–6.

Caporaso, J.G., Lauber, C.L., Costello, E.K., Berg-Lyons, D., Gonzalez, A., Stombaugh, J., Knights, D., Gajer, P., Ravel, J., Fierer, N., Gordon, J.I., Knight, R., 2011. Moving pictures of the human microbiome. Genome Biol. 12, R50.

Chen, T.-L., Chen, S., Wu, H.-W., Lee, T.-C., Lu, Y.-Z., Wu, L.-L., Ni, Y.-H., Sun, C.-H., Yu, W.-H., Buret, A.G., Yu, L.C.-H., 2013. Persistent gut barrier damage and commensal bacterial influx following eradication of Giardia infection in mice. Gut Pathog. 5, 26.

Claesson, M.J., Jeffery, I.B., Conde, S., Power, S.E., O'Connor, E.M., Cusack, S., Harris, H.M.B., Coakley, M., Lakshminarayanan, B., O'Sullivan, O., Fitzgerald, G.F., Deane, J., O'Connor, M., Harnedy, N., O'Connor, K., O'Mahony, D., van Sinderen, D., Wallace, M., Brennan, L., Stanton, C., Marchesi, J.R., Fitzgerald, A.P., Shanahan, F.,

Hill, C., Ross, R.P., O'Toole, P.W., 2012. Gut microbiota composition correlates with diet and health in the elderly. Nature 488, 178–84.

Clausen, M.R., Mortensen, P.B., 1994. Kinetic studies on the metabolism of short-chain fatty acids and glucose by isolated rat colonocytes. Gastroenterology 106, 423–32.

Clemente, J.C., Ursell, L.K., Parfrey, L.W., Knight, R., 2012. The impact of the gut microbiota on human health: an integrative view. Cell 148, 1258–70.

Cliffe, L.J., Grencis, R.K., 2004. The Trichuris muris system: a paradigm of resistance and susceptibility to intestinal nematode infection. Adv. Parasitol. 57, 255–307.

Cliffe, L.J., Humphreys, N.E., Lane, T.E., Potten, C.S., Booth, C., Grencis, R.K., 2005. Accelerated intestinal epithelial cell turnover: a new mechanism of parasite expulsion. Science 308, 1463–5.

Cliffe, L.J., Potten, C.S., Booth, C.E., Grencis, R.K., 2007. An increase in epithelial cell apoptosis is associated with chronic intestinal nematode infection. Infect. Immun. 75, 1556–64.

Coombes, J.L., Siddiqui, K.R.R., Arancibia-Cárcamo, C. V, Hall, J., Sun, C.-M., Belkaid, Y., Powrie, F., 2007. A functionally specialized population of mucosal CD103+ DCs induces Foxp3+ regulatory T cells via a TGF-beta and retinoic acid-dependent mechanism. J. Exp. Med. 204, 1757–64.

Cooper, P., Walker, A.W., Reyes, J., Chico, M., Salter, S.J., Vaca, M., Parkhill, J., 2013. Patent human infections with the whipworm, Trichuris trichiura, are not associated with alterations in the faecal microbiota. PLoS One 8, e76573.

Costello, E.K., Lauber, C.L., Hamady, M., Fierer, N., Gordon, J.I., Knight, R., 2009. Bacterial community variation in human body habitats across space and time. Science 326, 1694–7.

Cresci, G.A., Thangaraju, M., Mellinger, J.D., Liu, K., Ganapathy, V., 2010. Colonic gene expression in conventional and germ-free mice with a focus on the butyrate receptor GPR109A and the butyrate transporter SLC5A8. J. Gastrointest. Surg. 14, 449–61.

Croswell, A., Amir, E., Teggatz, P., Barman, M., Salzman, N.H., 2009. Prolonged impact of antibiotics on intestinal microbial ecology and susceptibility to enteric Salmonella infection. Infect. Immun. 77, 2741–53.

Cuff, M.A., Lambert, D.W., Shirazi-Beechey, S.P., 2002. Substrate-induced regulation of the human colonic monocarboxylate transporter, MCT1. J. Physiol. 539, 361–71.

Cummings, J.H., Pomare, E.W., Branch, W.J., Naylor, C.P., Macfarlane, G.T., 1987. Short chain fatty acids in human large intestine, portal, hepatic and venous blood. Gut 28, 1221–7.

D'Elia, R., Behnke, J.M., Bradley, J.E., Else, K.J., 2009. Regulatory T cells: a role in the control of helminth-driven intestinal pathology and worm survival. J. Immunol. 182, 2340–8.

Dea-Ayuela, M.A., Rama-Iñiguez, S., Bolás-Fernandez, F., 2008. Enhanced susceptibility to Trichuris muris infection of B10Br mice treated with the probiotic Lactobacillus casei. Int. Immunopharmacol. 8, 28–35.

De Filippo, C., Cavalieri, D., Di Paola, M., Ramazzotti, M., Poullet, J.B., Massart, S., Collini, S., Pieraccini, G., Lionetti, P., 2010. Impact of diet in shaping gut microbiota revealed by a comparative study in children from Europe and rural Africa. Proc. Natl. Acad. Sci. U. S. A. 107, 14691–6.

De Vadder, F., Kovatcheva-Datchary, P., Goncalves, D., Vinera, J., Zitoun, C., Duchampt, A., Bäckhed, F., Mithieux, G., 2014. Microbiota-generated metabolites promote metabolic benefits via gut-brain neural circuits. Cell 156, 84–96.

den Besten, G., van Eunen, K., Groen, A.K., Venema, K., Reijngoud, D.-J., Bakker, B.M., 2013. The role of short-chain fatty acids in the interplay between diet, gut microbiota, and host energy metabolism. J. Lipid Res. 54, 2325–40.

Den Hond, E., Hiele, M., Evenepoel, P., Peeters, M., Ghoos, Y., Rutgeerts, P., 1998. In vivo butyrate metabolism and colonic permeability in extensive ulcerative colitis. Gastroenterology 115, 584–90.

Despommier, D.D., Müller, M., 1976. The stichosome and its secretion granules in the mature muscle larva of Trichinella spiralis. J. Parasitol. 62, 775–85.

Dirksen, P., Marsh, S.A., Braker, I., Heitland, N., Wagner, S., Nakad, R., Mader, S., Petersen, C., Kowallik, V., Rosenstiel, P., Félix, M.-A., Schulenburg, H., 2016. The native microbiome of the nematode Caenorhabditis elegans: gateway to a new host-microbiome model. BMC Biol. 14, 38.

Dominguez-Bello, M.G., Costello, E.K., Contreras, M., Magris, M., Hidalgo, G., Fierer, N., Knight, R., 2010. Delivery mode shapes the acquisition and structure of the initial microbiota across multiple body habitats in newborns. Proc. Natl. Acad. Sci. 107, 11971–11975.

Donaldson, G.P., Melanie Lee, S., Mazmanian, S.K., 2015. Gut biogeography of the bacterial microbiota. Nat. Publ. Gr. 14.

Donohoe, D.R., Garge, N., Zhang, X., Sun, W., O'Connell, T.M., Bunger, M.K., Bultman, S.J., 2011. The Microbiome and Butyrate Regulate Energy Metabolism and Autophagy in the Mammalian Colon. Cell Metab. 13, 517–526.

Donohoe, D.R., Wali, A., Brylawski, B.P., Bultman, S.J., 2012. Microbial regulation of glucose metabolism and cell-cycle progression in mammalian colonocytes. PLoS One 7, e46589.

Earley, Z.M., Akhtar, S., Green, S.J., Naqib, A., Khan, O., Cannon, A.R., Hammer, A.M., Morris, N.L., Li, X., Eberhardt, J.M., Gamelli, R.L., Kennedy, R.H., Choudhry, M.A., 2015. Burn Injury Alters the Intestinal Microbiome and Increases Gut Permeability and Bacterial Translocation. PLoS One 10, e0129996.

Eckburg, P.B., Bik, E.M., Bernstein, C.N., Purdom, E., Dethlefsen, L., Sargent, M., Gill, S.R., Nelson, K.E., Relman, D.A., 2005. Diversity of the human intestinal microbial flora. Science 308, 1635–8.

Edwards, C., Canfield, J., Copes, N., Rehan, M., Lipps, D., Bradshaw, P.C., 2014. D-beta-hydroxybutyrate extends lifespan in C. elegans. Aging (Albany. NY). 6, 621–44.

Else, K.J., Finkelman, F.D., Maliszewski, C.R., Grencis, R.K., 1994. Cytokine-mediated regulation of chronic intestinal helminth infection. J. Exp. Med. 179, 347–51.

Else, K.J., Grencis, R.K., 1996. Antibody-independent effector mechanisms in resistance to the intestinal nematode parasite Trichuris muris. Infect. Immun. 64, 2950–4.

Engel, P., Moran, N.A., 2013. The gut microbiota of insects - diversity in structure and function. FEMS Microbiol. Rev. 37, 699–735.

Ergin, A., Syrbe, U., Scheer, R., Thiel, A., Adam, T., Büssow, K., Duchmann, R., Zeitz, M., Sieper, J., 2011. Impaired peripheral Th1 CD4+ T cell response to Escherichia coli proteins in patients with Crohn's disease and ankylosing spondylitis. J. Clin. Immunol. 31, 998–1009.

Espey, M.G., 2013. Role of oxygen gradients in shaping redox relationships between the human intestine and its microbiota. Free Radic. Biol. Med. 55, 130–40.

Fadrosh, D.W., Ma, B., Gajer, P., Sengamalay, N., Ott, S., Brotman, R.M., Ravel, J., 2014. An improved dual-indexing approach for multiplexed 16S rRNA gene sequencing on the Illumina MiSeq platform. Microbiome 2, 6.

Faith, J.J., Guruge, J.L., Charbonneau, M., Subramanian, S., Seedorf, H., Goodman, A.L., Clemente, J.C., Knight, R., Heath, A.C., Leibel, R.L., Rosenbaum, M., Gordon, J.I., 2013. The long-term stability of the human gut microbiota. Science 341, 1237439.

Faulkner, H., Renauld, J.C., Van Snick, J., Grencis, R.K., 1998. Interleukin-9 enhances resistance to the intestinal nematode Trichuris muris. Infect. Immun. 66, 3832–40.

Ferreyra, J.A., Wu, K.J., Hryckowian, A.J., Bouley, D.M., Weimer, B.C., Sonnenburg, J.L., 2014. Gut microbiota-produced succinate promotes C. difficile infection after antibiotic treatment or motility disturbance. Cell Host Microbe 16, 770–7.

Fischbach, M., Sonnenburg, J., 2011. Eating for two: how metabolism establishes interspecies interactions in the gut. Cell Host Microbe 10, 336–347.

Forman, R.A., DeSchoolmeester, M.L., Hurst, R.J.M., Wright, S.H., Pemberton, A.D., Else, K.J., 2012. The Goblet Cell Is the Cellular Source of the Anti-Microbial Angiogenin 4 in the Large Intestine Post Trichuris muris Infection. PLoS One 7, e42248.

Foster, J., Ganatra, M., Kamal, I., Ware, J., Makarova, K., Ivanova, N., Bhattacharyya, A., Kapatral, V., Kumar, S., Posfai, J., Vincze, T., Ingram, J., Moran, L., Lapidus, A., Omelchenko, M., Kyrpides, N., Ghedin, E., Wang, S., Goltsman, E., Joukov, V., Ostrovskaya, O., Tsukerman, K., Mazur, M., Comb, D., Koonin, E., Slatko, B., 2005. The Wolbachia genome of Brugia malayi: endosymbiont evolution within a human pathogenic nematode. PLoS Biol. 3, e121.

Foth, B.J., Tsai, I.J., Reid, A.J., Bancroft, A.J., Nichol, S., Tracey, A., Holroyd, N., Cotton, J.A., Stanley, E.J., Zarowiecki, M., Liu, J.Z., Huckvale, T., Cooper, P.J., Grencis, R.K., Berriman, M., 2014. Whipworm genome and dual-species transcriptome analyses provide molecular insights into an intimate host-parasite interaction. Nat. Genet. 46, 693–700.

Frank, D.N., Robertson, C.E., Hamm, C.M., Kpadeh, Z., Zhang, T., Chen, H., Zhu, W., Sartor, R.B., Boedeker, E.C., Harpaz, N., Pace, N.R., Li, E., 2011. Disease phenotype and genotype are associated with shifts in intestinal-associated microbiota in inflammatory bowel diseases. Inflamm. Bowel Dis. 17, 179–84.

Frank, D.N., St Amand, A.L., Feldman, R.A., Boedeker, E.C., Harpaz, N., Pace, N.R., 2007. Molecular-phylogenetic characterization of microbial community imbalances in human inflammatory bowel diseases. Proc. Natl. Acad. Sci. U. S. A. 104, 13780–5.

Franks, A.H., Harmsen, H.J., Raangs, G.C., Jansen, G.J., Schut, F., Welling, G.W., 1998. Variations of bacterial populations in human feces measured by fluorescent in situ hybridization with group-specific 16S rRNA-targeted oligonucleotide probes. Appl. Environ. Microbiol. 64, 3336–45.

Franzosa, E.A., Hsu, T., Sirota-Madi, A., Shafquat, A., Abu-Ali, G., Morgan, X.C., Huttenhower, C., 2015. Sequencing and beyond: integrating molecular “omics” for microbial community profiling. Nat. Rev. Microbiol. 13, 360–72.

Friswell, M.K., Gika, H., Stratford, I.J., Theodoridis, G., Telfer, B., Wilson, I.D., McBain, A.J., 2010. Site and Strain-Specific Variation in Gut Microbiota Profiles and Metabolism in Experimental Mice. PLoS One 5, e8584.

Fukuda, S., Toh, H., Hase, K., Oshima, K., Nakanishi, Y., Yoshimura, K., Tobe, T., Clarke, J.M., Topping, D.L., Suzuki, T., Taylor, T.D., Itoh, K., Kikuchi, J., Morita, H., Hattori, M., Ohno, H., 2011. Bifidobacteria can protect from enteropathogenic infection through production of acetate. Nature 469, 543–7.

Fumagalli, M., Pozzoli, U., Cagliani, R., Comi, G.P., Riva, S., Clerici, M., Bresolin, N., Sironi, M., 2009. Parasites represent a major selective force for interleukin genes and shape the genetic predisposition to autoimmune conditions. J. Exp. Med. 206, 1395–408.

Furusawa, Y., Obata, Y., Fukuda, S., Endo, T.A., Nakato, G., Takahashi, D., Nakanishi, Y., Uetake, C., Kato, K., Kato, T., Takahashi, M., Fukuda, N.N., Murakami, S., Miyauchi, E., Hino, S., Atarashi, K., Onawa, S., Fujimura, Y., Lockett, T., Clarke, J.M., Topping, D.L., Tomita, M., Hori, S., Ohara, O., Morita, T., Koseki, H., Kikuchi, J., Honda, K., Hase, K., Ohno, H., 2013. Commensal microbe-derived butyrate induces the differentiation of colonic regulatory T cells. Nature 504, 446–50.

Galván-Moroyoqui, J.M., Del Carmen Domínguez-Robles, M., Franco, E., Meza, I., 2008. The interplay between Entamoeba and enteropathogenic bacteria modulates epithelial cell damage. PLoS Negl. Trop. Dis. 2, e266.

Ganesh, B.P., Klopfleisch, R., Loh, G., Blaut, M., 2013. Commensal Akkermansia muciniphila Exacerbates Gut Inflammation in Salmonella Typhimurium-Infected Gnotobiotic Mice. PLoS One 8, e74963.

Gao, C., Cao, T., Martin, R., Keenan, M., Greenway, F., Finley, J., Burton, J., Johnson, W., Enright, F., Zheng, J., 2014. Butyrate increased lifespan in C. elegans (1025.13). FASEB J. 28, 1025.13.

García-Villalba, R., Giménez-Bastida, J.A., García-Conesa, M.T., Tomás-Barberán, F.A., Carlos Espín, J., Larrosa, M., 2012. Alternative method for gas chromatography-mass spectrometry analysis of short-chain fatty acids in faecal samples. J. Sep. Sci. 35, 1906–13.

Garrett, W.S., Gallini, C.A., Yatsunenko, T., Michaud, M., DuBois, A., Delaney, M.L., Punit, S., Karlsson, M., Bry, L., Glickman, J.N., Gordon, J.I., Onderdonk, A.B., Glimcher, L.H., 2010. Enterobacteriaceae act in concert with the gut microbiota to induce spontaneous and maternally transmitted colitis. Cell Host Microbe 8, 292–300.

Gaudier, E., Jarry, A., Blottière, H.M., de Coppet, P., Buisine, M.P., Aubert, J.P., Laboisse, C., Cherbut, C., Hoebler, C., 2004. Butyrate specifically modulates MUC gene expression in intestinal epithelial goblet cells deprived of glucose. Am. J. Physiol. Gastrointest. Liver Physiol. 287, G1168-74.

Gerbaba, T.K., Gupta, P., Rioux, K., Hansen, D., Buret, A.G., 2015. Giardia duodenalis-induced alterations of commensal bacteria kill Caenorhabditis elegans: a new model to study microbial-microbial interactions in the gut. Am. J. Physiol. Gastrointest. Liver Physiol. 308, G550-61.

Gill, R.K., Dudeja, P.K., 2011. A novel facet to consider for the effects of butyrate on its target cells. Focus on “The short-chain fatty acid butyrate is a substrate of breast cancer resistance protein.” Am. J. Physiol. - Cell Physiol. 301.

Gill, S.R., Pop, M., Deboy, R.T., Eckburg, P.B., Turnbaugh, P.J., Samuel, B.S., Gordon, J.I., Relman, D.A., Fraser-Liggett, C.M., Nelson, K.E., 2006. Metagenomic analysis of the human distal gut microbiome. Science 312, 1355–9.

Goyal, N., Shukla, G., 2013. Probiotic lactobacillus rhamnosus GG modulates the mucosal immune response in giardia intestinalis-infected BALB/c Mice. Dig. Dis. Sci.

58, 1218–1225.

Green, G.L., Brostoff, J., Hudspith, B., Michael, M., Mylonaki, M., Rayment, N., Staines, N., Sanderson, J., Rampton, D.S., Bruce, K.D., 2006. Molecular characterization of the bacteria adherent to human colorectal mucosa. J. Appl. Microbiol. 100, 460–9.

Grencis, R.K., Humphreys, N.E., Bancroft, A.J., 2014. Immunity to gastrointestinal nematodes: mechanisms and myths. Immunol. Rev. 260, 183–205.

Gu, S., Chen, D., Zhang, J.-N., Lv, X., Wang, K., Duan, L.-P., Nie, Y., Wu, X.-L., 2013. Bacterial community mapping of the mouse gastrointestinal tract. PLoS One 8, e74957.

Guo, J., Xu, N., Li, Z., Zhang, S., Wu, J., Kim, D.H., Sano Marma, M., Meng, Q., Cao, H., Li, X., Shi, S., Yu, L., Kalachikov, S., Russo, J.J., Turro, N.J., Ju, J., 2008. Four-color DNA sequencing with 3'-O-modified nucleotide reversible terminators and chemically cleavable fluorescent dideoxynucleotides. Proc. Natl. Acad. Sci. U. S. A. 105, 9145–50.

Gusarov, I., Gautier, L., Smolentseva, O., Shamovsky, I., Eremina, S., Mironov, A., Nudler, E., 2013. Bacterial nitric oxide extends the lifespan of C. elegans. Cell 152, 818–30.

Hasnain, S., Evans, C.M., Roy, M., Gallagher, A.L., Kindrachuk, K.N., Barron, L., Dickey, B.F., Wilson, M.S., Wynn, T.A., Grencis, R.K., Thornton, D.J., 2011. Muc5ac: a critical component mediating the rejection of enteric nematodes. J. Exp. Med. 208, 893–900.

Hasnain, S.Z., McGuckin, M.A., Grencis, R.K., Thornton, D.J., 2012. Serine protease(s) secreted by the nematode Trichuris muris degrade the mucus barrier. PLoS Negl. Trop. Dis. 6, e1856. doi:10.1371/journal.pntd.0001856

Hasnain, S.Z., Thornton, D.J., Grencis, R.K., 2011. Changes in the mucosal barrier during acute and chronic Trichuris muris infection. Parasite Immunol. 33, 45–55.

Hayes, K.S., Bancroft, a J., Goldrick, M., Portsmouth, C., Roberts, I.S., Grencis, R.K., 2010. Exploitation of the intestinal microflora by the parasitic nematode Trichuris muris. Science 328, 1391–1394.

Haynes, M., Rohwer, F., 2011. The Human Virome, in: Nelson, K. (Ed.), Metagenomics of the Human Body. New York.

Hepworth, M.R., Monticelli, L.A., Fung, T.C., Ziegler, C.G.K., Grunberg, S., Sinha, R., Mantegazza, A.R., Ma, H.-L., Crawford, A., Angelosanto, J.M., Wherry, E.J., Koni, P.A., Bushman, F.D., Elson, C.O., Eberl, G., Artis, D., Sonnenberg, G.F., 2013. Innate lymphoid cells regulate CD4+ T-cell responses to intestinal commensal bacteria. Nature 498, 113–7.

Hill, D.A., Hoffmann, C., Abt, M.C., Du, Y., Kobuley, D., Kirn, T.J., Bushman, F.D., Artis, D., 2010. Metagenomic analyses reveal antibiotic-induced temporal and spatial changes in intestinal microbiota with associated alterations in immune cell homeostasis. Mucosal Immunol. 3, 148–58.

Hites, R., 1997. Gas Chromatography - Mass Spectrometry, in: Settle, F. (Ed.), Handbook of Instrumental Techniques for Analytical Chemistry. pp. 609–626.

Hoerauf, A., Mand, S., Volkmann, L., Büttner, M., Marfo-Debrekyei, Y., Taylor, M., Adjei, O., Büttner, D.W., 2003. Doxycycline in the treatment of human onchocerciasis: Kinetics of Wolbachia endobacteria reduction and of inhibition of embryogenesis in female Onchocerca worms. Microbes Infect. 5, 261–273.

Hoerauf, A., Nissen-Pähle, K., Schmetz, C., Henkle-Dührsen, K., Blaxter, M.L., Büttner, D.W., Gallin, M.Y., Al-Qaoud, K.M., Lucius, R., Fleischer, B., 1999. Tetracycline therapy targets intracellular bacteria in the filarial nematode Litomosoides sigmodontis and results in filarial infertility. J. Clin. Invest. 103, 11–18. d

Holm, J.B., Sorobetea, D., Kiilerich, P., Ramayo-Caldas, Y., Estellé, J., Ma, T., Madsen, L., Kristiansen, K., Svensson-Frej, M., 2015. Chronic Trichuris muris Infection Decreases Diversity of the Intestinal Microbiota and Concomitantly Increases the Abundance of Lactobacilli. PLoS One 10, e0125495.

Houlden, A., Hayes, K.S., Bancroft, A.J., Worthington, J.J., Wang, P., Grencis, R.K., Roberts, I.S., 2015. Chronic Trichuris muris Infection in C57BL/6 Mice Causes Significant Changes in Host Microbiota and Metabolome: Effects Reversed by Pathogen Clearance. PLoS One 10, e0125945.

Huda-Faujan, N., Abdulamir, A.S., Fatimah, A.B., Anas, O.M., Shuhaimi, M., Yazid, A.M., Loong, Y.Y., 2010. The impact of the level of the intestinal short chain Fatty acids in inflammatory bowel disease patients versus healthy subjects. Open Biochem. J. 4, 53–8.

Humen, M.A., De Antoni, G.L., Benyacoub, J., Costas, M.E., Cardozo, M.I., Kozubsky, L., Saudan, K.-Y., Boenzli-Bruand, A., Blum, S., Schiffrin, E.J., Pérez, P.F., 2005. Lactobacillus johnsonii La1 antagonizes Giardia intestinalis in vivo. Infect. Immun. 73, 1265–9.

Humphreys, N.E., Xu, D., Hepworth, M.R., Liew, F.Y., Grencis, R.K., 2008. IL-33, a potent inducer of adaptive immunity to intestinal nematodes. J. Immunol. 180, 2443–9.

Huttenhower, C., Gevers, D., Knight, R., Abubucker, S., Badger, J.H., Chinwalla, A.T., Creasy, H.H., Earl, A.M., FitzGerald, M.G., Fulton, R.S., *et al.*, 2012. Structure, function and diversity of the healthy human microbiome. Nature 486, 207–214.

Illumina, 2016. An Introduction to Next-Generation Sequencing Technology [WWW Document]. URL http://www.illumina.com/content/dam/illumina-marketing/documents/products/illumina_sequencing_introduction.pdf (accessed 9.15.16).

Jakobsson, H.E., Abrahamsson, T.R., Jenmalm, M.C., Harris, K., Quince, C., Jernberg, C., Björkstén, B., Engstrand, L., Andersson, A.F., 2014. Decreased gut microbiota diversity, delayed Bacteroidetes colonisation and reduced Th1 responses in infants delivered by caesarean section. Gut 63, 559–66.

Jakobsson, H.E., Rodríguez-Piñeiro, A.M., Schütte, A., Ermund, A., Boysen, P., Bemark, M., Sommer, F., Bäckhed, F., Hansson, G.C., Johansson, M.E. V, 2015. The composition of the gut microbiota shapes the colon mucus barrier. EMBO Rep. 16, 164–77.

Jenkins, T., 1969. Electron microscope observations of the body wall of Trichuris suis, Schrank, 1788 (Nematoda: Trichuroidea). I. The cuticle and bacillary band. Zeitschrift für Parasitenkd. Berlin, Ger. 32, 374–87.

Jernberg, C., Löfmark, S., Edlund, C., Jansson, J.K., 2007. Long-term ecological impacts of antibiotic administration on the human intestinal microbiota. ISME J. 1, 56–66.

Jiménez, E., Fernández, L., Marín, M.L., Martín, R., Odriozola, J.M., Nueno-Palop, C., Narbad, A., Olivares, M., Xaus, J., Rodríguez, J.M., 2005. Isolation of Commensal Bacteria from Umbilical Cord Blood of Healthy Neonates Born by Cesarean Section. Curr. Microbiol. 51, 270–274.

Jiménez, E., Marín, M.L., Martín, R., Odriozola, J.M., Olivares, M., Xaus, J., Fernández,

L., Rodríguez, J.M., 2008. Is meconium from healthy newborns actually sterile? Res. Microbiol. 159, 187–193. 7

Johansson, M.E. V, Phillipson, M., Petersson, J., Velcich, A., Holm, L., Hansson, G.C., 2008. The inner of the two Muc2 mucin-dependent mucus layers in colon is devoid of bacteria. Proc. Natl. Acad. Sci. U. S. A. 105, 15064–9.

Kashyap, P.C., Marcobal, A., Ursell, L.K., Larauche, M., Duboc, H., Earle, K.A., Sonnenburg, E.D., Ferreyra, J.A., Higginbottom, S.K., Million, M., Tache, Y., Pasricha, P.J., Knight, R., Farrugia, G., Sonnenburg, J.L., 2013. Complex Interactions Among Diet, Gastrointestinal Transit, and Gut Microbiota in Humanized Mice. Gastroenterology 144, 967–977.

Kelly, C.J., Zheng, L., Campbell, E.L., Saeedi, B., Scholz, C.C., Bayless, A.J., Wilson, K.E., Glover, L.E., Kominsky, D.J., Magnuson, A., Weir, T.L., Ehrentraut, S.F., Pickel, C., Kuhn, K.A., Lanis, J.M., Nguyen, V., Taylor, C.T., Colgan, S.P., 2015. Crosstalk between Microbiota-Derived Short-Chain Fatty Acids and Intestinal Epithelial HIF Augments Tissue Barrier Function. Cell Host Microbe 17, 662–71.

Khan, W.I., Richard, M., Akiho, H., Blennerhasset, P.A., Humphreys, N.E., Grencis, R.K., Van Snick, J., Collins, S.M., 2003. Modulation of intestinal muscle contraction by interleukin-9 (IL-9) or IL-9 neutralization: correlation with worm expulsion in murine nematode infections. Infect. Immun. 71, 2430–8.

Klampfer, L., Huang, J., Sasazuki, T., Shirasawa, S., Augenlicht, L., 2003. Inhibition of interferon gamma signaling by the short chain fatty acid butyrate. Mol. Cancer Res. 1, 855–62.

Klementowicz, J.E., Travis, M.A., Grencis, R.K., 2012. Trichuris muris: a model of gastrointestinal parasite infection. Semin. Immunopathol. 34, 815–28.

Koyama, K., Ito, Y., 2000. Mucosal mast cell responses are not required for protection against infection with the murine nematode parasite Trichuris muris. Parasite Immunol. 22, 13–20.

Kozich, J.J., Westcott, S.L., Baxter, N.T., Highlander, S.K., Schloss, P.D., 2013. Development of a dual-index sequencing strategy and curation pipeline for analyzing amplicon sequence data on the MiSeq Illumina sequencing platform. Appl. Environ. Microbiol. 79, 5112–20.

Kunin, C.M., Chalmers, T.C., Leevy, C.M., Sebastyen, S.C., Lieber, C.S., Finland, M., 1960. Absorption of orally administered neomycin and kanamycin with special reference to patients with severe hepatic and renal disease. N. Engl. J. Med. 262, 380–5.

Kurokawa, K., Itoh, T., Kuwahara, T., Oshima, K., Toh, H., Toyoda, A., Takami, H., Morita, H., Sharma, V.K., Srivastava, T.P., Taylor, T.D., Noguchi, H., Mori, H., Ogura, Y., Ehrlich, D.S., Itoh, K., Takagi, T., Sakaki, Y., Hayashi, T., Hattori, M., 2007. Comparative metagenomics revealed commonly enriched gene sets in human gut microbiomes. DNA Res. 14, 169–81.

Lane, D., 1991. 16S/23S rRNA sequencing, in: Stackebrandt, E., Goodfellow, M. (Eds.), Nucleic. Acids Techniques in Bacterial Systematics. Wiley, New York, pp. 115–147.

Langille, M., Meehan, C.J., Koenig, J.E., Dhanani, A.S., Rose, R.A., Howlett, S.E., Beiko, R.G., Gi Langille, M., Meehan, C.J., Koenig, J.E., Dhanani, A.S., Rose, R.A., Howlett, S.E., Beiko, R.G., 2014. Microbial shifts in the aging mouse gut. Microbiome 2, 50.

Lathrop, S.K., Bloom, S.M., Rao, S.M., Nutsch, K., Lio, C.-W., Santacruz, N., Peterson, D.A., Stappenbeck, T.S., Hsieh, C.-S., 2011. Peripheral education of the immune

system by colonic commensal microbiota. Nature 478, 250–4.

Lee, A., Gemmell, E., 1972. Changes in the mouse intestinal microflora during weaning: role of volatile fatty acids. Infect. Immun. 5, 1–7.

Lee, D., 1965. The Physiology of Nematodes. Oliver and Boyd Ltd, Edinburgh.

Lee, S.C., Tang, M.S., Lim, Y.A.L., Choy, S.H., Kurtz, Z.D., Cox, L.M., Gundra, U.M., Cho, I., Bonneau, R., Blaser, M.J., Chua, K.H., Loke, P., 2014. Helminth colonization is associated with increased diversity of the gut microbiota. PLoS Negl. Trop. Dis. 8, e2880.

Lewis, K., Lutgendorff, F., Phan, V., Söderholm, J.D., Sherman, P.M., McKay, D.M., 2010. Enhanced translocation of bacteria across metabolically stressed epithelia is reduced by butyrate†. Inflamm. Bowel Dis. 16, 1138–1148.

Ley, R.E., Bäckhed, F., Turnbaugh, P., Lozupone, C.A., Knight, R.D., Gordon, J.I., 2005. Obesity alters gut microbial ecology. Proc. Natl. Acad. Sci. U. S. A. 102, 11070–5.

Ley, R.E., Peterson, D.A., Gordon, J.I., 2006a. Ecological and evolutionary forces shaping microbial diversity in the human intestine. Cell 124, 837–48.

Ley, R.E., Turnbaugh, P.J., Klein, S., Gordon, J.I., 2006b. Microbial ecology: human gut microbes associated with obesity. Nature 444, 1022–3. doi:10.1038/4441022a

Li, H., Limenitakis, J.P., Fuhrer, T., Geuking, M.B., Lawson, M.A., Wyss, M., Brugiroux, S., Keller, I., Macpherson, J.A., Rupp, S., Stolp, B., Stein, J. V, Stecher, B., Sauer, U., McCoy, K.D., Macpherson, A.J., 2015. The outer mucus layer hosts a distinct intestinal microbial niche. Nat. Commun. 6, 8292.

Li, R.W., Wu, S., Li, W., Navarro, K., Couch, R.D., Hill, D., Urban, J.F., 2012. Alterations in the porcine colon microbiota induced by the gastrointestinal nematode Trichuris suis. Infect. Immun. 80, 2150–7.

Louis, P., Young, P., Holtrop, G., Flint, H.J., 2010. Diversity of human colonic butyrate-producing bacteria revealed by analysis of the butyryl-CoA:acetate CoA-transferase gene. Environ. Microbiol. 12, 304–14.

Lupp, C., Robertson, M.L., Wickham, M.E., Sekirov, I., Champion, O.L., Gaynor, E.C., Finlay, B.B., 2007. Host-Mediated Inflammation Disrupts the Intestinal Microbiota and Promotes the Overgrowth of Enterobacteriaceae. Cell Host Microbe 2, 119–129.

Macpherson, A., Khoo, U.Y., Forgacs, I., Philpott-Howard, J., Bjarnason, I., 1996. Mucosal antibodies in inflammatory bowel disease are directed against intestinal bacteria. Gut 38, 365–75.

Manichanh, C., Rigottier-Gois, L., Bonnaud, E., Gloux, K., Pelletier, E., Frangeul, L., Nalin, R., Jarrin, C., Chardon, P., Marteau, P., Roca, J., Dore, J., 2006. Reduced diversity of faecal microbiota in Crohn's disease revealed by a metagenomic approach. Gut 55, 205–11.

Mariat, D., Firmesse, O., Levenez, F., Guimarães, V., Sokol, H., Doré, J., Corthier, G., Furet, J.-P., 2009. The Firmicutes/Bacteroidetes ratio of the human microbiota changes with age. BMC Microbiol. 9, 123.

Mascie-Taylor, C.G.N., Karim, E., 2003. The burden of chronic disease. Science 302, 1921–2.

Mazmanian, S.K., Liu, C.H., Tzianabos, A.O., Kasper, D.L., 2005. An immunomodulatory molecule of symbiotic bacteria directs maturation of the host immune system. Cell 122, 107–18.

Mazmanian, S.K., Round, J.L., Kasper, D.L., 2008. A microbial symbiosis factor prevents intestinal inflammatory disease. Nature 453, 620–5.

Meehan, C.J., Beiko, R.G., 2014. A phylogenomic view of ecological specialization in the Lachnospiraceae, a family of digestive tract-associated bacteria. Genome Biol. Evol. 6, 703–13.

Mendoza-Macías, C.L., Barrios-Ceballos, M.P., de la Peña, L.P.C., Rangel-Serrano, A., Anaya-Velázquez, F., Mirelman, D., Padilla-Vaca, F., 2009. Entamoeba histolytica: effect on virulence, growth and gene expression in response to monoxenic culture with Escherichia coli 055. Exp. Parasitol. 121, 167–74.

Miyauchi, S., Gopal, E., Fei, Y.-J., Ganapathy, V., 2004. Functional identification of SLC5A8, a tumor suppressor down-regulated in colon cancer, as a Na(+)-coupled transporter for short-chain fatty acids. J. Biol. Chem. 279, 13293–6.

Montalvo-Katz, S., Huang, H., Appel, M.D., Berg, M., Shapira, M., 2013. Association with soil bacteria enhances p38-dependent infection resistance in Caenorhabditis elegans. Infect. Immun. 81, 514–20.

Morelli, L., 2008. Postnatal development of intestinal microflora as influenced by infant nutrition. J. Nutr. 138, 1791S–1795S.

Moter, A., Göbel, U.B., 2000. Fluorescence in situ hybridization (FISH) for direct visualization of microorganisms. J. Microbiol. Methods 41, 85–112.

Muyzer, G., de Waal, E.C., Uitterlinden, A.G., 1993. Profiling of complex microbial populations by denaturing gradient gel electrophoresis analysis of polymerase chain reaction-amplified genes coding for 16S rRNA. Appl. Environ. Microbiol. 59, 695–700.

Muyzer, G., Smalla, K., 1998. Application of denaturing gradient gel electrophoresis (DGGE) and temperature gradient gel electrophoresis (TGGE) in microbial ecology. Antonie Van Leeuwenhoek 73, 127–41.

Myers, R.M., Fischer, S.G., Lerman, L.S., Maniatis, T., 1985. Nearly all single base substitutions in DNA fragments joined to a GC-clamp can be detected by denaturing gradient gel electrophoresis. Nucleic Acids Res. 13, 3131–45.

Nakagawa, H., Shiozaki, T., Kobatake, E., Hosoya, T., Moriya, T., Sakai, F., Taru, H., Miyazaki, T., 2016. Effects and mechanisms of prolongevity induced by Lactobacillus gasseri SBT2055 in Caenorhabditis elegans. Aging Cell 15, 227–36.

Natividad, J.M.M., Hayes, C.L., Motta, J.-P., Jury, J., Galipeau, H.J., Philip, V., Garcia-Rodenas, C.L., Kiyama, H., Bercik, P., Verdu, E.F., 2013. Differential induction of antimicrobial REGIII by the intestinal microbiota and Bifidobacterium breve NCC2950. Appl. Environ. Microbiol. 79, 7745–54.

Nava, G.M., Friedrichsen, H.J., Stappenbeck, T.S., 2011. Spatial organization of intestinal microbiota in the mouse ascending colon. ISME J. 5, 627–38.

Nguyen, T.L.A., Vieira-Silva, S., Liston, A., Raes, J., 2015. How informative is the mouse for human gut microbiota research? Dis. Model. Mech. 8, 1–16.

Niu, Q., Zhang, L., Zhang, K., Huang, X., Hui, F., Kan, Y., Yao, L., 2016. Changes in intestinal microflora of Caenorhabditis elegans following Bacillus nematocida B16 infection. Sci. Rep. 6, 20178.

Nolan, T., Hands, R.E., Bustin, S.A., 2006. Quantification of mRNA using real-time RT-PCR. Nat. Protoc. 1, 1559–1582.

O'Hara, A.M., Shanahan, F., 2006. The gut flora as a forgotten organ. EMBO Rep. 7, 688–93.

Oudhoff, M.J., Antignano, F., Chenery, A.L., Burrows, K., Redpath, S.A., Braam, M.J., Perona-Wright, G., Zaph, C., 2016. Intestinal Epithelial Cell-Intrinsic Deletion of Setd7 Identifies Role for Developmental Pathways in Immunity to Helminth Infection. PLoS Pathog. 12, e1005876.

Padilla-Vaca, F., Ankri, S., Bracha, R., Koole, L.A., Mirelman, D., 1999. Down regulation of Entamoeba histolytica virulence by monoxenic cultivation with Escherichia coli O55 is related to a decrease in expression of the light (35-kilodalton) subunit of the Gal/GalNAc lectin. Infect. Immun. 67, 2096–102.

Panesar, T.S., Croll, N.A., 1980. The location of parasites within their hosts: site selection by Trichuris muris in the laboratory mouse. Int. J. Parasitol. 10, 261–73.

Parsons, R., 1977. Drug absorption in gastrointestinal disease with particular reference to malabsorption syndromes. Clin. Pharmacokinet. 2, 45–60.

Payne, S.H., Loomis, W.F., 2006. Retention and loss of amino acid biosynthetic pathways based on analysis of whole-genome sequences. Eukaryot. Cell 5, 272–6.

Pédron, T., Mulet, C., Dauga, C., Frangeul, L., Chervaux, C., Grompone, G., Sansonetti, P.J., 2012. A crypt-specific core microbiota resides in the mouse colon. MBio 3.

Pérez, P.F., Minnaard, J., Rouvet, M., Knabenhans, C., Brassart, D., De Antoni, G.L., Schiffrin, E.J., 2001. Inhibition of Giardia intestinalis by extracellular factors from Lactobacilli: an in vitro study. Appl. Environ. Microbiol. 67, 5037–42.

Petrosino, J.F., Highlander, S., Luna, R.A., Gibbs, R.A., Versalovic, J., 2009. Metagenomic pyrosequencing and microbial identification. Clin. Chem. 55, 856–66.

Phillips, B.P., Wolfe, P.A., 1959. The use of germ free guinea pigs in studies on the microbial interrelationships in amoebiasis. Ann. N. Y. Acad. Sci. 78, 308–314.

Preston, C.M., Jenkins, T., 1985. Parasitenkunde Trichuris muris: Structure and formation of the egg polar plugs. Z Parasitenkd 71, 373–381.

Qin, J., Li, R., Raes, J., Arumugam, M., Burgdorf, K.S., Manichanh, C., Nielsen, T., Pons, N., Levenez, F., Yamada, T., Mende, D.R., Li, J., Xu, J., Li, S., Li, D., Cao, J., Wang, B., Liang, H., Zheng, H., Xie, Y., Tap, J., Lepage, P., Bertalan, M., Batto, J.-M., Hansen, T., Le Paslier, D., Linneberg, A., Nielsen, H.B., Pelletier, E., Renault, P., Sicheritz-Ponten, T., Turner, K., Zhu, H., Yu, C., Li, S., Jian, M., Zhou, Y., Li, Y., Zhang, X., Li, S., Qin, N., Yang, H., Wang, J., Brunak, S., Doré, J., Guarner, F., Kristiansen, K., Pedersen, O., Parkhill, J., Weissenbach, J., MetaHIT Consortium, Bork, P., Ehrlich, S.D., Wang, J., 2010. A human gut microbial gene catalogue established by metagenomic sequencing. Nature 464, 59–65.

Rae, R., Riebesell, M., Dinkelacker, I., Wang, Q., Herrmann, M., Weller, A.M., Dieterich, C., Sommer, R.J., 2008. Isolation of naturally associated bacteria of necromenic Pristionchus nematodes and fitness consequences. J. Exp. Biol. 211, 1927–36.

Ramanan, D., Bowcutt, R., Lee, S.C., Tang, M.S., Kurtz, Z.D., Ding, Y., Honda, K., Gause, W.C., Blaser, M.J., Bonneau, R.A., Lim, Y.A.L., Loke, P., Cadwell, K., 2016. Helminth infection promotes colonization resistance via type 2 immunity. Science 352, 608–12.

Rao, A.U., Carta, L.K., Lesuisse, E., Hamza, I., 2005. Lack of heme synthesis in a free-living eukaryote. Proc. Natl. Acad. Sci. U. S. A. 102, 4270–5.

Rao, R., Weil, G.J., 2002. In vitro effects of antibiotics on Brugia malayi worm survival and

reproduction. J. Parasitol. 88, 605–611.

Rao, R., Moussa, H., Weil, G.J., 2002. Brugia malayi : effects of antibacterial agents on larval viability and development in vitro. Exp. Parasitol. 101, 77–81.

Rao, S., Kupfer, Y., Pagala, M., Chapnick, E., Tessler, S., 2011. Systemic absorption of oral vancomycin in patients with Clostridium difficile infection. Scand. J. Infect. Dis. 43, 386–8.

Rausch, S., Held, J., Fischer, A., Heimesaat, M.M., Kühl, A. a., Bereswill, S., Hartmann, S., 2013. Small Intestinal Nematode Infection of Mice Is Associated with Increased Enterobacterial Loads alongside the Intestinal Tract. PLoS One 8, 1–13.

Reikvam, D.H., Erofeev, A., Sandvik, A., Grcic, V., Jahnsen, F.L., Gaustad, P., McCoy, K.D., Macpherson, A.J., Meza-Zepeda, L.A., Johansen, F.-E., 2011. Depletion of murine intestinal microbiota: effects on gut mucosa and epithelial gene expression. 6, e17996.

Reuter, J.A., Spacek, D. V, Snyder, M.P., 2015. High-throughput sequencing technologies. Mol. Cell 58, 586–97.

Reynolds, L.A., Smith, K.A., Filbey, K.J., Harcus, Y., Hewitson, J.P., Redpath, S.A., Valdez, Y., Yebra, M.J., Finlay, B.B., Maizels, R.M., 2014. Commensal-pathogen interactions in the intestinal tract: lactobacilli promote infection with, and are promoted by, helminth parasites. Gut Microbes 5, 522–32.

Rigottier-Gois, L., 2013. Dysbiosis in inflammatory bowel diseases: the oxygen hypothesis. ISME J. 7, 1256–1261.

Rivera-Chávez, F., Zhang, L.F., Faber, F., Lopez, C.A., Byndloss, M.X., Olsan, E.E., Xu, G., Velazquez, E.M., Lebrilla, C.B., Winter, S.E., Bäumler, A.J., 2016. Depletion of Butyrate-Producing Clostridia from the Gut Microbiota Drives an Aerobic Luminal Expansion of Salmonella. Cell Host Microbe 19, 443–454.

Robertson, B.R., O'Rourke, J.L., Neilan, B.A., Vandamme, P., On, S.L.W., Fox, J.G., Lee, A., 2005. Mucispirillum schaedleri gen. nov., sp. nov., a spiral-shaped bacterium colonizing the mucus layer of the gastrointestinal tract of laboratory rodents. Int. J. Syst. Evol. Microbiol. 55, 1199–204.

Rocha, E.., Herren, C.D., Smalley, D.J., Smith, C.., 2003. The complex oxidative stress response of Bacteroides fragilis: the role of OxyR in control of gene expression. Anaerobe 9, 165–173.

Rodríguez, J.M., Murphy, K., Stanton, C., Ross, R.P., Kober, O.I., Juge, N., Avershina, E., Rudi, K., Narbad, A., Jenmalm, M.C., Marchesi, J.R., Collado, M.C., 2015. The composition of the gut microbiota throughout life, with an emphasis on early life. Microb. Ecol. Health Dis. 26, 26050.

Rooks, M.G., Garrett, W.S., 2016. Gut microbiota, metabolites and host immunity. Nat. Rev. Immunol. 16, 341–52.

Round, J.L., Lee, S.M., Li, J., Tran, G., Jabri, B., Chatila, T.A., Mazmanian, S.K., 2011. The Toll-like receptor 2 pathway establishes colonization by a commensal of the human microbiota. Science 332, 974–7.

Round, J.L., Mazmanian, S.K., 2009. The gut microbiota shapes intestinal immune responses during health and disease. Nat Rev Immunol 9, 313–323.

Saenz, S.A., Siracusa, M.C., Perrigoue, J.G., Spencer, S.P., Urban, J.F., Tocker, J.E., Budelsky, A.L., Kleinschek, M.A., Kastelein, R.A., Kambayashi, T., Bhandoola, A., Artis, D., 2010. IL25 elicits a multipotent progenitor cell population that promotes

T(H)2 cytokine responses. Nature 464, 1362–6.

Saiki, R.K., Gelfand, D.H., Stoffel, S., Scharf, S.J., Higuchi, R., Horn, G.T., Mullis, K.B., Erlich, H.A., 1988. Primer-directed enzymatic amplification of DNA with a thermostable DNA polymerase. Science 239, 487–91.

Sambrook, J., Russell, D.W., 2001. Molecular Cloning: A Laboratory Manual, Third Edit. ed. Cold Spring Harbor Laboratory Press.

Sartor, R.B., Mazmanian, S.K., 2012. Intestinal Microbes in Inflammatory Bowel Diseases. Am. J. Gastroenterol. Suppl. 1, 15–21.

Sawant, D. V, Gravano, D.M., Vogel, P., Giacomin, P., Artis, D., Vignali, D.A.A., 2014. Regulatory T cells limit induction of protective immunity and promote immune pathology following intestinal helminth infection. J. Immunol. 192, 2904–12.

Schopf, L.R., Hoffmann, K.F., Cheever, A.W., Urban, J.F., Wynn, T.A., 2002. IL-10 is critical for host resistance and survival during gastrointestinal helminth infection. J. Immunol. 168, 2383–92.

Segain, J.P., Raingeard de la Blétière, D., Bourreille, A., Leray, V., Gervois, N., Rosales, C., Ferrier, L., Bonnet, C., Blottière, H.M., Galmiche, J.P., 2000. Butyrate inhibits inflammatory responses through NFkappaB inhibition: implications for Crohn's disease. Gut 47, 397–403.

Severance, S., Rajagopal, A., Rao, A.U., Cerqueira, G.C., Mitreva, M., El-Sayed, N.M., Krause, M., Hamza, I., 2010. Genome-wide analysis reveals novel genes essential for heme homeostasis in Caenorhabditis elegans. PLoS Genet. 6, 1–16.

Sheffield, H.G., 1963. Electron microscopy of the bacillary band and stichosome of Trichuris muris. J. Parasitol. 49, 998–1009.

Sheffield, V.C., Beck, J.S., Stone, E.M., Myers, R.M., 1992. A simple and efficient method for attachment of a 40-base pair, GC-rich sequence to PCR-amplified DNA. Biotechniques 12, 386–8.

Shin, N.-R., Whon, T.W., Bae, J.-W., 2015. Proteobacteria: microbial signature of dysbiosis in gut microbiota. Trends Biotechnol. 33, 496–503.

Smith, H.L., Rajan, T. V, 2000. Tetracycline Inhibits Development of the Infective-Stage Larvae of Filarial Nematodes in Vitro. Exp. Parasitol. 95, 265–270.

Sonnenburg, J.L., Bäckhed, F., 2016. Diet-microbiota interactions as moderators of human metabolism. Nature 535, 56–64.

Spencer, S.P., Wilhelm, C., Yang, Q., Hall, J.A., Bouladoux, N., Boyd, A., Nutman, T.B., Urban, J.F., Wang, J., Ramalingam, T.R., Bhandoola, A., Wynn, T.A., Belkaid, Y., 2014. Adaptation of innate lymphoid cells to a micronutrient deficiency promotes type 2 barrier immunity. Science 343, 432–7.

Stepek, G., Lowe, A.E., Buttle, D.J., Duce, I.R., Behnke, J.M., 2006. In vitro and in vivo anthelmintic efficacy of plant cysteine proteinases against the rodent gastrointestinal nematode, Trichuris muris. Parasitology 132, 681–9.

Stephenson, L.S., Holland, C. V, Cooper, E.S., 2000. The public health significance of Trichuris trichiura. Parasitology 121 Suppl, S73-95.

Suzuki, M.T., Taylor, L.T., DeLong, E.F., 2000. Quantitative analysis of small-subunit rRNA genes in mixed microbial populations via 5'-nuclease assays. Appl. Environ. Microbiol. 66, 4605–14.

Swidsinski, A., Ladhoff, A., Pernthaler, A., Swidsinski, S., Loening-Baucke, V., Ortner, M., Weber, J., Hoffmann, U., Schreiber, S., Dietel, M., Lochs, H., 2002. Mucosal flora in inflammatory bowel disease. Gastroenterology 122, 44–54.

Tap, J., Mondot, S., Levenez, F., Pelletier, E., Caron, C., Furet, J.-P.P., Ugarte, E., Muñoz-Tamayo, R., Paslier, D.L.E., Nalin, R., Dore, J., Leclerc, M., 2009. Towards the human intestinal microbiota phylogenetic core. Environ. Microbiol. 11, 2574–2584.

Taylor, M.J., Bandi, C., Hoerauf, A., 2005a. Wolbachia bacterial endosymbionts of filarial nematodes. Adv. Parasitol. 60, 245–84.

Taylor, M.J., Makunde, W.H., McGarry, H.F., Turner, J.D., Mand, S., Hoerauf, A., 2005b. Macrofilaricidal activity after doxycycline treatment of Wuchereria bancrofti: a double-blind, randomised placebo-controlled trial. Lancet (London, England) 365, 2116–21.

Thangaraju, M., Cresci, G., Itagaki, S., Mellinger, J., Browning, D.D., Berger, F.G., Prasad, P.D., Ganapathy, V., 2008. Sodium-coupled transport of the short chain fatty acid butyrate by SLC5A8 and its relevance to colon cancer. J. Gastrointest. Surg. 12, 1773-81–2.

Thibault, R., De Coppet, P., Daly, K., Bourreille, A., Cuff, M., Bonnet, C., Mosnier, J.-F., Galmiche, J.-P., Shirazi-Beechey, S., Segain, J.-P., 2007. Down-regulation of the monocarboxylate transporter 1 is involved in butyrate deficiency during intestinal inflammation. Gastroenterology 133, 1916–27.

Thoene-Reineke, C., Fischer, A., Friese, C., Briesemeister, D., Göbel, U.B., Kammertoens, T., Bereswill, S., Heimesaat, M.M.M., 2014. Composition of intestinal microbiota in immune-deficient mice kept in three different housing conditions. PLoS One 9, e113406.

Thomsen, L.E., Petkevicius, S., Bach Knudsen, K.E., Roepstorff, A., 2005. The influence of dietary carbohydrates on experimental infection with Trichuris suis in pigs. Parasitology 131, 857–65.

Tian, L., Altin, J.A., Makaroff, L.E., Franckaert, D., Cook, M.C., Goodnow, C.C., Dooley, J., Liston, A., 2011. Foxp3^{+} regulatory T cells exert asymmetric control over murine helper responses by inducing Th2 cell apoptosis. Blood 118, 1845–53.

Tielens, A.G.M.M., van Grinsven, K.W.A.A., Henze, K., van Hellemond, J.J., Martin, W., 2010. Acetate formation in the energy metabolism of parasitic helminths and protists. Int. J. Parasitol. 40, 387–97.

Tilney, L.G., Connelly, P.S., Guild, G.M., Vranich, K.A., Artis, D., 2005. Adaptation of a nematode parasite to living within the mammalian epithelium. J. Exp. Zool. A. Comp. Exp. Biol. 303, 927–45.

Torres, M.R., Silva, M.E., Vieira, E.C., Bambirra, E.A., Sogayar, M.I., Pena, F.J., Nicoli, J.R., 1992. Intragastric infection of conventional and germfree mice with Giardia lamblia. Brazilian J. Med. Biol. Res. 25, 349–52.

Turnbaugh, P.J., Hamady, M., Yatsunenko, T., Cantarel, B.L., Duncan, A., Ley, R.E., Sogin, M.L., Jones, W.J., Roe, B.A., Affourtit, J.P., Egholm, M., Henrissat, B., Heath, A.C., Knight, R., Gordon, J.I., 2009a. A core gut microbiome in obese and lean twins. Nature 457, 480–4.

Turnbaugh, P.J., Ley, R.E., Mahowald, M.A., Magrini, V., Mardis, E.R., Gordon, J.I., 2006. An obesity-associated gut microbiome with increased capacity for energy harvest. Nature 444, 1027–31.

Turnbaugh, P.J., Ridaura, V.K., Faith, J.J., Rey, F.E., Knight, R., Gordon, J.I., 2009b. The

effect of diet on the human gut microbiome: a metagenomic analysis in humanized gnotobiotic mice. Sci. Transl. Med. 1, 6ra14.

van der Waaij, D., Berghuis-de Vries, J.M., Lekkerkerk Lekkerkerk-v, 1971. Colonization resistance of the digestive tract in conventional and antibiotic-treated mice. J. Hyg. (Lond). 69, 405–11.

van Der Wielen, P.W., Biesterveld, S., Notermans, S., Hofstra, H., Urlings, B.A., van Knapen, F., 2000. Role of volatile fatty acids in development of the cecal microflora in broiler chickens during growth. Appl. Environ. Microbiol. 66, 2536–40.

Vieites, J.M., Guazzaroni, M.-E., Beloqui, A., Golyshin, P.N., Ferrer, M., 2009. Metagenomics approaches in systems microbiology. FEMS Microbiol. Rev. 33, 236–55.

Vital, M., Howe, A.C., Tiedje, J.M., 2014. Revealing the Bacterial Butyrate Synthesis Pathways by Analyzing (Meta)genomic Data. MBio 5, e00889-14-e00889-14.

Walk, S.T., Blum, A.M., Ewing, S.A.-S., Weinstock, J. V, Young, V.B., 2010. Alteration of the murine gut microbiota during infection with the parasitic helminth Heligmosomoides polygyrus. Inflamm. Bowel Dis. 16, 1841–9.

Walker, A.W., Ince, J., Duncan, S.H., Webster, L.M., Holtrop, G., Ze, X., Brown, D., Stares, M.D., Scott, P., Bergerat, A., Louis, P., McIntosh, F., Johnstone, A.M., Lobley, G.E., Parkhill, J., Flint, H.J., 2011a. Dominant and diet-responsive groups of bacteria within the human colonic microbiota. ISME J. 5, 220–230.

Walker, A.W., Sanderson, J.D., Churcher, C., Parkes, G.C., Hudspith, B.N., Rayment, N., Brostoff, J., Parkhill, J., Dougan, G., Petrovska, L., 2011b. High-throughput clone library analysis of the mucosa-associated microbiota reveals dysbiosis and differences between inflamed and non-inflamed regions of the intestine in inflammatory bowel disease. BMC Microbiol. 11, 7.

Walter, J., 2008. Ecological role of lactobacilli in the gastrointestinal tract: implications for fundamental and biomedical research. Appl. Environ. Microbiol. 74, 4985–96.

Waterman, M., Xu, W., Stempak, J.M., Milgrom, R., Bernstein, C.N., Griffiths, A.M., Greenberg, G.R., Steinhart, A.H., Silverberg, M.S., 2011. Distinct and overlapping genetic loci in Crohn's disease and ulcerative colitis: correlations with pathogenesis. Inflamm. Bowel Dis. 17, 1936–42.

Wehkamp, J., Harder, J., Weichenthal, M., Schwab, M., Schäffeler, E., Schlee, M., Herrlinger, K.R., Stallmach, A., Noack, F., Fritz, P., Schröder, J.M., Bevins, C.L., Fellermann, K., Stange, E.F., 2004. NOD2 (CARD15) mutations in Crohn's disease are associated with diminished mucosal alpha-defensin expression. Gut 53, 1658–64.

Whitman, W.B., Coleman, D.C., Wiebe, W.J., 1998. Prokaryotes: the unseen majority. Proc. Natl. Acad. Sci. U. S. A. 95, 6578–83.

Wilhelm, C., Harrison, O.J., Schmitt, V., Pelletier, M., Spencer, S.P., Urban, J.F., Ploch, M., Ramalingam, T.R., Siegel, R.M., Belkaid, Y., 2016. Critical role of fatty acid metabolism in ILC2-mediated barrier protection during malnutrition and helminth infection. J. Exp. Med. 213, 1409–18.

Willing, B.P., Russell, S.L., Finlay, B.B., 2011. Shifting the balance: antibiotic effects on host-microbiota mutualism. Nat. Rev. Microbiol. 9, 233–243.

Wilson, K.H., Blitchington, R.B., 1996. Human colonic biota studied by ribosomal DNA sequence analysis. Appl. Environ. Microbiol. 62, 2273–8.

Wimmersberger, D., Tritten, L., Keiser, J., 2013. Development of an in vitro drug sensitivity assay for Trichuris muris first-stage larvae. Parasit. Vectors 6, 42.

Winter, S.E., Thiennimitr, P., Winter, M.G., Butler, B.P., Huseby, D.L., Crawford, R.W., Russell, J.M., Bevins, C.L., Adams, L.G., Tsolis, R.M., Roth, J.R., Bäumler, A.J., 2010. Gut inflammation provides a respiratory electron acceptor for Salmonella. Nature 467, 426–9.

Wohlgemuth, S., Haller, D., Blaut, M., Loh, G., 2009. Reduced microbial diversity and high numbers of one single Escherichia coli strain in the intestine of colitic mice. Environ. Microbiol. 11, 1562–71.

Wold, A.E., 1998. The hygiene hypothesis revised: is the rising frequency of allergy due to changes in the intestinal flora? Allergy 53, 20–5.

Wolk, K., Sabat, R., 2006. Interleukin-22: a novel T- and NK-cell derived cytokine that regulates the biology of tissue cells. Cytokine Growth Factor Rev. 17, 367–80.

Worthington, J.J., Klementowicz, J.E., Rahman, S., Czajkowska, B.I., Smedley, C., Waldmann, H., Sparwasser, T., Grencis, R.K., Travis, M.A., 2013. Loss of the TGFβ-Activating Integrin αvβ8 on Dendritic Cells Protects Mice from Chronic Intestinal Parasitic Infection via Control of Type 2 Immunity. PLoS Pathog. 9, e1003675.

Wright, K.A., Chan, J., 1973. Sense receptors in the bacillary band of trichuroid nematodes. Tissue Cell 5, 373–80.

Wu, S., Li, R.W., Li, W., Beshah, E., Dawson, H.D., Urban, J.F., 2012. Worm burden-dependent disruption of the porcine colon microbiota by Trichuris suis infection. PLoS One 7, e35470.

Xiao, L., Feng, Q., Liang, S., Sonne, S.B., Xia, Z., Qiu, X., Li, X., Long, H., Zhang, J., Zhang, D., Liu, C., Fang, Z., Chou, J., Glanville, J., Hao, Q., Kotowska, D., Colding, C., Licht, T.R., Wu, D., Yu, J., Sung, J.J.Y., Liang, Q., Li, J., Jia, H., Lan, Z., Tremaroli, V., Dworzynski, P., Nielsen, H.B., Bäckhed, F., Doré, J., Le Chatelier, E., Ehrlich, S.D., Lin, J.C., Arumugam, M., Wang, J., Madsen, L., Kristiansen, K., 2015. A catalog of the mouse gut metagenome. Nat. Biotechnol. 33, 1103–1108.

Yamamoto, I., Abe, A., Saito, H., Ishimoto, M., 1984. The pathway of ammonia assimilation in Bacteroides fragilis. J. Gen. Appl. Microbiol. 30, 499–508.

Yang, Y.-W., Chen, M.-K., Yang, B.-Y., Huang, X.-J., Zhang, X.-R., He, L.-Q., Zhang, J., Hua, Z.-C., 2015. Use of 16S rRNA Gene-Targeted Group-Specific Primers for Real-Time PCR Analysis of Predominant Bacteria in Mouse Feces. Appl. Environ. Microbiol. 81, 6749–56.

Yatsunenko, T., Rey, F.E., Manary, M.J., Trehan, I., Dominguez-Bello, M.G., Contreras, M., Magris, M., Hidalgo, G., Baldassano, R.N., Anokhin, A.P., Heath, A.C., Warner, B., Reeder, J., Kuczynski, J., Caporaso, J.G., Lozupone, C.A., Lauber, C., Clemente, J.C., Knights, D., Knight, R., Gordon, J.I., 2012. Human gut microbiome viewed across age and geography. Nature 486, 222–7.

Zaiss, M.M., Rapin, A., Lebon, L., Dubey, L.K., Mosconi, I., Sarter, K., Piersigilli, A., Menin, L., Walker, A.W., Rougemont, J., Paerewijck, O., Geldhof, P., McCoy, K.D., Macpherson, A.J., Croese, J., Giacomin, P.R., Loukas, A., Junt, T., Marsland, B.J., Harris, N.L., 2015. The Intestinal Microbiota Contributes to the Ability of Helminths to Modulate Allergic Inflammation. Immunity 43, 998–1010.

Zambell, K.L., Fitch, M.D., Fleming, S.E., 2003. Acetate and butyrate are the major substrates for de novo lipogenesis in rat colonic epithelial cells. J. Nutr. 133, 3509–15.

Zhu, H., Li, Y.R., 2012. Oxidative stress and redox signaling mechanisms of inflammatory bowel disease: updated experimental and clinical evidence. Exp. Biol. Med. (Maywood). 237, 474–80.